UNIVERSIDAD DE SALAMANCA

FACULTAD DE FARMACIA

Departamento de Ciencias Farmacéuticas

OBTENCIÓN DE COMPUESTOS HETEROCÍCLICOS CON ACTIVIDAD ANTIINFECCIOSA

TESIS DOCTORAL

NEREA ESCALA SAGASTA

Bajo la dirección de

Dra. Esther del Olmo

2023

OBTENCIÓN DE COMPUESTOS HETEROCÍCLICOS CON ACTIVIDAD ANTIINFECCIOSA

VNiVERSiDAD D SALAMANCA

CAMPUS DE EXCELENCIA INTERNACIONAL

Memoria de Tesis Doctoral para optar al Grado de Doctora en Farmacia con Mención Internacional por la Universidad de Salamanca, presentada por:

Nerea Escala

Dª. Nerea Escala Sagasta

Vº Bº

Esther del Olmo

Prof. Dra. Esther del Olmo Fernández

Directora del Departamento de
Ciencias Farmacéuticas

Dña. Esther del Olmo Fernández, catedrática del Departamento de Ciencias Farmacéuticas: Área de Química Farmacéutica, de la Facultad de Farmacia de la Universidad de Salamanca,

CERTIFICA:

Que la graduada en Farmacia por la Universidad del País Vasco, Dña. **NEREA ESCALA SAGASTA** ha realizado en este departamento, bajo su dirección, la tesis titulada "**Obtención de compuestos heterocíclicos con actividad antiinfecciosa**" para optar al título de Doctora en Farmacia por la Universidad de Salamanca y considera que reúne los requisitos necesarios por lo que autoriza su presentación para ser evaluada.

Para que así conste, firma el presente certificado en Salamanca, a 17 de mayo de 2023.

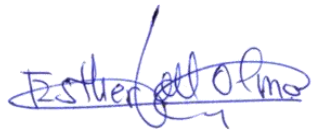

Esther del Olmo

Tesis Doctoral en formato de compendio de artículos

El presente Trabajo de Tesis para optar a la mención de Doctora por la Universidad de Salamanca corresponde a un compendio de cuatro artículos, tres de ellos publicados y uno enviado.

- **Anthelmintic activity of benzalphthalides and phthalazinones against *Teladorsagia circumcincta*: synthesis and structure-activity relationship**

  Nerea Escala, Elora Valderas-García, Bianca Barboza, Sobinson Arsène, Matheus C. Romeiro Miranda, Rafael Balaña-Fouce, María Martínez-Valladares, Esther del Olmo

  Enviado a: *Revista Brasilera de Parasitología Veterinaria*, 2023.

- **Synthesis, bioevaluation and docking studies of some 2-phenyl-1*H*-benzimidazole derivatives as anthelminthic agents against the nematode *Teladorsagia circumcincta***

  Nerea Escala, Elora Valderas-García, María Álvarez Bardón, Verónica Castilla Gómez de Agüero, Ricardo Escarcena, José Luis López-Pérez, Francisco A. Rojo-Vázquez, Arturo San Feliciano, Rafael Balaña-Fouce, María Martínez-Valladares, Esther del Olmo

  European Journal of Medicinal Chemistry, 2020, 208, 112554. doi: 10.1016/j.ejmech.2020.112554

- **Further and new target-based benzimidazole anthelmintics active against *Teladorsagia circumcincta***

  Nerea Escala, Elora Valderas-García, María Álvarez Bardón, Verónica Castilla Gómez de Agüero, José Luis López-Pérez, Francisco A. Rojo-Vázquez, Arturo San Feliciano, Rafael Balaña-Fouce, María Martínez-Valladares, Esther del Olmo

  Journal of Molecular Structure 2022, 1269, 133735. doi: 10.1016/j.molstruc.2022.133735

- **Antiplasmodial activity, structure–activity relationship and studies on the action of novel benzimidazole derivatives**

  Nerea Escala, Laura M. Pineda, Michelle G. Ng, Lorena M. Coronado, Carmenza Spadafora, Esther del Olmo

  Scientific Reports, 2023, 13, 285. doi: 10.1038/s41598-022-27351-z

Además, ha dado lugar a la publicación de otros tres artículos de investigación:

- **Novel compound shows in vivo anthelmintic activity in gerbils and sheep infected by *Haemonchus contortus***

  Elora Valderas-García, **Nerea Escala**, María Álvarez-Bardón, Verónica Castilla-Gómez de Agüero, María Cambra-Pellejà, Laura González del Palacio, Raquel Vallejo García, Jennifer de la Vega, Arturo San Feliciano, Esther del Olmo, María Martínez-Valladares

  Scientific Reports, 2022, 12, 13004. doi: 10.1038/s41598-022-17112-3
- **Benzimidazole and aminoalcohol derivatives show in vitro anthelmintic activity against *Trichuris muris* and *Heligmosomoides polygyrus***

  Elora Valderas-García, Cècile Häberli, María Álvarez-Bardón, **Nerea Escala**, Verónica Castilla-Gómez de Agüero, Jennifer de la Vega, Esther del Olmo, Rafael Balaña-Fouce, Jennifer Keiser, María Martínez-Valladares

  Parasites & Vectors, 2022, 15, 243. doi: 10.1186/s13071-022-05347-y
- **Semisynthesis, antiplasmodial activity, and mechanism of action studies of isocoumarin derivatives**

  Lorena Coronado, Xue-Quing Zhang, Doriana Dorta, **Nerea Escala**, Laura M. Pineda, Michelle G. Ng, Esther del Olmo, Chang-Yun Wang, Yu-Cheng Gu, Chang-Lun Shao, Carmenza Spadafora

  Journal of Natural Products, 2021, 84, 1434–1441. doi: 10.1021/acs.jnatprod.0c01032

El trabajo que aquí se presenta ha formado parte de los siguientes proyectos de investigación:

- **Control of ovine trichostrongyloidosis: drug design, synthesis and clinical trials of new antihelminthic molecules**. MINECO-RETOS, AGL2016-79813-C2-2-R. 2017-2020.
- **Antivirals for Dengue. Evaluation of mechanisms of action of semi-synthetic active products using in vitro models**. COLCIENCIAS; Basic Sciences: 712-2015, Project 55595, 2017-2020.

A mis padres, Elixabete y Juan Ignacio

A mis tíos, Maite y Agustín

Agradecimientos

Habiendo concluido este trabajo de tesis doctoral, deseo expresar mi agradecimiento a las personas que han ayudado de manera directa e indirecta a su realización. En primer lugar, quiero agradecer a la persona que más presente ha estado durante este proceso, por los conocimientos y el apoyo brindado, por ser mi guía y abrirme camino, por su infinita humanidad y valiosas enseñanzas; mil gracias, Esther, por ser mucho más que una directora. Gracias por confiar en mí.

Agradezco a la Dra. Carmenza Spadafora por darme la oportunidad de trabajar con su equipo, por enseñarme y transmitirme esa pasión por la investigación. Gracias a todo su equipo por acogerme y hacerme sentir una más. En especial, a Laura Pineda por la ayuda y la paciencia, y a Doriana Dorta por ser familia.

A Ricardo Escarcena, por enseñarme a dar los primeros pasos en el laboratorio y, sobre todo, por la infinita paciencia.

Al Dr. Atanasio Pandiella, por abrirme las puertas de su laboratorio y darme la oportunidad de iniciarme en los ensayos biológicos.

Al Dr. José Luis López Pérez, por su disponibilidad y la realización de los estudios de acoplamiento y modelado molecular que se incluyen en este trabajo.

A Itxaso Quintana y Arantza Maneiro; me siento afortunada de teneros. Habéis sido mi ancla durante todos estos años. Demostráis que la distancia no impide caminar de la mano. Mila esker, bihotzez.

A Jenny, porque haber empezado y terminado esta etapa contigo ha hecho que todo sea mucho más sencillo; no puedo imaginar estos años en Salamanca sin ti.

Al mejor grupo de amigos con el que podía contar. Mario, Sergio y Raúl, gracias por la energía, la complicidad y el apoyo; a Cris, por el cariño y la dulzura. Por los colores, por vosotros, ¡a los ojos! A Miguel, Noelia, Sara y a todos con los que he compartido este tiempo, porque fue más fácil hacerlo con vosotros cerca.

Índice

Abreviaturas y acrónimos

A	
AcOH	Ácido Acético
ADN	Ácido desoxirribonucléico
ADNk	ADN del kinetoplasto
Ar	Aromático
Art.	Artículo
ACT	Terapia combinada con artemisinina en malaria

B	
Boc_2O	Dicarbonato de di-*terc*-butilo
Bf	Benzalftalida
Bu	Butilo
Bz	Benzimidazol
Bzi	2-aminobenzimidazol intermedio
Bzo	Benzimidazolona

C	
ºC	Grado Celsius
CCF	Cromatografía de capa fina
CC	Cromatografía en columna
CC_{50}	Concentración citotóxica 50%
$CDCl_3$	Cloroformo deuterado
CDI	1,1´-Carbonildiimidazol
CHIKV	Chikungunya
CI_{50}	Concentración inhibitoria 50%
CE_{50}	Concentración efectiva 50%
CL_{50}	Concentración letal 50%
col.	Colaboradores
Cont.	Continuación
Comp.	Compuesto

D	
d	Doblete
da	Doblete ancho
DALY	Disability-adjusted life years
DCM	Diclorometano
dd	Doble doblete
ddd	Doble doble doblete
DEN	Dengue
DHPS	Dihidropteroato sintetasa
DHFR	Dihidrofolato reductasa
DMF	*N*,*N*-dimetilformamida
$DMSO\text{-}D_6$	Dimetilsulfóxido deuterado
dt	Doble triplete

E	
EHI	Inhibición de la eclosión de huevos
EIs	Enfermedades infecciosas
EtOH	Etanol
et al.	Y otros

F	
FDA	*"Food and Drug Administration"*
Fig.	Figura
Ft	Ftalazinona

G	
g	Gramo
GABA	Ácido 4-aminobutírico
GluCl	Canales de cloro activados por glutamato

H	
HR-MS	Espectrometría de masas de alta resolución
Hz	Hercio

I	
IR	Infrarrojo
IUPAC	*"International Union of Pure and Applied Chemistry"*
IS	Índice de selectividad

J	
J	Constante de acoplamiento

L	
L3	Larva 3 - fase infectiva
LD_{50}	Dosis letal 50%
LMI	Inhibición de la migración larvaria

M	
m	Multiplete
mg	Miligramo
mL	Mililitro
μM	Micromolar
μL	Microlitro
MPRA	*"Multidrug resistance-associated protein A"*
MTT	Bromuro de 3-(4,5-dimetiltiazol-2-il)-2,5,-difeniltetrazolio

N	
n-Hex	Hexano
nAChR	Receptores nicotínicos
$Na_2S_2O_5$	Metabisulfito sódico
NGI	Nematodos gastrointestinales
nM	Nanomolar
NTD	*"Neglected Tropical Diseases"*
NTR	Nitroreductasa

O	
OMS	Organización Mundial de la Salud

P	
PBS	Tampón fosfato salino
pCI_{50}	$-\log(CI_{50})$
Pd-C	Paladio sobre carbón activo
Pf	*Plasmodium falciparum*
Ph	Fenilo
PIC	Porcentaje de inhibición de crecimiento
ppm	Partes por millón

Q	
q	Quartete

R	
REA	Relación estructura-actividad
RMN	Resonancia magnética nuclear
2D-RMN	Bidimensionales

S	
s	Singlete
sa	Singlete ancho
STD	*"Soil-transmitted diseases"*

T	
t	Triplete
t.a.	Temperatura ambiente
Tc	*Trypanosoma cruzi*
TEA	Trietilamina
THF	Tetrahidrofurano

V	
V	Voltio

Z	
ZIK	Zika

Símbolos	
δ	Desplazamiento químico

Resumen

En este Trabajo de Doctorado se plantea la búsqueda nuevos prototipos de fármacos, que puedan constituir una alternativa para el tratamiento de las infecciones por nematodos gastrointestinales en rumiantes, y en más en concreto en el ganado ovino. Basándose en resultados positivos de actividad del grupo de investigación con compuestos de tipo benzalftalida y ftalazinona, se planteó ampliar las variantes estructurales con nuevas modificaciones sobre los anillos aromáticos, y sobre el sustituyente del nitrógeno amídico en el caso de las ftalazinonas.

Con el fin de ampliar la variación estructural se decidió obtener derivados de benzimidazol de tipo 2-fenilbenzimidazol, por lo que hubo que poner a punto los procesos de síntesis. Los resultados positivos de actividad obtenidos, condujeron al planteamiento de nuevas familias 2-(fenil/aril/hetaril)-aminometilbenzimidazol (familia II), -amidobenzimidazol (familia III) y relacionados, incluso de benzimidazolonas.

Todos los compuestos obtenidos han sido purificados mediante técnicas cromatográficas y cristalización en algún caso, y caracterizados mediante propiedades física y espectroscópicas: IR, HR-MS, RMN ^{1}H y RMN ^{13}C, con apoyo de técnicas bidimensionales en algún caso. Además, en el caso de los benzimidazoles se realizaron estudios de docking y modelado molecular sobre la β-tubulina de *Teladorsagia circumcincta.*

Se seleccionó un compuesto de la familia III para realizar ensayos in vivo, con el fin de determinar su toxicidad en ratones, y su eficacia en jerbos y en corderos infectados con *Haemonchus contortus*.

Se ampliaron los estudios de bioactividad frente a otros microorganismos. Así, quince compuestos de la familia III fueron evaluados frente a otros nematodos: *Trichuris muris* y *Heligmosomoides polygyrus*. Compuestos de las diferentes familias fueron evaluados frente a protozoos: *Plasmodium falciparum, Leishmania donovani, Trypanosoma cruzi*. Además, algunos benzimidazoles fueron ensayados frente a tres líneas tumorales. HeLa, MDA-MB-231 y MCF-7, y frente a algunos virus: dengue, zika, chikungunya.

Abstract

In this Doctoral Thesis, the search for new drug prototypes is proposed, which may constitute an alternative for the treatment of gastrointestinal nematode infections in ruminants, and more specifically in sheep. Based on the positive results of the research group's activity with compounds benzalphthalide and phthalazinone nucleus, it was proposed to expand the structural variants with new modifications on the aromatic rings, and on the amide nitrogen substituent in the case of phthalazinones.

In order to enlarge the structural variation, it was decided to obtain 2-phenylbenzimidazole derivatives of benzimidazole, so the synthesis processes had to be fine-tuned. The positive activity results obtained led to the proposal of new 2-(phenyl/aryl/hetaryl)-aminomethylbenzimidazole (family II), -amidobenzimidazole (family III) and related families, including benzimidazolones.

All the compounds obtained have been purified by chromatographic techniques and crystallization in some cases, and characterized by physical and spectroscopic properties: IR, HR-MS, ^{1}H NMR and ^{13}C NMR, with the support of two-dimensional techniques in some cases. In addition, in the case of benzimidazoles, docking and molecular modelling studies were carried out on β-tubulin from *Teladorsagia circumcincta*.

A compound of family III was selected for in vivo testing to determine its toxicity in mice, and its efficacy in gerbils and in lambs infected with *Haemonchus contortus*.

Bioactivity studies against other microorganisms were extended. Thus, fifteen family III compounds were evaluated against other nematodes: *Trichuris muris* and *Heligmosomoides polygyrus*. Compounds from the different families were evaluated against protozoa: *Plasmodium falciparum*, *Leishmania donovani*, *Trypanosoma cruzi*. In addition, some benzimidazoles were tested against three tumoral lines. HeLa, MDA-MB-231 and MCF-7, and against some viruses: dengue, zika, chikungunya.

I. INTRODUCCIÓN

I.1. ENFERMEDADES INFECCIOSAS

Por enfermedades infecciosas (EIs) se entiende aquellas causadas por microorganismos, generalmente, bacterias, virus, hongos o parásitos o, por sus productos tóxicos, y que aparecen después de la transmisión del agente infeccioso desde una persona infectada, un animal o un reservorio, a un hospedador susceptible. El proceso infeccioso depende de diferentes factores, como las características del microorganismo, la cantidad del inóculo, y factores dependientes del huésped como la respuesta inmunitaria.[1]

El acceso a los sistemas de Sanidad Pública ha aumentado a nivel global, así como las condiciones de higiene y la seguridad alimentaria.[2] Sin embargo, las EIs continúan siendo una carga elevada para los sistemas de salud, lo que supone una amenaza importante para la seguridad sanitaria global y la estabilidad económica de los países.[3] El desarrollo de los agentes antimicrobianos en el siglo pasado y de la inmunoterapia hicieron pensar que en algún momento se alcanzaría el control de las EIs, pero aún hoy en día continúa afectando a millones de personas, sobre todo en países de bajos recursos económicos. Por otro lado,

[1] Ausina, V.; Prets, G. Principales grupos de seres vivos con capacidad patógena para el hombre. En: *Tratado SEIMC de enfermedades infecciosas y microbiología clínica*; Ausina Ruiz, V.; Moreno Guillen, S., Ed.; Médica Panamericana; Madrid, 2005; pp 1–18.

[2] Baker, R.E.; Mahmud, A.S.; Miller, I.F.; Rajeev, M.; Rasambainarivo, F.; Rice, B.L.; Takahashi, S.; Tatem, A.J.; Wagner, C.E.; Wang, L.F.; Wesolowski, A.; Metcalf, C.J.E. Infectious disease in an era of global change. *Nat. Rev. Microbiol.* **2022**, 20, 193–205. doi: 10.1038/s41579-021-00639-z

[3] Bloom, D.E.; Cadarette, D. Infectious disease threats in the twenty-first century: strengthening the global response. *Front. Inmunol*. **2019**, 10, 549. doi: 10.3389/fimmu.2019.00549

han ido reapareciendo enfermedades que se creían controladas, surgiendo nuevos patógenos, o incluso apareciendo microorganismos resistentes a la mayoría de los agentes antimicrobianos disponibles en la actualidad.[4]

Las EIs pueden clasificarse teniendo en cuenta numerosos y variados criterios. Atendiendo a la transmisibilidad se clasifican en enfermedades de transmisión directa o indirecta. Las primeras se propagan directamente desde el individuo infectado, a través de sus secreciones, su piel o sus mucosas o, indirectamente, a partir de la contaminación del aire, de los alimentos o el agua. En las segundas, se requieren circunstancias especiales ya sean medioambientales (vectores intermediarios), accidentales (transfusiones de sangre) u otras (jeringas de uso compartido), para la transmisión del microorganismo.

En esta Memoria se expondrá de manera sucinta la etiología y tratamiento de una enfermedad transmitida por el suelo, producida concretamente por *Teladorsagia circumcincta*, y de tres enfermedades transmitidas por vectores, malaria, leishmaniasis y Chagas, estando las dos últimas incluidas dentro del grupo de las enfermedades tropicales desatendidas según la OMS.

I.1.1. ENFERMEDADES TRANSMITIDAS POR EL SUELO

Entre las enfermedades transmisibles, las transmitidas por el suelo (STD, por sus siglas en inglés: *Soil-transmitted diseases*) o geohelmintiasis, constituyen las infecciones más prevalentes a nivel global, tanto en humanos como animales de pastoreo, y se transmiten por la ingesta de huevos presentes en suelos contaminados, o por la penetración activa a través de la piel de las larvas que se encuentran en el suelo.[5]

Las STDs afectan a escala mundial a más de mil millones de personas, mayormente en África sub-Sahariana, América y este de Asia incluyendo a China,[5] y más concretamente, a los niños, disminuyendo la escolarización y agudizando la malnutrición. En los adultos supuso 1,97 millones de DALYs en 2019.[6]

[4] Kok, M.; Pechere, J.C. Nature and pathogenicity of micro-organisms. En *Infectious diseases*, 2ª edición; Cohen, J.; Powderly, W.G., Ed.; Mosby, Edinbourgh: 2004; pp 3–29.
[5] WHO, Soil-transmitted helminth infections. Disponible en: https://www.who.int/news-room/fact-sheets/detail/soil-transmitted-helminth-infections. (Acceso 2 mayo 2023)
[6] Intestinal nematode infections — level 3 cause | Institute for Health Metrics and Evaluation n.d. Disponible en: http://www.healthdata.org/results/gbd_summaries/2019/intestinal-nematode-infections-level-3-cause. (Acceso 2 mayo 2023)

Por otro lado, en el caso de los animales de pastoreo las infecciones por nematodos gastrointestinales (NGI) son las más prevalentes,[7] constituyendo un problema importante de salud en los rumiantes, especialmente en las ovejas, ya que produce retraso en el crecimiento, disminuye la producción de leche, genera lana de mala calidad, incluso disminuye la fertilidad, llegando a producir la muerte cuando la carga de vermes es muy alta.[8,9] Todo ello ocasiona pérdidas económicas muy elevadas en las explotaciones ganaderas de animales de pastoreo.

Las especies de tricostrongílidos más importantes que infectan a las ovejas son *Teladorsagia circumcincta*, *Trichostrongylus* spp. y *Haemonchus contortus*.[7] La distribución geográfica de estos parásitos está muy relacionada con las variaciones climáticas, así, *H. contortus* tiende a vivir en zonas más cálidas, mientras que *T. circumcincta* predomina en áreas templadas.[7] Sin embargo, los factores ambientales actuales, como el calentamiento global y el cambio climático, podrían alterar tanto la distribución como la epidemiología de estas parasitosis, agravando la salud de los animales, y disminuyendo las ganancias de los ganaderos.[10]

Teladorsagia circumcincta

T. circumcincta es, entre los NGIs, el parásito más prevalente en pequeños rumiantes y también, el que ha desarrollado más resistencias.[11] Además, constituye un buen modelo experimental de nematodo intestinal para infecciones parasitarias en ovejas.[12]

[7] Morgan, E.R.; van Dijk, J. Climate and the epidemiology of gastrointestinal nematode infections of sheep in Europe. *Vet. Parasitol.* **2012**, 189, 8-14. doi: 10.1016/j.vetpar.2012.03.028

[8] Craig, T.M. Gastrointestinal Nematodes, Diagnosis and Control. *Vet. Clin. North Am. Food Anim. Pract.* **2018**, 34(1), 185–199. doi: 10.1016/j.cvfa.2017.10.008

[9] Moje, N.; Gurmesa, A.; Regassa, G. Gastro-intestinal tract nematodes of small ruminants: Prevalence and their identification in and around Alage, Southern Ethiopia. *Vet. Clin. North Am. Food Anim. Pract*, **2021**, 9(3), 65-72. doi: 10.11648/j.avs.20210903.14

[10] Bautista-Garfias, C.R.; Castañeda-Raírez, G.S.; Estrada-Reyes, Z.M.; de Freitas Soares, F.E.; Ventura-Cordero, J.; González-Pech, P.; Morgan, E.R.; Soria-Ruiz, J.; López-Guillén, G.; Aguilar-Marcelino, L. A review of the impact of climate change on the epidemiology of gastrointestinal nematode infections in small ruminants and wildlife in tropical conditions pathogens, **2022**, 11(2), 148. doi: 10.3390/pathogens11020148

[11] Valderas-García, E.; de la Vega, J.; Álvarez-Bardón, M.; Castilla-Gómez de Agüero, V.; Escarcena, R.; López-Pérez, J. L.; Rojo-Vázquez, F.A.; San Feliciano, A.; del Olmo, E.; Balaña-Fouce, R; Martínez-Valladares, M. Anthelmintic activity of aminoalcohol and diamine derivatives against the gastrointestinal nematode *Teladorsagia circumcincta*. *Vet. Parasitol.* **2021**, 296, 109496. doi: 10.1016/j.vetpar.2021.109496

[12] Escala, N.; Valderas-García, E.; Álvarez-Bardón, M.; Castilla Gómez de Agüero, V.; López-Pérez, J. L.; Rojo-Vázquez, F.A.; San Feliciano, A.; Martínez-Valladares, M.; Balaña-Fouce, R.; del Olmo, E. Further and new target-based benzimidazole anthelmintics active against *Teladorsagia circumcincta*. **2022**, *J. Mol. Struct*., 1269, 133735. doi: 10.1016/j.molstruc.2022.133735

Con un ciclo de vida similar al de los nematodos gastrointestinales (Fig. I.1), los vermes adultos copulan en el abomaso liberando los huevos al medio a través de las heces, donde, en condiciones óptimas de temperatura, humedad y oxígeno, al cabo de dos semanas, desarrollan, pasando por los estadios L1 y L2, la tercera fase infectiva (L3). Las L3 migran de las heces a la hierba y el nuevo hospedador se infecta mediante su ingestión, donde continúa el desarrollo con dos mudas más del parásito (L4 y L5) antes de convertirse en sexualmente maduros en la superficie de la mucosa del abomaso.[13]

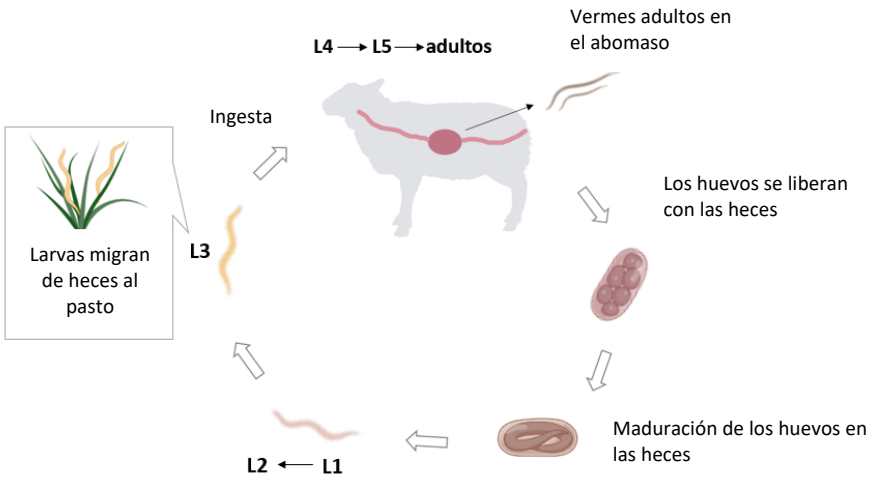

Figura I.1. Ciclo de vida de *Teladorsagia circumcincta*.[14]

La patología comienza cuando los primeros vermes adultos emergen de las glándulas gástricas alterando la estructura del abomaso, y reduciendo la secreción de ácido clorhídrico, cursando, además, con edema en los pliegues abomasales, y llegando a generar el desprendimiento de la mucosa. Los efectos fisiológicos más frecuentes son anorexia, diarrea, deshidratación, edema intermandibular y, la consecuente pérdida de peso,[15] con una reducción en su ganancia de entre 10-47%,[16] poniendo en riesgo la vida del animal.

[13] Taylor, M.A.; Coop, R.L.; Wall, R.L. *Veterinary parasitology*, 4ª edición; John Wiley & Sons, Chichester: UK, 2016.
[14] Figura creada con https://biorender.com/
[15] Anderson, D.E.; Rings, M. Current veterinary therapy: food animal practice, 5ª edición; Saunders Elsevier, St. Louis, MO, 2009.
[16] Charlier, J.; van der Voort, M.; Kenyon, F.; Skuce, P.; Vercruysse, J. Chasing helminths and their economic impact on farmed ruminants. *Trends Parasitol*. **2014**, 30, 361-367. doi: 10.1016/j.pt.2014.04.009

Fármacos actuales: mecanismo de acción y limitaciones de uso

Los fármacos antihelmínticos son los más utilizados en medicina veterinaria. Se dispone de un amplio número de fármacos vermífugos para el tratamiento de las infecciones por NGIs, que pueden clasificarse por similitud estructural en compuestos heterocíclicos (tiabendazol, albendazol, pirantel, etc.), lactonas macrocíclicas (ivermectina y derivados), o amino-acetonitrilos (monepantel), entre otros (Fig. I.2).

Desde la introducción del tiabendazol, compuesto con estructura de **benzimidazol** (Bz), para el tratamiento de las STDs en el año 1961 por Brown,[17] se han introducido nuevos análogos y derivados, como el albendazol, mebendazol, etc. Estos últimos muestran mejor eficacia en comparación con el tiabendazol, mayor espectro de acción, así como una menor toxicidad para el hospedador, y representan, además, el grupo de fármacos más utilizados para el tratamiento de estas parasitosis.

Dos décadas más tarde, se introdujeron las **lactonas macrocíclicas**, avermectinas y milbemicinas, que son compuestos obtenidos por semisíntesis a partir de metabolitos producidos por bacterias del suelo del género *Streptomyces,* y que muestran una alta capacidad nematicida a concentraciones del orden de µg/Kg.

Compuestos con estructura de **imidazotiazoles**, como el levamisol o tetramisol,[18] y las **tetrahidropirimidinas**, como el pirantel y morantel, actúan con un mecanismo similar, por lo que se suelen clasificar dentro del mismo grupo.

En el año 2009 se introdujo en el arsenal terapéutico uno de los últimos antihelmínticos nematicidas, el monepantel, compuesto derivado de **amino-acetonitrilo**.[19]

[17] Brown, H.D.; Matzuk, A.R.; Ilves, I.R.; Peterson, L.H.; Harris, S.A.; Sarett, L.H.; Egerton, J.R.; Yakstis, J.J.; Campbell, W.C.; Cuckler, A.C. Antiparasitic drugs. iv. 2-(4'-thiazolyl)-benzimidazole, a new anthelmintic. *J. Am. Chem. Soc.* **1961**, 83(7), 1764–1765. doi: 10.1021/ja01468a052

[18] Zajac, A.M.; Garza, J. Biology, epidemiology, and control of gastrointestinal nematodes of small ruminants. *Vet. Clin. North Am. Food Anim. Pract*. **2020**, 36(1), 73–87. doi: 10.1016/j.cvfa.2019.12.005

[19] Kaminsky, R.; Gauvry, N.; Schorderet, W.S.; Skripsky, T.; Bouvier, J.; Wenger, A.; Schroeder, F.; Desaules, Y.; Hotz, R.; Goebel, T.; Hosking, B.C.; Pautrat, F.; Wieland-Berghausen, S.; Ducray, P. Identification of the amino-acetonitrile derivative monepantel (AAD 1566) as a new anthelmintic drug development candidate. *Parasitol. Res*. **2008**, 103, 931–939. doi: 10.1007/s00436-008-1080-7

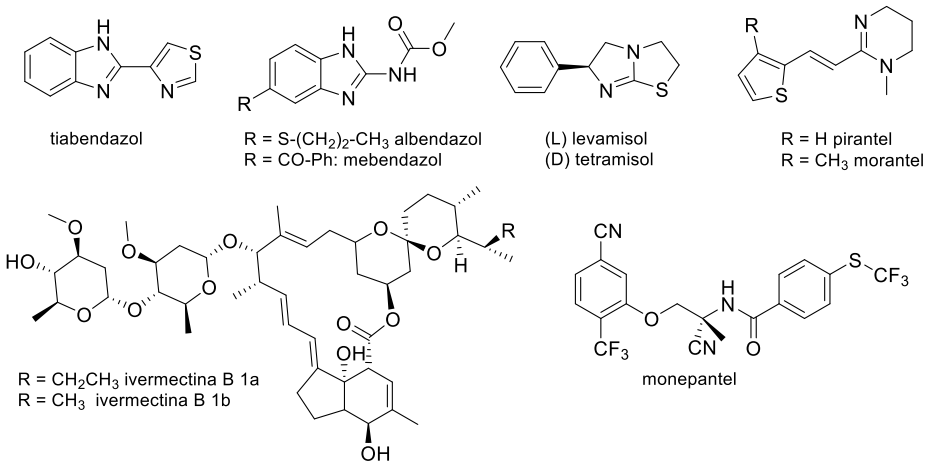

Figura I.2. Estructuras de algunos fármacos nematicidas de uso veterinario.

Sin embargo, a pesar del amplio arsenal terapéutico disponible para el tratamiento de las infecciones por NGIs, el uso masivo de estos fármacos y la incorrecta dosificación han generado resistencias en los parásitos a los tratamientos establecidos.[20] Así, desde hace más de una década se conocen especies de *T. circumcincta* resistentes a una o dos clases de nematicidas, incluso especies multirresistentes, es decir, resistentes a más de dos clases de fármacos.[21]

Las resistencias a los Bzs antihelmínticos se extienden a escala mundial desde Nueva Zelanda[22] a Sudáfrica[23] o México[24], con una prevalencia muy elevada en Europa, registrándose casos en la mayor parte de los países. También se han encontrado resistencias a los imidazotiazoles en Reino Unido e Italia, incluso resistencias a las lactonas macrocíclicas

[20] Papadopoulos, E.; Gallidis, E.; Ptochos, S. Anthelmintic resistance in sheep in Europe: A selected review. *Vet. Parasitol.* **2012**, 189, 85-88. doi: 10.1016/j.vetpar.2012.03.036

[21] Sargison, N.D. Pharmaceutical treatments of gastrointestinal nematode infections of sheep-Future of anthelmintic drugs. *Vet. Parasitol*., **2012**, 189, 79-84. doi: 10.1016/j.vetpar.2012.03.035

[22] Waghorn, T.S.; Leathwick, D.M.; Rhodes, A.P.; Lawrence, K.E.; Jackson, R.; Pomroy, W.E.; West, D.M; Moffat, J.R. Prevalence of anthelmintic resistance on sheep farms in New Zealand. *NZ Vet. J.* **2006**, 54, 271-277. doi: 10.1080/00480169.2006.36710

[23] Tsotetsi, A.M.; Njiro, S.; Katsande, T.C.; Moyo, G.; Baloyi, F.; Mpofu, J. Prevalence of gastrointestinal helminths and anthelmintic resistance on small-scale farms in Gauteng Province, South Africa. *Trop. Anim. Health Prod*. **2013**, 45, 751-761. doi: 10.1007/s11250-012-0285-z

[24] Alcalá-Canto, Y.; Camberos, L.O.; López, H.S.; Olvera, L.G.; Pérez, G.T. Anthelmintic resistance status of gastrointestinal nematodes of sheep to the single or combined administration of benzimidazoles and closantel in three localities in Mexico. *Vet. Mexico*. **2016**, 3, 1-11. doi: 10.21753/vmoa.3.4.374

en Europa, desde el Reino Unido a España e Italia.[20,25] Hace algo más de una década se encontraron resistencias a los amino-acetonitrilos en Nueva Zelanda.[26]

A continuación, se describen los mecanismos de acción (Fig. I.3) y los principales mecanismos de resistencia de estas familias de agentes nematicidas (Tabla I.1):

Los **Bzs** se unen de manera selectiva y con alta afinidad a la β-tubulina del nematodo, acoplándose al sitio de colchicina, de esta manera inhiben la formación de los microtúbulos, y como consecuencia dañan la estructura celular, bloquean el transporte de vesículas secretoras y/o la secreción de enzimas al citoplasma, provocando la lisis celular y desencadenando la muerte del parásito.[27] Los Bz antihelmínticos son los fármacos más utilizados para el tratamiento de las helmintiasis, por lo que se conocen bien sus mecanismos de resistencia.

Muchos de los Bzs presentan en posición C-2 del núcleo de benzimidazol un grupo carbamato, que está asociado a mutaciones de tres residuos en la β-tubulina, F200, F167 y E198. Las mutaciones generan una menor afinidad por el sitio de unión de la colchicina y, por lo tanto, disminuyen la eficacia del fármaco.

La mayoría de los fármacos nematicidas actúan sobre el sistema nervioso de los parásitos, así los **imidazotiazoles** actúan como agonistas colinérgicos de los receptores nicotínicos (nAChR) musculares subtipo-L 35pS del parásito, abriendo los canales catiónicos mediados por acetilcolina. Esto produce la despolarización y parálisis espástica del músculo del parásito, causando su expulsión del hospedador.[28] La resistencia frente a estos fármacos se produce debido a la sobrexpresión de la glicoproteína-G, una bomba de eflujo de fármacos que provoca su expulsión desde las células.

Las **tetrahidropirimidinas**, actúan sobre los mismos receptores nAChR musculares provocando parálisis espástica y la consiguiente muerte del parásito.[27,29] Mientras que los derivados de **amino-acetonitrilo** actúan como moduladores alostéricos de los nAChR

[25] Traversa, D.; von Samson-Himmelstjerna, G. Anthelmintic resistance in sheep gastro-intestinal strongyles in Europe. *Small Ruminant Res*. **2016**, 135, 75-80. doi: 10.1016/j.smallrumres.2015.12.014

[26] Scott, I.; Pomroy, W.E.; Kenyon, P.R.; Smith, G.; Adlington, B.; Moss, A. Lack of efficacy of monepantel against *Teladorsagia circumcincta* and *Trichostongylus colubriformis*. *Vet. Parasitol*. **2013**, 198, 166-171. doi: 10.1016/j.vetpar.2013.07.037

[27] McKellar, Q.A.; Jackson, F. Veterinary anthelmintics: old and new. *Trends Parasitol*. **2004**, 20(10), 456-461. doi: 10.1016/j.pt.2004.08.002

[28] Furgasa, W. Review on anthelmintic resistance against gastrointestinal nematodes of small ruminants: its status and future perspective in Ethiopia. *J. Vet. Sci. Anim. Husb*. **2018**, 6(4).

[29] Köhler, P. The biochemical basis of anthelmintic action and resistance. *Int. J. Parasitol.* **2001**, 31, 336-345. doi: 10.1016/S0020-7519(01)00131-X

neuronales del parásito, provocando, igualmente parálisis espástica y la subsiguiente muerte del parásito (Kaminsky, 2008)[30]. Las resistencias descritas para ambas familias están relacionadas con mutaciones en los genes que codifican sus receptores[27,28].

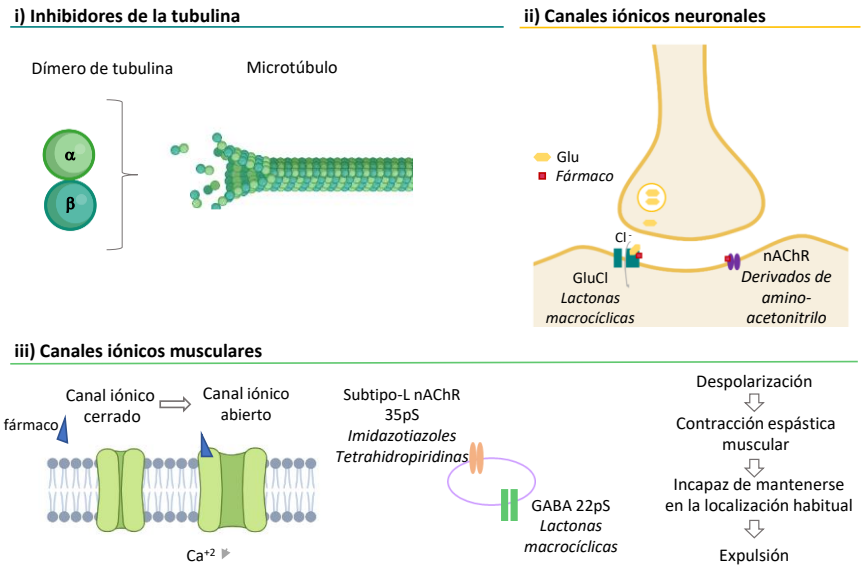

Figura I.3. Mecanismos de acción de los nematicidas comerciales. i) Subunidades α y β de la tubulina, inhibición de la polimerización de la tubulina; ii) Canales iónicos neuronales: GluCl y nAChR; iii) Canales iónicos musculares.[14]

Las **lactonas macrocíclicas** actúan fundamentalmente como agonistas selectivos de los canales de cloro activados por glutamato (GluCl) situados en las neuronas y músculos de la faringe de los nematodos (y artrópodos), pero no en humanos. Esto induce la apertura de los canales, provocando la hiperpolarización de la membrana celular. Así, se genera una parálisis flácida del músculo de la faringe, se interrumpe la ingestión, y se desencadena la muerte del parásito por la inanición. Adicionalmente, las avermectinas actúan como antagonistas del ácido 4-aminobutírico 22pS (GABA) y de los receptores nicotínicos expresados en las células musculares somáticas de los nematodos.[28,29] Las glicoproteínas-P están expresadas en altas concentraciones en las células intestinales y faríngeas, lugar de

[30] Kaminsky, R.; Ducray, P.; Jung, M.; Clover, R.; Rufener, L.; Bouvier, J.; Weber, S.S.; Wenger, A.; Wieland-Berghausen, S.; Goebel, T. A new class of anthelmintics effective against drug-resistant nematodes. *Nature*. **2008**, 452(7184), 176–180. doi: 10.1038/nature06722

acción de estos fármacos. Estas células aumentan la capacidad de eflujo de fármaco cambiando su distribución y provocando, por tanto, la inactividad del antihelmíntico.[31]

Tabla I.1. Mecanismos de resistencia y mutaciones de los fármacos nematicidas.

Fármacos	Mecanismo de resistencia
Benzimidazoles	Mutaciones en el gen que codifica la β-tubulina: F200Y (Fen→Ala), F167Y (Fen→Tyr), E198A (Glu→Ala)[32,33] y E198L (Glu→Leu)[34]
Imidazotiazoles	Mutaciones en los genes que codifican los receptores nAChR: *Cel-unc-29*, *Cel-unc-38*, *Cel-unc-64* y *Cel-acr-8* [35]
Lactonas macrocíclicas	Sobreexpresión de la glicoproteína-P por mutación en gen *Tc-Pgp-9*

Por todo lo acabado de exponer, es necesario y urgente encontrar nuevas alternativas terapéuticas para el tratamiento de las infecciones por NGIs.

I.1.2. ENFERMEDADES TRANSMITIDAS POR VECTORES

Las enfermedades transmitidas por vectores constituyen más del 17% de todas las EIs y producen más de 700.000 muertes anuales, afectando desproporcionadamente a las poblaciones más pobres de las regiones tropicales y subtropicales. Actualmente, y debido a diferentes factores, están apareciendo en zonas templadas y frías.[36] Debido a los escasos recursos de las regiones donde se encuentran, no han recibido la atención necesaria. Sin embargo, hoy en día por la influencia de la globalización, y la mejora en los métodos de

[31] Xu, M.; Molento, M.; Blackhall, W.; Ribeiro, P.; Beech, R.; Prichard, R. Ivermectin resistance in nematodes may be caused by alteration of P-glycoprotein homolog. *Mol. Biochem. Parasitol*. **1998**, 91(2), 327-335. doi: 10.1016/S0166-6851(97)00215-6

[32] Aguayo-Ortiz, R.; Méndez-Lucio, O; Romo-Mancillas, A.; Castillo, R.; Yépez-Mulia, L.; Medina-Franco, J.L.; Hernández-Campos, A. Molecular basis for benzimidazole resistance from a novel β-tubulin binding site model. *J. Mol. Graph. Model*. **2013**, 45, 26-37. doi: 10.1016/j.jmgm.2013.07.008

[33] Erez, M.S.; Kozan, E. Anthelmintic resistance in farm animals. *Kocatepe Vet. J.* **2018**, 11(3), 322-330. doi: 10.30607/kvj.429795

[34] Martínez-Valladares, M.; Valderas-García, E.; Gandasegui, J.; Skuce, P.; Morrison, A.; Castilla Gómez de Agüero, V.; Cambra-Pellejà, M.; Balaña-Fouce, R.; Rojo-Vázquez, F.A. *Teladorsagia circumcincta* beta tubulin: the presence of the E198L polymorphism on its own is associated with benzimidazole resistance. *Parasites Vectors*. **2020**, 13(1), 453. doi: 10.1186/s13071-020-04320-x

[35] Choi, Y.J.; Bisset, S.A.; Doyle, S.R.; Hallsworth-Pepin, K.; Martin, J.; Grant, W.N.; Mitreva, M. Genomic introgression mapping of field-derived multiple-anthelmintic resistance in *Teladorsagia circumcincta*. *PLoS Genet*. **2017**, 13(6), e1006857. doi: 10.1371/journal.pgen.1006857

[36] Fouque, F.; Reeder, J.C. Impact of past and on-going changes on climate and weather on vector-borne diseases transmission: a look at the evidence. *Infect. Dis. Poverty*. **2019**, 8, 51. doi: 10.1186/s40249-019-0565-1

diagnóstico y tratamiento comienzan a ver la luz. Dentro de estas enfermedades se encuentran la malaria, la leishmaniasis y la enfermedad de Chagas.[37]

1. Malaria

La malaria o paludismo es una enfermedad febril y potencialmente mortal causada por protozoos del género *Plasmodium* y que es transmitida por la picadura de mosquitos hembra infectados del género *Anopheles*.[38] Entre las enfermedades transmitidas por vectores, es la que mayor número de muertes causa. Según los datos de la OMS en el año 2021 hubo 247 millones de casos de paludismo causando 619.000 muertes. La región de África es la más afectada, concentrando en el año 2021 el 95% de los casos de paludismo y el 96% de las defunciones por esta enfermedad, correspondiendo el 80% a niños menores de los 5 años.[39]

Se conocen cinco especies de *Plasmodium* que afectan al ser humano, siendo *P. falciparum* la más frecuente y agresiva, seguido de *P. vivax*. La primera se encuentra fundamentalmente en el continente africano, mientras que la segunda se da principalmente en la región del sureste asiático y pacífico este y, región de América Latina.

El ciclo de vida se alterna entre el mosquito hembra y el hospedador vertebrado (Fig. I.4). Una vez los esporozoitos ingresan en el hospedador infectan los hepatocitos, donde se replican y liberan como merozoitos a la sangre. Los parásitos comienzan un ciclo sanguíneo se reproducen en el eritrocito, se liberan los merozoitos e infectan nuevamente otro eritrocito repitiéndose el proceso varias veces. Las formas sexuales, micro- y macrogametocitos, que se pueden desarrollar durante la etapa sanguínea son ingeridas en

[37] WHO, Enfermedades transmitidas por vectores. Disponible en: https://www.who.int/es/news-room/fact-sheets/detail/vector-borne-diseases. (Acceso 2 mayo 2023)
[38] Ashley, E.A.; Pyae Phyo, A.; Woodrow, C.J. Malaria. *The Lancet*, **2018**, 391(10130), 1608–1621. doi: 10.1016/s0140-6736(18)30324-6
[39] WHO, World Malaria Report. (2022). Disponible en: https://www.who.int/publications/i/item/9789240064898. (Acceso 2 mayo 2023)

la alimentación de un mosquito no infectado completando así, el ciclo.[40]

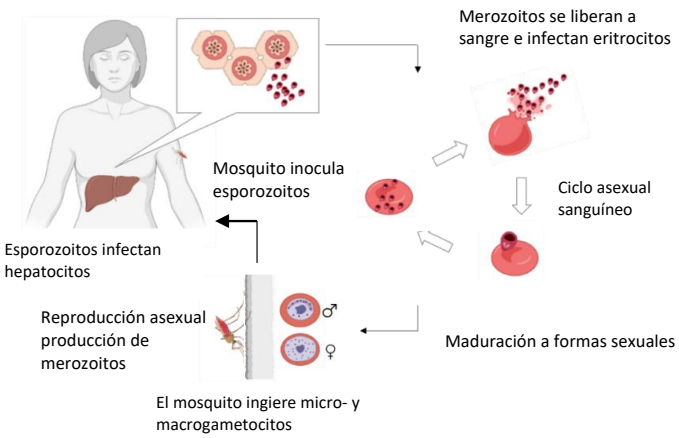

Figura I.4. Ciclo vital de *Plasmodium* spp.[14]

1.1. Fármacos actuales y limitaciones de uso

La malaria es una enfermedad prevenible y curable. Desde el año 2021 la OMS recomienda el uso de la vacuna RTS,S/AS01 (Mosquirix™) en niños que viven en regiones con transmisión de moderada a alta de *P. falciparum*.[41]

La **quinina***, compuesto aislado de los árboles del género *Cinchona* constituyó el primer fármaco clínicamente útil para el tratamiento de la malaria. Posteriormente, se desarrollaron varios análogos de síntesis, entre los que se encuentra la **cloroquina**. En la década de 1960, emergieron las primeras resistencias a este fármaco, y se sintetizaron nuevos análogos como la **amodiaquina**, los arilaminoalcoholes, **mefloquina**, halofantrina y **lumefantrina**, y más recientemente la **piperaquina**, entre otros. Estos fármacos actúan en procesos como la degradación de la hemoglobina e inhiben la formación de cristales de hemozoína. Sin embargo, a finales de 1980, se encontraron resistencias a estos nuevos fármacos. Las resistencias a la cloroquina y amodiaquina están estrechamente ligadas a las

*en negrita compuestos para los que se indica su estructura

[40] CDC, Malaria - biology. Disponible en: https://www.cdc.gov/malaria/about/biology/index.html. (Acceso 2 mayo 2023)

[41] Olotu, A.; Fegan, G.; Wambua, J.; Nyangweso, G.; Leach, A.; Lievens, M.; Kaslow, D.C.; Njuguna, P.; Marsh, K.; Bejon, P. Seven-year efficacy of RTS,S/AS01 Malaria vaccine among young african children. *N. Engl. J. Med*. **2016**, 374, 2519-2529. doi: 10.1056/NEJMoa1515257

mutaciones de los transportadores de membrana *Pf*CRT y *Pf*MDR-1.[42] En la Fig. I.5 se muestran las estructuras de algunos fármacos antipalúdicos.

La **sulfadoxina**, **pirimetamina** y el **proguanil** bloquean la síntesis de folatos, el primer fármaco por la inhibición de la enzima dihidropteroato sintasa (DHPS) y los dos últimos por inhibición de la dihidrofolato reductasa (DHFR). En los años 60 se detectaron las primeras resistencias a sulfadoxina y pirimetamina, que están asociadas a los genes *dhps* y *dhfr*.[43] En el caso de proguanil, se detectó la primera resistencia en la década de los años 40 y está asociada a mutaciones en la enzima DHFR.[44]

El descubrimiento de la **artemisinina**, compuesto natural aislado de *Artemisia annua* en 1972 por Tu Youyou constituyó una excelente alternativa para el tratamiento de la malaria[45]. Se obtuvieron análogos de semisíntesis químicamente más estables como **artemeter** o **arteeter**. La artemisinina y sus derivados presentan varios mecanismos de acción a nivel de la vacuola, retículo sarcoplasmático y membrana mitocondrial, produciendo la liberación de radicales libres.[46] La artemisinina y sus derivados se usan en **terapias combinadas (ACT)** con el fin de lograr una rápida y completa eliminación de los parásitos y evitar las manifestaciones graves de la enfermedad. Existen diferentes opciones: artemeter-lumefantrina, artesunato-amodiaquina, artesunato-mefloquina, artesunato-sulfadoxina-pirimetamina y dihidroartemisinina-piperaquina. Recientemente se ha añadido una sexta ACT, artesunato-pironaridina.[47] En el año 2008 se encontraron los primeros casos de resistencia a artemisinina en la frontera entre Camboya y Tailandia, extendiéndose en la actualidad a otras regiones. La principal resistencia está ligada a las mutaciones Y493H, R539T, I543T y C580Y en la proteína Kelch13, la cual es importante para la supervivencia del parásito.[48]

---

[42] Wicht, K.; Mok, S.; Fidock, D.A. Molecular mechanisms of drug resistance in *Plasmodium falciparum* malaria. *Annu. Rev. Microbiol.* **2020**, 74, 431–454. doi: 10.1146/annurev-micro-020518-115546

[43] Wongsrichanalai, C.; Pickard, A.L.; Wernsdorfer, W.H.; Meshnick, S.R. Epidemiology of drug-resistant malaria. *Lancet Infect. Dis*. **2002**, 2(4), 209-218. doi: 10.1016/S1473-3099(02)00239-6

[44] Le Bras, J.; Durand, R. The mechanism of resistance to antimalarial drugs in *Plasmodium falciparum*. *Fundam. Clin Pharmacol*. **2003**, 17(2), 147-153. doi: 10.1046/j.1472-8206.2003.00164.x

[45] Tu, Y. The discovery of artemisinin (qinghaosu) and gifts from Chinese medicine. *Nat. Med.* **2011**, 17, 1217–1220. doi: 10.1038/nm.2471

[46] Kumar Rai, S.; Apoorva; Kumar Rai, K.; Pandey-Rai, S. New perspectives of the *Artemisia annua* bioactive compounds as an affordable cure in treatment of malaria and cancer. En *Natural Bioactive Compounds: Technological Advancements,* 1ª edición; Sinha, R.; Häder, D.P., Eds; Elsevier: Países Bajos, 2021; pp 229-315. doi: 10.1016/B978-0-12-820655-3.00015-X

[47] WHO, Guidelines for malaria. Disponible en: https://www.who.int/publications/i/item/guidelines-for-malaria. (Acceso 2 mayo 2023)

[48] Menard, D.; Dondorp, A. Antimalarial drug resistance: a threat to malaria elimination. *Cold Spring Harb. Perspect. Med.* **2017**, 7(7), a025619. doi: 10.1101/cshperspect.a025619

La **atovaquona** descubierta en 1992 actúa a nivel de la cadena de transporte de electrones en la mitocondria del parásito. En 1996 se encontraron las primeras resistencias asociadas a mutaciones en el citocromo b (CYT b), que forma el complejo CYT bc_1 de la cadena de transporte de electrones que inhibe este fármaco.[49] La atovaquona en combinación con proguanil (Malarone®) muestran sinergia, y el uso de ambos fármacos combinados retrasa el desarrollo de resistencias. Sin embargo, su alto coste hace que no sea posible su uso extendido en África.[43]

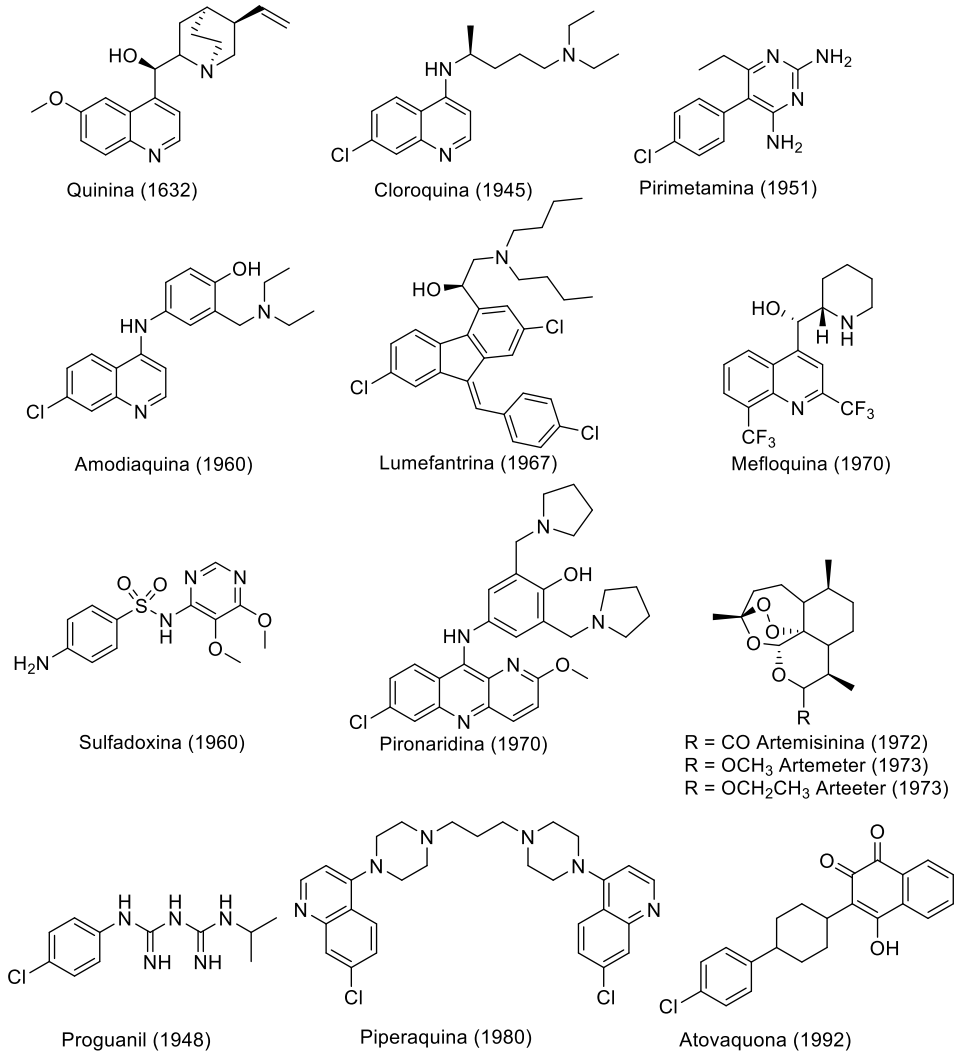

Figura I.5. Estructuras de algunos fármacos antipalúdicos.

[49] Korsinczky, M.; Chen, N.; Kotecka, B.; Saul, A.; Rieckmann, K.; Cheng, Q. Mutations in *Plasmodium falciparum* cytochrome b that are associated with atovaquone resistance are located at a putative drug-binding site. *Antimicrob. Agents Chemother.* **2000**, 44(8), 2100-2108. doi: 10.1128/AAC.44.8.2100-2108.2000

2. Leishmaniasis

Bajo el término leishmaniasis se engloba un grupo de enfermedades causadas por protozoos del género *Leishmania*, que afecta a las poblaciones más pobres del planeta (unos 99 países) y se extienden desde Asia, África, Medio Oriente a América Central y del Sur, [50] y se incluye dentro de las Enfermedades Tropicales Olvidadas (NTD, por sus siglas en inglés, *Neglected Tropical Diseases*).[51] Se conocen más de veinte especies que pueden infectar al humano y, dependiendo de las manifestaciones clínicas, se clasifican en tres categorías: leishmaniasis cutánea, leishmaniasis mucocutánea y leishmaniasis visceral. *Leishmania donovani* es una de las especies causantes de leishmaniasis visceral y está considerada la más agresiva.

Según la OMS se estima que entre 700.000 y 1 millón de personas se infectan anualmente, y en el caso de la leishmaniasis visceral causa la muerte en el 95% de los casos si no se trata a tiempo. En la actualidad continúa siendo un reto importante para la salud pública, ya que, según la OMS es una de las parasitosis con más capacidad de generar brotes y producir la muerte.[52] En la leishmaniasis visceral, los parásitos afectan a los órganos internos principales, como el bazo y el hígado, y al sistema linfático.[53]

Las leishmanias se transmiten por la picadura de flebótomos hembra infectados, que inoculan los promastigotes a través de la piel. Posteriormente, son fagocitados por los macrófagos transformándose en amastigotes. Estos se multiplican en los macrófagos de diferentes tejidos y, después, el flebótomo los ingiere al alimentarse. Dentro del vector, los amastigotes se transforman nuevamente en promastigotes, cerrando así el ciclo (Fig. I.6).[54]

[50] Mann, S.; Frasca, K.; Scherrer, S.; Henao-Martínez, A.; Newman, S.; Ramanan, P.; Suarez, J.A. A Review of leishmaniasis: Current knowledge and future directions. *Curr. Trop. Med. Rep*. **2021**, 8, 121–132. doi: 10.1007/s40475-021-00232-7

[51] WHO, Neglected Tropical Diseases. Disponible en: https://www.who.int/health-topics/neglected-tropical-diseases#tab=tab_1. (Acceso 2 mayo 2023)

[52] WHO, Leishmaniasis. Disponible en: https://www.who.int/news-room/fact-sheets/detail/leishmaniasis. (Acceso 2 mayo 2023)

[53] CDC, Leishmaniasis - disease. Disponible en: https://www.cdc.gov/parasites/leishmaniasis/disease.html. (Acceso 2 mayo 2023)

[54] CDC, Leishmaniasis - biology. Disponible en: https://www.cdc.gov/parasites/leishmaniasis/biology.html. (Acceso 2 mayo 2023)

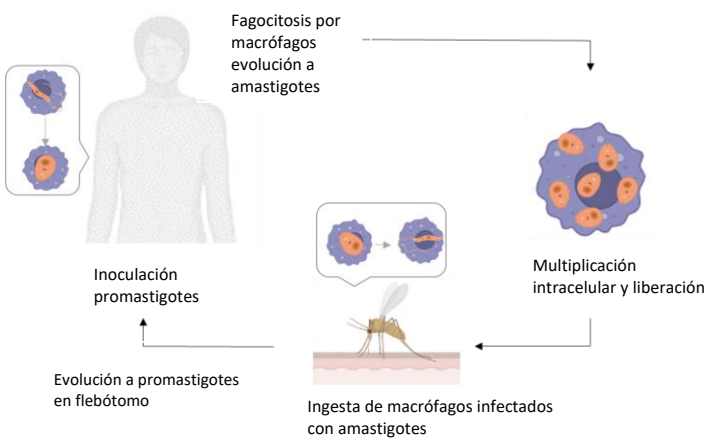

Figura I.6. Ciclo de vida de *Leishmania* spp.[14]

2.1. Fármacos actuales y limitaciones de uso

Los fármacos de primera elección para el tratamiento de la leishmaniasis son muy antiguos y tóxicos, en la Fig. I.7 se muestran las estructuras de los fármacos disponibles. Los **antimoniales pentavalentes**, estibogluconato de sodio y antimoniato de meglumina, son los fármacos de primera línea. Se administran vía intravenosa, en lesiones o en músculos, y actúan por inhibición de la glicólisis y oxidación de los ácidos grasos, sin embargo, el desarrollo de resistencias ha limitado su uso. Se han encontrado diferentes mecanismos de resistencia asociados a los antimoniales, como la disminución de la reducción de Sb(V) a Sb(III), el eflujo de tioles y Sb(III) a través de bombas de transporte ABC, vesículas enriquecidas con MRPA (por sus siglas en inglés, *multidrug resistance-associated protein A*) o el aumento del potencial redox de tioles. Además, en el subcontinente indio se ha encontrado disminución de sensibilidad de las acuaporinas AQP1 en *L. donovani*, encargadas de transportar metaloides trivalentes.[55]

La anfotericina B liposomal y la pentamidina son fármacos de segunda elección. La **anfotericina B**, descubierta inicialmente por sus propiedades antifúngicas, muestra actividad leishmanicida que, por unión al ergosterol de la membrana citoplasmática de los parásitos, modifica la permeabilidad selectiva de K^+ y Mg^{2+}. Para evitar la toxicidad aguda

[55] Sundar, S.; Chakravarty, J.; Meena, L.P. Leishmaniasis: treatment, drug resistance and emerging therapies. *Expert Opin. Orphan Drugs.* **2018**, 7(1), 1-10. doi: 10.1080/21678707.2019.1552853

producida por el fármaco y mejorar su biodisponibilidad se han desarrollado formas liposomales, de costo más elevado lo que limita su uso. Por otro lado, la **pentamidina**, es una diamidina aromática que interfiere con la síntesis de ADN y modifica la morfología del kinetoplasto, disminuyendo el potencial de membrana mitocondrial por acumulación en la mitocondria. La resistencia a pentamidina se basa en la modificación de la secuencia de ADNk, el eflujo de fármaco y la disminución de la captación mitocondrial, esto unido a su elevada toxicidad ha llevado al cese de su uso.

La **miltefosina**, actúa sobre la biosíntesis de fosfolípidos y el metabolismo de alquil-lípidos, por acumulación intracelular en el parásito. Su administración oral constituye una ventaja. Sin embargo, es teratogénica y podría generar resistencias por su larga duración en el organismo. El principal mecanismo de resistencia es la disminución en la introducción del fármaco en el parásito y su eflujo.[55]

Por último, la **paromomicina** es un antibiótico aminoglucósido aislado por fermentación de *Streptomyces rimosus*, y aunque su mecanismo de acción no está del todo establecido, hay estudios que demuestran su implicación en la inhibición de la biosíntesis de proteínas. La duración del tratamiento es corta, no obstante, se le atribuyen varios efectos adversos y existe cierta variación en su efectividad dependiendo del área geográfica, lo que aumenta el desarrollo de resistencias.[56,57,58] Debido a su escaso uso, ha desarrollado pocas resistencias, entre las que se encuentran la disminución de captación del fármaco, la disminución en la síntesis de proteínas mitocondriales y citoplasmáticas, y la reducción de la acumulación de fármaco asociada a la reducción de la unión inicial a la superficie celular.[55]

[56] Ghorbani, M.; Farhoudi, R. Leishmaniasis in humans: drug or vaccine therapy? *Drug Des. Devel. Ther*. **2018**, 12, 25–40. doi: 10.2147/DDDT.S146521

[57] Matos, A.P.S.; Viçosa, A.L.; Ré, M.I.; Ricci-Júnior, E.; Holandino, C. A review of current treatments strategies based on paromomycin for leishmaniasis. *J. Drug Deliv. Sci. Technol*. **2020**, 57, 101664. doi: 10.1016/j.jddst.2020.101664

[58] Pradhan, S.; Schwartz, R.A.; Grabbe, S.; Goldust, M. Treatment options for leishmaniasis. Clin. Exp. Dermatol. **2021**, 47, 3, 516-521. doi: 10.1111/ced.14919

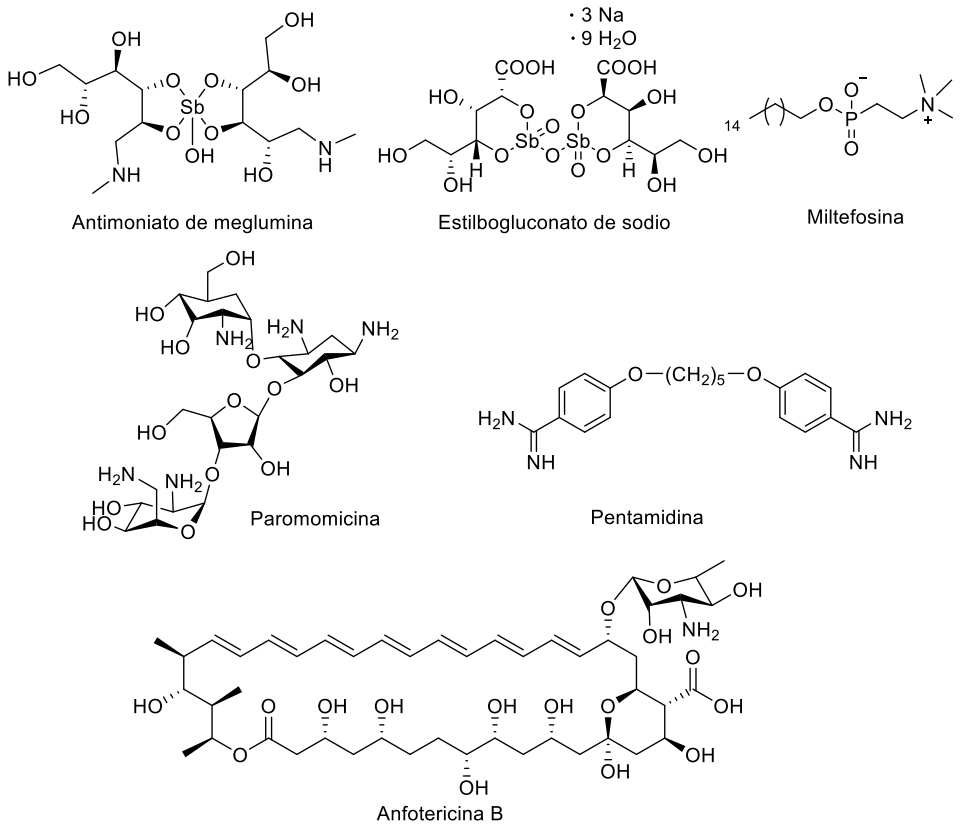

Figura I.7. Estructuras de los fármacos de primera y segunda línea para el tratamiento por infección de *Leishmania* spp.

3. Chagas

La enfermedad de Chagas o tripanosomiasis americana está englobada también dentro de las NTDs.[51] Es causada por el protozoo flagelado *Trypanosoma cruzi*, y se transmite, mayormente, a través de las heces de triatominos, aunque también existen otras vías de contagio como transfusiones de sangre, trasplantes de órganos, o la transmisión congénita, que hacen que la enfermedad se expanda fuera de su territorio.[59]

La enfermedad es endémica en 21 países de América, desde el sur de Estados Unidos hasta el norte de Chile y Argentina.[59,60] Se estima que hay entre 6 y 7 millones de personas

[59] WHO, Chagas Disease. Disponible en: https://www.who.int/news-room/fact-sheets/detail/chagas-disease-(american-trypanosomiasis). (Acceso 2 mayo 2023)

[60] Pérez-Molina, J.A.; Molina, I. Chagas disease. *Lancet.* **2018**, 391, 82-94. doi: 10.1016/S0140-6736(17)31612-4

infectadas en el mundo, 75 millones están en riesgo de contraer la infección y produce unas 12.000 muertes anuales, lo que genera un problema significativo de salud pública en América Latina.[59] Además, en los últimos años a causa de la movilidad de las poblaciones entre América Latina y el resto del mundo, el número de casos diagnosticados en Estados Unidos y Europa ha ido aumentando.[59,61]

Durante la ingesta de sangre, el triatomino muerde al huésped mamífero y libera los tripomastigotes con las heces cerca de la mordedura. Los parásitos penetran a través de la herida o de la mucosa, y en el huésped, invaden las células próximas al lugar de inoculación, diferenciándose en amastigotes intracelulares. Estos se multiplican por fisión binaria y se diferencian en tripomastigotes, que son liberados al torrente sanguíneo infectando las células de diferentes tejidos comportándose como nuevos focos de infección. El triatomino se infecta por ingestión de tripomastigotes en la sangre de un hospedador infectado cerrando así el ciclo (Fig. I.8).[62]

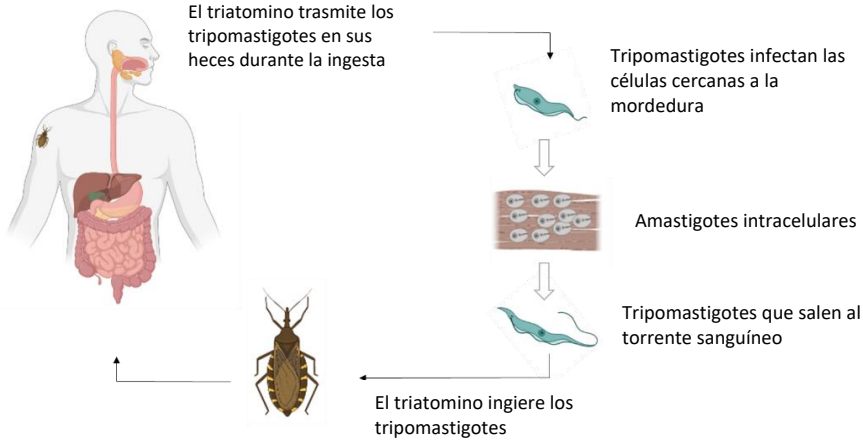

Figura I.8. Ciclo vital de *Trypanosoma cruzi*.[14]

La enfermedad cursa con fiebre, tos, lesiones cutáneas ligadas a la mordedura, dolor abdominal o cefalea. Sin embargo, también puede cursar de forma asintomática y, en el 70% de los casos no se manifiesta a lo largo de la vida del individuo. El 30% de los pacientes entran

[61] Pinazo, M.J.; Gascon, J. The importance of the multidisciplinary approach to deal with the new epidemiological scenario of Chagas disease (global health). *Acta Trop.* **2015**, 151, 16-20. doi: 10.1016/j.actatropica.2015.06.013
[62] CDC, American Trypanosomiasis - biology. Disponible en: https://www.cdc.gov/dpdx/trypanosomiasisamerican/index.html. (Acceso 2 mayo 2023)

en la etapa crónica de la enfermedad desarrollando signos irreversibles en el sistema nervioso, digestivo, sistema inmune, y mayormente el cardíaco.[63]

3.1. Fármacos actuales y limitaciones de uso

La cura del Chagas es posible en la primera etapa de la enfermedad con los dos fármacos disponibles: **nifurtimox** (Lampit®) comercializado en 1965 y el **benznidazol** (Rochagan®, Radanil®), seis años después (Fig. I.9).[64] Ambos son compuestos de tipo heterocíclico nitroaromático que actúan por la reducción del grupo nitro a amino mediado por las nitroreductasas (NTR), generando radicales libres y/o metabolitos electrofílicos. En el caso de nifurtimox se produce un superóxido altamente tóxico, mientras que en el caso del benznidazol los compuestos intermedios reducidos actúan formando enlaces covalentes con biomacromoléculas tales como lípidos, proteínas o el ADN, modificándolos y dañándolos.[65] Sin embargo, hay algunos autores que no aceptan esta hipótesis.

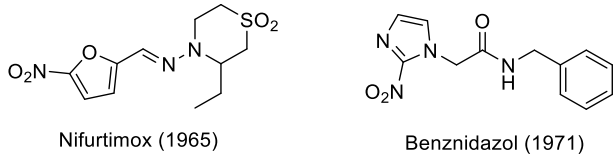

Nifurtimox (1965) Benznidazol (1971)

Figura I.9. Estructuras de los fármacos de referencia para el tratamiento de *T. cruzi.*

Los dos compuestos muestran una elevada toxicidad y baja eficacia en algunos casos.[60] Entre los efectos adversos del nifurtimox están la hipersensibilidad, anorexia, vómitos, polineuritis y depresión, por lo que está en desuso en muchos países de Centro- y Sudamérica. Por lo tanto, el fármaco más utilizado es el benznidazol, aunque sus efectos secundarios como la hepatitis, polineuropatía periférica, y la intolerancia digestiva y anorexia limitan su uso.[66] La utilidad de ambos se limita a la fase temprana de la infección y

[63] Echeverria, L.E.; Morillo, Carlos A. American Trypanosomiasis (Chagas Disease). *Infect. Dis. Clin. North Am.* **2019**, 33(1), 119–134. doi: 10.1016/j.idc.2018.10.015

[64] Lascano, F.; García Bournissen, F.; Altcheh, J. Review of pharmacological options for the treatment of Chagas disease. *Br. J. Clin. Pharmacol.* **2020**, 88(2), 383-402. doi: 10.1111/bcp.14700

[65] Maya, J.D.; Cassels, B.K.; Iturriaga-Vásquez, P.; Ferreira, J.; Faúndez, M.; Galanti, N.; Ferreira, A.; Morello, A. (2007). Mode of action of natural and synthetic drugs against *Trypanosoma cruzi* and their interaction with mammalian host. *Comp. Biochem. Physiol.* **2007**, 146(4), 601-620. doi: 10.1016/j.cbpa.2006.03.004

[66] Mansoldo, F.R.P.; Carta, F.; Angeli, A., da Silva Cardoso, V.; Supuran, C.T.; Vermelho, A.B. Chagas Disease: Perspectives on the past and present and challenges in drug discovery. *Molecules*. **2020**, 25(22), 5483. doi: 10.3390/molecules25225483

no está indicado en mujeres embarazadas, niños, ni en pacientes con insuficiencia renal o hepática, de la misma manera que en personas con afecciones neurológicas o psiquiátricas.[59] Además, el tratamiento es muy prolongado (60-90 días).

No se han descrito resistencias relevantes asociadas a estos fármacos. Sin embargo, hay estudios que explican un posible desarrollo de resistencias cruzadas debido a que ambos se activan a través de la NTR tipo I. Una mutación en el gen que codifica para esta proteína podría ser la causa de la resistencia cruzada.[67]

En este apartado se han revisado de manera breve y concisa los ciclos infectivos de las enfermedades (malaria, leishmaniasis y Chagas), los fármacos disponibles en el arsenal terapéutico, así como su mecanismo de acción y desarrollo de resistencias. El número de moléculas disponibles para malaria dista considerablemente de las otras dos enfermedades. De manera general, se puede decir que son compuestos bastante tóxicos, que han desarrollado resistencias rápidamente y en algunos casos tienen un precio elevado, en la Tabla I.2 se muestra un resumen de ellos. Por todo lo expuesto queda patente que es necesario el desarrollo y hallazgo de nuevas alternativas terapéuticas.

Tabla I.2. Enfermedades protozoarias transmitidas por vectores. Fármacos disponibles y sus limitaciones.

Enfermedad	Fármaco	Limitaciones
Malaria	Quinina y derivados Pirimetamina Amodiaquina Mefloquina Halofantrina ACT	Resistencias emergentes
Leishmaniasis	Antimoniales pentavalentes	Administración, resistencias emergentes
	Anfotericina B	Costo, toxicidad, resistencias emergentes
	Pentamidina Paromomicina	Toxicidad y resistencias emergentes
	Miltefosina	Teratogénica y resistencias emergentes
Chagas	Nifurtimox	Efectos secundarios gastrointestinales y del sistema nervioso central, activo en fase aguda
	Benznidazol	Inusuales, pero efectos secundarios severos, resistencias emergentes, activo en fase aguda

[67] Wilkinson, S.R.; Taylor, M.C.; Horn, D.; Kelly, J.M.; Cheeseman, I. A mechanism for cross-resistance to nifurtimoxand benznidazole in trypanosomes. *Proc. Natl. Acad. Sci. U.S.A.* **2008**, 105(13), 5022-5027. doi: 10.1073/pnas.0711014105

I.2. COMPUESTOS HETEROCÍCLICOS NITROGENADOS

Los compuestos heterocíclicos constituyen la base de numerosos compuestos bioactivos que se encuentran en nuestro entorno, como son los ácidos nucleicos, los aminoácidos, las vitaminas, los precursores de coenzimas, entre otros. Además, presentan una amplia variedad estructural, tienen aplicaciones muy diversas y juegan un papel notable en Química Médica. Dentro de ellos, están los compuestos que contienen nitrógeno.

El núcleo heterocíclico nitrogenado es una estructura química rica en electrones capaz de aceptar o donar electrones, lo que, además, permite la formación de enlaces intermoleculares por puentes de hidrógeno, interacción dipolo-dipolo, efecto hidrofóbico, fuerzas van der Waals e interacciones de apilamiento π, y que puedan unirse a diferentes dianas con alta afinidad, constituyendo, así, un significativo punto de partida en la obtención de agentes terapéuticos. De hecho, más del 75% de los fármacos aprobados por la FDA y que están disponibles en el mercado muestran esqueleto de heterociclo nitrogenado.[68]

En este trabajo hemos seleccionado los núcleos de ftalazinona y benzimidazol como potenciales agentes terapéuticos, con propiedades nematicidas (*T. circumcincta*) y/o antiprotozoarias (malaria, leishmaniosis, Chagas), debido a la experiencia del grupo de investigación en el que se ha desarrollado este Trabajo de Tesis en la obtención de estos compuestos.

I.2.1. FTALAZINONAS

El núcleo de ftalazinona está formado por dos anillos de seis eslabones unidos entre sí que contienen dos nitrógenos en posiciones 2 y 3 y un carbonilo en posición 1. En disolución suele estar en equilibrio con la forma lactima, aunque predomina la forma lactámica (cetona) (Fig. I.10).[69]

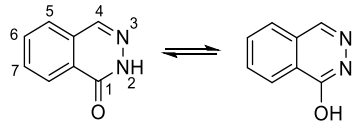

Figura I.10. Tautomería de ftalazinona.

[68] Kerru, N.; Gummidi, L.; Maddila, S.; Gangu, K.K.; Jonnalagadda, S.B. A review on recent advances in nitrogen-containing molecules and their biological applications. *Molecules*. **2020**, 25, 1909. doi: 10.3390/molecules25081909
[69] Vila, N.; Besada, P.; Costas, T.; Costas-Lago, M.C.; Terán, C. Phthalazin-1(2*H*)-one as a remarkable scaffold in drug discovery. *Eur. J. Med. Chem*. **2015**, 97, 462-482. doi: 10.1016/j.ejmech.2014.11.043

Las modificaciones del núcleo de ftalazinona han dado lugar a compuestos muy variados y con actividades farmacológicas muy diferentes. Muchos de los fármacos presentes en el arsenal terapéutico presentan un núcleo de ftalazinona, como la **azelastina** y **flezelastina** con actividad antihistamínica, **ponalrestat** inhibidor de la aldosa reductasa con actividad antidiabética, su análogo **zopolrestat** que muestra adicionalmente un fragmento de benzotiazol sobre el nitrógeno amídico, o el **olaparib**, inhibidor de las proteínas PARP para el tratamiento del cáncer de ovario avanzado, incluso en pacientes con mutaciones en los genes BRCA1 y/o BRCA2 (Fig. I.11).[70]

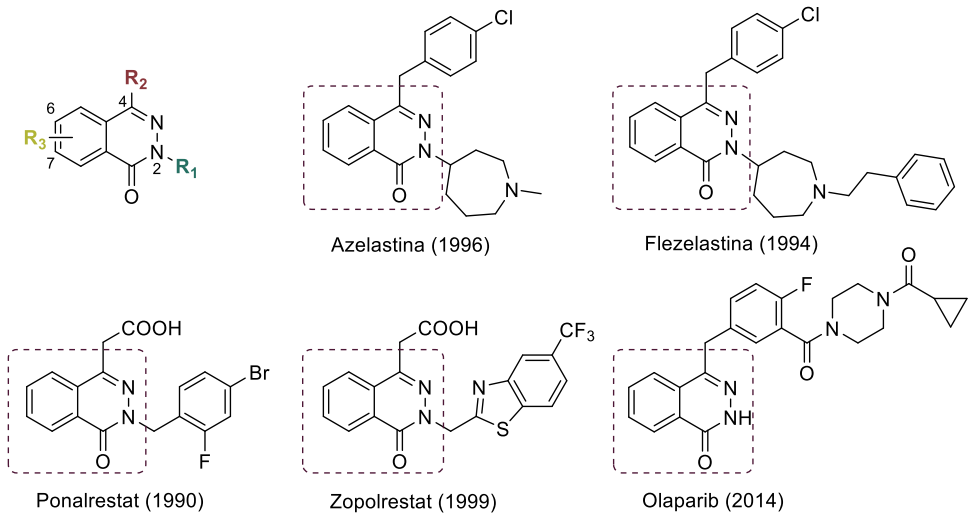

Figura I.11. Estructuras de algunos fármacos con esqueleto de ftalazinona.

[70] Terán, C.; Besada, P.; Vila, N.; Costas-Lago, M.C. Recent advances in the synthesis of phthalazin-1(2*H*)-one core as a relevant pharmacophore in medicinal chemistry. *Eur. J. Med. Chem.*, **2019**, 161, 468-478. doi: 10.1016/j.ejmech.2018.10.047

Además, en la bibliografía se pueden encontrar otro tipo de aplicaciones para estos compuestos como la antihipertensiva,[71,72] antiasmática,[73] vasorelajante,[74,75] antitumoral,[76,77,78] o la antituberculosa[79].

En relación con la actividad antiparasitaria de ftalazinonas y análogos, del Olmo y *col.* en el año 2003[80] obtuvieron compuestos con este núcleo que fueron evaluados frente a *P. falciparum*, obteniendo valores de CI_{50} de 3,6 y 3,8 µM. Estos mismos compuestos habían sido evaluados frente a *L. braziliensis*, *L. amazonensis* y *L. donovani* en el año 2001[81] por el mismo grupo de investigación, no encontrando actividad leishmanicida. Sijm y *col.* (2019)[82] obtuvieron análogos de hexahidroftalazinonas que mostraron actividad frente a *L. infantum* en rango micromolar. En el año 2021, De Araújo y *col*.[83] evaluaron la actividad frente a amastigotes intracelulares de *L. amazonensis* y *L. infatum* de un compuesto con núcleo de

[71] Demirayak, S.; Karaburun, A.C.; Beis, R. Some pyrrole substituted aryl pyridazinone and phthalazinone derivatives and their antihypertensive activities. *Eur. J. Med. Chem*. **2005**, 39(12), 1089-1095. doi: 10.1016/j.ejmech.2004.09.005

[72] Cherkez, S.; Herzig, J.; Yellin, H. Synthesis, saludiuretic, and antihypertensive activity of 6,7-disubstituted 1(2*H*)- and 3,4-dihydro-1(2*H*)-phthalazinones. *J. Med. Chem*. **1986**, 29(6), 947–959. doi: 10.1021/jm00156a011

[73] Yamaguchi, M.; Kamei, K.; Koga, T.; Akima, M.; Kuroki, T.; Ohi, N. (1993). Novel antiasthmatic agents with dual activities of thromboxane A2 synthetase inhibition and bronchodilation. 1. 2-[2-(1-Imidazolyl)alkyl]-1(2*H*)-phthalazinones. *J. Med. Chem.* **1993**, 36(25), 4052–4060. doi: 10.1021/jm00077a008

[74] del Olmo, E.; Barboza, B.; Ybarra, M.I.; López-Pérez, J.L.; Carrón, R.; Sevilla, M.A.; Boselli, C.; San Feliciano, A. Vasorelaxant activity of phthalazinones and related compounds. *Bioorg. Med. Chem. Lett*. **2006**, 16(10), 2786–2790. doi: 10.1016/j.bmcl.2006.02.003

[75] Munín, J.; Quezada, E.; Viña, D.; Uriarte, E.; Delogu, G.L.; Gil-Longo, J. Discovery of new phthalazinones as vasodilator agents and novel pharmacological tools to study calcium channels. *Future Med. Chem.* **2019**, 11(3), 179-191. doi: 10.4155/fmc-2018-0250

[76] Almahli, H.; Hadchity, E.; Jaballah, M.Y.; Daher, R.; Ghabbour, H.A.; Kabil, M.M.; Al-shakliah, N.S.; Eldehna, W.M. Development of novel synthesized phthalazinone-based PARP-1 inhibitors with apoptosis inducing mechanism in lung cancer. *Bioorg. Chem.* **2018**, 77, 443–456. doi: 10.1016/j.bioorg.2018.01.034

[77] Okunlola, F.O.; Olotu, F.A.; Soliman, M.E.S. Unveiling the mechanistic roles of chlorine substituted phthalazinone-based compounds containing chlorophenyl moiety towards the differential inhibition of poly (ADP-ribose) polymerase-1 in the treatment of lung cancer. *J. Biomol. Struct. Dyn*. **2021**, 10878-10886. doi: 10.1080/07391102.2021.1951354

[78] Singh, J.; Suryan, A.; Kumar, S.; Sharma, S. Phthalazinone scaffold: emerging tool in the development of target based novel anticancer agents. *Curr. Med. Chem. Anticancer Agents*. **2020**, 20(18), 2228-2245. doi: 10.2174/1871520620666200807220146

[79] Santoso, K.T, Cheung, C.Y.; Hards, K., Cook, G.M.; Stocker, B.L.; Timmer, M.S.M. Synthesis and investigation of phthalazinones as antitubercular agents. *Chem. Asian J.* **2019**, 14(8), 1278-1285. doi: 10.1002/asia.201801805

[80] del Olmo, E.; García Armas, M.; Ybarra, M.I.; López-Pérez, J.L.; Oporto, P.; Gimenez, A.; Deharo, E.; San Feliciano, A. The imidazo[2,1-*a*]isoindole system. A new skeletal basis for antiplasmodial compounds. *Bioorg. Med. Chem. Lett*. **2003**, 13(16), 2769-2772. doi: 10.1016/S0960-894X(03)00509-2

[81] del Olmo, E.; García Armas, M.; López-Pérez, J.L.; Muñoz, V.; Deharo, E.; San Feliciano, A. Leishmanicidal activity of some stilbenoids and related heterocyclic compounds. *Bioorg. Med. Chem. Lett*. **2001**, 11(16), 2123-2126. doi: 10.1016/S0960-894X(01)00387-0

[82] Sijm, M.; de Heuvel, E.; Matheeussen, A.; Caljon, G.; Maes, L.; Sterk, G.J.; de Esch, I.J.P.; Leurs, R. Identification of phenylphthalazinones as a new class of *Leishmania infantum* inhibitors. *ChemMedChem*, **2019**, 15(2), 219-227. doi: 10.1002/cmdc.201900538

[83] De Araújo, J.S.; Peres, R.B.; da Silva, P.B.; Batista, M.M.; Sterk, G.J.; Maes, L.; Caljon, G.; Leurs, R.; de Koning, H.P.; Kalejaiye, T.D.; Soeiro, M.N.C. Tetrahydrophthalazinone inhibitor of phosphodiesterase with in vitro activity against intracellular trypanosomatids. *Antimicrob. Agents Chemother.* **2021**, 65(3). doi: 10.1128/AAC.00960-20

tetrahidroftalazinona diseñado, sintetizado por Blaazer y *col*. (2018)[84] y evaluado que mostró una actividad leishmanicida moderada (<10 µM). En el año 2020, el mismo grupo obtuvo buenos resultados con derivados del mismo núcleo (CI_{50} 5,1 µM) frente a la cepa *Tc*Tulahuen, que además mostraron baja toxicidad (IS >39).[85] Adicionalmente, evaluaron la actividad del compuesto frente a diferentes formas de *T. cruzi*, encontrando una CE_{50} en el rango de 6,6 a 39,5 µM.[85]

Por otro lado, se han descrito actividades de diferentes ftalazinonas frente a otros protozoos como *Cryptosporidium parvum*[86] y *Trypanosoma brucei*[87,88,89].

No se ha encontrado información sobre actividad nematicida de ftalazinonas. En la Tabla I.3 se resume las ftalazinonas encontradas con propiedades antimalárica, leishmanicida y anti-Chagas.

Tabla I.3. Ftalazinonas con propiedades anti-*Plasmodium*, leishmanicidas o anti-Chagas.

Tipo de compuesto	Organismo	Relevancia	Referencia
***Plasmodium* spp**			
Ftalazinona y 2-metilftalazinona	*Pf*F32	CI_{50} 3,6 y 3,8 µM.	Del Olmo, 2003[80]
***Leishmania* spp.**			
Ftalazinona y 2-metilftalazinona		Inactivos.	Del Olmo, 2001[81]
Hexahidroftalazinona	*L. infantum*	$pCI_{50}{}^{a}$ 4-6. IS 0,05 a >31	Sijm, 2019[82]
Tetrahidroftalazinona	*L. amazonensis y L. infantum*	CE_{50} 14,9 y 12,5 µM, respectivamente.	De Araújo, 2021[83]
Trypanosoma cruzi			

[84] Blaazer, A.R.; Singh, A.K.; de Heuvel, E.; Edink, E.; Orrling, K.M.; Veerman, J.J.N.; van den Bergh, T.; Jansen, C.; Balasubramaniam, E.; Mooij, W.J.; Custers, H.; Sijm, M.; Tagoe, D.N.A.; Kalejaiye, T.D.; Munday, J.C.; Tenor, H.; Matheeussen, A.; Wijtmans, M.; Siderius, M.; de Graaf, C.; Maes, L.; de Koning, H.P.; Bailey, D.S.; Sterk, G.J.; de Esch, I.J.P.; Brown, D.G.; Leurs, R. Targeting a subpocket in *Trypanosoma brucei* phosphodiesterase B1 (*Tbr*PDEB1) enables the structure-based discovery of selective inhibitors with trypanocidal activity. *J. Med. Chem*. **2018**, 61(9), 3870–3888. doi: 10.1021/acs.jmedchem.7b01670

[85] De Araújo, J.S.; da Silva, P.B.; Batista, M.M.; Peres, R.B.; Cardoso-Santos, C.; Kalejaiye, T.D.; Munday, J.C.; De Heuvel, E.; Sterk, G.J.; Augustyns, K.; Salado, I.G.; Matheeussen, A.; De Esch, I.; De Koning, H.P.; Leurs, R.; Maes, L.; Correia Soeiro, M.N. Evaluation of phthalazinone phosphodiesterase inhibitors with improved activity and selectivity against *Trypanosoma cruzi*. *J. Antimicrob. Chemother.* **2020**, 75(4), 958–967. doi: 10.1093/jac/dkz516

[86] Johnson, C.R.; Gorla, S.K.; Kavitha, M.; Zhang, M.; Liu, X.; Striepen, B.; Mead, J.R.; Cuny, G.D.; Hedstrom, L. Phthalazinone inhibitors of inosine-5'-monophosphate dehydrogenase from *Cryptosporidium parvum*. *Bioorg. Med. Chem*. **2013**, 23(4), 1004-1007. doi: 10.1016/j.bmcl.2012.12.037

[87] De Koning, H.P.; Gould, M.K.; Sterk, G.J.; Tenor, H.; Kunz, S.; Luginbuehl, E.; Seebeck, T. Pharmacological validation of *Trypanosoma brucei* phosphodiesterases as novel drug targets. *J. Infect. Dis.* **2012**, 206, 229-237. doi: 10.1093/infdis/jir857

[88] Salado, I.G.; Singh, A.K.; Moreno-Cinos, C.; Sakaine, G.; Siderius, M.; van der Veken, P.; Matheeussen, A.; van der Meer, T.; Sadek, P.; Gul, S.; Maes, L.; Sterk, G.J.; Leurs, R.; Brown, D.; Augustyns, K. Lead optimization of phthalazinone phosphodiesterase inhibitors as novel antitrypanosomal compounds. *J. Med. Chem.* **2020**, 63(7), 3485-3507. doi: 10.1021/acs.jmedchem.9b00985

[89] De Heuvel, E.; Kooistra, A.J.; Edink, E.; van Klaveren, S.; Stuijt, J.; van der Meer, T.; Sadek, P.; Mabille, D.; Caljon, G.; Maes, L.; Siderius, M.; de Esch, I.J.P.; Sterk, G.J.; Leurs, R. discovery of diaryl ether substituted tetrahydrophthalazinones as TbrPDEB1 inhibitors following structure-based virtual screening. *Front. Chem.* **2021**, 8, 608030. doi: 10.3389/fchem.2020.608030

Tetrahidroftalazinona	*Tc*Tulahuen y *Tc*Y	CE_{50} 5,1 µM. IS >39. Inhibidores de la enzima fosfodiesterasa.	De Araújo, 2020[85]
	*Tc*Tulahuen y *Tc*Y	CE_{50} 9,7, 6,6 y 39,5 µM. IS <20. Inhibidores de la enzima fosfodiesterasa.	De Araújo, 2021[83]

[a] pCI_{50}: logaritmo negativo de CI_{50} en molar

I.2.2. BENZIMIDAZOLES

El núcleo de benzimidazol, conocido también como 1*H*-benzimidazol o 1,3-benzodiazol, está formado por un anillo de benceno fusionado con un anillo de imidazol, y se encuentra en un gran número de compuestos con elevado interés farmacológico.[90,91] La presencia en su estructura de un protón sobre el nitrógeno imidazólico en posición 1, produce una tautomería imina-enamina (Fig. I.12) que da lugar a compuestos que interaccionan de manera diferente con su diana y que desde el punto de vista de su obtención conlleva aproximaciones químicas diferentes.[92]

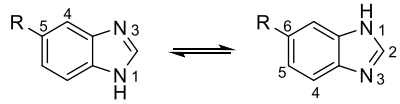

Figura I.12. Equilibrio tautomérico en benzimidazoles.

Sustituciones en las posiciones C-5(6) y C-4(7) sobre el anillo bencénico o en N-1 y C-2 del imidazol, le confieren actividades muy distintas. Así, se dispone de fármacos con estructura de Bz, como el **candesartán** (antihipertensivo), **omeprazol** (inhibidor de la bomba de protón-ATP), **bendamustina** (anticanceroso), **bilastina** (antihistamínico), mebendazol (antihelmíntico) o **benomilo** (fungicida), entre otros (Fig. I.13).[93]

[90] Barot, K.P.; Nikolova, S.; Ivanov I.; Ghate, M.D. Novel research strategies of benzimidazole derivatives: a review. *Mini Rev. Med. Chem.* **2013**, 13(10), 1421-47. doi: 10.2174/13895575113139990072

[91] Alaqeel, S.I. Synthetic approaches to benzimidazoles from o-phenylenediamine: A literature review. *J. Saudi Chem. Soc.* **2017**, 21, 229–237. doi: 10.1016/j.jscs.2016.08.001

[92] Claramunt, R.M.; López, C.; Santa María, M.D.; Sanz, D.; Elguero, J. The use of NMR spectroscopy to study tautomerism. *Prog. Nucl. Magn. Reason. Spectrosc.* **2006**, 49, 169–206. doi: 10.1016/j.pnmrs.2006.07.001

[93] Gaba, M.; Mohan, C. Development of drugs based on imidazole and benzimidazole bioactive heterocycles: recent advances and future directions. *Med. Chem. Res*. **2016**, 25, 173–210. doi: 10.1007/s00044-015-1495-5

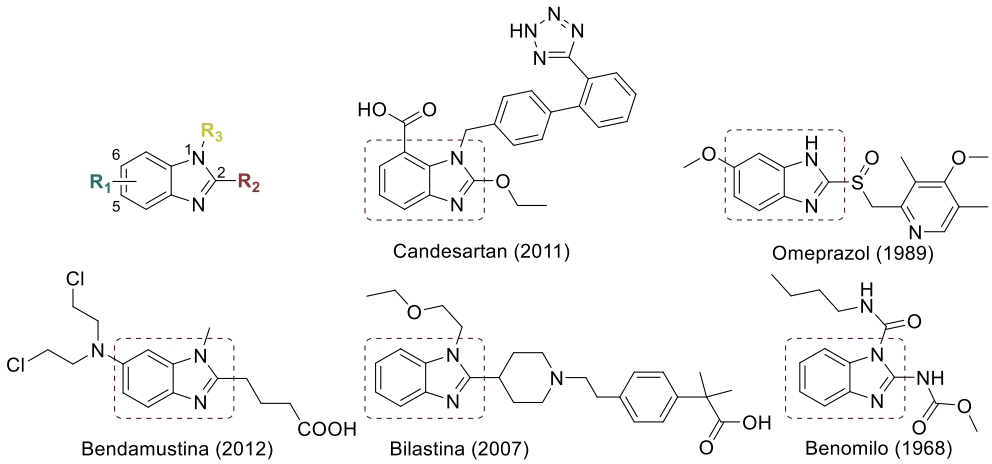

Figura. I.13. Fármacos comerciales con núcleo benzimidazólico.

El interés por este núcleo se remonta a los años 1940, cuando se especuló que podría interaccionar de manera semejante a las purinas, desencadenando determinadas respuestas biológicas. Las primeras investigaciones en este sentido fueron llevadas a cabo por Woolley en 1944[94]. Posteriormente, Brink *et al.* en 1949[95] y Emerron *et al.* en 1950[96] exploraron el núcleo de Bz y derivados, encontrando que el Bz es un producto de degradación de la vitamina B_{12}, y que algunos de estos derivados presentaban una actividad semejante a ella.

Desde entonces el interés por este núcleo no ha cesado, encontrándose nuevas aplicaciones biológicas como propiedades analgésicas y antiinflamatorias,[97] anticonvulsivantes,[98] antimicrobianas,[99] antivirales,[100] o antihipertensivas,[101] entre otras.

[94] Woolley, D.W. Some biological effects produced by benzimidazole and their reversal by purines. *J. Biol. Chem*. **1944**, 152(2), 225-232. doi: 10.1016/S0021-9258(18)72045-0

[95] Brink, N.G.; Folkers, K. Vitamin B12. VI. 5,6-dimethylbenzimidazole, a degradation product of vitamin B12. *J. Am. Chem. Soc.* **1949**, 71(8), 2951. doi: 10.1021/ja01176a532

[96] Emerron, G.; Folkers, K. Water-soluble vitamins. *Annu. Rev. Biochem.* **1950**, 20, 559-598. doi: 10.1146/annurev.bi.20.070151.003015

[97] Gaba, M.; Singh, S.; Mohan, C. Benzimidazole: An emerging scaffold for analgesic and anti-inflammatory agents. *Eur. J. Med. Chem*. **2014**, 76, 494-505. doi: 10.1016/j.ejmech.2014.01.030

[98] Ruhi, A.; Mohammad, A.K.; Nadeem, S. Past, present and future of antiepileptic drug therapy-finding a place for heterocyclics. *Mini Rev. Med. Chem*. **2015**, 15(12), 1024-1050. doi: 10.2174/1389557515121507311135 49

[99] Bansal, Y.; Kaur, M.; Bansal, G. Antimicrobial potential of benzimidazole derived molecules. *Mini Rev. Med. Chem.* **2019**, 19(8), 624-646. doi: 10.2174/1389557517666171101104024

[100] Kanwal, A.; Ahmad, M.; Aslam, S.; Naqvi, S.A.R.; Saif, M.J. Recent Advances in Antiviral Benzimidazole Derivatives: A Mini Review. *Pharm. Chem. J.* **2019**, 53, 179–187. doi: 10.1007/s11094-019-01976-3

[101] Danao, K.R.; Mahapatra, D.K. Recent Advances of Benzimidazole Derivatives as Anti-Hypertensive Agents. En *Biochemistry, Biophysics, and Molecular Chemistry,* 1ª edición; Torrens, F.; Mahapatra, D.K.; Haghi, A.K., Eds; Apple Academic Press: Nueva York, 2020.

Basado en el objetivo principal de este Trabajo de Tesis, centrado en el hallazgo de nuevas moléculas heterocíclicas con actividad nematicida y antiprotozoaria, se ha hecho una revisión bibliográfica sobre Bz con actividad nematicida, y/o antiprotozoaria con el fin de diseñar nuevos compuestos que puedan constituir una alternativa terapéutica, y que pueden servir en el caso de resistencias.

A continuación, se exponen los resultados más relevantes encontrados en la búsqueda, indicando primero Bzs sustituidos en C-2, directamente unidos a un arilo o heteroarilo o a través de espaciadores, después Bzs con sustituciones en N-1, seguido de análogos de otros fármacos, y de Bzs ciclados y, por último, Bzs organometálicos. Según Katsuno y *col.* (2015)[102] para que un compuesto sea considerado *hit compound* ha de presentar en *Plasmodium* una CI_{50} <1 µM, en *Leishmania* <10 µM y en *T. cruzi* <10 µM. Sin embargo, en el caso de las dos últimas enfermedades se ha aplicado una cota <4 µM con el fin de recoger en el texto los compuestos más activos sin poner límite de años, mientras que en el caso de *Plasmodium*, dada la abundancia de información, sólo se recogen datos de los últimos 5 años. Adicionalmente, en las Tablas I.4, I.5 y I.6 se recogen datos de actividad de derivados que muestran una potencia menor.

Benzimidazoles con actividad nematicida

No se ha encontrado información sobre derivados de Bz con actividad anti-*Teladorsagia*.

Benzimidazoles con actividad antimalárica

Algunos derivados de 2-fenilBz han mostrado buena actividad in vitro frente a *Plasmodium*. Los compuestos **1**, **2** y **3** tienen un grupo amida sustituido en la posición C-4´ y fueron evaluados frente a las cepas *Pf*NF54 y *Pf*Dd2 mostrando buenos valores de CI_{50} (0,96/0,41, 0,34/0,53 y 0,31/0,67 µM, respectivamente), además de excelentes índices de selectividad (IS), con valores entre 197 y 665.[103] Por otro lado, Purwono y *col.*[104] diseñaron

[102] Katsuno, K.; Burrows, J.; Duncan, K.; Hooft van Huijsduijnen, R.; Kaneko, T.; Kita, K.; Mowbray, C.E.; Schmatz, D.; Warner, P.; Slingsby. Hit and lead criteria in drug discovery for infectious diseases of the developing world. *Nat. Rev. Drug. Discov*. **2015**, 14, 751–758. doi: 10.1038/nrd4683

[103] L´abbate, F.P.; Müller, R.; Openshaw, R.; Combrinck, J.M.; de Villiers, K.A.; Hunter, R.; Egan, T.J. Hemozoin inhibiting 2-phenylbenzimidazoles active against malaria parasites. *Eur. J. Med. Chem*. **2018**, 159, 243-254. doi: 10.1016/j.ejmech.2018.09.060

[104] Purwono, B.; Nurohmah, B.A.; Fathurrohman, P.Z.; Syahri, J. Some 2-arylbenzimidazole derivatives as an antimalarial agent: synthesis, activity assay, molecular docking and pharmacological evaluation. *Rasayan J. Chem*. **2021**, 14(1), 94-100. doi: 10.31788/ RJC.2021.1416088

en 2021, una serie de compuestos dirigidos a inhibir las proteínas DHFR y timidilato sintasa de *P. falciparum*, encontrando una actividad moderada frente a la cepa *Pf*3D7 para el 2-(4-metoxifenil)-1*H*-Bz (CI_{50} 0,76 µM). Los compuestos **4** y **5**, presentan un grupo de guanidina en posición C-5 y grupos bifenilo y 4-(3,4-dimetoxifenoxi)fenilo en C-2, respectivamente, mostrando actividades en el rango nanomolar (0,071 y 0,129 µM), e IS próximo a 2000.[105]

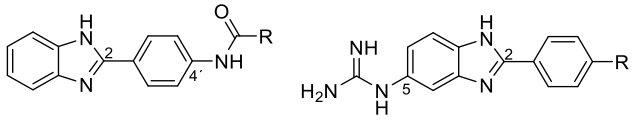

1 R = 5-Br-piridin-3-ilo
2 R = 2,6-diCl-piridin-4-ilo
3 R = 3,5-diNO_2-fenilo

4 R = fenilo
5 R = 3,4-diOCH_3fenoxilo

Figura I.14. Estructuras de algunos 2-fenil Bz activos frente a *Plasmodium* spp.

El uso de un espaciador entre el núcleo Bz y el sustituyente en C-2, confiere a la molécula la posibilidad de adoptar conformaciones diferentes y establecer otros enlaces a nivel del receptor. Así, los compuestos **6** y **7**, que contienen NH en C-2, mostraron actividad en el rango submicromolar (0,079/0,335 y 0,11/0,762 µM frente a las cepas *Pf*NF54/K1 y buenos IS (273 y 228). El grupo hidroxilo en posición 2´ del fenilo forma un puente de hidrógeno intramolecular con la amina terciaria situada en la cadena.[106] Se diseñaron compuestos con un grupo acrilonitrilo en C-2 para actuar de forma dual, la enzima falcipaína-2 y la formación de la hemozoína, que mostraron menor actividad antimalárica (**8**, CI_{50} 0,69 µM; IS 34,2).[107] Según describen Divatia y *col.* 2019,[108] los compuestos con agrupación hidrazona carbotioamida mostraron muy buena actividad inhibitoria frente a *P. falciparum*, siendo los compuestos **9**, **10**, **11** y **12** los más activos, con CI_{50} de 8.3, 29, 10 y 62 nM, respectivamente.

[105] Dognanc, F.; Celik, I.; Eren, G.; Kaiser, M.; Brun, R.; Goker, H. Synthesis, in vitro antiprotozoal activity, molecular docking and molecular dynamics studies of some new monocationic guanidinobenzimidazoles. *Eur. J. Med. Chem*. **2021**, 221, 113545. doi: 10.1016/j.ejmech.2021.113545

[106] Attram, H.D.; Wittlin, S.; Chibale, K. Incorporation of an intramolecular hydrogen bonding motif in the side chain of antimalarial benzimidazoles. *Med. Chem. Comm*. **2019**, 10, 450-455. doi: 10.1039/C8MD00608C

[107] Sharma, K.; Shrivastava, A.; Mehra, R.N.; Deora, G.S.; Alam, M.M.; Zaman, M.S.; Akhter, M. Synthesis of novel benzimidazole acrylonitriles for inhibition of *Plasmodium falciparum* growth by dual target inhibition. *Arch. Pharm. Chem. Life Sci.* **2017**, e1700251. doi: 10.1002/ardp.201700251

[108] Divatia, S.M.; Rajani, D.P.; Rajani, S.D., Patel, H.D. Novel thiosemicarbazone derivatives containing benzimidazole moiety: Green synthesis and anti-malarial activity. *Arab. J. Chem*. **2019**, 12, 1641-1651. doi: 10.1016/j.arabjc.2014.09.007

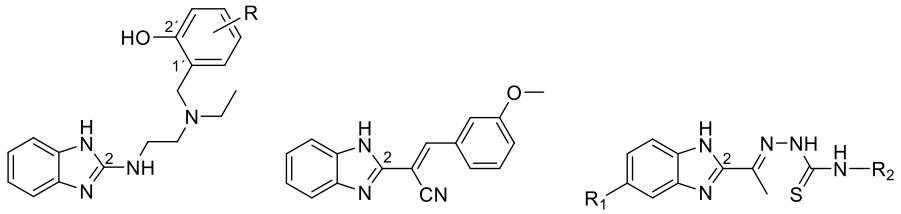

6 R = 4-Cl
7 R = 5-Cl

8 R = 4-Cl

9 R_1 = Cl; R_2 = 4-F-fenilo
10 R_1 = Cl; R_2 = 2,3-diCl-fenilo
11 R_1 = Cl; R_2 = 4-I-fenilo
12 R_1 = Cl; R_2 = CO-fenilo

Figura I.15. Estructuras de algunos C-2 arilalquilamino/ C-2 arilalquilo activos frente a *Plasmodium* spp.

La sustitución en N-1 concede al núcleo una configuración electrónica diferente, eliminando la posibilidad de formar puentes de hidrógeno y tautómeros. Así, la combinación entre el núcleo de Bz, con ftalimida, un isobutilmetilo como conector, y un triazol en N-1 confiere a los compuestos obtenidos por Kumar y *col.* (2017)[109] valores de CI_{50} a nivel submicromolar (0,7, 0,9 y 0,9 µM para **13**, **14** y **15**, respectivamente) frente a las cepas *Pf*3D7 y *Pf*W2, y buenos resultados frente a *P. berguei* en estudios in vivo. Además, los compuestos mostraron inhibición en diferentes estadios del parásito, y sinergia con cloroquina y dihidroartemisinina. Por otro lado, la presencia de fenilos en N-1 y una amina primaria en C-2, dio lugar a compuestos con actividad en rango nanomolar frente a la cepa *Pf*3D7 (CI_{50} 6,4 nM) y baja toxicidad (IS >1000) para **16**.[110] Los N-1 bencilo, C-2 arilamino derivados obtenidos por Dziwornu y *col.* (2021)[111] llevó a compuestos con muy buena actividad y baja toxicidad, como el Bz **17** (CI_{50} 0,19/0,08 µM, IS >263) que fue seleccionado para ensayos in vivo frente a *P. berguei* logrando una reducción de la parasitemia del 98% a dosis de 4 x 50 mg/Kg.

[109] Kumar, P.; Achieng, A.O.; Rajendran, V.; Ghosh, P.C.; Singh, B.K.; Rawat, M.; Perkins, D.J.; Kempaiah, P.; Rathi, B. S ynergistic blending of high-valued heterocycles inhibits growth of *Plasmodium falciparum* in culture and *P. berghei* infection in mouse model. *Sci. Rep*. **2017**, 7, 6724. doi: 10.1038/s41598-017-06097-z

[110] Devine, S.M.; Challis, M.P.; Kigotho, J.K.; Siddiqui, G.; de Paoli, A.; MacRaild, C.A.; Avery, V.M.; Creek, D.J.; Norton, R.S.; Scammells, P. J. Discovery and development of 2-aminobenzimidazoles as potent antimalarials. *Eur. J. Med. Chem.* **2021**, 221, 113518. doi: 10.1016/j.ejmech.2021.113518

[111] Dziwornu, G.A.; Coertzen, D.; Leshabane, M.; Korkor, C.M.; Cloete, C.K.; Njoroge, M.; Gibhard, L.; Lawrence, N.; Reader, J.; van der Watt, M.; Wittlin, S.; Birkholtz, L.M.; Chibale, K. *J. Med. Chem*. **2021**, 64, 5198-5215. doi: 10.1021/acs.jmedchem.1c00354

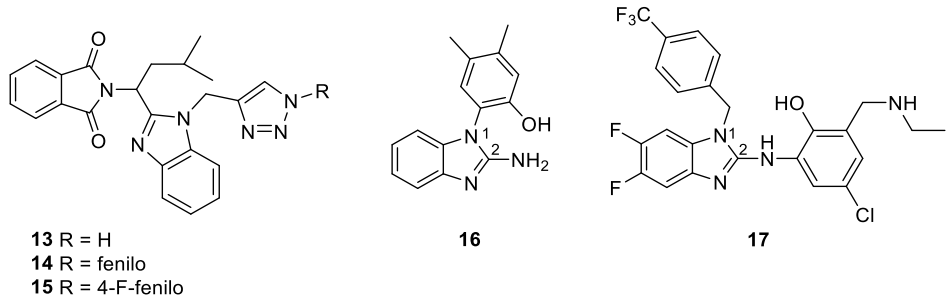

13 R = H
14 R = fenilo
15 R = 4-F-fenilo

16

17

Figura I.16. Estructuras de algunos Bz N-1, C-2 -sustituidos activos frente a *Plasmodium* spp.

La obtención de estructuras mixtas, siendo alguno de los fragmentos farmacológicamente activo, constituye una de las estrategias modernas en la búsqueda de nuevos fármacos. El lerisetrón, por ejemplo, es un antagonista de los receptores 5-HT_3 con actividades antieméticas que muestra además actividad antimalárica (CI_{50} 0,81 µM). Sus análogos **18** y **19** mostraron unas CI_{50} frente a la cepa *Pf*NF54 de 28 y 38 nM, y de 61 y 76 nM frente a la *Pf*K1, respectivamente. Además, los valores de IS fueron de 714 y 553.[112] Por otro lado, el astemizol, fármaco antihistamínico usado en el tratamiento de las alergias, muestra actividad anti-*Plasmodium* (*Pf*NF54 CI_{50} 0,086 µM; *Pf*3D7 CI_{50} 0,23 µM; *Pf*Dd2 CI_{50} 0,46 µM), basado en ello obtuvieron los compuestos **20** (*Pf*NF54 CI_{50} 47 nM; IS 860)[113] y **21** (*Pf*3D7 CI_{50} 29 nM; IS 110), con actividad en rango nanomolar.[114] Asimismo, el compuesto **22** mostró una CI_{50} de 0,20 y 1,14 µM frente a las cepas *Pf*NF54 y *Pf*K1, respectivamente, y un IS de 148. Este compuesto, además, mostró actividad frente al estadio sanguíneo y la etapa tardía del gametocito.[115]

[112] Mueller, R.; Reddy, V.; Nchinda, A.T.; Mebrahtu, F.; Taylor, D.; Lawrence, N.; Tanner, L.; Barnabe, M.; Eyermann, C.J.; Zou, B.; Kondreddi, R.R.; Lakshminarayana, S.B.; Rottmann, M.; Street, L.J.; Chibale, K. Lerisetron Analogues with antimalarial properties: synthesis, structure−activity relationship studies, and biological assessment. *ACS Omega*. **2020**, 5, 6967-6982. doi: 10.1021/acsomega.0c00327

[113] Kumar, M.; Okombo, J.; Mambwe, D.; Taylor, D.; Lawrence, N.; Reader, J.; van der Watt, M.; Fontinha, D.; Sanches-Vaz, M.; Bezuidenhout, B.C.; Lauterbach, S.; Liebenberg, D.; Birkholtz, L.M.; Coetzer, T.L.; Prudencio, M.; Egan, T.J.; Wittlin, S.; Chibale, K. Multistage antiplasmodium activity of astemizole analogues and inhibition of hemozoin formation as a contributor to their mode of action. *ACS Infect. Dis.* **2018**, 5(2), 303-315. doi: 10.1021/acsinfecdis.8b00272

[114] Tian, J.; Vadermosten, L.; Peigneur, S.; Moreels, L.; Rozenski, J.; Tytgat, J.; Herdewijn, P.; Van de Steen, P.E.; De Jonghe, S. Astemizole analogues with reduced hERG inhibition as potent antimalarial compounds. *Bioorg. Med. Chem.* **2017**, 25(17), 4553-4559. doi: 10.1016/j.bmc.2017.10.004

[115] Mambwe, D.; Kumar, M.; Ferger, R.; Taylor, D.; Njoroge, M.; Coertzen, D.; Reader, J.; van der Watt, M.; Birkholtz, L.M.; Chibale, K. *ACS Med. Chem. Lett*. **2021**, 12, 1333-1341. doi: 10.1021/acsmedchemlett.1c00328

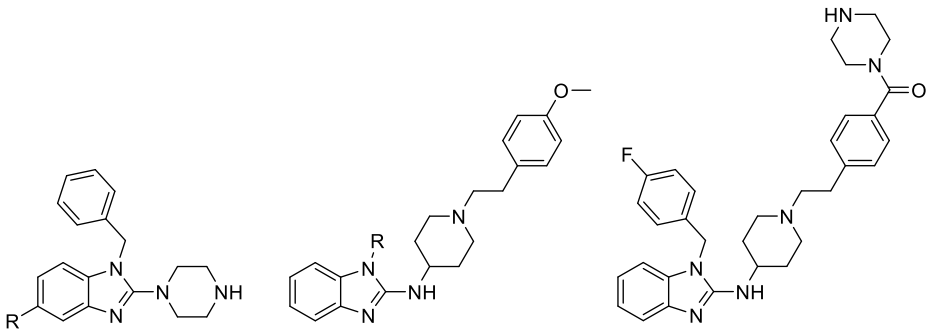

Figura I.17. Estructuras de algunos N-1, C-2-aquilamino Bz análogos de fármacos activos frente a *Plasmodium* spp.

El grupo de investigación de Chibale ha trabajado en la obtención de derivados de pirido[1,2-*a*]Bz obteniendo compuestos con resultados muy prometedores frente a *Plasmodium* spp., llegando a seleccionar algunos derivados para ensayos in vivo frente a *P. berghei*, que mostraron muy buena eficacia oral. Basándose en estudios antimaláricos preliminares llegaron al derivado **23** (*Pf*NF54 CI_{50} 0,12 y *Pf*K1 CI_{50} 0,11 µM, IS 13) que mostró buena eficacia oral en roedores (reducción del 97,5% a 4 x 25 mg/Kg),[116] por lo que progresaron con estos estudios. Así, los compuestos **24** y **25**, que contienen 3-(dietilaminometil)-4-hidroxifenilo, mostraron actividad antimalárica frente a las cepas *Pf*NF54 y *Pf*K1 en rango submicromolar (CI_{50} 0,11/0,18 µM para **24** y CI_{50} 0,07/0,07 µM en **25**) y valores elevados de IS, 1718 y 1429. Además, **24** en ensayos in vivo, a dosis de 4 x 50 mg/Kg redujo la parasitemia en un 95%.[117] El cambio de los átomos de flúor por cloro, compuesto **26**, llevó a un aumento de la actividad del orden nanomolar (CI_{50} de 18 nM y 19 nM frente a las cepas *Pf*NF54 y *Pf*K1, respectivamente) e IS de 188, además, mostró una eficacia oral de 99,7% a dosis de 4 x 30 mg/Kg.[118] Los compuestos **27** y **28**, mantuvieron la

[116] Ndakala, A. J.; Gessner, R. K.; Gitari, P. W.; October, N.; White, K. L.; Hudson, A.; Fakorede, F.; Shackleford, D. M.; Kaiser, M.; Yeates, C.; Charman, S. A.; Chibale, K. Antimalarial pyrido[1,2- *a*]benzimidazoles. *J. Med. Chem*. **2011**, 54, 4581–4589. doi: 10.1021/jm200227r

[117] Okombo, J.; Brunschwig, C.; Singh, K.; Dziwornu, G.A.; Barnard, L.; Njoroge, M.; Wittlin, S.; Chibale, K. Antimalarial pyrido[1,2-*a*]benzimidazole derivatives with Mannich base side chains: synthesis, pharmacological evaluation, and reactive metabolite trapping studies. *ACS Infect. Dis*. **2019**, 5(3), 372-384. doi: 10.1021/acsinfecdis.8b00279

[118] Singh, K.; Okombo, J.; Brunschwig, C.; Ndubi, F.; Barnard, L.; Wilkinson, C.; Njogu, P.M.; Njoroge, M.; Laing, L.; Machado, M.; Prudêncio, M.; Reader, J.; Botha, M.E.; Nondaba, S.H.; Birkholtz, L.M.; Lauterbach, S.; Churchyard, A.; Coetzer, T.L.; Burrows, J.N.; Yeates, C.L.; Denti, P.; Wiesner, L.; Egan, T.J.; Wittlin, S.; Chibale, K. Antimalarial pyrido[1,2-*a*]benzimidazoles: Lead optimization, parasite life cycle stage profile, mechanistic evaluation, killing kinetics and in vivo oral efficacy in a mouse mode. *J. Med. Chem*. **2017**, 60(4), 1432-1448. doi: 10.1021/acs.jmedchem.6b01641

actividad frente a las cepas *Pf*NF54 (CI_{50} 0,17 µM) y *Pf*K1 (CI_{50} 0,15 y 0,14 µM, respectivamente). Sin embargo, los valores de IS se redujeron, 25 para el **27** y 103 para el **28**. Adicionalmente, vieron que es poco probable que estas estructuras muestren resistencia cruzada con cloroquina.[119] Leshabane y *col.* (2021)[120] concluyeron que algunos compuestos con núcleo de pirido[1,2-*a*]Bz, como el **29**, eran capaces de actuar tanto frente a los estadios intraeritrocíticos asexuales sanguíneos (CI_{50} 94 nM), como frente a gametocitos transmisibles a concentraciones en rango submicromolar (CI_{50} 0,57 µM).

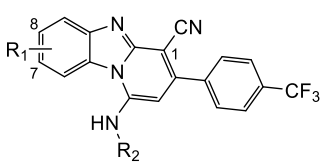

23 R_1 = H; R_2 = *N*-etil etilendiamina
24 R_1 = H; R_2 = 3´-CH_2-dietilamino, 4´-OH-fenilo
25 R_1 = 7,8-diF; R_2 = 3´-CH_2-dietilamino, 4´-OH-fenilo
26 R_1 = 7,8-diCl; R_2 = *N*-etiletilendiamina

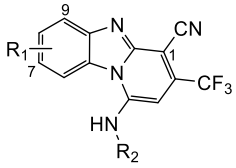

27 R_1 = H; R_2 = 4-OCF_3-fenilo
28 R_1 = 7,9-diCl; R_2 = CH_2-2-F-fenilo
29 R_1 = 7,8-diF; R_2 = 4-Cl-feniletilamina

Figura I.18. Estructuras de algunos pirido[1,2-*a*]Bz activos frente a *Plasmodium* spp.

Se analizó la acumulación intramolecular del derivado **24** y se estudió su mecanismo de acción, encontrando que actúa por una vía diferente a la inhibición de la formación de hemozoína.[121] En 2022, el grupo de investigación describió que la actividad antimalárica in vitro e in vivo de los pirido[1,2-*a*]Bz se debe a la capacidad de acumulación del compuesto dentro de las células del parásito y la supresión de la detoxificación del grupo hemo.[122]

El campo de la química bioorganometálica ha ofrecido alternativas muy interesantes a los fármacos tradicionales. Así, la **ferroquina**, diseñada por Biot y *col.* en

[119] Mayoka, G.; Njoroge, M.; Okombo, J.; Gibhard, L.; Sanches-Vaz, M.; Fontinha, D.; Birkholtz, L.M.; Reader, J.; van der Watt, M.; Coetzer, T.L.; Lauterbach, S.; Churchyard, A.; Bezuidenhout, B.; Egan, T.J.; Yeates, C.; Wittlin, S.; Prundêncio, M.; Chibale, K. Structure–activity relationship studies and *Plasmodium* life cycle profiling identifies pan-active *N*-aryl-3-trifluoromethyl pyrido[1,2-*a*]benzimidazoles which are efficacious in an in vivo mouse model of malaria. *J. Med. Chem*. **2018**, 62(2), 1022-1035. doi: 10.1021/acs.jmedchem.8b01769

[120] Leshabane, M.; Dziwornu, G.A.; Coertzen, D.; Reader, J.; Moyo, P.; van der Watt, M.; Chisanga, K.; Nsanzubuhoro, C.; Ferger, R.; Erlank, E.; Venter, N.; Koekemoer, L.; Chibale, K.; Birkholtz, L.M. Benzimidazole derivatives are potent against multiple life cycle stages of *Plasmodium falciparum* malaria parasites. *ACS Infect. Dis*. **2021**, 7(7), 1945-1955. doi: 10.1021/acsinfecdis.0c00910

[121] Korkor, C.M.; Garnei, L.F.; Amod, L.; Egan, T.J.; Chibale, K. Intrinsic fluorescence properties of antimalarial pyrido[1,2-*a*]benzimidazoles facilitate subcellular accumulation and mechanistic studies in the human malaria parasite *Plasmodium falciparum*. *Org. Biomol. Chem.* **2020**, 18, 8668-8676. doi: 10.1039/D0OB01730B

[122] Sousa, C.C.; Dziwornu, G.A.; Quadros, H.C.; Araujo-Neto, J.H.; Chibale, K.; Moreira, D.R.M. Antimalarial pyrido[1,2-*a*]benzimidazoles exert strong parasiticidal effects by achieving high cellular uptake and suppressing heme detoxification. *ACS Infect. Dis.* **2022**, 8, 1700-1710. doi: 10.1021/acsinfecdis.2c00326

1997,[123] un ferronilo unido al esqueleto base de cloroquina, presenta actividad frente a *P. falciparum* resistente a cloroquina, además de actuar por mecanismos de acción diferentes.[124] Varios grupos de investigación han trabajado desarrollando estructuras análogas, obteniendo compuestos con actividad antimalárica prometedora (Fig. I.19). Baartzes y *col.* (2019)[125] obtuvieron híbridos de aminoquinolina-Bz con ferroceno con valores de CI_{50} en rango submicromolar (0,33 µM *Pf*NF54 y 0,28 µM *Pf*K1, **30**), seleccionando el compuesto **31** para ensayos in vivo frente *P. berguei*, que redujo la parasitemia en un 92% a dosis de 4 x 50 mg/Kg. El grupo de Chibale antes mencionado, sintetizó y evaluó derivados de 2-fenilBz ciclometalizados, observando que los 2-fenilBz con complejos de rutenio(II), iridio(III) y rodio(III) mejoraban notablemente la actividad antimalárica a nivel submicromolar en comparación con los 2-fenilBz (CI_{50} >15 µM). Los derivados **32** y **33** mostraron CI_{50} de 0,12 y 0,19 frente a la cepa *Pf*NF64, respectivamente y **34** alcanzó una CI_{50} de 0,97 frente a la cepa *Pf*K1.[126] En 2020 el grupo desarrolló unos híbridos de aminoquinolina-Bz con complejos metálicos de Ir(II) y Rh(III). Los derivados **35** y **36** mostraron CI_{50} de 0,49 y 0,19 µM frente a *Pf*NF54, además **35** mantuvo la actividad frente a *Pf*K1 (CI_{50} 0,69 µM).[127] Jordaan y *col.* (2022)[128] estudiaron la actividad anti-*Plasmodium* de derivados de complejos metálicos de Rh(III) e Ir(III) ciclopentadienilo sustituidos con 2-(2-piridil)Bz. El compuesto más activo, el **37**, mostró una CI_{50} de 0,75 y 0,42 µM frente a las cepas *Pf*3D7 y *Pf*Dd2, respectivamente.

[123] Biot, C.; Glorian, G.; Maciejewski, L.A.; Brocard, J.S. Synthesis and antimalarial activity in vitro and in vivo of a new ferrocene-chloroquine analogue. *J Med Chem.* **1997**, 40(23), 3715-3718. doi: 10.1021/jm970401y

[124] Biot, C.; Nosten, F.; Fraisse, L.; Ter-Minassian, D.; Khalife, J.; Dive, D. The antimalarial ferroquine: from bench to clinic. *Parasite*. **2011**, 18(3), 207-214. doi: 10.1051/parasite/2011183207

[125] Baartzes, N.; Stringer, T.; Seldom, R.; Warner, D.F.; Taylor, D.; Wittlin, S.; Chibale, K.; Smith, G.S. Bioisosteric ferrocenyl aminoquinoline-benzimidazole hybrids: Antimicrobial evaluation and mechanistic insights. *Eur. J. Med. Chem.* **2019**, 180, 121-133. doi: 10.1016/j.ejmech.2019.06.069

[126] Rylands, L.; Welsh, A.; Maepa, K.; Stringer, T.; Taylor, D.; Chibale, K.; Smith, G.S. tructure-activity relationship studies of antiplasmodial cyclometallated ruthenium(II), rhodium(III) and iridium(III) complexes of 2-phenylbenzimidazoles. *Eur. J. Med. Chem*. **2019**, 161, 11-21. doi: 10.1016/j.ejmech.2018.10.019

[127] Baartzes, N.; Jordaan, A.; Warner, D.F.; Combrinck, J.; Taylor, D.; Chibale, K.; Smith, G.S. Antimicrobial evaluation of neutral and cationic iridium(III) and rhodium(III)aminoquinoline-benzimidazole hybrid complexes. *Eur. J. Med. Chem.* **2020**, 206, 112694. doi: 10.1016/j.ejmech.2020.112694

[128] Jordaan, L.; Ndlovu, M.T.; Mkhize, S.; Ngubane, S.; Loots, L.; Duffy, S.; Avery, V.M.; Chellan, P. Investigating the antiplasmodial activity of substituted cyclopentadienyl rhodium and iridium complexes of 2-(2-pyridyl)benzimidazole. *J. Organomet. Chem*. **2022**, 962, 122273. doi: 10.1016/j.jorganchem.2022.122273

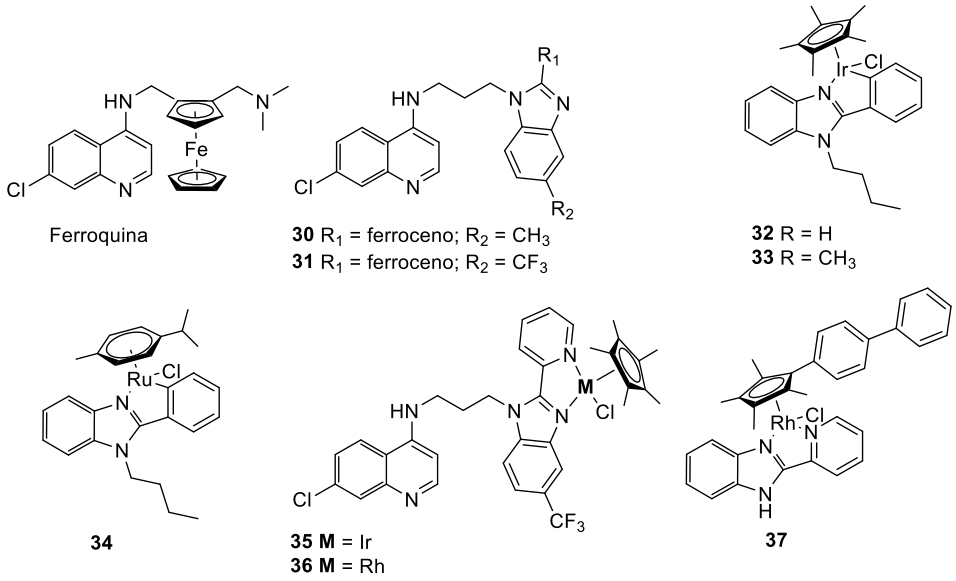

Figura I.19. Estructuras de algunos Bz organometálicos activos frente a *Plasmodium* spp.

En la Tabla I.4 se resumen los resultados de otros trabajos sobre Bz con menor actividad antimalárica publicados en los últimos cinco años.

Tabla I.4. Otros benzimidazoles con actividad antimalárica, últimos 5 años.

Tipo de derivado	**Cepa *Pf***	**Relevancia**	**Referencia**
2-Aril-1*H*-Bz-5-carboxamida. 5´-nitrofurano y 5´-nitrotiofeno en C-2	-	Inhibición de la β-hematina (2,0-88,7%). Evaluación in vivo frente a *P. berghei.* Resultados similares a cloroquina.	Romero, 2019[129]
N-metilBz	*Pf*NF54	CI_{50} 1,15-13,3 µM. Comparación de actividad antimalárica entre heterociclos 6,5-fusionados.	Jacobs, 2018[130]
Análogo de carvacrol	-	CI_{50} 0,48-1,76 µg/mL. Acoplamiento molecular frente a la enzima dihidrofolato reductasa de *P. falciparum*.	Bhoi, 2022[131]

[129] Romero, J.A.; Acosta, M.E.; Gamboa, N.D., Mijares, M.R., De Sanctis, J.B., Llovera, L.J.; Charris, J.E. Synthesis, antimalarial, antiproliferative, and apoptotic activities of benzimidazole-5-carboxamide derivatives. *Med. Chem. Res*. **2019**, 28, 13-27. doi: 10.1007/s00044-018-2258-x

[130] Jacobs, L.; de Kock, C.; Taylor, D.; Pelly, S.C.; Blackie, M.A.L. Synthesis of five libraries of 6,5-fused heterocycles to establish the importance of the heterocyclic core for antiplasmodial activity. *Bioorg. Med. Chem.* **2018**, 26(21), 5730-5741. doi: 10.1016/j.bmc.2018.10.029

[131] Bhoi, R.T.; Rajput, J.D.; Bendre, R.S. An efficient synthesis of rearranged new biologically active benzimidazoles derived from 2-formyl carvacrol. *Res. Chem. Intermed*. **2022**, 48, 401-422. doi: 10.1007/s11164-021-04601-9

Bases Schiff	*Pf*3D7	PIC[a] (50 µg/mL) 49-95 % in vitro. Bases de Schiff, compuestos 2-amidoBz.	Fonkui, 2019[132]
	*Pf*3D7	CI_{50} 12,8-18,4 µM. SI >10. Acoplamiento molecular frente a α-tubulina. Bases de Schiff. Complejos metálicos de La(III) y Ce(III).	Aragón-Muriel, 2021[133]
Bioorganometálicos. 2-(2-piridil)Bz	*Pf*NF54	CI_{50} 9,65-55,9 µM. Complejos metálicos con Ir(III), Rh(III) y Ru(II).	Munnik, 2022[134]

[a] PIC: porcentaje de inhibición de crecimiento.

Benzimidazoles con actividad leishmanicida

Algunos derivados de benzimidazol han mostrado actividad leishmanicida interesante. Así, **38** y **39** fueron seleccionados como cabezas de serie debido a su CI_{50} de 0,62 µg/mL frente a la cepa GP63 de *L. major*[135], Fig. I.20.

La introducción de un grupo amino en C-2 como espaciador llevó a los Bz **40** y **41** con actividades de 2,6 y 3,2 µM frente a promastigotes de *L. mexicana* y, de 0,28 y 0,26 µM en amastigotes, respectivamente.[136]

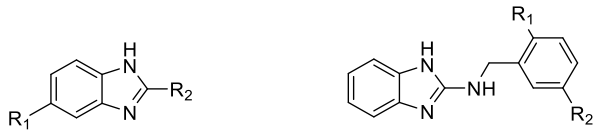

38 R_1 = H; R_2 = tiofen-2-ilo
39 R_1 = NO_2; R_2 = indol-3-ilo

40 R_1 = OH; R_2 = Br
41 R_1 = OCH_3; R_2 = H

Figura I.20. Estructuras de algunos C-2 hetarilo/C-2 metilamino Bz activos frente a *Leishmania* spp.

[132] Fonkui, T.Y.; Ikhile, M.I.; Njobeh, P.B.; Ndinteh, D.T. Benzimidazole Schif base derivatives: synthesis, characterization and antimicrobial activity. *BMC Chem*. **2019**, 13, 127. doi: 10.1186/s13065-019-0642-3

[133] Aragón-Muriel, A.; Liscano, Y.; Upegui, Y.; Robledo, S.M.; Ramírez-Apan, M.T.; Morales-Morales, D.; Oñate-Garzón, J.; Polo-Cerón, D. *Antibiotics*. **2021**, 10, 728. doi: 10.3390/antibiotics10060728

[134] Munnik, B.L.; Kaschula, C.H.; Watson, D.J.; Wiesner, L.; Loots, L.; Chellan, P. Synthesis and study of organometallic PGM complexes containing 2-(2-pyridyl)benzimidazole as antiplasmodial agents. *Inorganica Chim. Acta*. **2022**, 540, 121039. doi: 10.1016/j.ica.2022.121039

[135] Shaukat, A.; Mirza, H.M.; Ansari, A.H.; Yasinzai, M.; Zaidi, S.Z.; Dilshad, S.; Ansari, F.L. Benzimidazole derivatives: synthesis, leishmanicidal effectiveness, and molecular docking studies. *Med. Chem. Res*. **2013**, 22, 3606-3620. doi: 10.1007/s00044-012-0375-5

[136] Nieto-Maneses, R.; Castillo, R.; Hernández-Campos, A.; Maldonado-Rangel, A.; Matius-Ruiz, J.B.; Trejo-Soto, P.J.; Nogueda-Torres, B.; Dea-Ayuela, M.A.; Bolás-Fernández, F.; Méndez-Cuesta, C.; Yépez-Mulia, L. In vitro activity of new *N*-benzyl-1*H*-benzimidazol-2-amine derivatives against cutaneous, mucocutaneous and visceral *Leishmania* species. *Exp. Parasitol*. **2018**, 184, 82-89. doi: 10.1016/j.exppara.2017.11.009

De Luca y *col.* (2018),[137] encontraron resultados interesantes en derivados *N*-sustituidos, con CI_{50} 0,45-2,06 µM frente a *L. infatum*. Adicionalmente, realizaron estudios de acoplamiento molecular frente a la cisteína proteasa CPB2.8ΔCTE de *L. mexicana*. Por otro lado, la combinación de metilamina con derivados de piridina dio lugar a compuestos **42** y **43** con buena CI_{50} frente a *L. mexicana*, de 0,25 y 0,41 µM, respectivamente.[138]

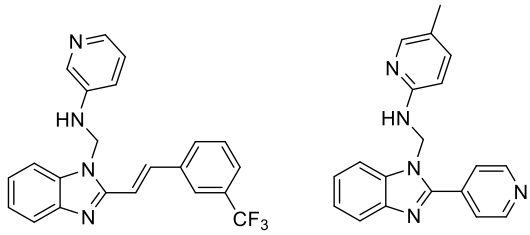

Figura I.21. Estructuras de algunos Bz activos frente a *Leishmania* spp.

Se han obtenido bis-benzimidazoles análogos de pentamidina que mostraron valores de actividad en rango submicromolar frente a *L. mexicana*, CI_{50} 0,38 y 0,71 µM para los compuestos **44** y **45**, respectivamente.[139] Como se ha indicado, los Bzs actúan por unión a la β-tubulina en el sitio de la colchicina, al igual que podofilotoxina. Así, Escudero-Martínez y *col.*[140] ensayaron la actividad de híbridos entre Bzs y podofilotoxina frente a promastigotes y amastigotes de *L. infantum* obteniendo unas CE_{50} de 2,2 y 2,5 µM e IS de 29 y <45,5 para los compuestos **46** y **47**, respectivamente.

[137] De Luca, L.; Ferro, S.; Buemi, M.R.; Monforte, A.M.; Gitto, R.; Schirmeister, T.; Maes, L.; Rescifina, A.; Micale, N. Discovery of benzimidazole-based Leishmania mexicana cysteine protease CPB2.8ΔCTE inhibitors as potential therapeutics for leishmaniasis. *Chem. Biol. Drug. Des.* **2018**, 92, 1585-1596. doi: 10.1111/cbdd.13326

[138] Patel, V.M.; Patel, N.B.; Chan-Bacab, M.J.; Rivera, G. *N*-Mannich bases of benzimidazole as a potent antitubercular and antiprotozoal agents: Their synthesis and computational studies. *Synth. Commun*. **2020**, 858-878. doi: 10.1080/00397911.2020.1725057

[139] Torres-Gómez, H.; Hernández-Núñez, E.; León-Rivera, I.; Guerrero-Álvarez, J.; Cedillo-Rivera, R.; Moo-Puc, R.; Argotte-Ramos, R.; Rodríguez-Gutiérrez, M.C.; Chan-Bacab, M.J.; Navarrete-Vázquez, G. Design, synthesis and in vitro antiprotozoal activity of benzimidazole-pentamidine hybrids. *Bioorg. Med. Chem. Lett*. **2018**, 18, 3147-3151. doi: 10.1016/j.bmcl.2008.05.009

[140] Escudero-Martínez, J.M.; Pérez-Pertejo, Y.; Reguera, R.M.; Castro, M.A.; Rojo, M.V.; Santiago, C.; Abad, A.; Anselmo García, P.; López-Pérez, J.L.; San Feliciano, A.; Balaña-Fouce, R. Antileishmanial activity and tubulin polymerization inhibition of podophyllotoxin derivatives on *Leishmania infantum*. *Int. J. Parasitol. Drugs Drug Resist.* **2017**, 7, 272-285. doi: 10.1016/j.ijpddr.2017.06.003

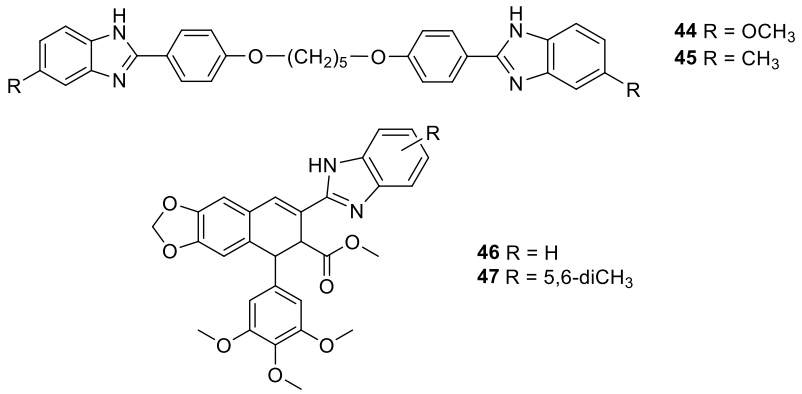

Figura I.22. Estructuras de algunos bis-Bz activos frente a *Leishmania* spp.

Al igual que en *Plasmodium*, se han obtenido derivados de compuestos organometálicos que mostraron buena actividad leishmanicida. Así, las sales de yoduro derivadas de *N*-ferrocenilmetil *N*-metilsustituidas **48** y **49**, presentaron muy buena actividad frente a la cepa L1 de *L. infantum* (CI_{50} de 0,5 µM).[141] Análogamente, se han obtenido y evaluado complejos de Bz con oro(I) y (III) frente a promastigotes de *L. amazonensis*, *L. braziliensis* y *L. major* obteniendo valores de CI_{50} en el rango micromolar (compuesto **50** CI_{50} 1,29 µM) e IS bajos.[142] Tonelli y *col.* (2017)[143], obtuvieron un gran número de derivados benzimidazólicos que fueron evaluados frente a *L. infantum* y *L. tropica*, mostrando actividades <1 µM, de ellos destacan las sales de yoduro **51**-**54**. Los compuestos **51** y **52** mostraron actividad de 0,28 y 0,27 µM frente a *L. infantum*, **53** de 0,19 y 0,34 µM para *L. tropica* y *L. infantum*, respectivamente, mientras que, en **54** fue de 0,49 µM para *L. tropica*.

[141] Howarth, J.; Hanlon, K. *N*-ferrocenylmethyl, *N´*-methyl-2-substituted benzimidazolium iodide salts with in vitro activity against the *Leishmania infantum* parasite strain L1. *Bioorg. Med. Chem. Lett*. **2003**, 13, 2017-2020. doi: 10.1016/S0960-894X(03)00327-5

[142] Mota, V.Z.; Gonçalves de Carvalho, G.S.; da Silva, A.D.; Sodré Costa, L.A.; de Almeida Machado, P.; Soares Coimbra, E.; Veríssima Ferreira, C.; Mika Shishido, D.; Cuin, A. *Biometals.* **2014**, 27, 183-194. doi: 10.1007/s10534-014-9703-1

[143] Tonelli, M.; Gabriele, E.; Piazza, F.; Basilico, N.; Parapini, S.; Tasso, B.; Loddo, R.; Sparatore, F.; Sparatore, A. Benzimidazole derivatives endowed with potent antileishmanial activity. *J. Enzym. Inhib. Med. Ch.* **2017**, 33(1), 210-226. doi: 10.1080/14756366.2017.1410480

Por último, el derivado de 2,3-dihidroimidazo[1,2-*a*]Bz, **55**, mostró actividad moderada a nivel micromolar frente a promastigotes (1,25 µM) y amastigotes (3,05 µM, IS >16,4) de *L. donovani*.[144]

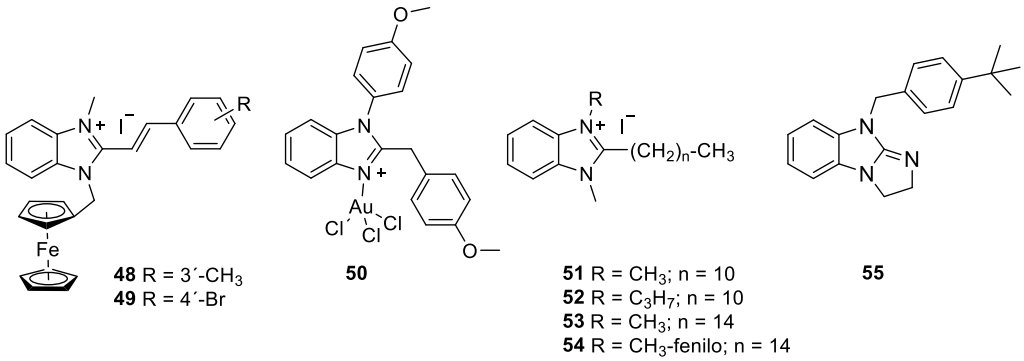

Figura I.23. Estructuras de algunos Bz activos frente a *Leishmania* spp.

En la Tabla I.5 se resumen otros resultados sobre los trabajos de Bz con actividad leishmanicida.

Tabla I.5. Benzimidazoles con baja actividad leishmanicida.

Tipo de derivado	**Cepa *Leishmania***	**Relevancia**	**Referencia**
2-(Fenantren-9-il)-1*H*-Bz	*L. mexicana*	CI_{50} de <5 µg/mL, valor similar a anfotericina.	Bandyopadhyay, 2017[145]
2-(4-((4-Nitrobenzil)oxi)fenil)-1*H*Bz	*L. donovani*	CI_{50} > 50 µM.	Kapil, 2019[146]
3'-Amido-2-fenilBz	*L. donovani*	PIC[a] (5 µM) 46 % in vitro.	Keurulainen, 2015[147]

[144] Oh, S.; Kim, S.; Kong, S.; Yang, G.; Lee, N.; Han, D.; Goo, J.; Siqueira-Neto, J.L.; Freitas-Junior, L.H.; Song, R. Synthesis and biological evaluation of 2,3-dihydroimidazo[1,2-*a*]benzimidazole derivatives against *Leishmania donovani* and *Trypanosoma cruzi*. *Eur. J. Med. Chem*. **2014**, 84, 395-403. doi: 10.1016/j.ejmech.2014.07.038

[145] Bandyopadhyay, D.; Samano, S.; Villalobos-Rocha, J.C.; Sánchez-Torres, L.E.; Nogueda-Torres, B.; Rivera, G.; Banik, B.K. A practical green synthesis and biological evaluation of benzimidazoles against two neglected tropical diseases: Chagas and Leishmaniasis. *Curr. Med. Chem*. **2017**, 24, 4714-4725. doi: 10.2174/0929867325666171201101807

[146] Kapil, S.; Singh, P.K.; Kashyap, A.; Silakari, O. Structure based designing of benzimidazole/benzoxazole derivatives as anti-leishmanial agents. *SAR and QSAR Environ. Res.* **2019**, 30(12), 919-933. doi: 10.1080/1062936X.2019.1684357

[147] Keurulainen, L.; Siiskonen, A., Nasereddin, A.; Kopelyanskiy, D.; Sacerdoti-Sierra, N.; Leino, T.O.; Tammela, P.; Yli-Kauhaluoma, J.; Jaffe, C.L.; Kiuru, P. Synthesis and biological evaluation of 2-arylbenzimidazoles targeting *Leishmania donovani*. *Bioorg. Med. Chem. Lett.* **2015**, 25, 1933-1937. doi: 10.1016/j.bmcl.2015.03.027

N-sustituidos	*L. mexicana*	CI_{50} de los dos mejores compuestos 52-82 µM. Acoplamiento molecular como inhibidores selectivos de arginasa de *L. mexicana*. IS bajos.	Betancourt-Conde, 2021[148]
2-(Trifluorometil)-1*H*-Bz	Promastigotes *L. mexicana*	CI_{50} 4,10-65,2 µM.	Hernández-Luis, 2010[149]
Schiff bases. Bioorganometálicos.	Amastigotes *L. braziliensis*	>4-106 µM. IS <3. Acoplamiento molecular frente a leishmanina.	Aragón-Muriel, 2021[133]
Bioorganometálicos. Derivados de plata.	Promastigotes y amastigotes de *L. major*	CI_{50} >5 µM. Baja selectividad (IS <3).	Khan, 2023[150]

[a] Porcentaje de inhibición de crecimiento

Benzimidazoles con actividad anti-Chagas

Por último, se indica la actividad anti-Chagas de algunos Bzs. Se obtuvieron derivados de 2-metilBz acoplados con *N*-acilhidrazona que mostraron buena actividad frente a la cepa Queretaro de *T. cruzi*, con valores de CI_{50} de 3 µM para el compuesto más activo, **56**.[151] Patel y *col.* (2020),[138] evaluaron la actividad anti-Chagas de los derivados piridínicos **42** y **43** (Fig. I.21), mencionados en el apartado de Bz leishmanicidas, obteniendo CI_{50} de 1,02 y 1,46 µg/mL, respectivamente, frente a la cepa *Tc*NINOA.

La sustitución en N-1 de Bz confiere a algunos derivados actividad anti-Chagas. Miana y *col.* (2019)[152] obtuvieron *N*-arilsulfonil-benzimidazoles, con valores de CI_{50} de 2,2-26,8 µM

[148] Betancourt-Conde, I.; Avitia-Domínguez, C.; Hernández-Campos, A.; Castillo, R.; Yépez-Mulia, L.; Oria-Hernández, J.; Méndez, S.T.; Sierra-Campos, E.; Valdez-Solana, M.; Martínez-Caballero, S.; Hermoso, J.A.; Romo-Mancillas, A.; Téllez-Valencia, A. Benzimidazole derivatives as new and selective inhibitors of arginase from *Leishmania mexicana* with biological activity against promastigotes and amastigotes. *Int. J. Mol. Sci.* **2021**, 22, 13613. doi: 10.3390/ijms222413613

[149] Hernández-Luis, F.; Hernández-Campos, A.; Castillo, R.; Navarrete-Vázquez, G.; Soria-Arteche, O.; Hernández-Hernández, M.; Yépez-Mulia, L. Synthesis and biological activity of 2-(trifluoromethyl)-1*H*-benzimidazole derivatives against some protozoa and *Trichinella spiralis*. *Eur. J. Med. Chem*. **2010**, 45, 3135-3141. doi: 10.1016/j.ejmech.2010.03.050

[150] Khan, T.A.; Mnasri, A.; Al Nasr, I.S.; Özdemir, I.; Gürbüzd, N.; Hamdi, N.; Biersack, B.; Koko, W.S. Activity of benzimidazole derivatives and their *N*-heterocyclic carbene silver complexes against *Leishmania major* promastigotes and amastigotes. *Biointerface Res. Appl. Chem.* **2023**, 13(3), 135. doi: 10.33263/BRIAC132.135

[151] Melchor-Doncel de la Torre, S.; Vázquez, C.; González-Chávez, Z.; Yépez-Mulia, L.; Nieto-Maneses, R.; Jasso-Chávez, R.; Saavedra, E.; Hernández-Luis, F. Synthesis and biological evaluation of 2-methyl-1*H*-benzimidazole-5-carbohydrazides derivatives as modifiers of redox homeostasis of *Trypanosoma cruzi*. *Bioorg. Med. Chem. Lett*. **2017**, 27, 3403-3407. doi: 10.1016/j.bmcl.2017.06.013

[152] Miana, G.E.; Ribone, S.R.; Vera, D.M.A.; Sánchez-Moreno, M.; Mazzieri, M.R.; Quevedo, M.A. Design, synthesis and molecular docking studies of novel *N*-arylsulfonyl-benzimidazoles with anti-*Trypanosoma cruzi* activity. *Eur. J. Med. Chem*. **2019,** 165, 1-10. doi: 10.1016/j.ejmech.2019.01.013

frente a epimastigotes de *T. cruzi*, concretamente, **57**, **58** y **59** mostraron actividades de 2,6 µM, 3,0 µM y 2,2 µM, respectivamente, además, presentaron IS superiores al benznidazol (0,8), con valores de 346,7, 68,5 y 205,3, respectivamente.

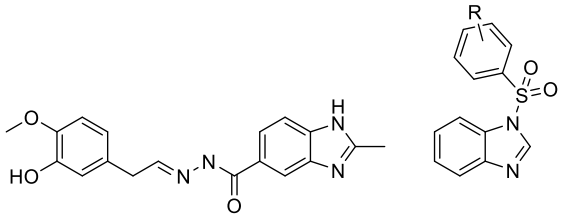

56

57 R = 4´-NO_2
58 R = 4´-$C(CH_3)_3$
59 R = 2´,3´,5´,7´-tetraCH_3

Figura I.24. Estructuras de varios benzimidazoles activos frente a *T. cruzi.*

El 2-amidoalquilBz **60**, sintetizado por el grupo de Díaz-Chiguer (2012)[153] como inhibidor de la cruzaína, mostró CI_{50} de 200 nM frente a las cepas *Tc*INC-5 y *Tc*NINOA de *T. cruzi*. Por otro lado, el mismo grupo de investigación obtuvo una serie de derivados de 2-mercapto-1*H*-Bz que mostraron actividad (CI_{50} <10 µM), e IS >50. Pauli y *col.* (2022),[154] basándose en los resultados previos del grupo, sintetizaron y evaluaron derivados de *N*-alquilbenzimidazol, como los compuestos **61** (CI_{50} 1,04 µM frente a *T. cruzi*) y **62** (CI_{50} 1,6 µM frente a *T. cruzi* y, de 0,8 µM frente a la cruzaína). Por otro lado, las N^1-alquil-2-fenilacetamidas también parecen ser estructuras prometedoras frente a *T. cruzi*. Así, los compuestos **63**-**66** mostraron CI_{50} del orden micromolar anti-Chagas.[155]

[153] Díaz-Chiguer, D.L.; Márquez-Navarro, A.; Nogueda-Torres, B.; León-Ávila, G.L.; Pérez-Villanueva, J.; Hernández-Campos, A.; Catillo, R.; Ambrosio, J.R.; Nieto-Maneses, R.; Yépez-Mulia, L.; Hernández-L. In vitro and in vivo trypanocidal activity of some benzimidazole derivatives against two strains of *Trypanosoma cruzi*. *Acta Trop*. **2012**, 122, 108-112. doi: 10.1016/j.actatropica.2011.12.009

[154] Pauli, I.; Rezende, C.O.; Slafer, B.W.; Dessoy, M.A.; de Souza, M.L.; Ferreira, L.L.G.; Adjanohun, A.L.M.; Ferreira, R.S.; Magalhães, L.G.; Krogh, R.; Michelan-Duarte, S.; Vaz del Pintor, R.; da Silva, F.B.R.; Cruz, F.C.; Días, L.C.; Andricopulo, A.D. Multiparameter optimization of trypanocidal cruzain inhibitors with in vivo activity and favorable pharmacokinetics. *Front. Pharmacol*. **2022**, 12, 774069. doi: 10.3389/fphar.2021.774069

[155] McNamara, N.; Rahmani, R.; Sykes, M.L.; Avery, V.M.; Baell, J. Hit-to-lead optimization of novel benzimidazole phenylacetamides as broad spectrum trypanosomacides. *RSC Med. Chem*. **2020**, 11(6), 685-695. doi: 10.1039/d0md00058b

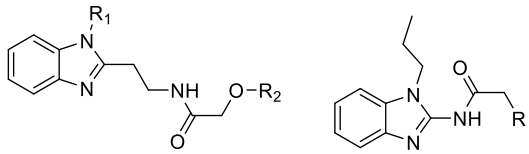

60 R_1 = Br-naft-2-ilo; R_2 = H
61 R_1 = fenilo; R_2 =CH_2-fenilo
62 R_1 = fenilo; R_2 =$(CH_2)_2$-fenoxilo

63 4´-CF_3-fenilo
64 4´-OCF_3-fenilo
65 4´,4´´-bifenilo
66 naft-1-ilo

Figura I.25. Estructuras de algunos Bz sustituidos en N1 y C-2 activos frente a *T. cruzi.*

Por último, Oh y *col.*[144] (2014) ensayaron la actividad anti-Chagas de los imidazoBz relacionados con **55**, ensayados frente a *Leishmania*, encontrando una CI_{50} <5 µM para los derivados más activos. Concretamente, **55** (Fig. I.23) mostró CI_{50} 1,10 µM e IS de 33.

En la Tabla I.6 se detallan los resultados de Bz que mostraron baja actividad frente a Chagas.

Tabla I.6. Benzimidazoles con baja actividad anti-Chagas.

Tipos de derivados	**Cepa**	**Relevancia**	**Referencia**
2-Mercapto-1*H*-Bz	Epimastigotes de *Tc*INC-5	CI_{50} > 28 µM. Inhibición de *Tc*TIM (enzima triosafosfato isomerasa).	Velázquez-López, 2015[156]
2-Aril-1*H*-Bz	Tripomastigotes de *Tc*INC-5	CI_{50} 4,9- >100 µg/mL. El compuesto más activo con ferroceno.	Bandyopadhyay, 2017[145]
N-(1*H*-Bz-2-il)-bencenosulfonamida	Tripomastigotes de *Tc*INC-5 y *Tc*NINOA	CL_{50} 49,98-101,46 µg/mL.	Bocanegra-García, 2012[157]
N-sustituidos	Epimastigotes CL-Luc:Neon	11,1-24,8 µM. IS bajos.	Beltrán-Hortelano, 2021[158]

[156] Velázquez-López, J.M.; Hernández-Campos, A.; Yépez-Mulia, L.; Téllez-Valencia, Flores-Carillo, P.; Nieto-Maneses, R.; Castillo, R. Synthesis and trypanocidal activity of novel benzimidazole derivatives. *Bioorg. Med. Chem. Lett*. **2015**, 26(17), 4377-4381. doi: 10.1016/j.bmcl.2015.08.018

[157] Bocanegra-García, V.; Villalobos-Rocha, J.C.; Nogueda-Torres, B.; Lemus-Hernández, M.E.; Camargo-Ordoñez, A.; Rosas-García, N.M.; Rivera, G. Synthesis and biological evaluation of new sulfonamide derivatives as potential anti-*Trypanosoma cruzi* agents. *Med. Chem.* **2012**, 8, 1039-1044. doi: 10.2174/157340612804075133

[158] Beltrán-Hortelano, I.; Atherton, R.L.; Rubio-Hernández, M.; Sanz-Serrano, J.; Alcolea, V.; Kelly, J.M.; Pérez-Silanes, S.; Olmo, F. Design and synthesis of Mannich base-type derivatives containing imidazole and benzimidazole as lead compounds for drug discovery in Chagas Disease. *Eur. J. Med. Chem*. **2021**, 223, 113646. doi: 10.1016/j.ejmech.2021.113646

N-sustituidos	Amastigotes	CI_{50} 1,3- >57 µM. Inhibidores reversibles no covalentes de la cruzaína. Buena selectividad.	Luci, 2013[159]
2-NO_2-Bz *N*-sustituidos	Epimastigotes de *Tc*MF	CI_{50} >60 µM. Espectrometría de UV y HPLC para caracterizar los compuestos.	Brain-Isasi, 2008[160]
Bioorganometálicos	Epimastigotes de *Tc*Dm28c	CI_{50} >80 µM. 2-ciretrenil-5-NO_2-Bz y 2-ferrocenil-5-NO_2-Bz y 2-fenil-5-NO_2-Bz	Barriga-González, 2021[161]
Bioorganometálicos	Amastigotes Tulahuen	13,6-179 µM. IS<3. Acoplamiento molecular frente a cruzaína. Bases de Schiff.	Aragón-Muriel, 2021[133]

[159] Luci, D.; Lea, W.; Ferreira, R.; Shoichet, B.; Simeonov, A.; Rodriguez, A.; Jadhav, A.; Maloney, D.J. Reversible and non-covalent benzimidazole-based in vivo lead for Chagas disease. En *Probe Reports from the NIH Molecular Libraries Program* [Internet]. Bethesda (MD): National Center for Biotechnology Information (US); 2010.

[160] Brain-Isasi, S.; Quezada, C.; Pessoa, H.; Morello, A.; Kogan, M.J.; Álvarez-Lueje, A. Determination and characterization of new benzimidazoles with activity against *Trypanosoma cruzi* by UV spectroscopy and HPLC. *Bioorg. Med. Chem*. **2008**, 16, 7622-7630. doi: 10.1016/j.bmc.2008.07.021

[161] Barriga-González, G.; Olivares-Petit, C.; Toro, P.M.; Klahn, A.H.; Olea-Azar, C.; Maya, J.D.; Huentupil, Y.; Arancibia, R. Electrochemical, ESR, theoretical studies and in vitro anti-*T. cruzi* activity of 2-organometallic-5-nitro benzimidazoles. *J. Chil. Chem. Soc.* **2020**, 65(1), 4692. doi: 10.4067/S0717-97072020000104692

II. PLANTEAMIENTO Y OBJETIVOS

II.1. PLANTEAMIENTO DEL TRABAJO

En el apartado de introducción se han expuesto algunas de las limitaciones que presentan los fármacos actuales para el tratamiento de determinadas enfermedades infecciosas, como la alta toxicidad, el elevado coste económico o el aumento de cepas resistentes a esos fármacos, lo que pone de manifiesto la necesidad de encontrar nuevas alternativas terapéuticas.

El grupo de investigación en el que se ha realizado este Trabajo de Tesis Doctoral presenta una amplia experiencia en diseño y síntesis de nuevas moléculas bioactivas, ya sea por modificación de metabolitos secundarios procedentes de plantas como la podofilotoxina (aislada de la resina de *Podophyllum* spp.), llegando a desarrollar compuestos antineoplásicos más potentes y selectivos, o el ácido isonotholaénico (aislado de *Notholaenea nivea* var. *nivea*) a partir del cual se obtuvieron moléculas con actividad antiparasitaria (anti-*Plasmodium*, leishmanicida, anti-Chagas), entre otros esqueletos, o bien por síntesis total generando compuestos con núcleo de benzalftalida, ftalazinona, imidazo-isoindol, aminoalcohol y diaminas alifáticas con actividades diversas, como antiparasitarias, antiadrenérgica, inmunomoduladora o antiinfecciosa, entre otras.

Es este Trabajo de Tesis se plantea, por un lado, obtener nuevos compuestos con actividad nematicida (anti-*Teladorsagia*), y por otro, compuestos con actividad antiparasitaria (anti-*Plasmodium*, anti-*Leishmania*, anti-Chagas). En el primer caso, se seleccionaron compuestos representativos de algunas familias (derivados de podofilotoxina, benzalftalida, ftalazinona, imidazo-isoindol, aminoalcohol y diaminas alifáticas), que fueron

ensayados in vitro frente a *Teladorsagia circumcincta* por el grupo de investigación del Dr. Balaña-Fouce de la Universidad de León (España), encontrándose resultados prometedores para algunas benzalftalidas y ftalazinonas, y moderados entre los aminoalcohol y diaminas alifáticas, por lo que se decidió ampliar las variantes de sustituyentes en las familias de benzalftalidas (Bf) y de ftalazinonas (Ft).

Benzalftalidas

Se diseñan nuevas Bf sin sustituir o con metilo en el anillo A, y grupos dadores y atractores de electrones en el anillo B, así como grupos voluminosos con el fin de estudiar la relación entre la estructura y la actividad, Fig. II.1.

Ftalazinonas

Se plantea obtener nuevas Ft sin sustituciones en el anillo A, y aumento en el tamaño del sustituyente R_3, diferentes a H y CH_3 iniciales, para determinar su influencia y establecer relaciones entre la estructura y la actividad, Fig. II.1.

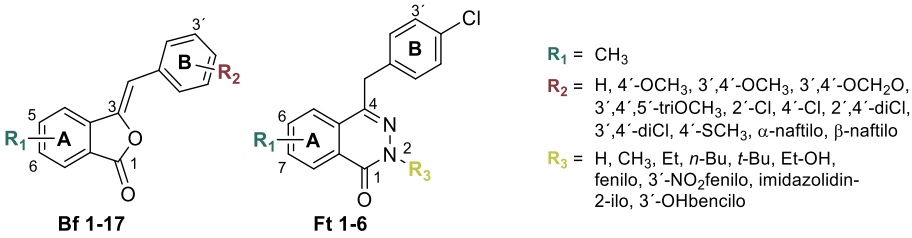

Figura II.1. Benzalftalidas y ftalazinonas obtenidas.

Benzimidazoles

Con el fin de ampliar el número y tipo de compuestos a obtener, y dado que en moléculas con estructura de lignano (podofilotoxina) o imidazo-isoindol no se obtuvieron resultados relevantes, se decidió obtener derivados con un núcleo diferente, concretamente el de benzimidazol.

En el apartado 2.2 de la introducción se ha indicado que el anillo de Bz está presente en numerosos fármacos existentes en el arsenal terapéutico, con aplicaciones muy variadas, como antihipertensivos, anticancerígenos, antihistamínicos, fungicidas o antiparasitarios,

entre otras, incluso en algunos medicamentos con actividad nematicida. Para esta última, los fármacos más extensamente utilizados (albendazol, mebendazol) poseen un grupo carbamato en la posición C-2 del Bz, y se ha visto que está estrechamente ligado a las mutaciones F200Y, F167Y y E198A en el isotipo-1 de la subunidad β de la tubulina, disminuyendo así su eficacia. Por lo que la sustitución de ese fragmento por otros ricos en electrones como puede ser un anillo de benceno o un heterociclo, unido a nuevas modificaciones sobre el anillo bencénico del Bz (R), permitiría obtener un amplio número de variantes estructurales, y ofrecería, quizá, la posibilidad de obtener compuestos activos frente a las cepas resistentes, mostrando además buena eficacia y tolerancia.

Por ello, en este trabajo de Tesis se plantea la obtención de compuestos de **tipo I**, con un anillo de benceno o un heterociclo directamente unido en la posición C-2; **tipo II** con un espaciador de amina entre el anillo de Bz y el Ar; y **tipo III** con un espaciador amida, acetamida ò acrilamida entre el anillo de Bz y el Ar, Fig. II.2.

Adicionalmente, se decidió explorar la actividad antiparasitaria (anti-*Plasmodium*, leishmanicida, anti-Chagas) de los compuestos obtenidos, ya que se encuentran numerosos artículos sobre la actividad antiprotozoaria de Bz en la bibliografía.

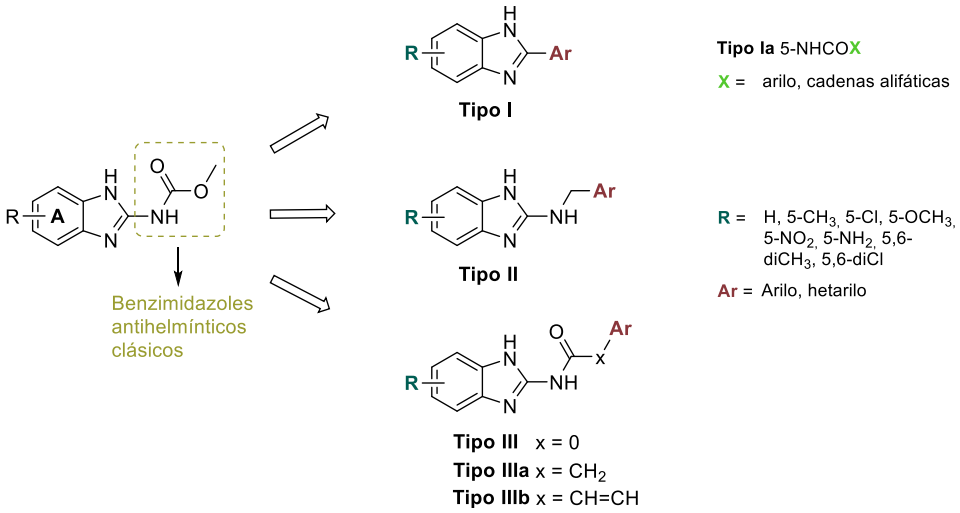

Figura II.2. Derivados de benzimidazol obtenidos.

Benzalftalidas y ftalazinonas

Resultados previos del grupo de investigación sobre benzalftalidas y ftalazinonas (compuestos intermedios en la ruta de síntesis) frente a algunos protozoos (Olmo, 2001[81])

(Olmo, 2003[80]), indicaban una buena actividad frente a epimastigotes de *Trypanosoma cruzi* (CI_{50} 2,3 μM; IS 12,4[162]) para **F-18061**, por lo que se ampliará la serie con compuestos del tipo **Ft-xx**.

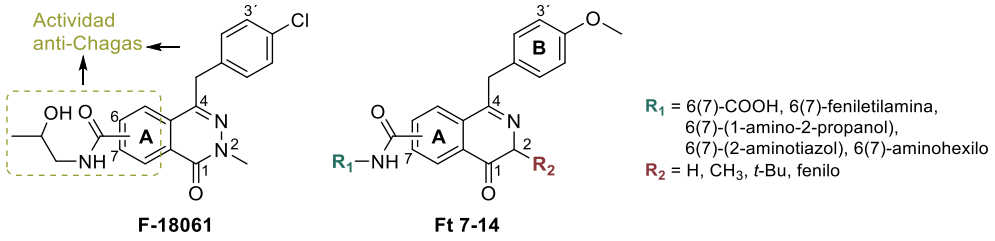

Figura II.3. Estructura general de las nuevas ftalazinonas a sintetizar.

Los ensayos de actividad antiprotozoaria se llevarán a cabo en el grupo de la Dra. Carmenza Spadafora del INDICAST-AIP de Panamá (Panamá).

Benzimidazoles

Todos los Bz obtenidos para ensayos frente a *Teladorsagia* serán testados frente a protozoos (*Plasmodium falciparum*, *Leishmania donovani*, *Trypanosoma cruzi*), ampliando las series cuando se considere oportuno, con el fin de establecer relaciones entre la estructura y la actividad.

Benzimidazolonas

Se ha encontrado en la bibliografía algunos trabajos que indican la actividad anti-*Plasmodium* de benzimidazolonas (Bzo). Así, se obtendrán nuevos derivados, cuya estructura se muestra en la Fig.II.4, que serán evaluados frente *P. falciparum*, *L. donovani* y *T. cruzi.*

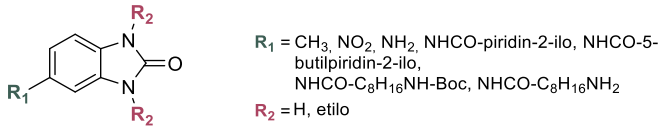

Figura II.4. Modificaciones sobre la estructura de benzimidazolonas.

[162] García Cadenas, Ana Esther. *Síntesis, actividad vasorrelajante y potencial quimioterápico de ftalazinonas y compuestos relacionados*. Tesis doctoral, Universidad de Salamanca, 2005.

II.2. OBJETIVOS

El **objetivo principal** de este Trabajo de Tesis consiste en el hallazgo de nuevas moléculas activas frente a *Teladorsagia circumcincta,* y frente a algunos protozoos (anti-*Plasmodium*, leishmanicida, anti-Chagas), con posible aplicación en el tratamiento de cepas resistentes. Para alcanzar este objetivo general, se plantean los siguientes **objetivos específicos**:

En la obtención de compuestos activos frente a Teladorsagia circumcincta

1. Considerando los resultados previos de actividad de **benzalftalidas** y **ftalazinonas** frente a *T. circumcincta*. Se diseñarán y obtendrán nuevos derivados con átomos atractores y dadores de electrones en R_1 y R_2, y un aumento el tamaño del sustituyente R_3 en el caso de las ftalazinonas.

2. Teniendo en cuenta que el principal mecanismo de acción de los **benzimidazoles** es su unión al sitio de colchicina en la β-tubulina. Se obtendrá la estructura 3D de la β-tubulina de *T. circumcincta* por homología molecular, que será validada con las herramientas informáticas adecuadas, para después realizar estudios de docking y modelado molecular con colchicina y algún fármaco comercial. Estos estudios permitirán definir las uniones fármaco-diana y determinar las distancias, lo que servirá para seleccionar el tamaño y geometría de las nuevas moléculas a sintetizar. También, se conocen los aminoácidos que mutan en casos de resistencias, lo que será de utilidad para el diseño de las moléculas a sintetizar.

3. Se pondrá a punto el proceso de obtención de los benzimidazoles diseñados (compuesto **tipo I**). Los compuestos serán purificados y caracterizados según propiedades fisicoquímicas y serán remitidos para su ensayo en *T. circumcincta.* Con los resultados obtenidos se establecerán relaciones entre la estructura y la actividad.

4. Se ampliará la serie de Bz, introduciendo un elemento espaciador entre el anillo de benzimidazol y el anillo aromático en posición C-2 con aminas (compuesto

tipo II) y amidas (compuesto **tipo III**). Con los resultados obtenidos se establecerán relaciones entre la estructura y la actividad.

5. Los resultados de actividad in vitro de los apartados 3 y 4, permitirán seleccionar uno o dos compuestos para ensayos in vivo en corderos infectados con *Haemonchus contortus.* Así, se obtendrán las cantidades necesarias de los compuestos seleccionados.

6. Se plantea la posibilidad de ampliar los ensayos de los Bzs obtenidos a otros nematodos gastrointestinales como *Heligmosomoides polygyrus* y *Trichuris muris.*

En la obtención de compuestos activos frente a protozoos

7. Se ensayarán las **benzalftalidas**, **ftalazinonas** y los **benzimidazoles** obtenidos frente a los protozoos indicados (*Plasmodium falciparum*, *Leishmania donovani*, *Trypanosoma cruzi*).
8. Se ampliarán las series de compuestos necesarios con el fin de establecer relaciones entre la estructura y la actividad.

II.3. OBSERVACIONES PREVIAS

Sistema de enumeración

Debido a la variedad de funciones, agrupaciones o anillos adicionales, se ha considerado oportuna la enumeración, que no siempre coincide con la establecida por la IUPAC, de los compuestos obtenidos para facilitar la compresión de la presentación. En el siguiente esquema, se presentan los tipos estructurales de los compuestos sintetizados en este trabajo de Tesis Doctoral y la numeración utilizada para cada uno de ellos.

Claves para las familias sintetizadas

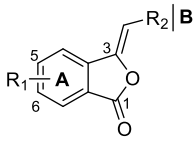

Benzalftalida
(Bf-xx)

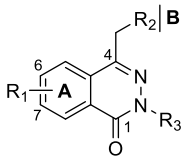

Ftalazinona
(Ft-xx)

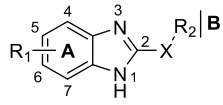

Benzimidazol
(Bz.xxx)

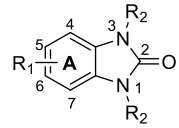

Benzimidazolona
(Bzo.xxx)

B = fenilo, arilo o hetarilo

Claves para las familias de benzimidazol sintetizadas

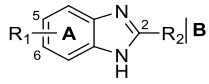

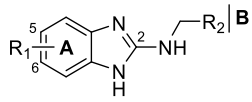

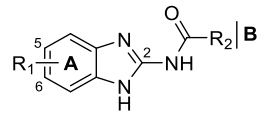

Ia: 5-NHCO-**X**; Ib: 3´-(**Y**CO-**Z**)-fenilo

IIIa:  ; IIIb: 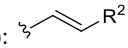

Tipo I
BzI.xxx
BzIa.xxx.xxx
BzIb.xxx.xxx
B = fenilo, arilo o hetarilo

Tipo II
BzII.xxx

Tipo III
BzIII.xxx

Claves para los sustituyentes en el anillo A de benzimidazol

Bz.0xxx	5-H	**Bz.5xxx**	5-NH_2
Bz.1xxx	5-CH_3	**Bz.6xxx**	5,6-diCH_3
Bz.2xxx	5-Cl	**Bz.7xxx**	5,6-diCl
Bz.3xxx	5-OCH_3	**Bz.8xxx**	5,6-benzo
Bz.4xxx	5-NO_2		

Claves para los sustituyentes en el anillo B de benzimidazol

X.x10	Ph	**X.300**	furan-2-ilo
X.x20	4´-CH_3Ph	**X.301**	5´-CH_3-furan-2-ilo
X.x30	4´-OCH_3Ph	**X.302**	5´-NO_2-furan-2-ilo
X.x40	4´-ClPh	**X.303**	benzofuran-2-ilo
X.x41	3´-ClPh	**X.304**	5´-Br-benzofuran-2-ilo
X.x50	4´-BrPh	**X.310**	tiofen-2-ilo
X.x60	4´-NO_2Ph	**X.311**	4´-CH_3-tiazol-5-ilo
X.x61	3´-NO_2Ph	**X.312**	2´-CH_3-piperazin-tiazol-5-ilo
X.x62	2´-NO_2Ph	**X.320**	2´-CH_3-imidazol-5-ilo
X.x70	4´-NH_2Ph	**X.321**	*N*-CH_3-indol-2-ilo
X.x71	3´-NH_2Ph	**X.330**	piridin-2-ilo
X.x81	3´-OHPh	**X.331**	3´-CH_3-piridin-2-ilo
X.x82	2´-OHPh	**X.332**	3´-Cl-piridin-2-ilo
X.x90	4´-(pirrolidin-1-ilo)Ph	**X.333**	4´-OCH_3-piridin-2-ilo
X.100	4´-Ph-Ph	**X.334**	5´-CH_3-piridin-2-ilo
X.110	3´-(4´´-COOH-Ph)Ph	**X.335**	5´-butilpiridin-2-ilo
X.120	4´-(4´´-toliloxilo)Ph	**X.336**	5´-CN-piridin-2-ilo
X.130	2´,4´-diF Ph	**X.337**	5´-Ph-piridin-2-ilo
X.140	2´,5´-diCH_3Ph	**X.338**	6´-CH_3-piridin-2-ilo
X.150	2´-Cl, 5´-NO_2Ph	**X.340**	piridin-3-ilo
X.160	3´-OH, 4´-OCH_3Ph	**X.350**	piridin-4-ilo
X.170	3´,4´-diOCH_3Ph	**X.360**	quinolin-2-ilo
X.180	3',4´-OCH_2OPh	**X.361**	6´-OCH_3-quinolin-2-ilo
X.190	3´-NO_2, 4´-OCH_3Ph	**X.362**	8´-OH-quinolin-2-ilo
X.200	3´-NH_2, 4´-OCH_3Ph	**X.370**	quinolin-3-ilo
X.210	3',5´-diOCH_3Ph	**X.380**	quinolin-4-ilo
X.220	naft-1-ilo	**X.390**	isoquinolin-1-ilo
X.230	6-NH_2-naft-2-ilo	α	2-Boc-aminododecanoilo
X.231	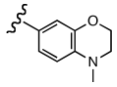	β	2-aminododecanoilo
		δ	2-Boc-decanoilo
		γ	2-aminodecanoilo
X.232	indol-5-ilo	ε	*terc*-butiloxicarbonilo
X.240	benzotriazol-5-ilo	τ	glutarilo
X.250	2´,3´,4´-triOCH_3Ph		
X.251	3´,5´-diOCH_3, 4´-OHPh		
X.252	3´,4´,5´-triOCH_3Ph		
X.260	α-OHbencilo		
X.270	ibuprofenilo		

III. PUBLICACIONES CIENTÍFICAS

Para esta Memoria de Tesis se ha elegido la modalidad de artículos científicos. A continuación, se expondrán los distintos trabajos en relación con los objetivos a alcanzar en el Trabajo de Tesis, algunos de ellos ya han sido publicados, otros están en proceso de revisión, y el resto en redacción.

III.1. ARTÍCULO 1

Este artículo está relacionado con el objetivo 1 del Trabajo de Tesis.

El uso indiscriminado de agentes antihelmínticos en la ganadería ha provocado la aparición de resistencias a los fármacos disponibles para el tratamiento de las infecciones por nematodos gastrointestinales, lo que evidencia la necesidad de buscar nuevas alternativas terapéuticas.

Basado en los resultados previos obtenidos por el grupo de investigación sobre la actividad de compuestos con estructura de benzalftalida y ftalazinonas contra *Teladorsagia circumcincta*, se realizó un diseño nuevo de derivados y se optimizaron los procesos de síntesis. Estos compuestos fueron evaluados in vitro frente a la cepa sensible de *T. circumcincta*, los resultados obtenidos condujeron a la selección de los dos compuestos más potentes para ser ensayados frente a una cepa resistente de *T. circumcincta*.

Anthelmintic activity of benzalphthalides and phthalazinones against *Teladorsagia circumcincta*: synthesis and structure-activity relationship

Nerea Escala, Elora Valderas-García, Bianca Barboza, Sobinson Arsène, Matheus C. Romeiro Miranda, Rafael Balaña-Fouce, María Martínez-Valladares, Esther del Olmo

En: Revista Brasileira de Parasitologia Veterinária

Factor de Impacto: 1,415
Quartil: Q2

Anthelmintic activity of benzalphthalides and phthalazinones against *Teladorsagia circumcincta*: synthesis and structure-activity relationship

Nerea Escala [a], Elora Valderas-García [b,c], Bianca Barboza [a], Sobinson Arsène [a], Matheus C. Romeiro Miranda[a,d], Rafael Balaña-Fouce [b], María Martínez-Valladares *[c,e], Esther del Olmo *[a]

[a] Departamento de Ciencias Farmacéuticas: Química Farmacéutica, Facultad de Farmacia, Universidad de Salamanca, CIETUS, IBSAL, 37007-Salamanca, Spain.
[b] Departamento de Ciencias Biomédicas, Facultad de Veterinaria, Universidad de León, 24071-León, Spain
[c] Instituto de Ganadería de Montaña, CSIC-Universidad de León, 24346-Grulleros, León, Spain.
[d] Instituto de Ciências Ambientais, Químicas e Farmacêuticas, Universidade Federal de São Paulo, Diadema, SP, Brazil.
[e] Departamento de Sanidad Animal, Facultad de Veterinaria, Universidad de León, 24071-León, Spain
*Corresponding authors: olmo@usal.es (E. del Olmo, Chemistry), rbalf@unileon.es (R. Balaña-Fouce, Toxicity studies), mmarva@unileon.es (M. Martínez-Valladares, in vitro helminth assays).

Abstract

Infections caused by nematodes are very common in both humans and animals. Among them, those produced by gastrointestinal nematodes (NGI) are one of the most prevalent in grazing ruminants, constituting an important health problem in livestock farms. Several drugs in the therapeutic arsenal for the treatment of GIN are available, however, their indiscriminate use has led to the development of resistance worldwide, which represents an important problem that needs an urgent solution. The aim of this study was to synthesize and tests the ovidical and larvicidal activity against *Teladorsagia circumcincta* (*T.c.*) of some heterocycle compounds, such as benzalphthalides (Bp) and phthalazinones (Pt). The activity of twenty-four Bp and thirteen Pt with modifications on ring B with electron donating or withdrawing groups attached to different positions of the phenyl ring, and bulky fragment such as α- or β-naphthyl were analyzed, they show non-substitution or a methyl in ring A. Pt **26** showed excellent nematocidal activity in the Egg Hatch Assay in both susceptible and resistant strain of *T.c.* at 10 µg/mL, with values of of 75.5 and 99.4%, respectively. **26** was also a good ovicidal, showing 99.0% LMT inhibition at 10 µg/mL in the *T.c* susceptible strain, which was higher than the control levamisole.

Resumo

Infecções causadas por nematóides são muito comuns em humanos e animais. Dentre eles, os produzidos por nematoides gastrointestinais (NGI) são um dos mais prevalentes em ruminantes em pastejo, constituindo um importante problema de saúde nas

fazendas pecuárias. Diversas drogas do arsenal terapêutico para o tratamento da GIN estão disponíveis, entretanto, seu uso indiscriminado tem levado ao desenvolvimento de resistência em todo o mundo, o que representa um problema importante que necessita de solução urgente. O objetivo deste estudo foi sintetizar e testar a atividade ovídica e larvicida contra *Teladorsagia circuncincta* (*T.c.*) de alguns compostos heterocíclicos, como benzalftalidas (Bp) e ftalazinonas (Pt). A atividade de vinte e quatro Bp e treze Pt com modificações no anel B com grupos doadores ou retiradores de elétrons ligados a diferentes posições do anel fenil e fragmentos volumosos como α- ou β-naftil foram analisados, eles mostram não substituição ou a metil no anel A. A Pt 26 apresentou excelente atividade nematocida no Ensaio de Eclosão de Ovos em cepas susceptíveis e resistentes de *T.c*. a 10 μg/mL, com valores de 75,5 e 99,4%, respectivamente. 26 também foi um bom ovicida, mostrando 99,0% de inibição de LMT a 10 μg/mL na cepa suscetível a T.c, que foi maior que o levamisol controle.

Keywords: Phthalazinones, synthesis, *Teladorsagia circumcincta*, in vitro assays, cytotoxicity, resistant strain

Introduction

The infections caused by gastrointestinal nematodes (GIN) are one of the most prevalent in grazing ruminants, constituting an important health problem, especially in sheep, due to lower growth, reduction in milk production, and poor quality of wool, decreased fertility and even produce death when the load of worms is very high (Moje *et al*., 2021) (Craig, 2018). All this generates considerable economic losses in livestock farms of grazing animals. Most frequent GIN infections are caused by *Teladorsagia* (Ostertagia) spp., *Haemonchus contortus*, *Trichostrongylus* spp., among others.

Various broad-spectrum anthelmintic agents in the therapeutic arsenal for the treatment of GIN (albendazole, fenbendazole, ivermectin, monepantel, etc.) are available. However, in the last decades, their incorrect and massive use has led to therapeutic failure and the generation of resistances worldwide (Sargison, 2012). In this context, new chemical entities for the GIN treatment are needed, for that, different approaches have been proposed, such as the identification of active natural products, the synthesis of novel chemical compounds, drug repurposing, or the synthesis of new derivatives of established drugs (Zajíčková *et al*., 2020).

The presence of a heterocyclic skeleton is very common in molecules of interest in medicinal chemistry. Among the great variety of heterocyclic compounds we can include those containing hydrazine, which show a wide structural variation and several pharmaceutical applications, such as antihypertensive (Demirayak *et al*., 2004), anticonvulsant (Sivakumar *et al*., 2002) or antimicrobial (Pathak S *et al*., 2013), among others, playing a considerable role in Medicinal Chemistry. Moreover, the phthalazinone skeleton represents a nucleus with a wide variety of applications, such as antihistaminic (azelastine), antidiabetic (ponalrestat) or antitumor (olaparib) activities (Terán *et al*., 2019).

Our research group has a great experience in heterocyclic derivatives obtaining, including arylindazoles (Viña *et al.* 2007), pyrazolophthalazines (Viña, *et al*. 2008) quinoline derivatives (Kouznetsov *et al.* 2012a), or imidazoisoindoles (Arsène *et al*. 2019), among others, some of those compounds were tested as antifungal. Recently, the group has worked on the synthesis of new molecules with nematocidal properties. In this context, they have obtained new derivatives of benzimidazole (BZ) type (Escala *et al*., 2020) (Escala *et al*., 2022), as well as of aliphatic aminoalcohol and diamine type (Valderas *et al*., 2021), some of these compounds showed excellent in vitro activity in sensitive and resistant strains of *Teladorsagia circumcincta* and were selected for in vivo tests in gerbils and sheep (Valderas *et al*., 2022). Following with this approach, we have decided to explore the nematocide profile of other heterocyclic nucleus, such benzalphthalides and phthalazinones, the former contains oxygen as a heteroatom and the latter an hydrazine group. In previous works, compounds from these families were tested as antiparasitics (*Leishmania* spp (del Olmo *et al.,* 2001), *Trypanosoma cruzi* (del Olmo *et al.,* 2001), *Plasmodium falciparum* (del Olmo *et al.,* 2003), or anti-HIV (Bedoya *et al*., 2006). Some benzalphthalides showed excellent anti-anxiety activity (Zamilpa *et al.,* 2005), and phthalazinones good vasorelaxant (del Olmo *et al.,* 2006), and antifungal results (Derita *et al.,* 2013).

Therefore, we describe here the synthesis and in vitro activity against *Teladorsagia circumcincta* of some benzalphthalides and phthalazinones, the latter are obtained from the former, and the influence of the substituents in rings A and B in relation to the activity were analyzed (Fig. 1). The compounds obtained were tested against eggs and larvae (L1) of a sensitive strain of *T. circumcincta*. The most potent compounds were selected to be tested on a resistant strain of *T. circumcincta.*

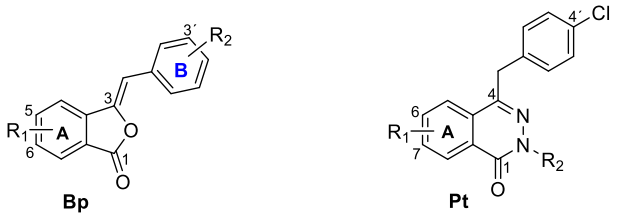

R1 = H, CH_3
R2 = H, 4´-OMe, 3´,4´-diOMe, etc.
B = α-naphthyl, β-naphthyl

R1 = H, CH_3
R2 = Me, Et, Allyl, But, etc.

Figure 1. General structure of the benzalphthalides and phthlazinones obtained.

Material and Methods

Chemistry. All commercial chemicals (Aldrich, Alpha, Fischer, SDS) were used as purchased and solvents (Fischer, SDS, Scharlau) purified by the standard procedures prior to use. Reactions were monitored by Thin Layer Chromatography (TLC) (Kieselgel 60 F254 precoated plates, E. Merck, Germany), the spots were detected by exposure to UV light at λ 254 nm, and colorization with 10% phosphomolybdic acid spray, with further heating of the plate. Melting points (Mp) were determined with Mel-Temp apparatus in open capillaries and were uncorrected. Separations by flash column chromatography were performed on Merck 60 silica gel (0.063-0.2 mesh). Infrared spectra were recorded on a FT-IR spectrometer Perkin Elmer System BX, using NaCl or KBr disks. NMR spectra were recorded on a Bruker Avance or Varian Mercury 200 and 400 MHz (200 MHz for ^{1}H, 50 MHz for ^{13}C; 400 MHz for ^{1}H, 100 MHz for ^{13}C). The spectra were measured either in $CDCl_3$, methanol-d4 or DMSO-d6, using tetramethylsilane (TMS) as internal standard, chemical shifts (δ) are given in ppm and coupling constants (*J*) in Hertz (Hz). High resolution mass spectra (HRMS) were obtained by electron spray ionisation-mass spectrometry (ESI-MS) technique (5 kV) on a QSTAR XL mass spectrometer. Microwave synthesis procedures were performed under selected conditions in a Monowave 300 microwave reactor (AP-MW; Anton Parr).

General procedures for preparation of compounds

Procedure for the synthesis of benzalphthalides 13, 14, 20-23 by Dean-Stark system. We have followed a procedure similar to that indicated by Zamilpa *et al*. (2005). 324.0 mg (2.0 mmol) of 5-methylphthalic anhydride, 459.0 mg (2.7 mmol) of 4-chlorophenylacetic acid and 25.6 mg (0.26 mmol) of potassium acetate were mixed in a two-necked flask. Then, dry toluene (5 mL) was added, and the mixture was maintained at 220 ºC in a Dean-Stark apparatus with magnetic stirring for 24 h. After completion of the reaction (monitored by

TLC), it was taken to dryness in a rotary evaporator, and the obtained crude was extracted with ethyl acetate (2 x 10 mL), the combined organic layers were washed with saturated sodium bicarbonate, and water to neutral pH, then, were dried with sodium sulphate, filtered and the solvent was removed under vacuum to provide a crude mixture that was purified by column chromatography with the properly movile phase. The reaction yield ranged from 46 to 65%.

Procedure for the synthesis of benzalphthalides 15-19 and 24 by microwave. We have applied a modification of the procedure indicated by Viña *et al*. (2009). 1 mmol of the phthalic anhydride, 1.4 mmol of the corresponding phenylacetic acid derivative and 0.13 mmol (13 mg) of potassium acetate were homogeneous mixed and introduced in a G4 MW flask, and the mixture was heated in a microwave at 230 ºC for 20 minutes. After the completion of the reaction (monitored by TLC), the crude was extracted in a separatory funnel with dichlorometane (3 x 10 mL) and washed with saturated sodium bicarbonate and water until neutral pH. Then, it was dried with sodium sulphate, filtered and the solvent was removed under vacuum to provide a crude mixture. Reaction crudes were purified by crystallization from CH_2Cl_2/ether. The reaction yield ranged from 51 to 80%.

*(Z)-3-(4-Chlorobenzylidene)-5(6)-methylisobenzofuran-1(3*H*)-one* **19**, Yield 70%; yellow crystal; mp 125-127 ºC; IR υ_{max} 3058, 2920, 1775, 1662, 1491, 1276, 1082, 976, 879, 284, 777 cm^{-1}. HRMS (ESI) *m/z*, calcd. for $C_{16}H_{11}ClO_2$ $[M+H]^+$: 271.0526, found: 271.0560.

*(Z)-3-(4-Chlorobenzylidene)-5-methylisobenzofuran-1(3*H*)-one* **19a**, ^{1}H-NMR (400 Hz, $CDCl_3$) δ 7.79 (d, *J* = 8.7 Hz, H-7), 7.54 (brs, H-4), 7.53 (d, *J* = 8.7 Hz, H-6), 7.76 (d, *J* = 8.8 Hz, H-2´+6´), 7.36 (d, *J* = 8.8 Hz, H-3´+5´), 6.31 (s, CH), 2.53 (s, CH_3); ^{13}C-NMR (100 Hz, $CDCl_3$) δ 167.0 (C-1), 146.0 (C-3), 145.1 (C-5), 140.9 (C-3a), 134.1 (C-1´), 131.7 (C-6), 131.5 (C-4´), 131.2 (C-2´+6´), 129.0 (C-3´+5´), 120.0 (C-4), 125.5 (C-7), 121.1 (C-7a), 105.3 (C-H), 22.3 (CH_3).

*(Z)-3-(4-Chlorobenzylidene)-6-methylisobenzofuran-1(3*H*)-one* **19b**, ^{1}H-NMR (400 Hz, $CDCl_3$) δ 7.82 (brs, H-7), 7.63 (d, *J* = 7.7 Hz, H-7), 7.74 (d, *J* = 8.8 Hz, H-2´+6´), 7.53 (d, *J* = 7.7 Hz, H-5), 7.35 (d, *J* = 8.8 Hz, H-3´+5´), 6.28 (s, CH), 2.49 (s, CH_3); ^{13}C-NMR (100 Hz, $CDCl_3$) δ 167.0 (C-1), 146.0 (C-3), 140.9 (C-3a), 138.2 (C-6), 135.9 (C-5), 134.1 (C-1´), 131.5 (C-4´), 131.2 (C-2´+6´), 129.0 (C-3´+5´), 119.7 (C-4), 125.5 (C-7), 123.6 (C-7a), 104.9 (C-H), 21.6 (CH_3).

Procedure for the synthesis of phthalazinones 25, 26, 30 and 32. In a round button flask fitted with a condenser, a methanol solution of 174 mg (0.68 mmol) of **7**, 2.03 mmol of the corresponding hydrazine and excess of triethylamine was heated under reflux at 80 °C

for 24 hours. Once the reaction was finished (monitored by TLC), it was extracted with ethyl acetate (3 x 10 mL) and washed with hydrochloric acid and water to neutral pH. Then, the combined organic phases were dried with sodium sulphate, filtered and the solvent removed under vacuum to provide a crude mixture that was purified by column chromatography with the properly solvent. Reaction yields ranged from 23 to 93%.

The spectroscopic data of compound **26** are in agreement with those indicated by Derita *et al*. (2013).

*4-(4-Chlorobenzyl)-2-methylphthalazin-1(2*H*)-one*, **26**. Yield 73%; light yellow crystal; mp 272-274 ºC; IR υ_{max} 3068, 2920, 1650, 1587, 1489, 1262, 1093, 815, 797, 749, 700 cm^{-1}. HRMS (ESI) *m/z*, calcd. for $C_{16}H_{13}ClN_2O$ $[M+H]^+$: 285.0795, found: 285.0776. ^{1}H-NMR (200 Hz, $CDCl_3$) δ 8.42 (m, 1H), 7.70 (m, 3H), 7.26 (d, *J* = 8.7, 2H), 7.20 (d, *J* = 8.7, 2H), 4.25 (s, 2H), 3.87 (s, 3H); ^{13}C-NMR (50 Hz, $CDCl_3$) δ 159.6, 144.5, 136.4, 132.8 (2C), 131.3, 129.8 (2C), 129.2, 128.9 (2C), 128.3, 127.2, 125.0, 39.4, 38.3.

Synthesis of compounds 27-29, 31 and 33-37 by reaction of compound 25 with the corresponding halide. In a one-necked frosted flask, 33.4 mg (0.24 mmol) of K_2CO_3 were added to a solution of 54 mg (0.20 mmol) of **25** in acetonitrile (7 mL) and the mixture was maintained at room temperature for 15 minutes. Then, 0.22 mmol of the corresponding halogen derivative was added dropwise and the mixture maintained at room temperature for 16 h under magnetic stirring. The reaction was controlled by TLC. Once the reaction was finished, the solvent was removed, and the resulting solid was purified by column chromatography. Yields ranged from 72 to 93%.

Biology

Animals. Two animals were used to obtain the necessary material to carry out the in vitro experiments. Two months-old Merino lambs were infected with 20,000 L3 of *T. circumcincta*. All protocols carried out were performed according to current national and European regulations of animal wellbeing (R.D 53/2013 and EU Directive 2010/63/EU) at the facilities of the Instituto de Ganadería de Montaña (IGM, CSIC, León, Spain).

Egg Hatch Assay (EHA). The eggs were extracted from fresh faecal material of infected animals by sieving, centrifugation, and flotation in a solution of saturated sodium chloride. Each compound was first tested in a susceptible strain of the GIN at concentration of 50 µg/mL to select those with activities higher than 96%. Then, their half maximal effective

concentration (EC_{50}) was calculated using eight serial dilutions (1:2) ranging from 50 to 10 µM. Thiabendazole at 0.49 µM (equivalent to 0.1 µg/mL) the known cut-off value used to classify field susceptible and resistant strains according to Coles *et al.,* (2006) was used as positive control and 0.5% DMSO as negative. The EHA was performed using a similar protocol described by Coles *et al*. Briefly, each compound was incubated with fresh eggs in 24-well culture plates for 48 hours at 23 ºC. The concentration of eggs per well was 150 in a final volume of 2 mL. All compounds were tested in duplicate during three different days to ensure the accuracy of results. After 48 hours of incubation, all eggs and larvae present in each well were counted and the ovicidal activity was estimated by following the formulas:

% Egg Hatching per well = (number of L1 / number of L1 larvae and eggs) x 100.

% Ovicidal activity = [100 – (% Egg hatching per well / % Egg hatching in control well)] x 100.

Dose-response curves were fitted by nonlinear regression using the computer program Sigma Plot V 10.0 (Systat Software, Inc., San José, California; USA). The EC_{50} values were calculated. The results were expressed as the mean of the EC_{50} and the standard error of the mean (SEM).

Larval mortality test (LMT). This test was carried out only on those compounds in which dead larvae appeared during the EHT reading (**19** and **26**), to discard a possible activity against this parasite stage. With the aim to obtain L1, fresh eggs (previously extracted from the faeces) were incubated during 24 h at 23 ºC. Then, larvae were collected in a known volume of water to obtain a density of 100-150 larvae per mL. The LMT was performed in the same way as the EHT but using the L1 instead. In this case a stock solution of levamisole at 10 mg/mL was added as positive control on every plate to reach a final concentration of 1 mg/mL per well. The number of dead and alive L1 present per well was counted using an inverted microscope to determine the larvicidal activity of the compound ([number of dead L1/number of dead and alive L1] x 100). Apparently motionless and rod-shaped larvae were considered dead, while those that presented some kind of movement or curvature in their body were considered alive. The efficacy of the compound was expressed by the percentage of viability inhibition using the following formula:

% Viability inhibition = (% larvicidal activity per well/% larvicidal activity in control well) x 100.

Cytotoxicity assay. Cytotoxicity assays were carried out on two human cell lines: the human colorectal adenocarcinoma Caco-2 (ATCC® HTB-37™) and the human hepatocarcinoma HepG2 (ATCC® HB-8065™), to assess the toxicity on a cell line of intestinal origin and to assess the systemic toxicity of the compounds, respectively. Briefly, 10,000 cells were seeded on 96 well-plates containing RPMI 1640 Medium supplemented with 2.0 g/L sodium bicarbonate (Fisher Scientific®), 1% (w/v) L-glutamine (Sigma-Aldrich®) and 25 mM HEPES buffer, pH 7.6, 10% (v/v) inactivated foetal bovine serum and antibiotic cocktail containing 100 U/mL penicillin, and 100 mg/mL streptomycin. Cultures were incubated at 37 ºC in a humidified atmosphere containing 5% CO_2. After 24 h, different concentrations of testing compounds (ranging 1 to 100 µM) were added for a period of 72 h. After this time, the viability of the cells was assessed using the Alamar Blue (Thermo Fisher) staining method according to manufacturer's recommendations.

Cell viability expressed as the fluorescence emitted by resorufin at 590 nm was plotted against the corresponding concentration added to cell culture and fitted using the software package for scientific data analysis SigmaPlot 10.0 with the aim to estimate the half cytotoxic concentration (CC_{50}) of each compound. As an estimation of the safety of each compound, selectivity index (SI) with respect to HepG2 cells was calculated by dividing CC_{50} by EC_{50}.

Results and Discussion

Chemistry. We have first obtained the corresponding benzalphthalide (Bp), and then, the phthalazinones (Figure 2). Initially, Bp without substitution on ring A were obtained (**1**-**12**), that included twelve modifications in ring B. Then, the same derivatives with a methyl in ring A were obtained (**13**-**24**). Next, Pt derivatives (**25**-**37**) based on the activity results of Bps were obtained.

Two different procedures for the synthesis of Bp were used. Method *A*) which was similar to that indicated by Zamilpa *et al*. (2005) that involves the use of toluene to improve the elimination of water generated during the reaction process. Thereby, the phthalic anhydride, the corresponding phenylacetic acid and potassium acetate were reacted in a Dean-Stark apparatus at 220 ºC during 2 h, to provide Bp derivatives **13**,**14** and **20**-**23** in 46-65%. On the other hand, Method *B*) was used to obtain compounds **15**-**19** and **24**, in which a homogeneous mixture of the reagents and potassium acetate were irradiated in a MW apparatus at 230 ºC for 20 minutes to provide the derivatives in 51 to 80%. In general, better yields were obtained using Method *B* than Method *A*.

Then, Bp compounds were reacted with different hydrazines (hydrazine, methyl-, *t*-butyl- and phenyl-hydrazine) and triethylamine at 80 ºC during 24 h to obtain phthalazinones (Pt) **25**, **16**, **30** and **32**, with yields ranging from 23 to 77%. Compounds **27** to **29**, **31** and **33** to **36** were obtained by an S_N2 reaction between amide **25** and the corresponding halide and in basic conditions. Compound **37** was obtained from **19** with methylhydrazine with the same procedure.

All the compounds obtained were properly characterized according to their physicochemical properties. MS, NMR and IR spectral data for Bp and Pt are reported in Supplementary Material.

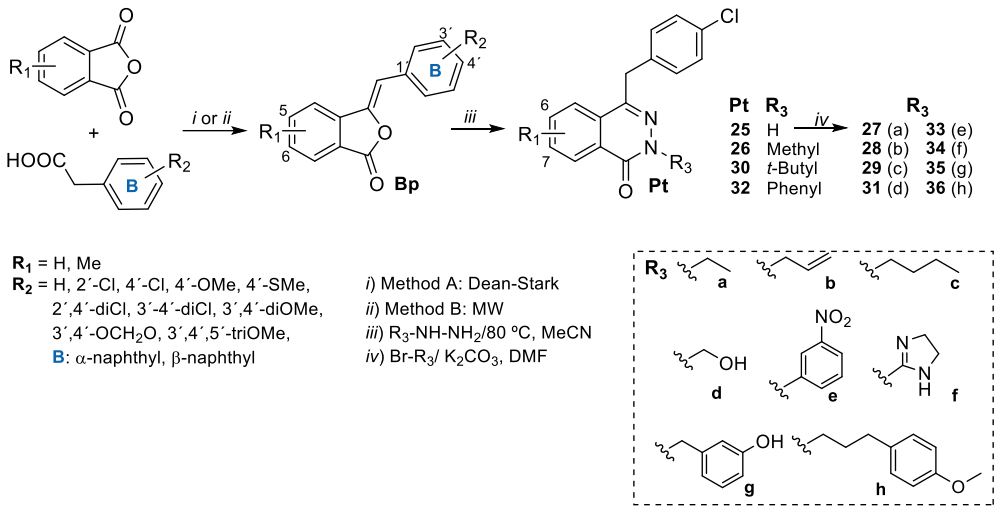

Figure 2. Synthesis procedure for benzalphthalide and phthalazinone derivatives.

Bioactivity. The nematocidal activity of all the compounds was evaluated at 50 µg/mL against *T. circumcincta* and EC_{50} values were determined for those compounds with egg hatching (EHT) higher than 96% inhibition. To determine their selectivity indexes (SI) cytotoxicity on HepG2 and Caco-2 cells was calculated.

Table 1 shows the inhibition percentage of egg hatching and larval migration of *T. circumcincta*. Twenty-four benzalphthalides were obtained and evaluated, twelve of them without substitution on ring A (**1** to **12**), and another twelve with a methyl group on ring A, which are mixtures of 5-Me/6-Me regioisomers (**13** to **24**). Regarding ring B, Bp compounds show non-substitution, or electron donating (Me, OMe, SMe) or withdrawing groups (Cl) attached to different positions of the phenyl ring, or moreover a bulky fragment such as α- or β-naphthyl.

Bearing in mind the results of Bp, we decide to obtain Pt without substitution on ring A combined with a 4´-chloro on ring B, and to explore the convenience of different size chains on the amide nitrogen (alkyl, aromatic, heteroaromatic), compounds **25** to **35**, Table 1. Regarding the methyl derivatives in ring A, only the result of compound **37** is indicated.

Among the compounds without substitution in ring A (**1** to **12**), **1** (R= H) and **7** (R = 4´-Cl) stand out due to their Egg Hatching Inhibition (EHI) of 97.7 and 96.7%, respectively, with EC_{50} values of 27.9 and 32.1 µM. The methoxy di-substituted **3**, and tri-substituted **5**, showed mild EHI with values of 66.8 and 36.7%, respectively. Similar results were obtained in the methyl analogues **13** to **24**, thus, **13** and the 4´-chloro **19** displayed 99.4 and 100% EHI, with EC_{50} values of 17.9 and 30.6 µM, respectively, and also the dimethoxy **15** showed moderated EHI of 57.0 %.

For compounds **1**, **7**, **13** and **19** the cytotoxicity on HepG2 and Caco-2 cells were calculated, in order to determine the safety of each compound, expressed as its selectivity index (SI). Cytotoxicity values were similar on HepG2 and Caco-2 cells, and those respecting to Caco-2 cells are shown in table 1. SI indexes rang from 3.70 for compound **1** to 9.14 and 10.23 for compounds **7** and **19**. Therefore, we have decided to obtained and tested Pt derivatives with ring A= H, and ring B = 4´-Cl and modification on the amide nitrogen with different aliphatic chains (Me, Et, allyl, *n*-But, CH_2CH_2OH), bulky (*t*-But), and aromatic groups (phenyl, 3´-nitrophenyl, 3´-hydroxibencyl, 3´-(4´-methoxyphenyl)propyl) or heteroaromatic fragments (imidazolidine-2-yl). Unluckily, only the methyl amide **26** (R_1 = H; R_2 = Me) showed 100% EHI activity with EC_{50} equal to 26.7 and SI of 13.64, subsequently, we obtained the methyl analogue **37**, which displayed slightly lower activity with 96.0% EHI, EC_{50} of 34.87and SI of 13.64.

Table 1. Results of egg hatching test (EHT) for obtained compounds against a susceptible strain of *T. circumcincta*. Cytotoxicity and selectivity index.

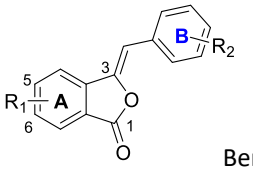

Benzalphthalides (Bp)

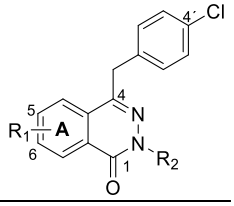

Phthalazinones (Pt)

Compound			*T. circumcincta* susceptible strain			
	R_1	R_2	EHT inhib. % at 50 µg/mL	Ovicidal EC_{50} µM	CC_{50}	SI
		Benzalphtalides				
1	H	H	**97.7**	**27.9**	103.2	3.70

2	H	4′-OMe	12.7	nc		
3	H	3′,4′-diOMe	**66.8**	nc		
4	H	3′,4′-OCH_2O	1.85	nc		
5	H	3′,4′,5′-triOMe	36.7	nc		
6	H	2′-Cl	4.54	nc		
7	H	4′-Cl	**96.7**	**32.1**	293.4	**9.14**
8	H	2′,4′-diCl	1.88	nc		
9	H	3′,4′-diCl	3.58	nc		
10	H	4′-SMe	4.72	nc		
11	H	α-naphthyl	0.74	nc		
12	H	β-naphthyl	0.33	nc		
13	Me	H	**99.4**	**17.9**	146.1	8.19
14	Me	4′-OMe	3.78	nc		
15	Me	3′,4′-diOMe	57.0	nc		
16	Me	3′,4′-OCH_2O	1.21	nc		
17	Me	3′,4′,5′-triOMe	0.05	nc		
18	Me	2′-Cl	0.00	nc		
19	Me	4′-Cl	**100**	**30.6**	313.0	**10.23**
20	Me	2′,4′-diCl	0.03	nc		
21	Me	3′,4′-diCl	0.03	nc		
22	Me	4′-SMe	0.86	nc		
23	Me	α-naphthyl	1.04	nc		
24	Me	β-naphthyl	2.56	nc		
		Phthalazinones				
25	H	H	5.02	nc		
26	H	Me	**100**	**26.7**	363.2	**13.64**
27	H	Et	3.94	nc		
28	H	Allyl	10.5	nc		
29	H	*n*-But	5.09	nc		
30	H	*t*-But	4.74	nc		
31	H	Et-OH	1.02	nc		
32	H	Ph	2.24	nc		
33	H	3′-nitroPh	3.31	nc		
34	H	Imidazolidin-2-yl	1.52	nc		
35	H	3′-hydroxiBn	1.02	nc		
36	H	3′-(4′-OCH_3Ph)Prop	2.54	nc		
37	Me	Me	**96.2**	**34.87**	241.7	6.93
Thiabendazole			**100**			

nc: not calculated. Hatching inhibition values > 96%, the EC_{50} values, and the SI values > 10 have been bolded to facilitate comparisons. Cytotoxicity (CC_{50}) in evaluated against HepG2 and Caco-2 for all compounds was >100 μM.

Bp **19** and Pt **26** were selected to be evaluated at lower doses of 10 μg/mL in eggs and larvae (L1) of a susceptible strain of *T. circumcincta* in the EHI and larval migration inhibition (LMT) tests, and in egg of a resistant strain of *T. circumcincta*, Table 2. Compounds **19** and **26** almost maintained the previous inhibition values at 10 μg/mL in the susceptible strain, with 76.3 and 76.1% EHI, respectively, without reaching the value of thiabendazol

used at 1mg/mL, however, in the resistant strain, this relationship is reversed, and we have found that Pt **26** shows almost complete inhibition of eggs hatching, 99.4% EHI, which is almost double the activity of the reference compound. In addition to that, Pt **26** in the LMT at 10 µg/mL was more potent than control levamisole, with also a nearly complete inhibition of larvae migration, 99.0% LMT.

Table 2. Results of EHT and LMT inhibition at 10 µg/mL against a susceptible and resistant strain of *T. circumcincta*.

Compound			*T. circumcincta* susceptible strain		*T. circumcincta* resistant strain
	R^1	R^2	EHT inhib. % at 10 µg/mL	LMT inhib % at 10 µg/mL	EHT inhib. % at 10 µg/mL
19	Me	4´-Cl	**76.3**	23.7	**75.5**
26	H	Me	**76.1**	**99.0**	**99.4**
Thiabendazole			**100**[a)]	-	55.0
Levamisole			-	nc	-

[a)] Thiabendazole tested at 1 µg/mL; levamisole 1 used at 1 mg/mL. nc: not calculated.

Druglikeness and toxicity risk predictions.

To analyse the druggability of the most active compounds, a prediction study by the online free webs ADMETsar (lmmd.ecust.edu.cn/admetsar2/) and Molinspiration (www.molinspiration.com/) was performed (Table 3). Briefly, compounds **19** and **26** fulfil the Lipinski´s Rule of Five with MW values between of 270.7 and 284.8 amu, clogP values in the range of 3.18 and 4.32, and the H-bond acceptors between 2 and 4, although they did not show H-bond donors. To ensure the distribution of the drug values as solubility (Log S = -3.06 and -4.63), topological polar surface area (TPSA = 30.21 and 34.90), intestinal absorption (HIA >97%) and plasma protein binding (100% and 96.4%) were predicted. The most active compound Pt **26** was neither mutagenic nor tumorigenic.

Table 3. *In silico* predicted physicochemical and ADMET properties of compounds **19** and **26**.

				Physicochemical properties				
Compounds	**MW**	**H-A**[a]	**H-D**[a]	**Log *P***	**Rot. bonds**	**TPSA**	**Druglikeness**	**Leadlikeness**
19	270.7	2	0	4.32	1	30.21	Yes	No
26	284.8	3	0	3.18	2	34.90	Yes	Yes
				ADMET properties				
Compounds	**Log S**	**HIA**	**BBB**	**PPB**		**P-g substrate**	**Mutagenic**	**Tumorigenic**

19	-3.06	High	Yes	100%	No	Yes	No
26	-4.63	High	Yes	96.4%	No	No	No

MW, molecular weight; [a] H-A; Acceptor, H-D; Donor; Log *P*, lipophilicity; PSA, Topological Polar Surface Area Å^2; Log S, aqueous solubility; HIA, Human intestinal absorption %; BBB, Blood-Brain Barrier; PPB, Plasma Protein Binding %.

Conclusion

In summary, in this study we described the synthesis and anthelmintic activity of series of benzaphthalide and phthalazinone derivatives. Among them, the benzaphthalide **19** and the phthalazinone **26** exhibited remarkable nematocidal activity on eggs of *T. circumcincta* in both susceptible and resistant strain at 10 µg/mL, especially in the latest results of 75.5 and 99.4% EHI were higher than the one found for the reference thiabendazole of 55.0%. Compound **26** showed excellent results in the LMT with 99.0% inhibition at 10 µg/mL in the susceptible strain with respect to the control levamisole. Compound **26** fulfil the Lipinski´s Rule of Five, and its ADME/toxicity-risks predictions, were in agreement with a leadlikeness, either **19** or **26** could be selected as an interesting starting point for the development of new anthelmintic compounds.

Acknowledgments

Financial support came from MINECO: RETOS (AGL2016-79813-C2-1R/2R) and Junta de Castilla y León co-financed by FEDER, UE [LE020P17]. EVG was funded by FPU17/00627; VCGA and MAB are recipients of Junta de Castilla y Leon (JCyL) (LE082-18, LE051-18, respectively) and MMV by the Spanish “Ramon y Cajal” Programme (Ministerio de Economía y competitividad; MMV, RYC-2015-18368).

Conflict of interest

The authors declare they have no conflict of interest.

References

Arsène S, Gómez-Pérez V, Escarcena R, Abengózar MA, García-Hernández R, Nácher-Vázquez M, San Feliciano A, Gamarro F, Rivas L, del Olmo E. Imidazo[2,1-*a*]isoindole scaffold as an uncharted structure active on *Leishmania donovani* 2019, 182, 111568. https://doi.org/10.1016/j.ejmech.2019.111568

Barkow K, Heun R, Üstün B, Berger M, Bermejo I, Gaebel W, Harter M, Schneider F, Stieglitz R, Maier W. Identification of somatic and anxiety symptoms which contribute to the

detection of depression in primary health care. *Eur Psych* 2004, 19(5), 250-257. https://doi.org/10.1016/j.eurpsy.2004.04.015

Bedoya L, Olmo E, Sancho R, Barboza B, Beltrán M, García-Cadenas A, Sánchez-Palomino S, Lopez JL, Muñoz E, San Feliciano A, Alcamí J. Anti-HIV activity of stilbene-related heterocyclic compounds. *Bioorg Med Chem Lett* 2006, 16, 4075–4079. https://doi.org/10.1016/j.bmcl.2006.04.087

Coles GC, Jackson F, Pomroy WE, Prichard RK, Von Samson-Himmelstjerna G, Silvestre A, Taylor MA, Vercruysse J. The detection of anthelmintic resistance in nematodes of veterinary importance. *Vet Parasitol* 2006, 136, 167–185. https://doi.org/10.1016/j.vetpar.2005.11.019

Craig TM. Gastrointestinal Nematodes, Diagnosis and Control. *Vet Clin North Am Food Anim Pract* 2018, 34(1), 185–199. https://doi.org/10.1016/j.cvfa.2017.10.008

Del Olmo E, García Armas M, López JL, Muñoz V, Deharo E, San Feliciano A. Leishmanicidal Activity of Some Stilbenoids and Related Heterocyclic Compounds. *Bioorg Med Chem Lett* 2001b, 11, 2123–2126. https://doi.org/10.1016/S0960-894X(01)00387-0

Del Olmo E, García Armas M, López JL, Ruiz G, Vargas F, Giménez A, Deharo E, San Feliciano A. Anti-Trypanosoma Activity of Some Natural Stilbenoids and Synthetic Related Heterocyclic Compounds. *Bioorg Med Chem Lett* 2001a, 11, 2755–2757. https://doi.org/10.1016/S0960-894X(01)00562-5

Del Olmo E, García Armas M, Ybarra MI, López JL, Oporto P, Giménez A, Deharo E, San Feliciano A. The imidazo[2,1-*a*]isoindole system. A new skeletal basis for antiplasmodial compounds. *Bioorg Med Chem Lett* 2003, 13, 2769-2772. https://doi.org/10.1016/S0960-894X(03)00509-2

Del Olmo E, Barboza B, Ybarra M, López JL, Carrón R, Sevilla A, Boselli C, San Feliciano A. Vasorelaxant activity of phtalazinones and related compounds. *Bioorg Med Chem Lett* 2006, 16, 2786-2790. https://doi.org/10.1016/j.bmcl.2006.02.003

Demeler J, Küttler U, Von Samson-Himmelstjerna G. Adaptation and evaluation of three different in vitro tests for the detection of resistance to anthelmintics in gastrointestinal nematodes of cattle. *Vet Parasitol* 2010, 170, 61–70. https://doi.org/10.1016/j.vetpar.2010.01.032

Demirayak S, Karaburun AC, Beis R. Some pyrrole substituted aryl pyridazinone and phthalazinone derivatives and their antihypertensive activities. *Eur J Med Chem* 2004, 39, 1089–1095. https://doi.org/10.1016/j.ejmech.2004.09.005

Derita M, del Olmo E, Barboza B, García-Cadenas AE, López-Pérez JL, Andújar S, Enriz D, Zacchino S, San Feliciano A. Synthesis, bioevaluation and structural study of substituted phthalazin-1(2*H*)-ones acting as antifungal agents. *Molecules* 2013, 18, 3479-3501. https://doi.org/10.3390/molecules18033479

Kouznetsov VV, Meléndez Gómez CM, Rojas Ruíz FA, del Olmo E. Simple entry to new 2-alkyl-1,2,3,4-tetrahydroquinoline and 2,3-dialkylquinoline derivatives using $BiCl_3$-catalyzed three component reactions of anilines and aliphatic aldehydes in the presence (or lack) of *N*-vinyl amides. *Tetrahedron Lett* 2012a, 53, 3115-3118. https://doi.org/10.1016/j.tetlet.2012.04.008

Moje N, Gurmesa A, Regassa G. Gastro-intestinal tract nematodes of small ruminants: Prevalence and their identification in and around Alage, Southern Ethiopia. *Vet Clin North Am Food Anim Pract* 2021, 9(3), 65-72. doi: https://doi.org/10.11648/j.avs.20210903.14

Pathak S, Debnath K, Hossain Sk T, Mukherjee SK, Pramanik A. Synthesis of biologically important phthalazinones, 2,3-benzoxazin-1-ones and isoindolinones from ninhydrin and their antimicrobial activity. *Tetrahedron Lett* 2013, 54, 3137–3143. https://doi.org/10.1016/j.tetlet.2013.04.015

Sargison ND. Pharmaceutical treatments of gastrointestinal nematode infections of sheep-Future of anthelmintic drugs. *Vet Parasitol* 2012, 189, 79-84. https://doi.org/10.1016/j.vetpar.2012.03.035

Sivakumar R, Kishore Guanasam S, Ramachandran S, Leonard JT. Pharmacological evaluation of some new 1-substituted-4-hydroxyphthalazines. *Eur J Med Chem* 2002, 37, 793–801. https://doi.org/10.1016/S0223-5234(02)01405-8

Terán C, Besada P, Vila N, Costas-Lago MC. Recent advances in the synthesis of phthalazin-1(2*H*)-one core as a relevant pharmacophore in medicinal chemistry. *Eur J Med Chem* 2019, 161, 468-478. https://doi.org/10.1016/j.ejmech.2018.10.047

Valderas-García E, de la Vega J, Álvarez Bardón M, Castilla Gómez de Agüero V, Escarcena R, López-Pérez JL, Rojo-Vázquez FA, San Feliciano A, del Olmo E, Balaña-Fouce R, Martínez-Valladares. Anthelmintic activity of aminoalcohol and diamine derivatives against the gastrointestinal nematode *Teladorsagia circumcincta*. *Vet Parasitol* 2021, 296, 109496. https://doi.org/10.1016/j.vetpar.2021.109496

Valderas-García E, Escala N, Álvarez-Bardón M, Castilla-Gómez de Agüero V, Cambra-Pellejà M, González del Palacio L, Vallejo García R, del la Vega J, San Feliciano A, del Olmo E, Martínez-Valladares M, Balaña-Fouce R. Novel compound shows in vivo anthelmintic activity

in gerbils and sheep infected by *Haemonchus contortus. Sci Rep* 2022, 12, 13004. https://doi.org/10.1038/s41598-022-17112-3

Viña D, del Olmo E, López-Pérez JL, San Feliciano A. Regioselective Synthesis of 1-alkyl- or 1-aryl-1*H*-indazoles via copper-catalyzed cyclizations of 2-haloarylcarbonylic compounds. *Org Lett* 2007, 9, 525-528. https://doi.org/10.1021/ol062890e

Viña D, del Olmo E, López-Pérez JL, San Feliciano A. Pyrazolo[3,4,5-*de*]phthalazine. Synthesis of a practically unknown heterocyclic system. *Tetrahedron* 2009, 65, 1574–1580. https://doi.org/10.1016/j.tet.2008.12.072

Zamilpa A, Herrera-Ruiz M, Olmo E, López JL, Tortoriello J, San Feliciano A. Anxiolytic effects of benzalphthalides. *Bioorg Med Chem Lett* 2005, 15, 3483–3486. https://doi.org/10.1016/j.bmcl.2005.06.031

Zajíčková M, Nguyen LT, Skálová L, Raisová Stuchlíková L, Matoušková P. Anthelmintics in the future: current trends in the discovery and development of new drugs against gastrointestinal nematodes. *Drug Discov Today* 2020, 25, 430-437. https://doi.org/10.1016/j.drudis.2019.12.007

Supplementary material

Supplementary material accompanies this paper.

1. Physicochemical properties some obtained compounds

   1a. Benzalphthalides (**13** to **24**)

   1b. Phthalazinones (**25** to **37**).

2. Spectroscopic data of benzalphthalide **19** and phthalazinone **26**.

III.2. ARTÍCULO 2

Este artículo está relacionado con los objetivos 2 y 3 del Trabajo de Tesis.

Se sabe que los Bzs con propiedades nematicidas actúan sobre el sitio de colchicina de la β-tubulina inhibiendo la formación de los microtúbulos, lo que conduce a la destrucción de la estructura celular y por tanto a la muerte del parásito. También, se conocen las principales mutaciones asociadas al desarrollo de resistencias, que afectan a tres aminoácidos (F167Y, E198A y F200Y) y producen una disminución en la afinidad por la β-tubulina, y por tanto reducción en la eficacia del fármaco.

Se diseñaron las estructuras de los Bzs a obtener, que muestran un anillo aromático directamente unido al Bz en C-2, se pusieron a punto los procesos de síntesis, se purificaron y caracterizaron los compuestos obtenidos según sus propiedades fisicoquímicas, y se prepararon las muestras para ensayo in vitro en una cepa sensible de *T. circumcincta*. Aquellos compuestos que dieron mejores resultados se ensayaron en una cepa resistente.

Se buscó la secuencia de β–tubulina de *T. circumcincta* y se obtuvo la estructura 3D por homología molecular con la herramienta SWISS-MODEL Workspace, y a continuación fue validada con el servidor Rampage (http://mordred.bioc.cam.ac.uk/ ~rapper/rampage.php), que predice la calidad estereoquímica y la precisión del modelo generado. Posteriormente, se realizaron estudios de modelado y docking de todas las moléculas obtenidas y ensayadas, con el fin de analizar su interacción con la β-tubulina en relación con los resultados de actividad.

Synthesis, bioevaluation and docking studies of some 2-phenyl-1*H*-benzimidazole derivatives as anthelminthic agents against the nematode *Teladorsagia circumcincta*

Nerea Escala, Elora Valderas-García, María Álvarez Bardón, Verónica Castilla Gómez de Agüero, Ricardo Escarcena, José Luis López-Pérez, Francisco A. Rojo-Vázquez, Arturo San Feliciano, Rafael Balaña-Fouce, María Martínez-Valladares, Esther del Olmo

En: *European Journal of Medicinal Chemistry* 2020, 208, 112554;
doi: 10.1016/j.ejmech.2020.112554

Factor de Impacto: 6,514
Quartil: Q1
5/63 en Química Médica

European Journal of Medicinal Chemistry 208 (2020) 112554

Contents lists available at ScienceDirect

European Journal of Medicinal Chemistry

journal homepage: http://www.elsevier.com/locate/ejmech

Research paper

Synthesis, bioevaluation and docking studies of some 2-phenyl-1*H*-benzimidazole derivatives as anthelminthic agents against the nematode *Teladorsagia circumcincta*

Nerea Escala [a, 1], Elora Valderas-García [b, c, 1], María Álvarez Bardón [b], Verónica Castilla Gómez de Agüero [c, d], Ricardo Escarcena [a], José Luis López-Pérez [a, e], Francisco A. Rojo-Vázquez [d], Arturo San Feliciano [a, f], Rafael Balaña-Fouce [b, **], María Martínez-Valladares [c, d, ***], Esther del Olmo [a, *]

[a] Departamento de Ciencias Farmacéuticas: Química Farmacéutica, Facultad de Farmacia, Universidad de Salamanca, CIETUS, IBSAL, 37007, Salamanca, Spain
[b] Departamento de Ciencias Biomédicas, Facultad de Veterinaria, Universidad de León, 24071, León, Spain
[c] Instituto de Ganadería de Montaña, CSIC-Universidad de León, 24346, Grulleros, León, Spain
[d] Departamento de Sanidad Animal, Facultad de Veterinaria, Universidad de León, 24071, León, Spain
[e] Facultad de Medicina, Universidad de Panamá, Panamá, R. de Panamá
[f] Programa de Pós-graduaçao em Ciências Farmacêuticas, Universidade do Vale do Itajaí, UNIVALI. Itajaí, SC, Brazil

ARTICLE INFO

Article history:
Received 10 April 2020
Received in revised form
3 June 2020
Accepted 7 June 2020
Available online 7 July 2020

Keywords:
2-Phenyl-1*H*-benzimidazoles
Teladorsagia circumcincta
in vitro assays
Cytotoxicity
Tubulin docking studies

ABSTRACT

Gastrointestinal nematode infections are the main diseases in herds of small ruminants. Resistance to the main established drugs has become a worldwide problem. The purpose of this study is to obtain and evaluate the *in vitro* ovicidal and larvicidal activity of some 2-phenylbenzimidazole derivatives on susceptible and resistant strains of *Teladorsagia circumcincta*. Compounds were prepared by known procedures from substituted *o*-phenylenediamines and arylaldehydes or intermediate sodium 1-hydroxyphenylmethanesulfonate derivatives. Egg Hatch Test (EHT), Larval Mortality Test (LMT) and Larval Migration Inhibition Test (LMIT) were used in the initial screening of compounds at 50 μM concentration, and EC_{50} values were determined for the most potent compounds. Cytotoxicity evaluation of compounds was conducted on human Caco-2 and HepG2 cell lines to calculate their Selectivity Indexes (SI). At 50 μM concentration, nine out of twenty-four compounds displayed more than 98% ovicidal activity on a susceptible strain, and four of them showed more than 86% on one resistant strain. The most potent ovicidal benzimidazole (BZ) **3** showed EC_{50} = 6.30 μM, for the susceptible strain, while BZ **2** showed the lowest EC_{50} value of 14.5 μM for the resistant strain. Docking studies of most potent compounds in a modelled *Teladorsagia* tubulin indicated an inverted orientation for BZ **1** in the colchicine binding site, probably due to its fair interaction with glutamic acid at codon 198, which could justify its inactivity against the resistant strain of *T. circumcincta*.

1. Introduction

Nematodes are roundworms belonging to the group of parasitic helminths that affect different host species, including humans and animals. Soil transmitted helminths (STH) infected more than one billion people around the world and contributed to 3.45 million disability adjusted life-years (DALYs) in 2016 [1]. Although these infections are more prevalent in low-income countries, they also occur in wealthy countries, such as the USA, Australia and some countries of the Mediterranean basin [2–4]. Moreover, infections produced by gastrointestinal nematodes (GIN)s are one of the most prevalent parasitic diseases affecting grazing ruminants worldwide. Their importance is due to the significant economic losses they produce as a result of decreased production and increased healthcare costs [5–7].

* Corresponding author.
** Corresponding author.
*** Corresponding author.
E-mail addresses: rbalf@unileon.es (R. Balaña-Fouce), mmarva@unileon.es (M. Martínez-Valladares), olmo@usal.es (E. Olmo).
[1] Both authors shared the first position.

https://doi.org/10.1016/j.ejmech.2020.112554
0223-5234/

The control of GIN infections is based on the strategic application of anthelmintic drugs, but their massive and incorrect administration have led to the development of anthelmintic resistance (AR), especially in ruminants. The emergence of AR has been described in the three classes of broad-spectrum anthelmintic drugs most commonly used in animals: benzimidazoles such as fenbendazole, mebendazole and albendazole, among others, macrocyclic lactones (MLs) such as ivermectin and moxidectin, and imidazothiazoles (IMs) such as levamisole [8–10]. Of these three classes of anthelmintic drugs, the BZ group that usually interferes tubulin polymerization and functions in parasites is the most popular and used in the control of GIN infections. Unfortunately, the current situation of resistance to this family of drugs in animals represents a serious problem for livestock production, mainly in sheep. This phenomenon is widely distributed, since resistant populations have been reported all over the world [11–14].

In humans, the World Health Organisation (WHO) recommends preventive chemotherapy, as a public health intervention to at-risk people living in endemic STH areas by mass administration of BZs, mainly albendazole or mebendazole. In consequence, there are already studies showing the decrease of BZ efficacy against some STH and the possible development of AR after years of mass drug administration campaigns [15].

It is well known that the mechanism of action of BZs is targeted to the selective binding of the high affinity colchicine site of parasite β-tubulin that prevents the formation of microtubules, which results in the destruction of cell structure and consequently in the death of the parasite [11]; in fact, competitive inhibition studies in mammalian isolated tubulins show that colchicine and BZ bind at the same site near the *N*-terminal domain [16]. Computational studies performed with BZs support this finding [17]. Three amino acid mutations (F167Y, E198A and F200Y) have been associated with major causes of anthelmintic drug resistance due to loss of drug affinity by β-tubulin [18], which seems to indicate that these amino acids would be located at or close to the colchicine binding site.

The problem of AR is seriously aggravated by the limited development of novel anthelmintic drugs during the last years. Classical BZ derivatives with nematocidal properties, such as albendazole, fenbendazole, mebendazole, oxibendazole, parbendazole or luxabendazole display a carbamate fragment at position C-2. Their activity is due to disruption of functions on the microtubule system [19]. The carbamate fragment can be substituted by an electron rich fragment such as a phenyl ring [20]. Here we report on the synthesis and bio-evaluation of some BZ derivatives containing a substituted phenyl group attached to the C-2 position of the benzimidazole system.

According to Zajíčková et al. [21] an effective approach to obtain new anthelmintics is to exploit the old ones, synthesizing derivatives and analogues of known drugs with an approved usage. Interestingly, although many 2-phenylbenzimidazole derivatives were synthesized and tested against viruses, fungi, and bacteria infecting humans or animals [22–24], and most rarely against helminths, no evaluation of BZs against *Teladorsagia circumcincta* could be found. In a previous study, the south Indian adult earth worm *Pheretima posthuma* was used as a model for testing the anthelmintic activity of 2-phenylbenzimidazole derivatives [25]. However, it is important to note that *P. posthuma* is not a parasitic worm, does not belong to phylum Nematoda, and therefore it is not the most suitable model for parasitic infections.

In this context, the goal of the present study is to synthesize several series of BZ derivatives, aiming to obtain new drugs with improved therapeutic profiles compared to those already marketed, as well as to evaluate *in vitro* their anthelmintic activity against *Teladorsagia circumcincta*, which is a good experimental model for sheep parasitic nematode infections, as well as one of the most prevalent GIN species in small ruminants worldwide, specifically in template areas [26]. Our research includes *in vitro* cytotoxicity tests in order to define candidate molecules for *in vivo* efficacy and toxicity assays. With these aims, the anthelmintic activity has been assessed in three life-cycle stages (eggs and larvae at two levels of growth) of *Teladorsagia circumcincta*, by means of assaying the BZs on two isolates, one susceptible and the other resistant to marketed drugs as albendazole, levamisole and ivermectin. The cytotoxicity evaluation has been carried out on Caco-2 (human colorectal adenocarcinoma) and the HepG2 (hepatocarcinoma) cells.

2. Results and discussion

2.1. Chemistry

Ten BZ derivatives were obtained by a reported two steps procedure. First, the sodium 1-hydroxyphenylmethanesulfonate derivatives were prepared from the corresponding aldehydes, and then coupled with substituted *o*-phenylenediamines in *N*,*N*-dimethylformamide (DMF) at 110–120 °C, to provide the desired BZs in 43–87% yield [27]. Eleven BZs were obtained in a single step by direct condensation of 1,2-phenylenediamines with the corresponding benzaldehyde derivative in DMF and in the presence of sodium metabisulfite ($Na_2S_2O_5$) under reflux for 16–20 h [28], (Scheme 1). The wide range of yields observed in these syntheses is similar or even lower than those reported by other authors. It can be mainly justified by the diverse electronic nature of the substituents and the influence of their inductive and mesomeric effects on the electrophilia of the aldehyde carbonyl or on the sulfonate α-carbon, and at a lesser level by the nucleophilia of the amino groups. Actually, when the substituents involved are *p*-Cl and the *m*-NO_2 groups at ring B, the yields are the highest.

The original articles referenced above comprise proposals for the reaction mechanisms involved in these BZ syntheses. More recently, Penieres-Castillo et al. [29] have published a more complete study on the subject in which they described different reaction conditions.

BZs **13** and **18** were obtained by reduction of the corresponding nitrobenzimidazoles with H_2 under Pd–C catalysis, while BZ **19** was obtained in 70% yield from the amine **18** by reaction with picolinic acid in the presence of 1,1-carbonyldiimidazole (CDI) as coupling agent. Scheme 2.

Physicochemical, MS and NMR spectral data for all the BZs are reported in the experimental section. IR spectra of BZs showed strong or very strong stretching (*str*) absorption bands of the benzimidazole moiety near 3315 (N–H), 1613 and 1535 (Ar C–C), 1460 and 1384 (C=N) cm^{-1}; along with those associated to the substituents on rings A and B, near 1521 and 1349 cm^{-1} (NO_2 *asym* and *sym str* bands, respectively), 1255 cm^{-1} (C–O), 731 cm^{-1} (C–Cl), 679 cm^{-1} (C–Br) or 1663 cm^{-1} (HN–C=O amide I *str* band). NMR spectra were run either in methanol-d_4 or DMSO-d_6. ^{1}H NMR and ^{13}C NMR spectra of BZs **1**, **2**, **3**, **23** and **24** resulted simplified due to the symmetry of their structures. As an example, in the ^{1}H NMR spectrum of BZ **1,** five signals were appreciated; one singlet at 3.84 ppm, corresponding to the methoxy group; two doublets ($J = 8.6$ Hz) at 7.06 and 7.99 ppm, that correspond to H-3′+5′and H-2′+6′, respectively, and two multiplets at 7.23 and 7.56 ppm corresponding to H-5+6 and H-4+7, respectively. With respect to the ^{13}C NMR spectrum eight signals were observed, one of a O$\underline{C}H_3$ at 54.5 ppm, three of aromatic methines at 114.1 (~double intensity),

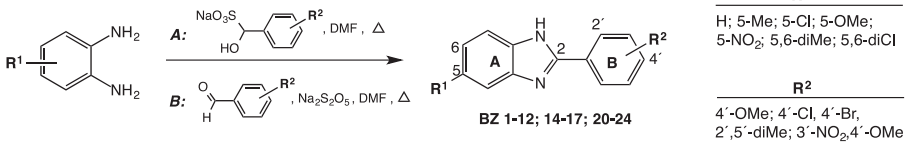

Scheme 1. Two procedures for the synthesis of 2-phenylbenzimidazole derivatives.

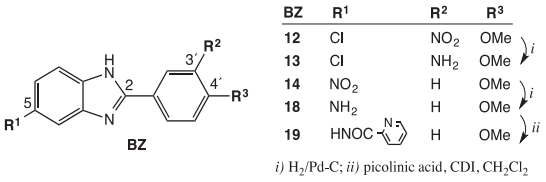

Scheme 2. The preparation of BZs 13, 18 and 19.

122.4 and 128.0 ppm assigned to C-3′+5′and C-4+7, C-5+6 and C-2′+6′, respectively, and four of non-protonated carbons at 121.7, 138.5, 152.0 and 161.7 ppm, corresponding to C-1′, C-3a+7a, C-2 and C-4′, respectively. Regarding ^{1}H NMR spectra of 5-substituted BZs, the signals corresponding to different protons were assigned taking into account their splitting patterns and chemical shifts. Related to the benzimidazole fragment, the signal corresponding to proton H-4 resonates in the 7.1–7.6 ppm range. The chemical shift corresponding to H-6 appears at 7.1–7.4 ppm, except in the presence of nitrogen substituents, such as NO_2 (fairly downfield, ~8.2 ppm), NH_2 (fairly upfield, 6.7 ppm) or NHCO (slightly downfield, 7.5 ppm). The signal for H-7 resonates in the 7.4–7.6 ppm interval, though with changes similar to those just above indicated in presence of nitrogen substituents. ^{13}C NMR spectra of 5-substituted BZs, related to the benzimidazole fragment, showed signals of four non protonated carbons, C-2 (150–157 ppm), C-5 (127–158 ppm), C-3a (131–141 ppm) and C-7a (132–147 ppm). Related the last two carbons, low and broad signals were observed in some spectra due to poor relaxation caused by their proximity to nitrogen atoms. Additionally, the signals of three methines C-4 (96–116 ppm), C-6 (113–124 ppm) and C-7 (112–116 ppm) were appreciated. Chemical shifts of the signals corresponding to ring B were also appropriately assigned considering the substitution pattern of that ring.

2D-NMR experiments on BZ **19** allowed the assignment of the additional signals corresponding to the pyridine portion. In the ^{1}H NMR spectrum, those multiplets at 7.62, 8.23, 8.29 and 8.73 ppm, corresponding to H-5, H-4, H-3 and H-6, respectively, are correlated with signals at 127.9, 139.1, 123.3 and 149.7 ppm, respectively in the ^{13}C NMR spectrum.

2.2. Biological assays

2.2.1. Anthelmintic activity and toxicity

All the compounds synthesized according to Schemes 1 and 2 were tested against a susceptible strain of *T. circumcinta* and their ovicidal (egg hatching inhibition) effects were determined (see Table 1). Those compounds showing ovicidal activity >98% were also tested against one resistant strain. Cytotoxicity was assessed on human Caco-2 and HepG2 cells cultures. Compounds listed in Table 1 are organized in first place by the number and type of substituents at position C-5 (C-6) of the benzimidazole system, and second, by the substituents on the 2-phenyl ring. From the results included in Table 1, it can be observed that several compounds displaying R^1 = H, Me, OMe or Cl, in combination with R^2 = 4-OMe, 4-Cl or 4-Br showed both inhibitory effects, on egg hatching (EHT) and on larvae motility (LMT) at 50 μM final concentration. Notably, nine BZs displayed their anti-hatching effect between 98.2 and 100% on the susceptible strain, and five of them showed this effect between 81.1 and 98.9% on the resistant strain. Additionally, two BZs caused the death of first stage larvae (L1) at 50 μM. On the other hand, compounds with polar groups such as NO_2, NH_2 or picolinamido in R^1, did not show a measurable effect on the nematodes, nor on the susceptible or the resistant strain. Similarly, double substitutions on ring A, as those 5,6-dimethyl (BZ **23**) or 5,6-dichloro (BZ **24**), also led to inactivity.

It is also interesting to verify that the type of substituent on C-4′ of the B-phenyl ring conditioned the anthelmintic potency of active compounds. Curiously, some substituents as $-OCH_3$ and -Cl displayed higher effects at such 4′-position than if they are attached to the BZ moiety. Thus, with respect to ring A, the unsubstituted BZs **1**, **2** and **3**, the 5-CH_3 (BZs **4** and **5**), the 5-Cl (BZs **8** and **9**) and the 5-OCH_3 (BZs **21** and **22**) were able to arrest the hatching of wild-type *T. circumcinta* eggs in more than 98% at the pre-established 50 μM concentration. Among them, the BZs **2**, **4**, **8**, **9** and **22** were also able to produce a significant hatching inhibition on eggs, between 81.1 and 98,9%, of the resistant strain of *T. circumcincta* used in this study. Surprisingly, despite its structural similarity with the most potent substances in the series, BZ **1** is the only one that loses much of its inhibitory capacity against the resistant strain.

Egg-hatching dose/response curves of the compounds of interest were performed in at least 6 final concentrations in order to determine an EC_{50} value that could be comparable with mammalian cytotoxicity (in the Supporting Information). Eight out of the nine hits mentioned above showed similar EC_{50} values within the 6.30–15.78 μM range. The most effective ovicidal BZs were **3** and **9**, which displayed significantly low EC_{50} values of 6.30 and 6.54 μM, respectively, that is, around 14 times less active than thiabendazole. The EC_{50} values of the most potent compounds on the resistant strain ranged between 14.47 and 25.76 μM, which are 9 and 17 times less active than the reference drug, respectively.

When analysing the effect of this series of 2-phenyl benzimidazole compounds on mammalian cells, all the compounds were significantly cytotoxic within a range of 9.07–83.17 μM. Considering only those compounds that have a significant effect against *T. circumcincta*, namely BZs **1**–**5**, **8**, **9**, **21** and **22**, their CC_{50} values were very homogeneous between Caco-2 and HepG2. This determined the SI values calculated for these compounds in the susceptible strain of the parasite to be comprised between 6.22 (BZ **3**) and 0.95 (BZ **4**) for Caco-2 cells and 6.22 (BZ **3**) and 0.87 (BZ **22**) for HepG2 cells. In the case of the resistant strain, the SI values were slightly lower and are comprised between 2.94 (BZ **2**) and 0.47 (BZ **4**) for the Caco-2 cells and between 3.56 and 0.76 for the same compounds and HepG2 cells.

In order to study the killing effect of the twenty-four compounds

Table 1
Inhibitory effects of BZs on hatching of wild type and resistant eggs of *Teladorsagia circumcinta*. Cytotoxicity and selectivity indexes.

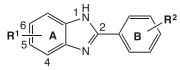

Compound			*T. circumcincta* susceptible strain		*T. circumcincta* resistant strain		Cytotoxicity [a] CC_{50}, μM		Selectivity Indexes[b]			
BZ	R^1	R^2	Hatch inhib. % at 50 uM	Ovicidal EC_{50}, μM	Hatch inhib. % at 50 μM	Ovicidal EC_{50}, μM	Caco-2	HepG2	SIs Caco-2	SIr Caco-2	SIs HepG2	SIr HepG2
1	H	4-OMe	**100**	**15.78 ± 0.12**	18.2	> 50	56.80 ± 8.12	43.08 ± 3.42	3.60	< 1	2.73	< 1
2	H	4-Cl	**99.5**	**9.04 ± 0.23**	**86.4**	**14.47 ± 1.05**	42.63 ± 6.50	51.46 ± 6.27	**4.72**	2.94	**5.69**	3.56
3	H	4-Br	**99.8**	**6.30 ± 0.23**	65.8	< 50	39.17 ± 2.46	38.36 ± 2.36	**6.22**	nc	**6.09**	nc
4	5-Me	4-OMe	**100**	**12.21 ± 0.29**	**81.1**	24.80 ± 0.99	11.60 ± 3.42	18.75 ± 1.92	0.95	0.47	1.53	0.76
5	5-Me	4-Cl	**99.5**	**15.23 ± 0.78**	71.8	< 50	28.06 ± 1.35	27.11 ± 1.69	1.84	< 1	1.78	< 1
6	5-Me	2,5-diMe	0,80	> 50	na	nc	9.14 ± 2.32	> 25	nc	nc	nc	nc
7	5-Me	3-NO_2,4-OMe	1.11	> 50	na	nc	9.07 ± 2.35	> 25	nc	nc	nc	nc
8	5-Cl	4-OMe	**100**	**13.74 ± 0.46**	**89.6**	25.76 ± 3.48	37.38 ± 3.38	36.03 ± 3.02	2.72	1.45	2.62	1.39
9	5-Cl	4-Cl	**99.6**	**6.54 ± 0.40**	**94.0**	20.90 ± 0.50	22.58 ± 1.69	17.54 ± 0.91	3.45	1.08	2.68	0.84
10	5-Cl	4- NO_2	1.25	> 50	na	nc	19.14 ± 2.05	21.73 ± 1.65	nc	nc	nc	nc
11	5-Cl	2,5-diMe	4.00	> 50	na	nc	23.28 ± 2.47	30.22 ± 3.35	nc	nc	nc	nc
12	5-Cl	3-NO_2,4-OMe	0.97	> 50	na	nc	67.31 ± 15.31	53.43 ± 16.61	nc	nc	nc	nc
13	5-Cl	3-NH_2,4-OMe	1.00	> 50	na	nc	34.70 ± 4.32	44.91 ± 5.94	nc	nc	nc	nc
14	5-NO_2	4-OMe	3.16	> 50	na	nc	14.37 ± 3.69	22.98 ± 19.57	nc	nc	nc	nc
15	5-NO_2	4-Cl	1.61	> 50	na	nc	12.29 ± 1.09	14.64 ± 0.83	nc	nc	nc	nc
16	5-NO_2	2,5-diMe	4.02	> 50	na	nc	16.78 ± 9.16	> 12.5	nc	nc	nc	nc
17	5-NO_2	3-NO_2,4-OMe	0.88	> 50	na	nc	13.38 ± 3.02	13.64 ± 4.85	nc	nc	nc	nc
18	5-NH_2	4-OMe	0.50	> 50	na	nc	> 25	> 50	nc	nc	nc	nc
19	5-NHpic [c]	4-OMe	17.1	> 50	na	nc	83.17 ± 45.84	22.76 ± 2.08	nc	nc	nc	nc
20	5-OMe	4-OMe	44.1	> 50	na	nc	21.80 ± 1.47	19.11 ± 3.68	nc	nc	nc	nc
21	5-OMe	4-Cl	**98.2**	25.60 ± 1.25	70.6	< 50	28.94 ± 1.47	21.33 ± 1.20	1.13	nc	0.83	nc
22	5-OMe	4-Br	**99.9**	**15.34 ± 0.55**	**98.9**	**15.99 ± 0.42**	21.69 ± 1.61	13.48 ± 0.64	1.41	1.36	0.87	0.84
23	5,6-diMe	4-OMe	17.4	> 50	na	nc	13.01 ± 1.23	31.66 ± 4.09	nc	nc	nc	nc
24	5,6-diCl	4-OMe	0.44	> 50	na	nc	16.68 ± 1.46	26.37 ± 2.29	nc	nc	nc	nc
Thiabendazole (TBZ)			100	0.43 ± 0.02	100	1.53 ± 0.06	> 300	>300	>697	>196	>697	>196

[c] picolinamide; *na*: not appreciable; *nc*: not calculated. Hatching inhibition values > **80%** and > **90%**, the EC_{50} values < **10** and < **20** μM, and the SI values > **4** have been bolded to facilitate comparisons.

[a] Determined by the Alamar Blue method.

[b] Selectivity index: SI = CC_{50}(Caco-2 or HepG2)/EC_{50}(*T.c.*), relative to susceptible (SIs) and resistant (SIr) strains.

on both susceptible and resistant *T. circumcincta* L1, we used the LMT assay with levamisol (LEV) as reference drug for comparison. Interestingly, three compounds of this series showed activity at this stage of the parasite: BZ **4** with a larvicidal activity higher than 40%, and BZ **9** and **22**, with lesser cytotoxicity which produced 100% death of susceptible L1 larvae of *T. circumcincta*. Table 2 includes the larvicidal results showing that these compounds proved much more potent than LEV, and in the case of BZ **9** also fairly more selective. Nevertheless, it must be taken into account that SIs,*r* values in Table 2 are just indicative, because they were calculated using the cytotoxicity CC_{50} values on human cells, whereas the EC_{50} values were determined on a complete and living organism, the nematode larvae. Independently, the SI is a useful parameter to compare the relative toxicities and selectivities of BZs with those of the currently used anthelmintic drug LEV. The EC_{50} values for susceptible L1 were 5.01 and 28.06 μM for BZs **9** and **22**, respectively (see also Supporting Information). The activity of BZ **9** on larvae was much potent than on *Teladorsagia* eggs, while the activity of BZ **22** was more potent on *Teladorsagia* eggs.

Very interestingly, as it can be seen in Table 2, BZs **9** and **22** killed practically all L1 larvae of both susceptible and resistant strains at 50 μM, with EC_{50} values in de low-medium μM range. Furthermore, both BZs were fairly more potent than the reference drug LEV, and BZ **9**, the most active compound, also showed higher SI values than LEV.

The effect of the compounds against the infective form of the parasite, third stage larvae (L3), was assessed using the LMIT assay. The results showed that they did not produce a significant inhibition of motility, since the highest percentage of inhibition of L3 migration was barely 30% in the case of BZ **23**.

In order to analyze the drugability of the active BZs, a preliminary prediction study was performed online through the Osiris Data Warrior and preADMET free web services (see Experimental section *4.2.6* for details. Detailed results are shown in Table S1 of Supporting Information). To sum up, all the active BZs fulfil Lipinski's Rule of Five with MW values in the range of 224.3–303.2 amu, clogP values between 2.8 and 4.1, and the H-bond acceptors and donors (2–3 and 1, respectively) under the established limits. Other properties as their solubility (>1–100 μM), total and polar surfaces (171–196 and 28–38 $Å^2$, respectively), very good intestinal absorption (>92%) and plasma protein binding (<90%) ensuring their distribution, as well as their qualification within the 90% cut-off in the World Drug Index, contributed to configure their Drug Score values in the range 0.40–0.69 of the Osiris algorithm. Most significantly, none of the active BZs was predicted to show any of those toxicity risks, mutagenic, tumorigenic, reproductive effective or irritant effects, considered in the Osiris panel.

2.3. Molecular docking studies

In order to justify the differential activity of these compounds against susceptible and resistant strains of *T. circumcincta* and further understand the molecular basis of its inhibitory properties, all compounds described in this study were subjected to molecular docking with the *T. circumcincta* tubulin, previously obtained by homology modelling as described in the experimental section *4.2.7.*

Table 2
Larvicidal effects of active BZs on susceptible and resistant larvae of *Teladorsagia circumcincta*.

	T. circumcincta L1 susceptible strain		*T. circumcincta* L1 resistant strain		Cytotoxicity [a]	Selectivity Indexes [b]
BZ	Mortality % at 50 μM	Larvicidal EC_{50} μM	Mortality % at 50 μM	Larvicidal EC_{50} μM	SIs Caco-2	SIr Caco-2
4	40.9	> 50	*nt*	*nd*	0.95	0.47
9	100	**5.01 ± 0.04**	100	**11.66 ± 0.21**	**4.51**	1.94
22	100	**28.06 ± 2.95**	99.3	**28.99 ± 3.32**	0.77	0.75
LEV	0	1782 ± 26	0	2410 ± 23	1.63	1.20

[a,b] reproduced from Table 1 for comparison with the reference drug levamisol (LEV). SI = CC_{50}(Caco-2) / EC_{50}(L1). *s,r*: related to L1 of susceptible and resistant strains, respectively. *nd:* not determined. *nt*: not tested. EC_{50} values **<10** and **<30** μM and SI values **>4** have been bolded to facilitate comparisons.

Taking into account the possibility of tautomerism of the benzimidazole system, which may lead to mixtures in dynamic equilibrium of asymmetrically substituted compounds, computational calculations at the DFT level, MN15/6-31+G(d,p), as described in the experimental section *4.2.8* were conducted with the most potent BZs of this study. The results obtained indicate that the tautomer with the substituent at C-6 (**B**) is about 0.5–1 kcal/mol more stable than the substituent at C-5 (**A**) (Scheme 3).

The activity ranking of the docked compounds of Table 1 in the mentioned *T. circumcincta* tubulin homology model is in agreement with the ovicidal EC_{50} results. In fact, all BZs that show a value of EC_{50} in the μM range (Table 1) appear positioned in the first places of the energetic ranking according the GlideScore function implemented in GLIDE (*see* section 4.2.8). Interestingly, the active conformation of the most efficient compounds corresponds to that of the lowest energy tautomer. The docking poses of some significant ligands can be visualized in Fig. 1 and 2 D maps of interactions in Fig. 2 and Supporting Information p. S41.

Looking at the docked molecules of Fig. 1 and the 2D-maps of tubulin-BZs interactions of Fig. 2, it can be seen that with the exception of BZ **1,** the active compounds are arranged with the same orientation in the site, while other aspects can be deduced from deeper examinations. Experimentally active ligands have none or only one substituent in the benzene ring of the benzimidazole system, whereas the presence of two substituents results in a loss of activity. Those with only one substituent bind tubulin through the lowest energy tautomer; that is, with the substituent located at C-6 according to the systematic IUPAC numbering. The possibility of interaction of the ligands in the tautomer substituted at C-5 results unfavourable due to the steric effect exerted by the methyl group of Ala314. This effect is clearly evident in 5,6-disubstituted BZs, as for example, in the cases of the BZ pairs **4**/**23** or **8**/**24**. A decrease in potency is also observed in those BZs with the potent electron attracting substituent $-NO_2$ located on any benzene ring. This group is placed in an unfavourable hydrophobic environment and provokes bad contacts with several amino acids of the binding site (Fig. 3).

In the colchicine binding site, the active compounds commonly establish a hydrogen bond with the peptide carbonyl of Val236 through their BZN-H acting as a donor. Additionally, some of the most potent compounds present π-stacking interactions between the BZ moiety and the tubulin Phe200 (Fig. 4).

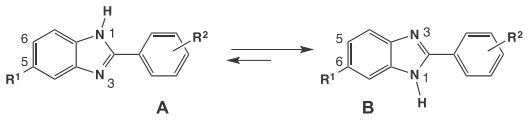

Scheme 3. Tautomeric equilibrium shift and systematic numbering for non-symmetrically 5(6)-monosubstituted BZs.

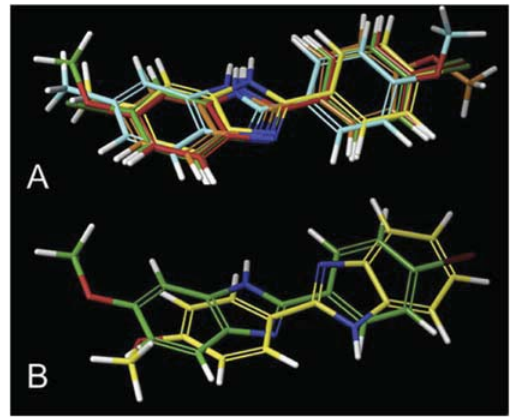

Fig. 1. A: Superimposition of the most potent BZs (**4**: cyan, **5**: yellow, **8**: brown **9**: red, and **22**: green) **as docked in the colchicine site of the *T. circumcincta* tubulin model. B: Superimposition of docked BZs 1** (yellow) **and 22** (green). (For interpretation of the references to color in this figure legend, the reader is referred to the Web version of this article.)

Interestingly, as shown in Figs. 1, 2 and 4, BZ **1** without any substituent on ring A interacts with tubulin in an inverse arrangement with respect to most compounds of the series, (also BZ **8** in Supporting Information, p. S41). As a consequence, it establishes its own BZN-H bond with the γ-carboxyl group of Glu198 instead of the amide carbonyl of Val236. Most of BZs establish a common H-bond acceptor with Val236 and also display π-stacking interactions with the phenyl group of Phe200 through its imidazole nucleus (Fig. 4). This different model of interaction could account for the loss of activity of this compound against resistant strains. Indeed, as described in the literature [18], the mutations associated with BZ-resistant strains for *T. circumcincta* and *Haemonchus contortus* are actually Phe167Tyr, Glu198Ala and Phe200Tyr, and as shown graphically and stated above, Glu198 and Phe200 are directly involved in tubulin - BZs interactions, which should result perturbed in some extension by such mutations.

3. Conclusions

In summary, we have identified some 2-phenylbenzimidazoles that exhibit promising nematocidal activity. Nine compounds displayed more than 98% ovicidal activity on *T. circumcincta* susceptible strain at 50 μM, and five of them showed more than 80% ovicidal activity on a resistant strain of *T. circumcincta* at the same concentration. BZ **3** was the most potent ovicidal on the susceptible strain, with an EC_{50} value of 6.30 μM and SI of 6.22 in relation to Caco-2 cells. BZ **2**, showed the lowest EC_{50} value of 14.47 μM on the

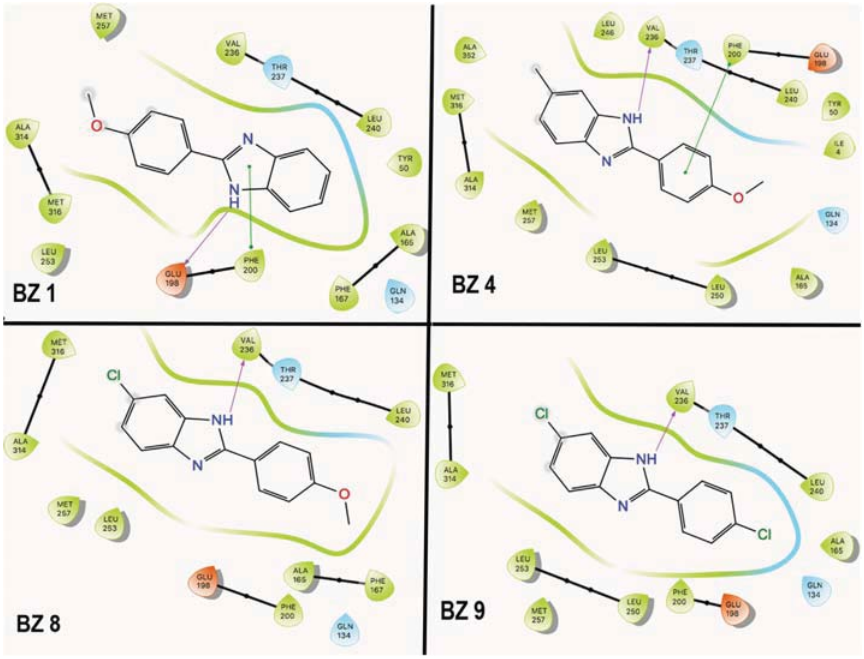

Fig. 2. 2D interaction maps resulting from the docking studies of several selected compounds at the colchicine site of *T. circumcincta* tubulin model. (For other 2D maps, see suppl. info).

resistant strain and SI of 2.94 on Caco-2 cells. Two BZs produced the motility inhibition and death of *T. circumcincta* L1, though none of them showed significant motility inhibition on the L3 stage. Docking studies of most active BZs on a modelled tubulin of *T. circumcincta* indicated a steric orientation of BZs **1** and **8** in their interaction with tubulin, that fairly differ from the other BZs of this study, and that could justify the lack of effect of BZ **1** against the resistant strain of *T. circumcincta*. Globally, these results do not seem very good, mainly because the infective L3 larvae were resistant to the 24 BZs assayed, however, they constitute a promising starting point to design and synthesize other compounds with improved tubulin affinity and higher antiparasitic efficacy.

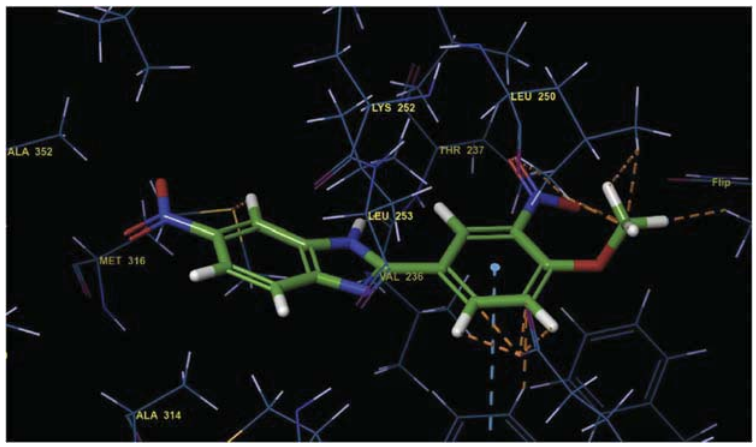

Fig. 3. Bad contacts (pink broken lines) **of nitro and methoxy groups of BZ 17.** (For interpretation of the references to color in this figure legend, the reader is referred to the Web version of this article.)

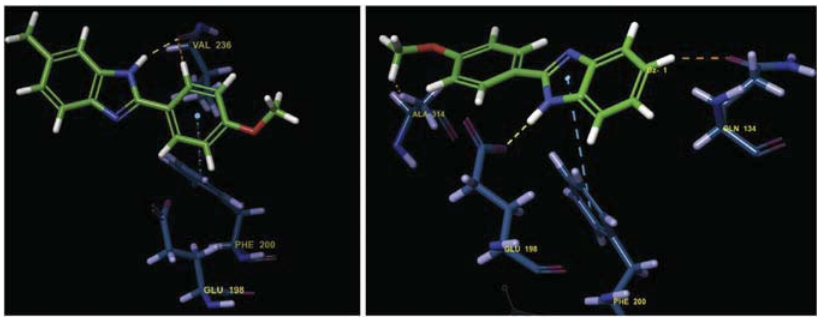

Fig. 4. BZ 4 establishes a hydrogen bond (yellowish broken line) **between its 1-BZN-H and the amide carbonyl of Val236** *(left)*, **while BZ 1 establishes the hydrogen bond with Glu198** (*right*).

Preliminarily, supported by its activity/selectivity profile and acceptable ADME/toxicity-risks predictions, BZ **9** could be selected for *in vivo* efficacy and acute toxicity evaluation on infected laboratory animals. The combined use of BZ **9** and other approved anthelminthic agent acting through a different mechanism against the parasite, also looking for additive or synergic effects could also be considered. However, further and more complete research will be first carried out to obtain better candidates with effects on L3 larvae, with a greater nematocidal potency and a higher selectivity index.

4. Experimental

4.1. Chemistry

4.1.1. Chemistry general

All commercial chemicals (Aldrich, Alpha, Fischer, SDS) were used as purchased and solvents (Fischer, SDS, Scharlau) purified by the standard procedures prior to use [30]. Reactions were monitored by Thin Layer Chromatography (TLC) (Kieselgel 60 F254 precoated plates, E. Merck, Germany), the spots were detected by exposure to UV light at λ 254 nm, and colorization with 10% ninhydrin spray, and further heating of the plate. Melting points (Mp) were determined with a Büchi apparatus in open capillaries and were uncorrected. Separations by flash column chromatography were performed on Merck 60 silica gel (0.063–0.2 mesh). Infrared spectra were recorded on a FT-IR spectrometer PerkinElmer, System BX using solid samples in KBr disks. NMR spectra were recorded on a Bruker Avance 400 MHz (400 MHz for ^{1}H, 100 MHz for ^{13}C) and Varian Mercury 200 MHz ((200 MHz for ^{1}H, 50 MHz for ^{13}C). The spectra were measured either in methanol-d_6 or DMSO-d_6, using tetramethylsilane (TMS) as internal standard, chemical shifts (δ) are given in ppm and coupling constants (J) in Hertz. High resolution mass spectra (HRMS) were obtained by electron spray ionisation-mass spectrometry (ESI-MS) technique (5 kV) on a QSTAR XL mass spectrometer.

4.1.2. Synthesis

4.1.2.1. Method A. General procedure for the synthesis of intermediate sodium hydroxy-(4-methoxyphenyl)methanesulfonate, ***SMS-1***. 4-methoxybenzaldehyde (7.34 mmol) and ethanol (22 mL) were added to a round-bottom flask equipped with a magnetic stir bar under argon atmosphere; then a 16% solution of $Na_2S_2O_5$ (5 mL) was added. The reaction mixture was vigorously stirred for 1 h at room temperature, and kept overnight a 4 °C in a refrigerator. The resulting precipitate was filtered off under vacuum to obtain a white solid in quantitative yield.

4.1.2.1.1. Sodium hydroxy-(4-methoxyphenyl)methanesulfonate, ***SMS-1***. White crystalline solid (100% yield); thermal decomposition of the compound prohibits melting point measurement. IR (KBr), ν_{max}: 3435, 3200, 2980, 1610, 1517, 1250, 1114, 839 cm^{-1}. ^{1}H NMR (C_2D_6SO): δ 3.70 (s, 3H), 4.85 (d, J = 5.0 Hz, D_2O, 1H), 5.65 (d, J = 5.0 Hz, 1H), 6.77 (d, J = 8.6 Hz, 2H), 7.31 (d, J = 8.6 Hz, 2H). ^{13}C NMR (C_2D_6SO): δ55.8, 83.7, 114.5 (2C), 128.1 (2C), 133.2, 159.2. HRMS (ESI^+) calcd. for $C_8H_9Na_2O_5S[M+Na]^+$: 262.9961; found: 262.9959.

4.1.2.1.2. Sodium hydroxy-(4-chlorophenyl)methanesulfonate, ***SMS-2***. White crystalline solid (100% yield); thermal decomposition of the compound prohibits melting point measurement. IR (KBr): ν_{max} 3440, 2930, 1660, 1595, 1244, 1136, 832, 621 cm^{-1}. ^{1}H NMR (C_2D_6SO): δ 4.91 (d, J = 5.4 Hz, D_2O, 1H), 5.94 (d, J = 5.4 Hz, 1H), 7.26 (d, J = 8.4 Hz, 2H), 7.41 (d, J = 8.4 Hz, 2H). ^{13}C NMR (C_2D_6SO): δ 84.2, 126.8 (2C), 129.5 (2C), 131.2, 138.8. HRMS (ESI^+) calcd. for $C_7H_7ClNaO_4S$ $[M+Na]^+$: 266.9465, found: 266.9462.

4.1.2.2. General procedure for the preparation of 2-phenylbenzimidazole derivatives from intermediates ***SMS-1*** *and* ***SMS-2*** *(compounds* ***1***, ***2***, ***4***, ***5***, ***8***, ***9***, ***14***, ***15***, ***23*** *and* ***24****).* 0.82 mmol of the corresponding intermediate was dissolved in *N*,*N*-dimethylformamide (2 mL) and 0.58 mmol of the substituted 1,2-phenylenediamine was added. The mixture was heated at 110–120 °C for 20–24 h with magnetic stirring. After cooling, the reaction crude was poured on a mixture of ice/water (150 mL) to give a solid that was filtered off in a Büchner funnel. The resulted solid was purified by column chromatography on silica gel with solvent gradient (hexane/ethyl acetate from 9:1 to 8:2), and recrystallized from the adequate solvent. Reaction yields ranged within 43–87%.

*4.1.2.2.1. 2-(4-Methoxyphenyl)-1*H*-benzimidazole,* **1**. Yield: 43%. Compound crystallized from EtOH to give a yellow solid, Mp: 229–230 °C. IR (KBr): ν_{max} 3460, 2836, 1611, 1436, 1254, 1179, 1035, 836, 803, 744 cm^{-1}. ^{1}H NMR (400 MHz, CD_3OD): δ 3.84 (s, 3H), 7.06 (d, J = 8.6 Hz, 2H), 7.23 (m, 2H), 7.56 (m, 2H), 7.99 (d, J = 8.6 Hz, 1H). ^{13}C NMR (100 MHz, CD_3OD): δ 54.5 ($O\underline{C}H_3$), 114.1 (C-4 + C-7 + C3' + C-5′), 121.7 (C-1′), 122.4 (C-5 + C-6), 128.0 (C-2′ + C-6′), 138.5 (C3a + C-7a), 152.0 (C-2), 161.7 (C-4′). HRMS (ESI^+) calcd. for $C_{14}H_{13}N_2O$ $[M+H]^+$: 225.1028, found: 225.1027.

4.1.2.2.2. 2-(4-Chlorophenyl)-1H-benzimidazole, **2**. Yield: 65%. Compound crystallized from EtOH to give a white solid, Mp: 300–301 °C. IR (KBr): ν_{max} 3459, 2920, 1611, 1429, 1272, 1176, 1089, 831, 803, 745 cm^{-1}. ^{1}H NMR (400 MHz, CD_3OD): δ 7.27 (m, 2H), 7.57 (d, J = 8.0 Hz, 2H), 7.61 (m, 2H), 8.06 (d, J = 8.0 Hz, 2H). ^{13}C NMR (100 MHz, CD_3OD): δ 124.2 (2C), 129.3 (4C), 129.6, 130.4 (2C), 137.4 (3C), 152.2. HRMS (ESI^+) calcd. for $C_{13}H_{10}ClN_2$ $[M+H]^+$: 229.0533, found: 229.0536.

4.1.2.2.3. 2-(4-Methoxyphenyl)-5-methyl-1H-benzimidazole, **4**. Yield: 59%. Compound crystallized from EtOH to give a light yellow solid, Mp: 163–164 °C. IR (KBr): ν_{max} 3460, 2921, 1611, 1438, 1255, 1176, 1030, 836, 803, 738 cm^{-1}. ^1H NMR (200 MHz, CD_3OD): δ 2.46 (s, 3H), 3.87 (s, 3H), 7.07 (d, J = 8.6 Hz, 2H), 7.08 (d, J = 8.2 Hz, 1H), 7.36 (bs, 1H), 7.44 (d, J = 8.2 Hz, 1H), 7.99 (d, J = 8.6 Hz, 2H). ^{13}C NMR (50 MHz, CD_3OD): δ 20.3 ($\underline{C}H_3$), 54.4 (O$\underline{C}H_3$), 113.6 (C-7), 114.0 (C-4 + C-3′ + C-5′), 122.0 (C-1′), 123.7 (C-6), 127.8 (C-2′ + C-6′), 132.1 (C-5), 137.2 (C-7a), 138.6 (C-3a), 151.8 (C-2), 161.4 (C-4′). HRMS (ESI^+) calcd. for $C_{15}H_{15}N_2O$ $[M+H]^+$: 239.1184, found: 239.1180.

4.1.2.2.4. 2-(4-Chlorophenyl)-5-methyl-1H-benzimidazole, **5**. Yield: 87%. Compound crystallized from EtOH to give a white solid, Mp: 189–190 °C. IR (KBr): ν_{max} 3580, 2921, 1630, 1520, 1418, 1090, 965, 834, 801, 731, 676 cm^{-1}. ^1H NMR (200 MHz, CD_3OD): δ 2.46 (s, 3H), 7.10 (dd, J_1 = 7.8; J_2 = 1.0 Hz, 1H), 7.38 (d, J = 1.0 Hz, 1H), 7.47 (d, J = 7.8 Hz, 1H), 7.52 (d, J = 9.0 Hz, 2H), 8.02 (d, J = 9.0 Hz, 2H). ^{13}C NMR (50 MHz, CD_3OD): δ 20.3, 113.8, 114.4, 124.4, 127.7 (2C), 128.2, 128.9 (2C), 133.0, 135.8, 137.0, 138.4, 150.3. HRMS (ESI^+) calcd. for $C_{14}H_{12}ClN_2$ $[M+H]^+$: 243.0689, found: 243.0687.

4.1.2.2.5. 5-Chloro-2-(4-methoxyphenyl)-1H-benzimidazole, **8**. Yield: 63%. Compound crystallized from EtOH to give a white solid, Mp: 175–176 °C. IR (KBr): ν_{max} 3429, 2910, 1613, 1494, 1432, 1391, 1257, 1178, 924, 835, 739 cm^{-1}. ^1H NMR (200 MHz, CD_3OD): δ 3.83 (s, 3H), 7.03 (d, J = 8,6 Hz, 2H), 7.17 (dd, J_1 = 8.6; J_2 = 1,8 Hz, 1H), 7.47 (d, J = 8.6 Hz, 1H), 7.50 (d, J = 1,8 Hz, 1H), 7.95 (d, J = 8,6 Hz, 2H). ^{13}C NMR (50 MHz, CD_3OD): δ 54.5 (O$\underline{C}H_3$), 114.0 (C-7), 114.1 (C-3′ + C-5′), 115.0 (C-4), 121.3 (C-1′), 122.6 (C-6), 127.7 (C-5), 128.0 (C-2′ + C-3′), 137.2 (C-7a), 139.6 (C-3a), 153.3 (C-2), 161.8 (C-4′). HRMS (ESI^+) calcd. for $C_{14}H_{12}ClN_2O$ $[M+H]^+$: 259.0638; found: 259.0635.

4.1.2.2.6. 5-Chloro-2-(4-chlorophenyl)-1H-benzimidazole, **9**. Yield: 80%. Compound crystallized from EtOH to give a white solid, Mp: 229–230 °C. IR (KBr): ν_{max} 3510, 2923, 1621, 1582, 1480, 1422, 1302, 1086, 925, 833, 731 cm^{-1}. ^1H NMR (200 MHz, CD_3OD): δ 7.21 (dd, J_1 = 8.6; J_2 = 2.0 Hz, 1H), 7.48 (d, J = 8.6 Hz, 1H), 7.49 (d, J = 8.6 Hz, 2H), 7.54 (d, J = 2.0 Hz, 1H), 8.00 (d, J = 8.6 Hz, 2H). ^{13}C NMR (50 MHz, CD_3OD): δ 114.4, 115.5, 123.1, 127.9 (2C), 128.2, 128.9 (2C), 136.3 (2C), 137.6, 139.8, 152.1. HRMS (ESI^+) calcd. for $C_{13}H_9Cl_2N_2$ $[M+H]^+$: 263.0143; found: 263.0143.

4.1.2.2.7. 2-(4-Methoxyphenyl)-5-nitro-1H-benzimidazole, **14**. Yield: 75%. Compound crystallized from MeOH to give a brown-red solid, Mp: 237–239 °C. IR (KBr): ν_{max} 3351, 3085, 1621, 1574, 1509, 1347, 1277, 1012, 881, 817, 737 cm^{-1}. ^1H NMR (200 MHz, C_2D_6SO): δ 3.84 (s, 3H), 7.14 (d, J = 8.8 Hz, 2H), 7.70 (d, J = 9.0 Hz, 1H), 8.08 (dd, J_1 = 9.0; J_2 = 2.4 Hz, 1H), 8.15 (d, J = 8.8 Hz, 2H), 8.40 (d, J = 2.4 Hz, 1H). ^{13}C NMR (50 MHz, C_2D_6SO): δ 55.9 (O$\underline{C}H_3$), 108.0 (C-4), 111.8 (C-7), 115.0 (C-3′ + C-5′), 118.3 (C-6), 121.8 (C-1′), 129.1 (C-2′ + C-6′), 140.3 (C-3a), 142.9 (C-5), 143.6 (C-7a), 155.8 (C-2), 161.9 (C-4′). HRMS (ESI^+) calcd. for $C_{14}H_{12}N_3O_3$ $[M+H]^+$: 270.0879, found: 270.0884.

4.1.2.2.8. 2-(4-Chlorophenyl)-5-nitro-1H-benzimidazole, **15**. Yield: 85%. Compound crystallized from MeOH to give a yellow solid, Mp: 306–307 °C. IR (KBr): ν_{max} 3441, 2921, 1601, 1498, 1333, 1289, 1060, 837, 735 cm^{-1}. ^1H NMR (200 MHz, C_2D_6SO): δ 7.67 (d, J = 8.6 Hz, 2H), 7.76 (d, J = 9.0 Hz, 1H), 8.13 (dd, J_1 = 9.0 Hz; J_2 = 2.0 Hz, 1H), 8.21 (d, J = 8.6 Hz, 2H), 8.47 (d, J = 2.0 Hz, 1H). ^{13}C NMR (50 MHz, C_2D_6SO): δ 113.1, 115.0, 118.5, 128.3, 129.0 (2C), 129.6 (2C), 136.1, 138.8, 140.2, 143.2, 155.0. HRMS (ESI^+) calcd. for $C_{13}H_9ClN_3O_2$ $[M+H]^+$: 274.0383, found: 274.0394.

4.1.2.2.9. 2-(4-Methoxyphenyl)-5,6-dimethyl-1H-benzimidazole, **23**. Yield: 60%. Compound crystallized from EtOH to give a light yellow solid, Mp: 227–229 °C. IR (KBr): ν_{max} 3435, 2921, 1612, 1500, 1440, 1384, 1253, 1151, 1031, 923, 836, 795 cm^{-1}. ^1H NMR (200 MHz, CD_3OD): δ 2.14 (s, 6H), 4.07 (s, 3H), 7.02 (d, J = 8.9 Hz, 2H), 7.33 (s, 2H), 7.92 (d, J = 8.9 Hz, 2H). ^{13}C NMR (50 MHz, CD_3OD): δ 19.5 (2 x $\underline{C}H_3$), 54.6 (O$\underline{C}H_3$), 114.0 (C-4 + C-7), 114.4 (C-3′ + C-5′), 119.7 (C-1′), 128.2 (C-2′ + C-6′), 132.8 (C-5 + C-6), 134.9 (C-3a + C-7a), 150.2 (C-2), 162.1 (C-4′). HRMS (ESI^+) calcd. for $C_{16}H_{17}N_2O$ $[M+H]^+$: 253.1341, found: 253.1352.

4.1.2.2.10. 5,6-Dichloro-2-(4-methoxyphenyl)-1H-benzimidazole, **24**. Yield: 71%. Compound crystallized from EtOH to give a beige solid, Mp: 218–220 °C. IR (KBr): ν_{max} 3321, 2939, 1610, 1573, 1492, 1383, 1261, 1192, 1090, 1028, 969, 832, 735 cm^{-1}. ^1H NMR (200 MHz, CD_3OD): δ 3.87 (s, 3H), 7.08 (d, J = 7.4 Hz, 2H), 7.69 (s, 2H), 7.99 (d, J = 7.4 Hz, 2H). ^{13}C NMR (50 MHz, CD_3OD): δ 54.6 (O$\underline{C}H_3$), 114.3 (C-3′ + C-5′), 115.4 (C-4 + C-7), 120.9 (C-1′), 125.9 (C-5 + C-6), 128.3 (C-2′ + C-6′), 138.1 (C-3a + C-7a), 154.5 (C-2), 162.2 (C-4′). HRMS (ESI^+) calcd. for $C_{14}H_{11}Cl_2N_2O$ $[M+H]^+$: 293.0248, found: 293.0238.

4.1.2.3. Method B. General procedure for the preparation of 2-phenylbenzimidazole derivatives (compounds ***3****,* ***6****,* ***7****,* ***10****,* ***11****,* ***12****,* ***16****,* ***17****,* ***20****,* ***21*** *and* ***22****).* A mixture of the corresponding 1,2-phenylenediamine (1.00 mmol), the substituted benzaldehyde (1.00 mmol) and the $Na_2S_2O_5$ (1.00 mmol) in dry DMF (4 mL) was heated to reflux for 6–12 h.

Then, the reaction was cooled to room temperature and water (20 mL) was added to provide a solid that was filtered off in Büchner. The solid was purified by column chromatography on silica gel with hexane/ethyl acetate (8:2) as elution system, and recrystallized from the adequate solvent in most cases. Reaction yields ranged within 40–73%.

4.1.2.3.1. 2-(4-Bromophenyl)-1H-benzimidazole, **3**. Yield: 40%. Compound crystallized from EtOH to give an orange solid, Mp: 295–296 °C. IR (KBr): ν_{max} 3460, 2924, 1620, 1430, 1260, 1178, 1070, 835, 802, 670 cm^{-1}. ^1H NMR (400 MHz, CD_3OD): δ 7.26 (m, 2H), 7.60 (m, 2H), 7.70 (d, J = 8.0 Hz, 2H), 7.99 (d, J = 8.0 Hz, 2H). ^{13}C NMR (100 MHz, CD_3OD): δ 124.2 (2C), 126.3, 129.5 (2C), 129.9 (2C), 130.2, 133.4 (2C), 138.9 (2C), 152.3. HRMS (ESI^+) calcd. for $C_{13}H_{10}BrN_2$ $[M+H]^+$: 273.0027, found: 273.0026.

4.1.2.3.2. 2-(2,5-Dimethylphenyl)-5-methyl-1H-benzimidazole, **6**. Yield: 42%. Compound crystallized from EtOH to give a light yellow solid, Mp: 112–113 °C. IR (KBr): ν_{max} 3430, 2920, 1629, 1447, 1276, 1000, 805 cm^{-1}. ^1H NMR (200 MHz, CD_3OD): δ 2.33 (s, 3H), 2.43 (s, 3H), 2.45 (s, 3H), 7.07 (dd, J_1 = 8.2; J_2 = 1.2 Hz, 1H), 7.18 (bs, 2H), 7.38 (m, 2H), 7.46 (d, J = 8.2 Hz, 1H). ^{13}C NMR (50 MHz, CD_3OD): δ 18.7 ($\underline{C}H_3$ at C-2′), 19.5 ($\underline{C}H_3$ at C-5′), 20.3 ($\underline{C}H_3$ at C-5), 113.8 (C-7), 114.3 (C-4), 123.8 (C-6), 129.8 (C-1′), 130.0 (C-4′), 130.2 (C-3′), 130.6 (C-6′), 132.3 (C-5), 133.8 (C-2′), 135.3 (C-5′), 136.8 (C-7a), 138.1 (C-3a), 152.4 (C-2). HRMS (ESI^+) calcd. for $C_{16}H_{17}N_2$ $[M+H]^+$: 237.1392; found: 237.1396.

4.1.2.3.3. 5-Methyl-2-(4-methoxy-3-nitrophenyl)-1H-benzimidazole, **7**. Yield: 66%. Compound crystallized from MeOH to give a yellow solid, Mp: 221–222 °C. IR (KBr): ν_{max} 3313, 2936, 1622, 1550, 1521, 1436, 1336, 1267, 1010, 815, 793 cm^{-1}. ^1H NMR (200 MHz, CD_3OD): δ 2.45 (s, 3H), 4.02 (s, 3H), 7.09 (dd, J_1 = 8.2; J_2 = 1.6 Hz, 1H), 7.35 (d, J_2 = 1.6 Hz, 1H), 7.43 (d, J = 8.6 Hz, 1H), 7.45 (d, J = 8.2 Hz, 1H), 8.25 (dd, J_1 = 8.6; J_2 = 2.4 Hz, 1H), 8.49 (d, J = 2.4 Hz, 1H). ^{13}C NMR (50 MHz, CD_3OD): δ 20.3 ($\underline{C}H_3$), 56.0 (O$\underline{C}H_3$), 112.0 (C-7), 112.2 (C-4), 114.3 (C-5′), 122.3 (C-1′), 122.9 (C-2′), 124.3 (C-6), 131.6 (C-6′), 132.4 (C-5), 136.8 (C-7a), 137.2 (C-3a), 140.0 (C-3′), 151.2 (C-2), 153.7 (C-4′). HRMS (ESI^+) calcd. for $C_{15}H_{14}N_3O_3$ $[M+H]^+$: 284.1035, found: 284.1031.

4.1.2.3.4. 5-Chloro-2-(4-nitrophenyl)-1H-benzimidazole, **10**. Yield: 55%. Compound crystallized from MeOH to give a yellow solid, Mp: 249–250 °C. IR (KBr): ν_{max} 3314, 2900, 1604, 1511, 1413, 1349, 1109, 924, 854, 809, 707 cm^{-1}. ^1H NMR (200 MHz, CD_3OD): δ 7.25 (dd, J_1 = 8.6; J_2 = 2.0 Hz, 1H), 7.56 (d, J = 8.6 Hz, 1H), 7.58 (d, J = 2.0 Hz, 1H), 8.21 (d, J = 9.0 Hz, 2H), 8.34 (d, J = 9.0 Hz, 2H). ^{13}C NMR (50 MHz, CD_3OD): δ 113.9 (C-4), 116.1 (C-7), 123.8 (C-6), 123.9 (C-3′ + C-5′), 127.3 (C-2′ + C-6′), 131.6 (C-5), 131.9 (C-7a), 135.0 (C-1′), 141.3 (C-3a), 148.7 (C-4′), 151.2 (C-2). HRMS (ESI^+) calcd. for

$C_{13}H_9ClN_3O_2$: 274.0383; found: 274.0381.

*4.1.2.3.5. 5-Chloro-2-(2,5-dimethylphenyl)-1*H*-benzimidazole,* **11**. Yield: 62%. Compound crystallized from EtOH to give a beige solid, Mp: 192–193 °C. IR (KBr): ν_{max} 3435, 2919, 1613, 1584, 1496, 1440, 1375, 1275, 1060, 926, 807 cm^{-1}. ^1H NMR (200 MHz, CD_3OD): δ 2.35 (s, 3H), 2.44 (s, 3H), 7.23 (m, 3H) 7.42 (bs, 1H), 7.57 (d, J = 8.6 Hz, 1H), 7.58 (d, J = 2.0 Hz, 1H). ^{13}C NMR (50 MHz, CD_3OD): 18.7, 19.5, 114.3, 115.4, 122.7, 127.8, 129.3, 129.9, 130.5, 130.8, 134.0, 135.5, 136.9, 139.2, 154.1. HRMS (ESI^+) calcd. for $C_{15}H_{14}ClN_2$: 257.0846; found: 257.0845.

*4.1.2.3.6. 5-Chloro-2-(4-methoxy-3-nitrophenyl)-1*H*-benzimidazole,* **12**. Yield: 70%. Compound crystallized from MeOH to give a pale yellow solid, Mp: 239–240 °C. IR (KBr): ν_{max} 3306, 2920, 1626, 1515, 1442, 1343, 1267, 1011, 923, 891, 822, 643 cm^{-1}. ^1H NMR (200 MHz, C_2D_6SO): δ 4.00 (s, 3H), 7.21 (dd, J_1 = 8.6; J_2 = 2.4 Hz, 1H), 7.56 (d, J = 9.0 Hz, 1H), 7.60 (d, J = 8.6 Hz, 1H), 7.63 (d, J = 2.4 Hz, 1H), 8.42 (d, J_1 = 9.0; J_2 = 2.2 Hz, 1H), 8.64 (d, J = 2.2 Hz, 1H). ^{13}C NMR (50 MHz, C_2D_6SO): δ 57.5, 115.2, 115.6, 116.4, 122.6, 123.0, 123.6, 127.0, 132.9, 138.4, 139.6, 140.9, 151.1, 153.8. HRMS (ESI^+) calcd. for $C_{14}H_{11}ClN_3O_3$: 304.0489; found: 304.0478.

*4.1.2.3.7. 2-(2,5-Dimethylphenyl)-5-nitro-1*H*-benzimidazole,* **16**. Yield: 58%. Compound crystallized from MeOH to give a white solid, Mp: 257–258 °C. IR (KBr): ν_{max} 3420, 2923, 1626, 1510, 1469, 1334, 1287, 1065, 921, 884, 737 cm^{-1}. ^1H NMR (200 MHz, CD_3OD): δ 2.33 (s, 3H), 2.45 (s, 3H), 7.19 (d, J = 8.6 Hz, 1H), 7.21 (d, J = 8.6, 1H), 7.42 (s, 1H), 7.62 (d, J = 8.6 Hz, 1H), 8.09 (dd, J_1 = 8.6; J_2 = 2.0 Hz, 1H), 8.41 (d, J = 2.0 Hz, 1H). ^{13}C NMR (50 MHz, CD_3OD): δ 18.9, 19.5, 112.1, 114.0, 117.9, 128.6, 129.9, 131.0 (2C), 134.2, 135.6, 140.1, 141.9, 143.4, 157.2. HRMS (ESI^+) calcd. for $C_{15}H_{14}N_3O_2$ $[M+H]^+$: 268.1086; found: 268.1080.

*4.1.2.3.8. 2-(4-Methoxy-3-nitrophenyl)-5-nitro-1*H*-benzimidazole,* **17**. Yield: 43%. Compound crystallized from MeOH to give a dark yellow solid, Mp: 290–292 °C. IR (KBr): ν_{max} 3433, 3351, 2923, 1621, 1508, 1444, 1347, 1277, 1066, 1012, 881, 817, 736 cm^{-1}. ^1H NMR (200 MHz, C_2D_6SO): δ 4.02 (s, 3H), 7.61 (d, J = 9.0 Hz, 1H), 7.76 (d, J = 9.0 Hz, 1H), 8.12 (dd, J_1 = 9.0; J_2 = 2.4 Hz, 1H), 8.44 (d, J = 2.4 Hz, 1H), 8.46 (dd, J_1 = 9.0; J_2 = 2.4 Hz, 1H), 8.70 (d, J = 2.4 Hz, 1H). ^{13}C NMR (50 MHz, C_2D_6SO): δ 57.2, 113.0113.7, 115.3, 118.2, 121.4, 123.7, 132.9, 137.9, 139.1, 142.8, 145.3, 153.9, 154.0. HRMS (ESI^+) calcd. for $C_{14}H_{11}N_4O_5$ $[M+H]^+$: 315.0729; found: 315.0718.

*4.1.2.3.9. 5-Methoxy-2-(4-methoxyphenyl)-1*H*-benzimidazole,* **20**. Yield: 46%. Compound crystallized from EtOH to give a yellow solid, Mp: 150–152 °C. IR (KBr): ν_{max} 3350, 2920, 1623, 1512, 1430, 1335, 1330, 1285, 1220, 1060, 920, 818, 795 cm^{-1}. ^1H NMR (400 MHz, CD_3OD): δ 3.87 (s, 3H), 3.89 (s, 3H), 7.00 (dd, J_1 = 9.2; J_2 = 2.0 Hz, 1H), 7.12 (d, J = 2.0 Hz, 1H), 7.13 (d, J = 8.4 Hz, 2H), 7.52 (d, J = 9.2 Hz, 1H), 7.99 (d, J = 8.4 Hz, 2H). ^{13}C NMR (100 MHz, CD_3OD): δ 54.7 ($O\underline{C}H_3$), 54.9 ($O\underline{C}H_3$), 96.2 (C-4), 113.5 (C-6), 114.2 (C-7), 114.6 (C-3′ + C-5′), 118.9 (C-1′), 128.3 (C-2′ + C-6′) 130.4 (C-7a), 136.2 (C-3a), 150.5 (C-2), 157.7 (C-5), 162.5 (C-4′). HRMS (ESI^+) calcd. for $C_{15}H_{15}N_2O_2$ $[M+H]^+$: 255.1134, found: 255.1122.

*4.1.2.3.10. 2-(4-Chlorophenyl)-5-methoxy-1*H*-benzimidazole,* **21**. Yield: 65%. Compound crystallized from EtOH to give a yellow solid, Mp: 227–228 °C. IR (KBr): ν_{max} 3350, 2910, 1635, 1595, 1424, 1330, 1271, 1158, 1032, 966, 825, 724 cm^{-1}. ^1H NMR (200 MHz, CD_3OD): δ 3.84 (s, 3H), 6.90 (dd, J_1 = 8.6; J_2 = 2.2Hz, 1H), 7.07 (d, J = 2.2 Hz, 1H), 7.47 (d, J = 8.6 Hz, 1H), 7.51 (d, J = 8.6 Hz, 2H), 7.99 (d, J = 8.6 Hz, 2H). ^{13}C NMR (50 MHz, CD_3OD): δ 56.1, 97.8, 113.9, 117.0, 128.9 (2C), 129.9, 130.2 (2C), 136.9, 139.0, 142.2, 151.6, 158.4. HRMS (ESI^+) calcd. for $C_{14}H_{12}ClN_2O$ $[M+H]^+$: 259.0638, found: 259.0636.

*4.1.2.3.11. 2-(4-Bromophenyl)-5-methoxy-1*H*-benzimidazole,* **22**. Yield: 73%. IR (KBr): ν_{max} 3300, 2910, 1635, 1595, 1424, 1330, 1271, 1158, 1023, 966, 825, 724 cm^{-1}. ^1H NMR (400 MHz, CD_3OD): δ 3.85 (s, 3H), 6.90 (dd, J_1 = 8.8; J_2 = 1.6 Hz, 1H), 7.08 (d, J = 1.6 Hz, 1H), 7.49 (d, J = 8.8 Hz, 1H), 7.69 (d, J = 7.6 Hz, 2H), 7.95 (d, J = 7.6 Hz, 2H). ^{13}C NMR (100 MHz, CD_3OD): δ 54.7, 96.4, 112.6, 115.6, 123.7, 127.7 (2C), 128.8, 131.8 (2C), 136.0, 138.8, 150.3, 157.1. HRMS (ESI^+) calcd. for $C_{14}H_{12}BrN_2O$ $[M+H]^+$: 303.0133, found: 303.0128.

4.1.2.4. Procedure for the reduction of nitrobenzimidazoles (compounds ***13*** *and* ***18****).* A solution with 0.32 mmol of the nitrobenzimidazole in MeOH (3 mL) in a two-necked round bottom flask was prepared, then Pd–C catalyst (3 mg) was added. The air was removed, and a balloon with H_2 was attached to one of the necks. The mixture was kept at room temperature and under magnetic stirring for 2 h. Then, the Pd–C was removed by filtration through Celite, and the residue was washed with MeOH. The solvent was removed *in vacuo* to provide a dark yellow solid.

*4.1.2.4.1. 5-Chloro-2-(3-amino-4-methoxyphenyl)-1*H*-benzimidazole,* **13**. Yield: 91%. Compound crystallized from MeOH to give a light yellow solid, Mp: 185–186 °C. IR (KBr): ν_{max} 3306, 3210, 2918, 1618, 1501, 1453, 1340, 1243, 1026, 927, 802 cm^{-1}. ^1H NMR (200 MHz, CD_3OD): δ 3.91 (s, 3H), 6.96 (d, J = 8.2 Hz, 1H), 7.20 (dd, J_1 = 8.6; J_2 = 1.6 Hz, 1H), 7.38 (dd, J_1 = 8.2; J_2 = 2.0 Hz, 1H), 7.42 (d, J = 2.0 Hz, 1H), 7.49 (d, J = 8.6 Hz, 1H), 7.52 (d, J = 1.6 Hz, 1H). ^{13}C NMR (50 MHz, CD_3OD): δ 54.7, 110.0, 112.7, 113.9, 114.9, 117.0, 121.6, 122.4, 127.6, 137.3, 139.8, 140.0, 149.7, 154.0. HRMS (ESI^+) calcd. for $C_{14}H_{13}ClN_3O$: 274,0747, found: 304.0735.

*4.1.2.4.2. 5-Amino-2-(4-methoxyphenyl)-1*H*-benzimidazole,* **18**. Yield: 65%. Compound crystallized from MeOH to give a brown-red solid, Mp: 195–197 °C. IR (KBr): ν_{max} 3300, 2910, 1626, 1573, 1355, 1330, 1267, 1011, 923, 820, 795 cm^{-1}. ^1H NMR (200 MHz, CD_3OD): δ 3.84 (s, 3H), 6.73 (dd, J_1 = 8.6; J_2 = 1.8 Hz, 1H), 6.92 (d, J = 1.8 Hz, 1H), 7.03 (d, J = 9.0 Hz, 2H), 7.35 (d, J = 8.6 Hz, 1H), 7.94 (d, J = 9.0 Hz, 2H). ^{13}C NMR (50 MHz, CD_3OD): δ 54.4 ($O\underline{C}H_3$), 99.0 (C-4), 112.9 (C-6), 113.9 (C-3′ + C-5′), 115.4 (C-7), 122.3 (C-1′), 127.4 (C-2′ + C-6′), 133.9 (C-7a), 138.5 (C-3a), 143.1 (C-5), 150.9 (C-2), 161.0 (C-4′). HRMS (ESI^+) calcd. for $C_{14}H_{14}N_3O$ $[M+H]^+$: 240.1137, found: 240.1131.

4.1.2.5. Coupling of BZ **18** *with picolinic acid,* **19**. 79 mg (0.49 mmol) of 1,1-carbonildiimidazole (CDI) was added to a solution of 50 mg (0.41 mmol) of picolinic acid in dry DMF (2 mL), and the mixture was maintained at room temperature for 1 h. Then, 88 mg (0.37 mmol) of compound BZ **18** was added, and the mixture was kept at room temperature with magnetic stirring for 16 h. The progress of the reaction was monitored by TLC, and a mixture of *n*-hexane/ethyl acetate (1:9) was used as eluent. After completion of the reaction, the solvent was removed under *vacuum* on a rotary evaporator, and the solid purified by column chromatography with *n*-hexane/ethyl acetate (2:8) as eluent gave 40 mg (67% yield) of an orange solid.

*4.1.2.4.3. 2-(4-Methoxyphenyl)-5-picolinamidil-1*H*-benzimidazole,* **19**. Yield: 70%. IR (KBr): ν_{max} 3300, 2910, 1626, 1573, 1355, 1330, 1267, 1011, 923, 820, 795 cm^{-1}. ^1H NMR (400 MHz, CD_3OD): δ 3.88 (s, 3H), 7.09 (d, J = 8.0 Hz, 2H), 7.50 (dd, J_1 = 8.6; J_2 = 1.8 Hz, 1H), 7.58 (d, J = 8.6 Hz, 1H), 7.62 (m, 1H), 8.03 (d, J = 8.0 Hz, 2H), 8.04 (d, J = 1.8 Hz, 1H), 8.23 (m, 1H), 8.29 (m, 1H), 8.73 (m, 1H). ^{13}C NMR (100 MHz, CD_3OD): δ 55.9 ($O\underline{C}H_3$), 107.1 (C-4), 115.6 (C-3′ + C-5′), 116.2 (C-7), 117.7 (C-6), 123.1 (C-1′), 123.3 (C-3″), 127.9 (C-5″), 129.4 (C-2′ + C-6′), 134.6 (C-5), 139.1 (C-4″), 139.2 (C-3a), 140.1 (C-7a), 149.7 (C-6″), 151.2 (C-2″), 154.2 (C-2), 163.1 (C-4′), 164.4 (CONH). HRMS (ESI^+) calcd. for $C_{20}H_{17}N_4O_2$ $[M+H]^+$: 345,1352, found: 345.1340.

4.2. Biological evaluation

4.2.1. Chemicals and drugs

Stock solutions of all the compounds and positive controls were prepared in DMSO (Sigma 276855), while the final dilutions were made with distilled water in order to maintain a maximum

concentration of 0.5% DMSO per well. To perform the different *in vitro* tests, thiabendazole (TBZ, Sigma T8904) or ivermectin (IVM, Sigma I8898) were used as positive controls, while 0.5% DMSO was used as negative control in all tests. Levamisole (LEV, Sigma 31742) was also used as positive control but in this case, the stock solution was prepared in distilled water.

4.2.2. Teladorsagia circumcincta

Different *in vitro* tests were carried out to test the anthelmintic activity of the new compounds in three stages of the parasite: eggs, first stage larvae (L1) and third stage larvae (L3). All of these tests were performed using two different strains, one susceptible and one resistant to BZs, LEV and IVM (the latter kindly provided by Dr. Dave Bartle, Moredun Research Institute, Edinburgh, UK).

4.2.3. Animals

To obtain biological material for further experiments, six 3 months-old Merino lambs were infected with 25,000 L3 of *T. circumcincta* at the facilities of the "Instituto de Ganadería de Montaña" (León, Spain). As indicated above, four of them were infected with a susceptible strain and the other two with the resistant one. All study protocols were revised and approved by the University of León Animal Care Committee (León, Spain) to AGL2016-79813-C2-1R/2R, according to current national and European regulations of animal wellbeing (R.D 53/2013 and EU Directive 2010/63/EU).

4.2.4. In vitro tests

A total of three *in vitro* experiments were undertaken to determine the activity of the 24 BZ derivatives against different stages of *T. circumcincta* using a susceptible strain of the parasite. An initial screening of the compounds was performed using a first discriminant concentration of 50 μM by the Egg Hatch Test (EHT), and the Larval Migration Inhibition Test (LMIT). The next step was to calculate the half maximal effective concentration (EC_{50}) in those compounds with activities higher than 90% at this initial screening. Then, with those compounds, the same initial screening at a discriminant dose of 50 μM within a resistant strain of the parasite was performed, and as in the previous case, EC_{50} was later calculated in those compounds with efficacies higher than 80%. When the EHT was carried out, some compounds showed larvicidal activity, so a Larval Mortality Test (LMT) was also performed in parallel. The procedure in this case was the same as in the EHT: an initial screening at a discriminant dose of 50 μM and the estimation of their EC_{50}.

All compounds were tested at least in duplicate at 3 different days to accurate the results.

Cytotoxicity assays were conducted on human Caco-2 and HepG2 cell lines with the aim to define the Selectivity Indexes (SI) for those compounds in which the EC_{50} was determined, and to compare the SI with those of the reference drug thiabendazole (TBZ).

4.2.4.1. Egg hatching test (EHT). EHT is based on a modification of a protocol previously described by Ref. [31]. Briefly, parasite eggs were freshly obtained from lamb faeces experimentally infected with *T. circumcincta* and distributed in 24-well cell culture plates (Costar®, CLS3738) at a density of 100–150 eggs per well in a volume of 1 mL. To carry out the initial testing, a 10 mM stock solution was prepared by dissolving each compound in DMSO, from which working solutions were prepared by further dilutions with distilled water. Each well included 1 mL of the egg suspension, 10 μL of a stock solution with each compound and distilled water up to 2 mL to achieve a final concentration in well of 50 μM. Additionally, in each plate TBZ was included at concentration of 0.1 μg/mL (0.5 μM) as positive control. After 48 h incubation at 23 °C, the number of L1 and eggs present per well were counted using an inverted microscope to determine the percentage of hatched eggs (number of L1/number of L1 larvae and eggs X 100). The ovicidal activity was expressed by the percentage of egg hatching inhibition using the following formula:

% Egg hatching inhibition = [100 − (% egg hatching per well/% egg hatching in control well)] x 100.

The EC_{50} of the compounds was calculated using 6 concentrations ranging from 50 μM to 1.56 μM.

4.2.4.2. Larval mortality test (LMT). This test was carried out only on those compounds in which dead larvae appeared during the EHT reading (BZs **4**, **9** and **22**), in order to discard a possible activity against this parasite stage.

With the aim to obtain L1, fresh eggs (previously extracted from the faeces) were incubated during 24 h at 23 °C. Then, larvae were collected in a known volume of water to obtain a density of 100–150 larvae per mL. The LMT was performed in the same way as the EHT but using the L1 instead. In this case a stock solution of LEV at 10 mg/mL was added as positive control on every plate to reach a final concentration of 1 mg/mL (4.15 mM) per well. The number of dead and alive L1 present per well was counted using an inverted microscope to determine the larvicidal activity of the compound ([number of dead L1/number of dead and alive L1] X 100). Apparently motionless and rod-shaped larvae were considered dead, while those that presented some kind of movement or curvature in their body were considered alive. The efficacy of the compound was expressed by the percentage of viability inhibition using the following formula:

% Viability inhibition = (% larvicidal activity per well/% larvicidal activity in control well) x 100.

The EC_{50} of each compound was calculated using 6 concentrations ranging from 50 μM to 1.56 μM.

4.2.4.3. Larval migration inhibition test (LMIT). LMIT was conducted in following the method described previously by Ref. [32]. To obtain L3, faeces from infected lambs were cultured in aerated and humidified closed boxes twice a week and placed in a climatic chamber at 25 °C for 13 days. Briefly, L3 were exsheathed by incubation in 0.5% (v/v) sodium hypochlorite solution for 10 min at room temperature. After incubation, the larvae suspension was washed 3 times by adding distilled water and centrifugation for 15 min at 300 g. Then, the number of larvae was adjusted to a density of 1000 L3 per mL and aliquots of 100 μL were added to each well in a 96-well culture plate (VWR, 734–2327) containing 100 μL of a suspension of distilled water with the compounds. As in the other test, all compounds were tested at a single dose of 50 μM; and 100 μM final concentration IVM was used as positive control. Each compound was tested in triplicate on the same plate and at least two technical replicas were performed. After 24 h of incubation in the dark at 28 °C, the whole content of each well was transferred to a 96-wells MultiScreen-Mesh Filter Plate (Sigma-Aldrich, MANMN2010) and left for a further 24 h to allow the motile L3 to pass through the sieves (20 μm mesh size) for counting. The size of the mesh was 20 μm to prevent the "fall" of the larvae since the cross-diameter of these is slightly larger [33].

The efficacy was expressed by the percentage of larval migration inhibition using the following formula:

% Larval migration inhibition = [(number of larvae migrating through sieves in negative controls wells − number of larvae

migrating through sieves in treatment wells) / number of larvae migrating through sieves in negative controls wells.] x 100

The EC_{50} of each compound was calculated using 6 concentrations ranging from 50 μM to 1.56 μM.

4.2.5. Cytotoxicity assay and selectivity indexes

The cytotoxicity evaluation of 2-phenylbenzimidazoles was carried out on two human cell lines: the colorectal adenocarcinoma Caco-2 (ATCC® HTB-37™) and the hepatocarcinoma HepG2 (ATCC® HB-8065™). Briefly, 10,000 cells were seeded on 96 well-plates in RPMI 1640 Medium supplemented with 2.0 g/L sodium bicarbonate (Fisher Scientific®), 1% (w/v) L-glutamine (Sigma-Aldrich®), and 25 mM HEPES buffer, 10% (v/v) inactivated foetal bovine serum (FBS), and antibiotic mixture containing 10,000 U/mL penicillin and 10,000 μg/mL streptomycin. Cultures were incubated at 37 °C in a humidified atmosphere containing 5% CO_2. After 24 h, different concentrations of testing compounds (ranging from 1 to 100 μM) were added for 72 h. After this time, the viability of the cells was assessed using the Alamar Blue (BioRad) staining method according to manufacturer's recommendations (Invitrogen).

Cytotoxic concentration 50 (CC_{50}) values were determined by plotting the concentration of each compound *vs*. cell viability expressed as the fluorescence emitted by resorufin at 590 nm. Dose-response curves were fitted using non-linear regression plots, using Sigma Plot programme (10.0 Software, Inc., San José, California; USA).

As a safety parameter of each compound, selectivity index (SI) was calculated as the CC_{50}/EC_{50} ratio of those compounds with a measurable effect on eggs or larvae. Despite the fact that the SI was calculated using non-congruent magnitudes (cells *vs* organisms), we considered that it was useful to compare the relative toxicity of the compounds.

4.2.6. Predictive drug-likeness and ADME-Toxicity parameters for BZs

Compounds with the best nematocidal activity and weak cytotoxicity were submitted to *in silico* pharmacokinetic properties and adverse effects prediction. To predict the druggability of these compounds, we got the parameters (see supplementary data) related to Lipinski's rule of five, absorption rate, drug-likeness and potential toxicity risks provided online by the freely accessible web-based applications Osiris Data Warrior (http://www.openmolecules.org/datawarrior and https://www.organic-chemistry.org/prog/peo); and preADMET (https://preadmet.bmdrc.kr/adme/and https://preadmet.bmdrc.kr/druglikeness/).

4.2.7. Tubulin homology modelling

Homology modelling of *T. circumcincta* β-tubulin was performed with SWISS-MODEL Workspace [34]. The sequence of this protein was taken from the one published in the literature [35]. This protein has a highly conserved region, which includes the most representative amino acids of the active site. This conserved region was identified after comparison with other β-tubulin sequence species using GCG software. Residues 1–419 of chain B of the crystallographic structure of *Ovis aries* tubulin (PDB ID: 3N2G) were used as a template [36].

The protein structure was validated by the use of Rampage server (http://mordred.bioc.cam.ac.uk/~rapper/rampage.php) which predicts the stereochemical quality and accuracy of the generated model. Ramachandran plot analysis revealed 92.7% residues of modelled structure in the favoured region, 6.0% residues in the allowed region, and 1.3% residues in the disallowed region.

4.2.8. Molecular docking

Docking calculations were performed using Glide integrated into the Schrödinger Molecular Modelling Suite (Schrödinger, Inc., USA, 2016–4). *T. circumcinta* β-tubulin previously obtained by homology modelling was used as a target to further understand the molecular bases of the inhibitory properties of these compounds. This target was processed with the Protein Preparation Wizard available in the modelling package. The process preparation of the protein included assignation of bond orders, addition and optimization of hydrogens, filling in missing side chains, cap termini addition, optimization of protonation states of some residues, H-bond network optimization, etc. The model was refined using OPLS-2005 Force Field. The ligands which appear in Table 1 were processed with the LigPrep module implemented in the same package previous to optimizing the structure of each ligand; afterwards different tautomers were generated considering the different protonation states (pH 7.0 ± 2.0) and partial charges using the OPLS-2005 force-field were assigned.

A receptor grid was generated and centred in the colchicine binding site of the β-tubulin. The size of the box was 25x25x25 Å, with a van der Waals scaling factor of 1.0 and a partial charge cut-off of 0.25. Docking was carried out using the Extra Precision (XP) mode of Glide. The final pose was selected using the energetic parameter GlideScore function. The docking poses of some significant ligands can be visualized and analysed for the key elements of interaction with the target enzyme using the Maestro's Pose Viewer utility in Figs. 1–4 and supplementary material (section 4).

Author contributions

All authors participate in their respective areas of research and collaborate to the writing of the manuscript.

Declaration of competing interest

The authors declare that they have no known competing financial interests or personal relationships that could have appeared to influence the work reported in this paper.

Acknowledgements

We would like to express our gratitude to Dr. Dave Bartley at Moredun Research Institute for providing the triple-resistant strain of *T. circumcincta*. Authors thank Bioinformatic & Molecular Design Research Centre (BMDRC, Yonsey University, Seoul, Korea) and Idorsia Pharmaceuticals Ltd. (Allschwil, Switzerland) for complimentary access to preADMET and Osiris Data Warrior databases, respectively. RE thanks financiation from RICET-USAL Program RD16/0027/0018. Financial support came from MINECO: RETOS (AGL2016-79813-C2-1R/2R) and Junta de Castilla y León co-financed by FEDER, UE (LE020P17). EVG was funded by FPU16/03536, VCGA by Junta de Castilla y León and FSE (LE082-18), MAV by Junta de Castilla y León (LE051-18) and MMV by the Spanish "Ramon y Cajal" Programme (Ministerio de Economía y Competitividad; MMV, RYC-2015-18368), respectively.

Appendix A. Supplementary data

Supplementary data to this article can be found online at https://doi.org/10.1016/j.ejmech.2020.112554.

References

[1] World Health Organization, Schistosomiasis and Soiltransmitted Helminthiases: Numbers of People Treated in 2017 [WWW Document], vol. 93, 2018.

WHO. URL, http://www.who.int/wer2018. accessed 7.18.2019.
[2] P.J. Hotez, Aboriginal populations and their neglected tropical diseases, PLoS Neglected Trop. Dis. 8 (2014), e2286, https://doi.org/10.1371/journal.pntd.0002286.
[3] S.P. Montgomery, M.C. Starr, Soil-transmitted helminthiasis in the United States: a systematic review—1940–2010, Am. J. Trop. Med. Hyg. 85 (2011) 680–684, https://doi.org/10.4269/ajtmh.2011.11-0214.
[4] F. Schär, U. Trostdorf, F. Giardina, V. Khieu, S. Muth, H. Marti, P. Vounatsou, P. Odermatt, *Strongyloides stercoralis*: global distribution and risk factors, PLoS Neglected Trop. Dis. 7 (2013) e2288, https://doi.org/10.1371/journal.pntd.0002288.
[5] M.A. Cruz-Rojo, M. Martínez-Valladares, M.A. Álvarez-Sánchez, F.A. Rojo-Vázquez, Effect of infection with *Teladorsagia circumcincta* on milk production and composition in Assaf dairy sheep, Vet. Parasitol. 185 (2012) 194–200, https://doi.org/10.1016/j.vetpar.2011.10.023.
[6] A. Kloosterman, H.K. Parmentier, H.W. Ploeger, Breeding cattle and sheep for resistance to gastrointestinal nematodes, Parasitol. Today 8 (1992) 330–335, https://doi.org/10.1016/0169-4758(92)90066-B.
[7] A.R. Sykes, Parasitism and production in farm animals, Anim. Sci. 59 (1994) 155–172, https://doi.org/10.1017/S0003356100007649.
[8] F. Jackson, R.L. Coop, The development of anthelmintic resistance in sheep nematodes, Parasitology 120 (2000) 95–107, https://doi.org/10.1017/S0031182099005740.
[9] R.M. Kaplan, Drug resistance in nematodes of veterinary importance: a status report, Trends Parasitol. 20 (2004) 477–481, https://doi.org/10.1016/J.PT.2004.08.001.
[10] E. Papadopoulos, E. Gallidis, S. Ptochos, Anthelmintic resistance in sheep in Europe: a selected review, Vet. Parasitol. 189 (2012) 85–88, https://doi.org/10.1016/j.vetpar.2012.03.036.
[11] M. Abongwa, R.J. Martin, A.P. Robertson, A brief review on the mode of action of antinematodal drugs, Acta Vet. 67 (2017) 137–152, https://doi.org/10.1515/acve-2017-0013.
[12] D.B. Bhinsara, M. Sankar, D.N. Desai, J.J. Hasnani, P.V. Patel, N.D. Hirani, V.D. Chauhan, Benzimidazole resistance: an overview, Int. J. Curr. Microbiol. App. Sci 7 (2018) 3091–3104, https://doi.org/10.20546/ijcmas.2018.702.372.
[13] L.F.V. Furtado, A.C.P. de Paiva Bello, E.M.L. Rabelo, Benzimidazole resistance in helminths: from problem to diagnosis, Acta Trop. 162 (2016) 95–102, https://doi.org/10.1016/j.actatropica.2016.06.021.
[14] M. Martínez-Valladares, T. Geurden, D.J. Bartram, J.M. Martínez-Pérez, D. Robles-Pérez, A. Bohórquez, E. Florez, A. Meana, F.A. Rojo-Vázquez, Resistance of gastrointestinal nematodes to the most commonly used anthelmintics in sheep, cattle and horses in Spain, Vet. Parasitol. 211 (2015) 228–233, https://doi.org/10.1016/j.vetpar.2015.05.024.
[15] J. Vercruysse, M. Albonico, J.M. Behnke, A.C. Kotze, R.K. Prichard, J.S. McCarthy, A. Montresor, B. Levecke, Is anthelmintic resistance a concern for the control of human soil-transmitted helminths? Int. J. Parasitol. Drugs Drug Resist. 1 (2011) 14–27, https://doi.org/10.1016/j.ijpddr.2011.09.002.
[16] S.K. Tahir, P. Kovar, S.H. Rosenberg, S.C. Ng, Rapid colchicine competition binding scintillation proximity assay using biotin-labelled tubulin, Biotechniques 29 (2000) 156–160, https://doi.org/10.2144/00291rr02.
[17] R. Aguayo-Ortiz, O. Méndez-Lucio, J.L. Medina-Franco, R. Castillo, L. Yépez-Mulia, F. Hernández-Luis, A. Hernández-Campos, Towards the identification of the binding site of benzimidazoles to β-tubulin of *Trichinella spiralis*: insights from computational and experimental data, J. Mol. Graph. Model. 41 (2013) 12–19, https://doi.org/10.1016/j.jmgm.2013.01.007.
[18] R.N. Beech, P. Skuce, D.J. Bartley, R.J. Martin, R.K. Prichard, S. Gilleard, Anthelmintic resistance: markers for resistance or susceptibility? Parasitology 138 (2010) 160–174, https://doi.org/10.1017/S0031182010001198.
[19] W. Wang, D. Kong, H. Cheng, L. Tan, Z. Zhang, X. Zhuang, H. Long, Y. Zhou, Y. Xu, X. Yang, K. Ding, New benzimidazole-2-urea derivatives as tubulin inhibitors have been reported, Bioorg. Med. Chem. Lett 24 (2014) 4250–4253, https://doi.org/10.1016/j.bmcl.2014.07.035.
[20] G.A. Patani, E.J. LaVoie Bioisosterism, A Rational approach in drug design, Chem. Rev. 96 (1996) 3147–3176, https://doi.org/10.1021/cr950066q.
[21] M. Zajíčková, L.T. Nguyen, L. Skálová, L. Raisová Stuchlíková, P. Matoušková, Anthelmintics in the future: current trends in the discovery and development of new drugs against gastrointestinal nematodes, Drug Discov. Today 25 (2020) 430–437, https://doi.org/10.1016/j.drudis.2019.12.007.
[22] M. Tonelli, M. Simone, B. Tasso, F. Novelli, V. Boido, F. Sparatore, G. Paglietti, S. Prici, G. Giliberti, S. Blois, C. Ibba, G. Sanna, R. Laddo, P.L. Colla, Antiviral activity of benzimidazole derivatives II antiviral activity of 2-phenylbenzimidazole derivatives, Bioorg. Med. Chem. 18 (2010) 2937–2953, https://doi.org/10.1016/j.bmc.2010.02.037.
[23] M. Tonelli, F. Novelli, B. Tasso, I. Vazzana, A. Sparatore, V. Boido, F. Sparatore, P.L. Colla, G. Sanna, G. Giliberti, B. Busonera, P. Farci, C. Ibba, R. Loddo, Antiviral activity of benzimidazole derivatives. III. Novel anti-CVB-5, anti-RSV and anti-Sb-1 agents, Bioorg. Med. Chem. 22 (2014) 4893–4909, https://doi.org/10.1016/j.bmc.2014.06.043.
[24] S. Utku, M. Topal, A. Dögen, M.S. Serin, Synthesis, characterization, antibacterial and antifungal evaluation of some new platinum(II) complexes of 2-phenylbenzimidazole ligands, Turk. J. Chem. 34 (2010) 427–436, https://doi.org/10.3906/kim-1002-5.
[25] R. Sawant, D. Kawade, Synthesis and biological evaluation of some novel 2-phenyl benzimidazole-1-acetamide derivatives as potential anthelmintic agents, Acta Pharm. 61 (2011) 353–361, https://doi.org/10.2478/v10007-011-0029-z.
[26] E.R. Morgan, J. van Dijk, Climate and the epidemiology of gastrointestinal nematode infections of sheep in Europe, Vet. Parasitol. 189 (2012) 8–14, https://doi.org/10.1016/j.vetpar.2012.03.028.
[27] A. Shaukat, H.M. Mirza, A.H. Ansari, M. Yasinzai, S.Z. Zaidi, S. Dilshad, F.L. Ansari, Benzimidazole derivatives: synthesis, leishmanicidal effectiveness and molecular docking studies, Med. Chem. Res. 22 (2012) 3606–3620, https://doi.org/10.1007/S00044-012-0375-5.
[28] R. Sawant, D. Kawade, Synthesis and biological evaluation of some novel 2-phenyl benzimidazole-1-acetamide derivatives as potential anthelmintic agents, Acta Pharm. 61 (2011) 353–361, https://doi.org/10.2478/v10007-011-0029-z.
[29] J.G. Penieres-Carrillo, H. Ríos-Guerra, J. Pérez-Flores, B. Rodríguez-Molina, A. Torres-Reyes, F. Barrera-Téllez, J. González-Carrillo, L. Moreno-González, A. Martínez-Zaldívar, J.J. Nolasco-Fidencio, A.S. Matus-Meza, R.A. Luna-Mora, Reevaluating the synthesis of 2,5-disubstituted-1*H*-benzimidazole derivatives by different green activation techniques and their biological activity as antifungal and antimicrobial inhibitor, J. Heterocycl. Chem. 57 (2020) 436–455, https://doi.org/10.1002/jhet.3801.
[30] W.L.F. Armarego, D.D. Perrin, Purification of Laboratory Chemicals, fourth ed., Butterworth-Heinemann, Oxford. MA, 1997.
[31] G.C. Coles, C. Bauer, F.H.M. Borgsteede, S. Geerts, T.R. Klei, M.A. Taylor, P.J. Waller, World Association for the Advancement of Veterinary Parasitology (W.A.A.V.P.) methods for the detection of anthelmintic resistance in nematodes of veterinary importance, Vet. Parasitol. 44 (1992) 35–44, https://doi.org/10.1016/0304-4017(92)90141-U.
[32] J. Demeler, U. Küttler, G. von Samson-Himmelstjerna, Adaptation and evaluation of three different in vitro tests for the detection of resistance to anthelmintics in gastro intestinal nematodes of cattle, Vet. Parasitol. 170 (2010) 61–70, https://doi.org/10.1016/j.vetpar.2010.01.032.
[33] B. Rabel, R. Mcgregor, P.G.C. Douch, Improved bioassay for estimation of inhibitory effects of ovine gastrointestinal mucus and anthelmintics on nematode larval migration, Int. J. Parasitol. 24 (1994) 671–676, https://doi.org/10.1016/0020-7519(94)90119-8.
[34] A. Waterhouse, M. Bertoni, S. Bienert, G. Studer, G. Tauriello, R. Gumienny, F.T. Heer, T.A.P. de Beer, C. Rempfer, L. Bordoli, R. Lepore, T. Schwede, Swiss-Model, Homology modelling of protein structures and complexes, Nucleic Acids Res. 46 (2018) W296–W303, https://doi.org/10.1093/nar/gky427.
[35] L. Elard, A.M. Comes, J.F. Humbert, Sequences of beta-tubulin cDNA from benzimidazole-susceptible and -resistant strains of *Teladorsagia circumcincta*, a nematode parasite of small ruminants, Mol. Biochem. Parasitol. 79 (1996) 249–253, https://doi.org/10.1016/0166-6851(96)02664-3.
[36] P. Barbier, A. Dorleans, F. Devred, L. Sanz, D. Allegro, C. Alfonso, M. Knossow, V. Peyrot, J.M. Andreu, Stathmin and interfacial microtubule inhibitors recognize a naturally curved conformation of tubulin dimers, J. Biol. Chem. 285 (2010) 31672–31681, https://doi.org/10.1074/jbc.M110.141929.

III.3. ARTÍCULO 3

Este artículo está relacionado con los objetivos 2 y 4 del Trabajo de Tesis.

Como se ha expuesto anteriormente, las resistencias generadas a los nematicidas disponibles en el mercado ponen de manifiesto la necesidad de hallar nuevas alternativas terapéuticas. Teniendo en cuenta los resultados obtenidos en el Artículo 2, en este trabajo se pretende mejorar la afinidad y potencia antihelmíntica de derivados de Bz. Para ello, se realizaron nuevos estudios de docking y modelado molecular con β-tubulina, analizando la interacción de los distintos compuestos de las diferentes familias con la diana. Teniendo en cuenta los resultados teóricos, se seleccionan tres nuevos esqueletos de Bz (tipos II-IV).

Así, se obtienen, además de los 2-fenilBz (tipo I), las tres familias, que contienen espaciadores nitrogenados de dos (N-C, tipo II y III) o tres (N-C-C, tipo IIIa; IV en este artículo) átomos entre el núcleo benzimidazólico y el fragmento aromático (Fig. III.1). Se pusieron a punto los procesos de síntesis, se purificaron y caracterizaron convenientemente todos los compuestos obtenidos según sus propiedades fisicoquímicas, y se prepararon las muestras para ensayo in vitro en una cepa sensible de *T. circumcincta*.

Further and new target-based benzimidazole anthelmintics active against *Teladorsagia circumcincta*

Nerea Escala, Elora Valderas-García, María Álvarez Bardón, Verónica Castilla Gómez de Agüero, José Luis López-Pérez, Francisco A. Rojo-Vázquez, Arturo San Feliciano, María Martínez-Valladares, Rafael Balaña-Fouce, Esther del Olmo

En: *Journal of Molecular Structure* 2022, 1269, 133735; doi: 10.1016/j.molstruc.2022.133735

Factor de Impacto: 3,841
Quartil: Q2

Journal of Molecular Structure 1269 (2022) 133735

Contents lists available at ScienceDirect

Journal of Molecular Structure

journal homepage: www.elsevier.com/locate/molstr

Further and new target-based benzimidazole anthelmintics active against *Teladorsagia circumcincta*

Nerea Escala[a,1], Elora Valderas-García[b,c,1], María Álvarez Bardón[b], Verónica Castilla Gómez de Agüero[c,d], José Luis López-Pérez[a,e], Francisco A. Rojo-Vázquez[d], Arturo San Feliciano[a,f], María Martínez-Valladares[c,d,**], Rafael Balaña-Fouce[b,*], Esther del Olmo[a,*]

[a] Departamento de Ciencias Farmacéuticas: Química Farmacéutica, Facultad de Farmacia, Universidad de Salamanca, CIETUS, IBSAL, Salamanca 37007, Spain
[b] Departmento de Ciencias Biomédicas, Facultad de Veterinaria, Universidad de León, León 24071, Spain
[c] Instituto de Ganadería de Montaña, CSIC-Universidad de León, Grulleros, León 24346, Spain
[d] Departamento de Sanidad Animal, Facultad de Veterinaria, Universidad de León, León 24071, Spain
[e] Facultad de Medicina, Universidad de Panamá, Panamá
[f] Programa de Pós-graduaçao em Ciências Farmacêuticas, Universidade do Vale do Itajaí, UNIVALI. Itajaí, SC, Brazil

ARTICLE INFO

Article history:
Received 6 June 2022
Revised 14 July 2022
Accepted 15 July 2022
Available online 19 July 2022

Keywords:
Benzimidazole derivatives
Teladorsagia
Anthelmintic
Docking
Structure-activity relationships

ABSTRACT

Helminth infections are one of the most prevalent parasitic diseases affecting animals and humans worldwide. Anthelmintic resistance to the main drugs used to control these infections in animals, especially ruminants, is a major global problem that needs urgent solutions. The purpose of this study was to design and obtain new benzimidazole (BZ) derivatives to evaluate their *in vitro* ovicidal and larvicidal activities. Based on previous results from 2-phenylbenzimidazoles and new docking studies of different BZ-containing scaffolds in *Teladorsagia circumcincta* tubulin four structural groups of BZs were selected. In addition to several new members of those previously reported 2-phenylBZs (type I), some twenty 2-aminoBZ derivatives (type II) and twenty-five BZ amides (types III and IV) were prepared and evaluated for their ability to inhibit egg hatching and larval motility of *T. circumcincta* with results superior to those previously achieved. Nine of the fifty-five BZs tested displayed ovicidal activity higher than 90%, and fourteen induced more than 30% larval death in the assays at 50 μM. The benzamide BZ **42** showed the best ovicidal EC_{50} value of 0.92 μM with a selectivity index > 100 respecting HepG2 cells, while the benzylamine BZ **13** attained a higher than 50% larvicidal activity. Notably, the amide BZ **39** displayed both ovicidal (100%) and larvicidal (>50%) activities. The SAR analysis and the docking studies carried out led to the conclusion that, in addition to the effects on tubulin, pending experimental confirmation, there must be other mechanisms by which the evaluated BZs prevent hatching and limit the mobility of the parasitic larvae.

Introduction

Helminthic infections are a type of parasite infection that affects both human and animal species. In humans, these parasites are classified as soil transmitted helminths and affect more than a quarter of the world's population, causing substantial disease and disability [1]. In grazing ruminants, one of the most prevalent helminth parasites worldwide are gastrointestinal nematodes (GINs), which produce important economic losses mainly derived from decreased production and increased healthcare costs [2].

During recent decades, control strategies against GINs in livestock have been mainly focused on massive drug administration which has led to the development of high levels of anthelmintic resistance all over the world [3–5]. This problem is seriously aggravated by the reduced number of types of anthelmintic drugs available on the market, requiring the development of new drugs and formulations for the treatment of these diseases.

* Corresponding author at: Departamento de Ciencias Farmacéuticas: Química Farmacéutica, Facultad de Farmacia, Universidad de Salamanca, CIETUS, IBSAL, Salamanca 37007, Spain
** Corresponding author at: Departamento de Sanidad Animal, Facultad de Veterinaria, Universidad de León, León 24071, Spain.
E-mail addresses: mmarva@unileon.es (M. Martínez-Valladares), rbalf@unileon.es (R. Balaña-Fouce), olmo@usal.es (E. del Olmo).
[1] Both authors shared the first position.

https://doi.org/10.1016/j.molstruc.2022.133735

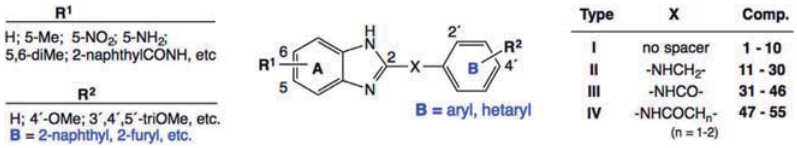

Fig. 1. General structures of types I–IV of the studied benzimidazoles.

In this context, different approaches have been proposed, such as the synthesis of novel chemical entities, drug repurposing, identification of active natural products or the synthesis of new derivatives [6]. The latter approach is a reasonable way of improving the properties and effectiveness of known drug scaffolds, as in the case of benzimidazoles (BZs), one of the most important classes of currently used anthelmintic agents. This well-known family of drugs includes good ovicidal and larvicidal agents, but they also present problems such as low water solubility, which limit their therapeutic effectiveness. Therefore, the preparation of new derivatives has been useful to develop soluble drugs, as in the case of mebendazole nitrate [7].

Previous studies of our research groups on 2-phenylbenzimidazole derivatives showed considerable ovicidal activity in GIN, *Teladorsagia circumcincta* infected sheep of compound 2-(4-bromophenyl)−1*H*-benzimidazole (EC_{50} = 6.30 μM) on a strain susceptible to albendazole, and that of compound 5-chloro-2-(4-chlorophenyl)−1*H*-benzimidazole (EC_{50} = 11.0 μM) on an albendazole-resistant strain of the same species [8]. The mechanism of action of BZs was associated with their high-affinity selective binding to the β-tubulin of the parasite, preventing the formation of microtubules, leading to the destruction of the cellular structure and the death of the parasite [9]. According to the reported docking results, the phenylBZs studied by Escala et al. [8] frequently established a hydrogen bond with the peptide carbonyl of Val236 through their BZN-H fragment acting as H-donor. Additionally, some of the most potent BZs presented π-stacking (T-shaped) aromatic ring interactions between the BZ moiety and the β-tubulin Phe200 residue.

Bearing these results in mind, and with the aim of going ahead to improve the potency and selectivity of BZ anthelmintic agents active against GIN, a planned virtual docking screening involving dozens of new structures and having different BZ arrangements and diverse functional groups, was carried out. The analysis of the results of such screening allowed discovery of some additional BZ-tubulin interactions, that led to the selection of three additional BZ scaffolds and the design of the compounds to be prepared and tested, as being described here.

2. Results and discussion

2.1. Chemistry

2.1.1. Design, synthesis and characterisation

As mentioned above, to the previous group of 2-phenylBZs (type I) three additional groups of BZ analogues derived from docking studies were added. They contain a nitrogen-based spacer of two (N-C, types II and III) or three (N-C-C, type IV) atoms between the main BZ (A) moiety and the aromatic fragment B, as represented in Fig. 1.

According to the preliminary docking results with predicted docking-score values better than −9 kcal/mol, the new compounds of type I (2-phenyl/aryl/hetarylBZs) to be prepared should contain, at the BZ fragment, any substituent able to establish additional favourable interactions with tubulin. To attain a similar or better score level, compounds of types II–IV would be guanidine (2-aminoimidazole) derivatives and should have a functional two- or three-atoms spacer between the aromatic systems A and B (Fig. 1). More than one hundred new BZ-containing structural entities including tautomers and protonated species, in addition to some of the previously reported BZs, were virtually docked in the modelled *T. circumcincta* tubulin [8], XP score values from GLIDE docking [10] found for 2-aminoBZs (type II) and 2-carbamoylBZs (types III and IV) attained levels better than −10 kcal/mol, ahead of those previously obtained for most type I BZs (see Table ST1 in Supporting Information). The increase in the scores was associated to some additional interactions found. Thus, with respect to the BZNH - Val236 H-bond and the π-stacking BZ - Phe200 interaction generally observed for the 2-phenylBZs of type I, those of type II – IV BZs complexes showed the additional H-bond donor interaction of the imidazole unit to the Glu198 residue of β-tubulin, which surely would contribute to increase the interaction energy and the docking score.

Therefore, some fifty BZ derivatives belonging to the four different types I - IV (Fig. 1) were synthesised, new and known compounds are indicated at the bottom of **Tables 1–3**. Compounds type I were prepared by known procedures from substituted *o*-phenylenediamines and aryl-aldehydes, while in the case of types II, III and IV of BZs, the 2-aminoBZ intermediates (BZ*i*) had to be previously prepared, and then condensed either, with the corresponding aldehydes followed by reduction to obtain type II 2-aminoBZs **11**–**30**, or with acids to obtain types III (**31**–**47**) and IV (**47**–**55**) of BZ amides.

Type II compounds have been reported as potential inhibitors of 12-lipoxygenase [11], and 5-lipoxygenase[12], as well as anti-*Helicobacter pylori* agents [13], anticancer [14], or as antiproliferative [15]. With respect to compounds types III and IV, descriptions on activities such as fungicidal [16–20], antimalarial, anti-*Trypanosoma brucei* [21], anthelmintic [22], against HIV-1 proteases, or hepatitis B virus [23], neuroprotective agents targeting mGluR5 [24], inhibitors of interleukin-1-receptor-associated kinase-4 [25] antiproliferative [26], or inhibitors of 5-lipoxygenase [12] can be found.

BZs **1** to **10** have in common a 4-methoxy group attached to ring B, and BZs **5** to **10** show different substitutions on the amino group at position C-5 of the BZ nucleus. BZs **1** and **2** were obtained in our previous work [8]. The nitrophenylBZ **3** was obtained by a single step condensation of 4-nitrobenzene-1,2-diamine with 4-methoxybenzaldehyde, in the presence of sodium metabisulfite, giving a yield of 75%, which was higher than the previously attained (65%). Reduction of BZ **3** with H_2 / Pd-C provided the aniline BZ **4** with a yield of 90% (Scheme 1), which was used to prepare BZs **5** to **10**.

The treatment of BZ **4** with di-*tert*-butyl dicarbonate (Boc_2O) gave the carbamate **5** a yield of 65%. The IR spectrum of BZ **5** showed absorption bands at 1693, 1391, 1366, 1250 and 1158 cm^{-1} of *tert*-butoxycarbonyl (Boc) fragment, and at 835 cm^{-1} of the *p*-substituted ring B. The ^{1}H NMR spectrum[1] of BZ **5** displayed with

[1] *Numbering priority:* To avoid confusion in spectral assignments through the sections, and to facilitate structural comparisons between the four types of BZs, the numbering priority has been attributed first, to the benzimidazole system (A), sec-

Table 1
Inhibition of egg hatching and larval migration of *Teladorsagia circumcincta* by type I BZ derivatives.

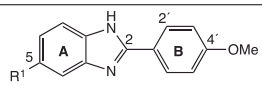

BZ	R [1]	Inhibition % (at 50 μM) Egg Hatching (EH)	Larval Migration (LM)
1	H	**100**[a]	11.5
2	Me	**100**[a]	**40.9**[a]
3	NO_2	3.2[a]	14.7
4	NH_2	< 1[a]	6.7
5	BocNH	< 1	8.7
6	TosylNH	< 1	**48.9**
7	2-NaphthylCH_2CONH	< 1	**43.8**
8	2-QuinolinylCONH	< 1	**38.7**
9	2-Boc-aminododecanoyl-NH	< 1	**39.1**
10	2-aminododecanoyl-NH	1.4	13.2
TBZ		**100**	*nd*
LEV		*nd*	**100**

Compounds **1** to **4** are known, while **5** to **10** are new. Boc = *tert*-butoxycarbonyl; *nd*: not determined
[a] Results taken from a previous study;[8] TBZ: thiabendazole; LEV: levamisol. EHI values >90% and LMI values >25% are bolded for comparison purposes.

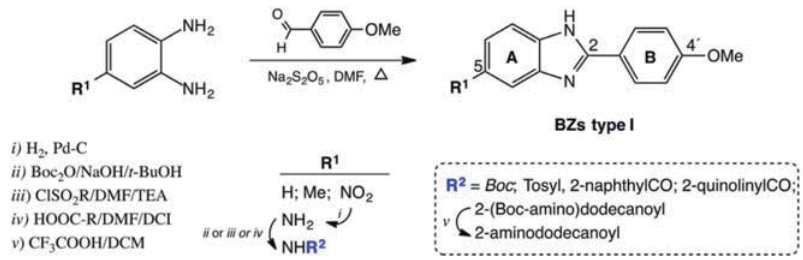

Scheme 1. Procedures for the synthesis of type I 2-methoxyphenylBZ derivatives.

respect to BZ **4** one intense singlet signal at 1.49 ppm that integrates for 9H and corresponds to the *tert*-butyl group, which resonate in ^{13}C NMR at 152.70, 80.34 and 28.8 ppm.

BZ **6** was obtained by tosylation of the aniline BZ **4** in 65% yield. Its IR and NMR spectral data reported in Section 4.1.2.4.1. confirm the sulfonamide formation and the incorporation of the *p*-tosyl group.

The amides BZs **7, 8** and **9** were obtained by coupling of BZ **4** with the corresponding acids in the presence of 1,1′-carbonyldiimidazole (CDI), with a yield of 67–94%, and the aminoamide BZ **10** by removal of the Boc-derivative **9** with trifluoroacetic acid. The 2-Boc-aminolauric acid used for the synthesis of BZ **9** was previously prepared by a reported procedure [27]. The ^{1}H and ^{13}C-NMR spectra of BZs **7** to **10** (Section 4.1.2.5) displayed the additional signals expected for the 2-naphthylmethyl, 2-quinolinyl, 1-Boc-aminoundecyl and 1-aminoundecyl groups, respectively.

To synthesise those type II–IV BZ derivatives, the corresponding BZ*is* had to be previously prepared by reaction of the corresponding 1,2-phenylenediamine with cyanogen bromide in aqueous methanol [28], which led to BZ*is* **1–5** at a yield of 62–85%. The physicochemical properties and spectral data of the resulting compounds were in accordance with the proposed structures (Section 4.1.2.7).

Type **II** BZs were obtained by a two-steps procedure (Scheme 2). BZ*is* **1–5** were reacted with different aldehydes in the presence of glacial acetic acid to obtain the corresponding imines, which were then reduced with $NaBH_4$ to provide BZs **11** to **30** in 17 with a 57% yield [29]. Physicochemical, MS, NMR and IR spectral data for BZs type II are reported in the experimental Sections 4.1.2.8.1-*20*. BZs **11** to **25** have a mono-substitution at position C-5 of the BZ unit with electron donating or withdrawing (Me, MeO, Cl) groups, while BZs **26** to **30** are di-substituted by either 5,6-dimethyl or 5,6-dichloro groups. Taken as an example of aminoBZs, the ^{1}H NMR of BZ **18** showed seven signals. Those corresponding to the BZ system resonate at 6.98 and 7.12 ppm as doublets (J = 7.8 Hz) for H-6 and H-7, respectively, and as a broad singlet at 7.18 for H-4. Regarding ring B, two doublets (J = 8.2 Hz) at 6.88 (H-3′+5′) and 7.32 (H-2′+6′) ppm were observed, in addition to a singlet at 3.77 of the methoxy group, and the signal at 4.56 ppm corresponding to the methylene group. In the ^{13}C NMR spectrum thirteen signals were observed, those corresponding to the B substituent at 113.98, 128.21, 131.72, 158.10 and 55.69 (methoxy group), those corresponding to the BZ system at 111.81, 118.8, 111.82, 120.11, 126.08, 134.00, 137.30 and 156.10 ppm, in addition to the signal at 45.99 ppm of the benzylic methylene.

The condensation of intermediate BZ*is* **1–5** with different acids in the presence of CDI, provided compounds III (BZs **31–46**) and IV (**47–55**) with yields ranging from 20% to 73% (Scheme 2). Variations in ring A included mono-substitution with electron donating or withdrawing groups (Me, MeO, Cl) and di-substitution (diMe, diCl). Variations on ring B were similar to those of type II BZs, in-

ond (with ′) to the homo or heterocyclic system B, and third, if necessary, (with ″) to the substituents attached to systems A or B. IUPAC names for all BZs are shown in the experimental section.

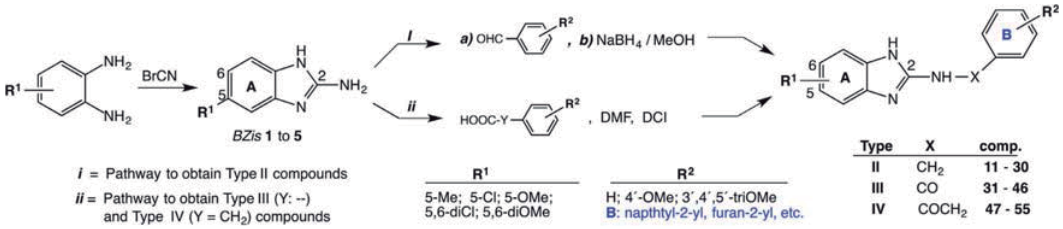

Scheme 2. Procedures for the synthesis of types II – IV BZs.

cluding homoaromatic systems (phenyl or naphthyl), heterocyclic (as thienyl, and pyridyl) and long-chain aliphatic substituents. BZs **47**–**53** were aryl/hetarylacetamides, while BZs **54** and **55** were lauroylamides.

Physicochemical, MS, NMR and some IR spectral data for type III and IV BZs are reported in the 4.1.2.9–11 sections. The IR spectra of these compounds showed the expected strong stretching absorption band for the amide carbonyl (NHC=O) at about 1680 cm^{-1}. ^{1}H and ^{13}C NMR spectral data for the picolinamide **42** (type III) and the aminophenacetamide **53** (type IV) are commented here. Thus, the ^{1}H NMR of BZ **42** showed eight signals, of which those corresponding to ring B resonate from 7.50 to 8.57 ppm; the ones associated to ring A resonate from 6.86 to 7.70 ppm, in addition to a singlet that integrate for three protons at 3.67 ppm ($OC\underline{H}_3$), and another at 11.83 ppm corresponding to the labile N-H protons. Its ^{13}C NMR showed fourteen signals, those of ring B resonated at 148.65, 148.17, 137.02, 127.32 and 122.73 ppm, signals associated to ring A resonate at 156.15, 147.87, 136.97, 129.93, 111.18, 110.80, 108.50 and 55.79 ppm, in addition to one at 163.54 ppm of the amide carbonyl. The ^{1}H and ^{13}C NMR spectra of BZ **53** showed the expected signals for ring A and B, with the simplification in the proton spectrum due to the double substitution on ring A, in addition to the singlet at 3.68 ppm in ^{1}H NMR and the corresponding one at 43.97 ppm in the ^{13}C spectrum of the benzylic methylene. For this compound and those type IV BZs the signal associated to the amide carbonyl appeared at 173.06 ppm, almost 10 ppm down field with respect to that of BZ 42 and those of type III.

2.2. Biological assays

2.2.1. Anthelmintic activity and selectivity

All the BZ derivatives were tested at a 50 μM concentration against a susceptible strain of *T. circumcincta* [30] and their ovicidal (egg hatching inhibition = EHI) and larvicidal (larval migration inhibition = LMI) results, determined through the corresponding assays (EHIA and LMIA), are shown in Tables 1 to 3. For those compounds showing an ovicidal activity higher than 90%, the EC_{50} values of EHI were determined, in addition to their cytotoxicity on Caco-2 and HepG2 cell cultures to calculate their selectivity indexes (Table 4).

Tables 1–3 show the inhibition percentage of type I–IV BZs on *T. circumcincta* egg hatching and larval migration. The compounds listed in Table 1 are organized according to either, the size and complexity of the substituents at the C-5 (C-6) of the benzimidazole system, or to the synthetic chemical sequence of their preparation, while all of them have a 4-methoxy group attached to ring B. In the previous work, Escala et al. reported [8] on the activity results for BZs **1**–**4**, which are included here again to facilitate comparisons between new and old members of type I derivatives.

As was previously reported the 5(6)-methylBZ **2** showed an excellent ovicidal activity (100%) and fair larvicidal effects (40.9%), whereas the introduction of nitro (BZ **3**) or amino (BZ **4**) groups at such position led to the practical loss of activity. Nevertheless, based on the preliminary virtual docking predictions a small group of BZ **4** derivatives those BZs **5**–**10** were prepared and evaluated. As can be seen, these BZs did not show any ovicidal activity, but four of the six new compounds showed good larvicidal activity, and two of them, the tosyl and naphthylamides BZs **6** and **7** substantially increased the larvicidal activity of their precursor BZ **4**, even surpassing that of BZ **2**, with values of 48.9% and 43.8%, respectively. As the main consequence of the results shown in Table 1, it follows that the acylation of BZ **4** with transformation of the 5-amino group into amides (BZs **6, 7** and **8**) or carbamates (BZs **5** and **9**) fairly contributed to enhance the larvicidal activity of type I BZs, reaching or exceeding the potency of those previously reported.

Type II BZs shown in Table 2 are ordered according to the number and size of the substituents, first in ring A, then in ring B. Such compounds (BZs **11** to **30**) had electron donating (5-Me, 5-MeO or 5,6-diMe) or withdrawing (5-Cl, or 5,6-diCl) substituents on ring A, while the benzene ring B were either non-substituted, mono- (4-MeO) or tri-substituted (3,4,5-triMeO), or changed by other aromatic (naphthyl) or heteroaromatic (furyl, 5-methylfuryl and thienyl) systems.

As in the case of type I BZs, none of those evaluated type II aminoBZs showed significant hatching inhibition effects; whereas, higher than 25% larval migration inhibition effects were observed for seven of the twenty aminoBZs tested. Globally, inhibition results in the 35–50% range were found for 5-methyl and 5,6-dimethyl BZs combined with phenyl (**11**), methoxyphenyl (**12** and **26**, respectively) or 2-naphthyl (**14**) groups as B systems. Similar though lower inhibition results were found for 5,6-dichloroBZ analogues **28** (phenyl) and **29** (methoxyphenyl), thus revealing that electron-donating substituents at ring A seem better, while the Me/Cl isosteric character, could be playing a certain role in such similarity. The BZ analogues containing furan, thiophene and other B ring configurations gave less relevant LMI results. On the other hand, it should be noted the strong negative influence for the activity that would be associated to the 3,4,5-trimethoxyphenyl group, whose presence practically removed the activity in BZs **19, 27** and **30**. This fact was independent of the substitution pattern of ring A, and in fair contrast with the overall positive influence of the structurally close 4-methoxyphenyl group. Most surprisingly, the regioisomeric 2,3,4-trimethoxyphenyl group, present in the most potent larvicidal BZ **13** (LMI: 54.9%), should be considered as the responsible for the 18.6% and 14.6% increases of the inhibitory potency in the respective comparison with the benzylamine **11** and the 4-methoxybenzylamine **12**. Consequently, the presence of the 2-methoxy group, which determines the absence of symmetry in the substituent and most likely an important rotational and conformational restriction, would be the ultimate cause of the great contribution of such 2,3,4-trimethoxyphenyl group to the activity. This fact must certainly be investigated through the preparation and evaluation of other benzylaminoBZ derivatives having an *ortho*-methoxy substituent, either alone or combined with other groups around ring B.

Table 2
Inhibition of egg hatching and larval migration of *Teladorsagia circumcincta* by type II 2-aminoBZ derivatives.

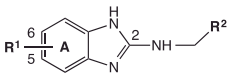

Type II BZ

BZ-II	R [1]	R [2]	Inhibition % (at 50 μM)	
			Egg Hatching (EH)	Larval Migration (LM)
11	5-methyl	phenyl	1.1	**36.3**
12	5-methyl	4-methoxyphenyl	1.1	**40.3**
13	5-methyl	2,3,4-trimethoxyphenyl	< 1	**54.9**
14	5-methyl	2-naphthyl	< 1	**41.5**
15	5-methyl	2-furyl	< 1	22.5
16	5-methyl	2-thienyl	< 1	< 1
17	5-chloro	phenyl	< 1	4.6
18	5-chloro	4-methoxyphenyl	< 1	12.1
19	5-chloro	3,4,5-trimethoxyphenyl	< 1	1.4
20	5-chloro	2-furyl	1.7	9.2
21	5-methoxy	phenyl	< 1	10.7
22	5-methoxy	4-methoxyphenyl	1.1	14.6
23	5-methoxy	4-(1-pyrrolidinyl)phenyl	1.0	16.4
24	5-methoxy	5-methylfur-2-yl	< 1	15.8
25	5-methoxy	2-thienyl	<1	20.0
26	5,6-dimethyl	4-methoxyphenyl	< 1	**49.8**
27	5,6-dimethyl	3,4,5-trimethoxyphenyl	< 1	< 1
28	5,6-dichloro	phenyl	2.1	**31.9**
29	5,6-dichloro	4-methoxyphenyl	1.3	**26.5**
30	5,6-dichloro	3,4,5-trimethoxyphenyl	< 1	< 1
TBZ			100.0	*nd*
LEV			*nd*	100.0

Compounds **11, 12, 15** to **18, 20** to **22** and **25** are known, while **13, 14, 19, 23, 24, 26** to **30** are new. TBZ: thiabendazole; LEV: levamisol. *nd*: not determined. LMI values >25% are bolded for comparison purposes.

An evaluation of the relative influence of ring A substituents on the activity of this type of BZs can be made by comparing those compounds having the same *p*-methoxybenzyl (B) moiety. In this way, the contribution order of the substituents to LMI resulted as follows: 5,6-diMe (BZ **26**: 49.8%) > 5-Me (**12**: 40.3) > 5,6-diCl (**29**: 26.5) > 5-MeO (**22**: 14.6) > 5-Cl (**18**: 12.1), corresponding to the respective detriments of 9.5, 12.5, 11.9 and 14.6 LMI% units, related to the successive disappearance or change of substituents from **26** to **18**. A similar sequence was observed for those aminoBZs having no-substitution on the benzene ring B, as that of BZs **11** (5-Me: 36.3%), **28** (5,6-diCl: 31.9%), **21** (5-MeO: 10.7%) and **17** (5-Cl: 4.6%). These sequences reveal for type II BZs the prevalence of the electron donating nature of the substituents on ring A, combined with the probable incidence of the mutual isosteric character of methyl and chloro substituents.

Other facts that can be mentioned are the 5.2% increase in LMI produced by changing the phenyl group in BZ **11** to the 2-naphthyl in BZ **14**, as well as the fair decreases of 13.8% and more than 35%, produced by its changing to 2-furyl (BZ **15**) and 2-thienyl (BZ **16**) groups, respectively. Since the four substituents in comparison are similarly aromatic and planar, such differences in the experimental results would have some significant influence on the global size of the hydrophobic aromatic B system on the activity.

FormamidoBZ derivatives **31**–**46** (type III), and acetamido and other acylamido derivatives BZs **47**–**55** (type IV), are shown in Table 3 with the results of their evaluation. BZs in this table have the same group of substituents on ring A, with differences in those attached to ring B, and are ordered in a similar way as in Tables 1 and 2. Regarding the B nucleus, the changing of the benzene ring by that of pyridine in BZs **36, 39** and **42**, or by an aliphatic long-chain in BZs **54** and **55** can be noted. Additional changes in the substitution pattern of the benzene ring B, with electron donating or withdrawing groups at position *meta* of either mono- or di-substituted nucleus were also introduced.

As can be seen by a first glance at the results in Table 3, globally considered, type III benzamidoBZs and picolinamidoBZs showed good hatching inhibition results, with 7 out of the 16 evaluated BZs, namely benzamides **31, 37, 40**, and **43** and the picolinamides **36, 39** and **42,** exceeded the 90% ovicidal level. A second relevant fact related to egg hatching by BZ benzamides refers to the inactivity of most compounds having any substituent attached to the benzene ring B, independently of the substituents on the BZ ring A, though with the relevant exception of the methoxybenzamide BZ **38**, which attained almost 40% hatching inhibition. In terms of structure-activity relationships, it would be more interesting to compare the respective decreases of 60% and 94% of inhibition power observed for the 4′-methoxyBZs **38** and **32**, with respect to the total inhibition produced by the non-substituted BZs **37** and **31**. This fact would demonstrate the existence of a true steric hindrance around ring B in the interaction with the target.

Significantly, and in sharp contrast with type-III formamido derivatives, all type IV phenyl and thienylacetamides and the two lauroylamides tested were practically inactive against hatching of *T. circumcincta* eggs. From such results, the inefficiency of the N-C-C spacer between the BZ and ring-B units was deduced. This, combined with the above mention about the inconvenience of the substitution at the ring B of benzamides, permit the establishment of the existence of a limited distance of around 7.5 Å from the N atom of 2-aminoBZ to the end of the B moiety, whether or not substituted.

Related to larval migration inhibition by type III BZs, the only relevant larvicide was the picolinamide **39**, which is also the principal dual BZ inhibitor with LMI and EHI values of 51.2% and 100%, respectively. Another compound of this group that could be mentioned is the benzamide **33**, which although devoid of activity on eggs, showed a LMI value of 22.5%, that could be associated to its double substitution by electron-withdrawing groups if, in terms of

Table 3
Inhibition of egg hatching and larval migration of *Teladorsagia circumcincta* by BZ amides of types III and IV.

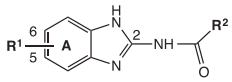

Types III and IV

BZ-III	R [1]	R [2]	Inhibition % (at 50 µM)	
			Egg Hatching (EH)	Larval Migration (LM)
31	5-methyl	phenyl	**95.5**	< 1
32	5-methyl	4-methoxyphenyl	< 1	8.8
33	5-methyl	2-chloro-5-nitrophenyl	< 1	22.5
34	5-methyl	3,5-dimethoxyphenyl	< 1	< 1
35	5-methyl	3,4,5-methoxyphenyl	< 1	6.9
36	5-methyl	2-pyridyl	**100.0**	< 1
37	5-chloro	phenyl	**100.0**	< 1
38	5-chloro	4-methoxyphenyl	39.9	< 1
39	5-chloro	2-pyridyl	**100.0**	**51.2**
40	5-methoxy	phenyl	**100.0**	15.1
41	5-methoxy	4-methoxyphenyl	< 1	< 1
42	5-methoxy	2-pyridyl	**100.0**	< 1
43	5,6-dimethyl	phenyl	**91.2**	7.2
44	5,6-dimethyl	4-methoxyphenyl	< 1	< 1
45	5,6-dichloro	Phenyl	< 1	3.6
46	5,6-dichloro	4-methoxyphenyl	< 1	3.3
BZ-IV				
47	5-methyl	3-nitrobenzyl	< 1	21.9
48	5-methyl	α-hydroxybenzyl	< 1	**34.2**
49	5-methyl	2-naphthylmethyl	< 1	2.3
50	5-methyl	2-thienylmethyl	1.00	**25.5**
51	5,6-dimethyl	3-chlorobenzyl	< 1	2.5
52	5,6-dichloro	3-nitrobenzyl	< 1	15.1
53	5,6-dichloro	3-aminobenzyl	< 1	**41.2**
54	5-methoxy	1-Boc-aminoundecyl	< 1	20.4
55	5-methoxy	1-aminoundecyl	< 1	< 1
TBZ			**100.0**	*nd*
LEV			*nd*	**100.0**

Compounds **31, 33, 35, 41, 44** and **49** are known, while **32, 34, 36** to **40, 42, 43, 45** to **48**, and 50 to **55** are new. TBZ: thiabendazole, LEV: levamisol. *nd*: not determined. EHI values >90% and LMI values >25% are bolded for comparison purposes.

Table 4
EC_{50} values of the most potent BZs against hatching of *T. circumcincta* eggs, cytotoxicity for Caco-2 and HepG2 cells and selectivity indexes (SI).

BZ	*T. circumcincta* EHI, EC_{50} (µM)	Caco-2 cells [a] (CC_{50}, µM)	HepG2 cells [a] (CC_{50}, µM)	SI [b]
31	1.51±0.03	**27.63±4.02**	**27.59±10.40**	18.3
36	1.52±0.03	7.56±1.25	**36.91±8.08**	**24.3**
37	1.58±0.03	18.24±4.23	**>50** [c]	**>31**
39	1.47±0.15	>12.50	**>25** [c]	>17
40	1.35±0.12	**61.93±32.19**	**>50** [c]	**>37**
42	**0.92±0.06**	14.35±3.40	**101.80±37.52**	**111**
TBZ [d]	**0.34±0.02**	**248.27±36.77**	**786.99±275.51**	**2315**

[a] Determined by the Alamar Blue method. [b] SI = CC_{50} (HepG2) / EC_{50} (*T.c.*). [c] Compounds with solubility problems. [d] Results for TBZ taken from a previous report.[8] Values of EC_{50} <1 µM, CC_{50} >25 µM and SI >20 are bolded to facilitate comparisons.

structure-activity relationship, it is compared with BZs **32, 34** and **35** which contain electron-donating groups.

Finally, related to LMI by acetamides and other acylamides of type IV, the inhibition values ranged from very low to suitable. Due to the diverse substitution patterns of both A and B ring systems, that makes any SAR analysis difficult, it is only worth mentioning those compounds exceeding 25% LM inhibition; namely, BZs **53** (41.2%), **48** (34.2%) and **50** (25.5%).

To obtain more precise data on the active compounds, EC_{50} values were determined for those BZs that reached inhibition levels higher than 90% in the initial EHI screening, and to establish their selectivity, their CC_{50} values of cytotoxicity for HepG2 cells (Table 4) were also determined.

As can be observed, all most potent ovicidal BZs included in Table 4 belong to type III BZ, and they are the benzamides **31, 37** and **40** and the isosteric picolinamides **36, 39** and **42**, with EC_{50} values under 1.6 µM, with BZ **42** as the most potent (0.92 µM); roughly equivalent to one-third the ovicidal potency of TBZ. Furthermore, it can be seen that all these BZs attained outstanding levels of selectivity, with BZ **42** also showing the highest index value (SI = 111). In the case of BZs **37, 39** and **40**, some solubility difficulties led to estimate their CC_{50} values as higher than 50, 25 and 50 µM, respectively.

2.3. Molecular docking, drug-likeness and toxicity risks predictions

2.3.1. Molecular docking studies

Considering the interaction of BZs with tubulin as a probable molecular mechanism for their anthelmintic effects, and aiming to find any correlation between the experimental results on eggs and larvae of *T. circumcincta* and their theoretical ability for tubulin inhibition, all BZs in this study were subjected to molecular docking with the *T. circumcincta* tubulin, as described in Section 4.1.3.

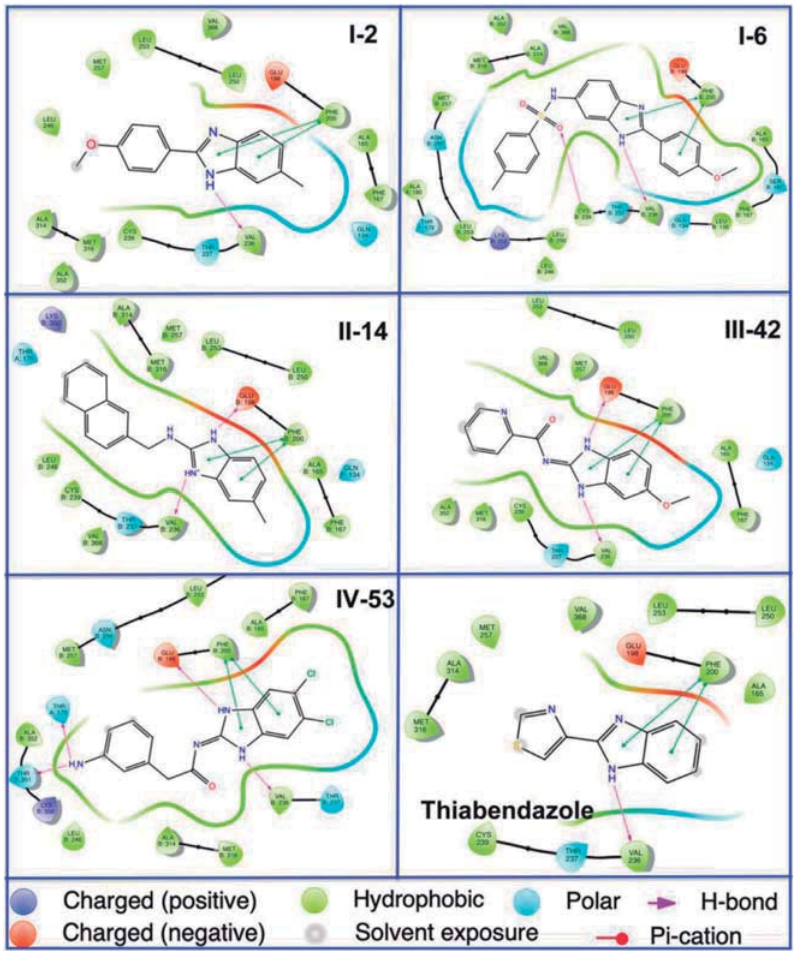

Fig. 2. 2D-maps of the docking interactions between BZs and the modelled *T. circumcincta* tubulin, with selected examples of the four BZ types, along the previously reported BZ **2** and the reference drug thiabendazole.

As in the previous study [8] the tautomerism of the BZ system was firstly examined on the four types of the compounds through a study performed with Spartan'20 (Vawefunction Inc) [10] using DFT at the RWB97X-D/6-31+G* level of theory in vacuo. The new 2-phenylBZs (Type I) behaved similarly to those previously studied, with the stability of 1H and 3H tautomers differing in some 0.5–1 kcal/mol in the presence of 5(6)-mono-substitution at ring A. The results for 2-aminoBZ derivatives (Type II) showed such equilibrium, though extended to a positively charged entity derived from protonation of the guanidine fragment in the interval of pH = 7 ± 2 applied in the study, and stabilised by charge distribution throughout the entire benzimidazole system (Scheme 3). Such a wide pH range results were appropriate in this case because *T. circumcinta* colonises the stomach and the intestine of ruminants. The BZ amides of Types III and IV showed a different behaviour with migration of the Δ^2-double bond towards the exocyclic nitrogen in most cases, surely stabilised by conjugation with the carbonyl group, and leaving two NH functions at positions 1 and 3 in such tautomer, with little difference in energy (about 1.5 kcal/mol) between the two tautomeric forms shown in the Scheme 3. These facts determine that both, the protonated amines type II and the amides III and IV with exocyclic tautomerisation, have more H-bond donors that can contribute to increasing their ability to interact with tubulin, which would potentially lead to greater affinities and more stable complexes.

The above statements are in agreement with the 2D interaction maps shown in Fig. 2, corresponding to the tubulin complexes with different BZs (additional 2D maps of some BZs are indicated in SF1 in Supporting Information). As can be seen, in addition to the BZN-H bond to Val236 residue of β-tubulin and the π-stacking interactions found for the previously reported 2-phenylBZ **2** (type I), some additional interactions can be observed for the new type I BZs and for those of types II–IV. Namely, the H-bond between de sulfonamide group of BZ **6** and the β-tubulin Cys239 residue, also the additional H-bond with Glu198 of the protonated amine **14** (type II) and of the exocyclic tautomers of BZ amides **42** (type III) and **53** (type IV).

It should also be considered that the presence of interactive functional groups in other parts of the ligand can add further positive interactions to the docking complex. Particularly, in the case

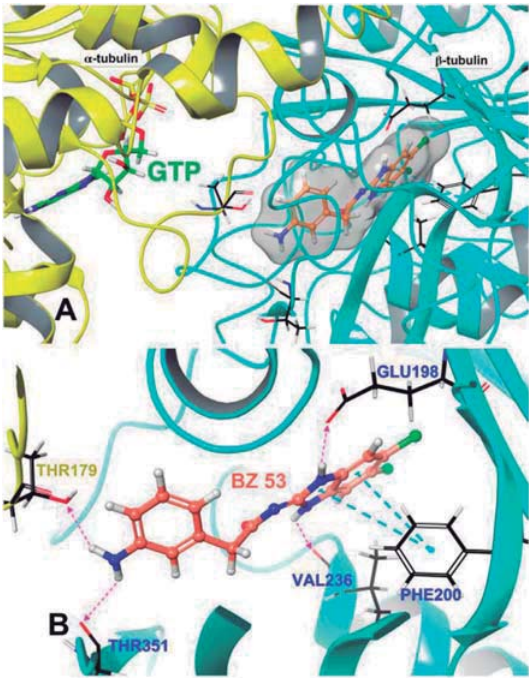

Fig. 3. (A) Docking of the amide BZ **53** into the colchicine site of the modelled *T. circumcincta* tubulin. (B) Details of the Phe200 - BZ π-stacking (T-shaped) interactions and the H-bonds of the N-H at positions 1 and 3 with Val236 and Glu198 residues of β-tubulin, as well as that between the 3-aminophenyl group and the α-tubulin (yellow) Thr179 residue, or the β-tubulin (blue) Thr 351 one.

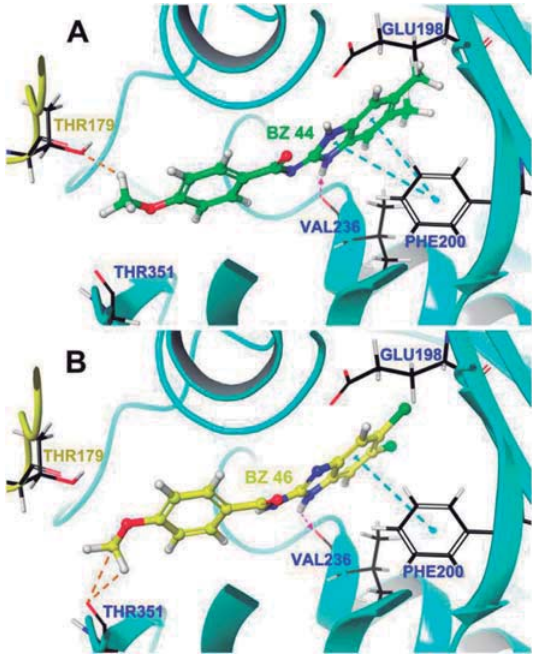

Fig. 4. (A) Docking complex of the benzamide BZ **44**, showing its bad interaction (gold broken line) with the Thr179 residue of α-tubulin, and without the usual H-bond for type III compounds between BZN-H and Glu198. (B) Similar complex of the dichloro analogue BZ **46** showing the bad interactions with the Thr351 residue of β-tubulin.

of BZ **53** the H-bonds of the *m*-amino group at the phenylacetic moiety with other β- or α-tubulin residues (Figs. 2 and 3) can be seen.

On the contrary, the presence of other substituents, although not too bulky, as in the cases of the methoxybenzamides **44** and **46** (Fig. 4), are enough to cause steric effects or bad contacts that would reduce the stability of the respective complexes (additional 3D maps of some BZs are indicated in SF2 in Supporting Information).

Interestingly, consistent with those favourable and unfavourable interactions shown in Figs. 3 and 4, the experimental LMI result for BZ **53** (41.2%) was much stronger than those found for BZs **46** (3.3%) and **44** (<1%), and such results also present a certain parallelism with the respective G-score values of −10.72, −10.42 and −9.98 predicted for the BZs (see Supporting Information, ST1).

Other aspects observed through the analysis of the BZ-tubulin complexes are related to the similarities and differences between BZs in the docking. Thus, it can be seen (Fig. 5A) that compounds of the four different types, BZs **2, 14, 34**, and **53** can dock in similar orientations into the colchicine site, whereas compounds of the same type II, as BZs **14** and **20** (Fig. 5B) are docked in practically opposed orientations. In agreement with this, they displayed very different experimental results on larval motility (LMI: 41.5 and 9.2%, respectively), and also fair differences between their predicted G-score values (−10.47 *vs* −9.20 kcal/mol), respectively (Fig. 5).

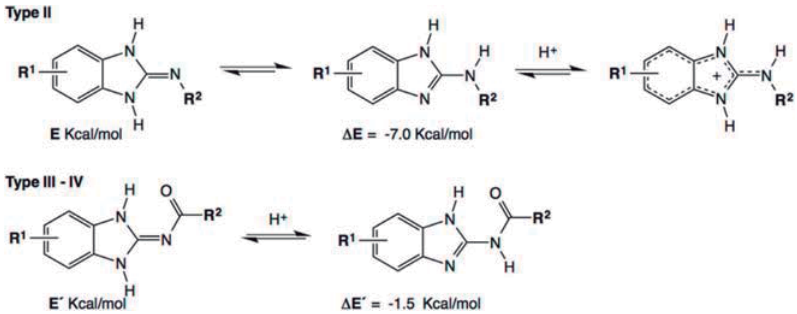

Scheme 3. Tautomeric and chemical equilibria for type II–IV BZ derivatives. Calculated generic energies (DFT RWB97X-D/6-31+G*) for BZ amines (E) and amides (E') and differences (Δ) between their respective tautomers.

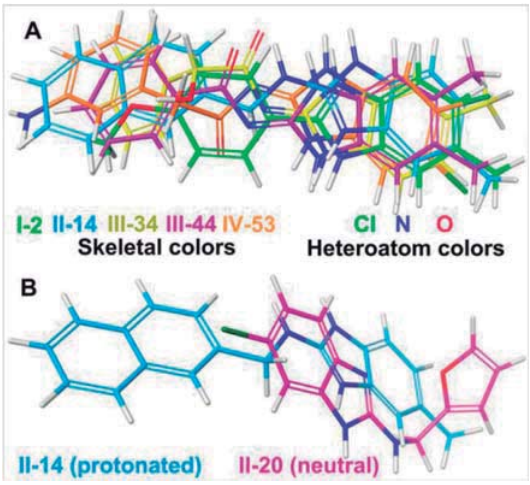

Fig. 5. (A) Superimposition of selected BZs of types I–IV as docked into the *T. circumcincta* tubulin model. (B) Different arrangement of the BZ (A) and furan (B) systems in the docked amines II–**14** and II–**20**.

Another interesting observation related to the GLIDE-Score function and the experimental activity, was that, whether on egg hatching or larval migration, the most efficient BZs presented between the best and the sufficient (−11.13 to −8.38 kcal/mol) G-Score docking values (see suppl. ST1), while commonly interacting with tubulin through their most stable tautomers or another of close stability. In apparent contrast, the current anthelmintic drug TBZ, while confirmed in this research as a very potent egg-hatching inhibitor, and having been reported to interact with the colchicine site of tubulin [31,32] (Fig. 3), attained a G-score value of −7.12 kcal/mol, substantially poorer than those mentioned above for the new active BZs. Nevertheless, it must be taken into account that TBZ is a broad-spectrum anti-infective drug, and that its tubulin polymerisation inhibition is actually complementary to the helminth-specific fumarate reductase inhibition and other biochemical mechanisms contributing to its anthelmintic action [33,34]. Something similar should happen with the new BZs, which in addition to inhibiting tubulin polymerisation, surely act through other as yet undiscovered mechanisms on the parasites.

2.3.2. Drug-likeness and toxicity risks predictions

In order to analyse the drugability of the active BZs, a virtual prediction study was performed online through the free web services SwissADME and ADMETsar platforms (see Supporting Information, ST2). To sum up, all the BZs included in Table 4 fulfil the Lipinski's Rule of Five, with MW values in the range of 251.2 and 272.7 amu (BZs **31** and **39**, respectively); clogP values between 1.48 and 2.79 (BZs **42** and **37**, respectively); H-bond acceptors between 2 and 4 (BZs **31** and **42**, respectively), and 2 H-bond donors in the six compounds. Other properties, such as their solubility above the μM level (clogS within the −3.98 to −5.14 range), and the total polar surface under 80 $Å^2$, contributed to their positive drug-likeness and lead-likeness qualifications. Most significantly, none of the active BZs in Table 4 were predicted to show any of those mutagenic, tumorigenic and irritant toxicity risks considered in the SwissADME panel.

3. Conclusions

In summary, we have synthetized and evaluated more than fifty 2-phenylbenzimidazoles, 2-(arylmethylamino)benzimidazoles, benzamides, picolinamides and other acyl derivatives of 2-aminobenzimidazoles, and a number of them exhibited promising nematocidal activities on eggs or larvae of *T. circumcincta*. Five amides of Type III displayed 100%, and two others, more than 90%, ovicidal activity on a TBZ susceptible strain at 50 μM. In addition, Ten BZs showed more than 40% larvicidal activity on such strain and at the same concentration. The amine BZ **13** was the most potent larvicide with 54.87% larval migration inhibition, while the amide BZ **39** showed both ovicidal and larvicidal activity, with an ovicidal EC_{50} value of 1.35 μM and SI value higher than 17 related to HepG2 cells. Most significantly, the amide BZ **42** resulted as the most potent and specific egg hatching inhibitor, showing the lowest ovicidal EC_{50} value of 0.92 μM and the highest SI of 110. Pending experimental confirmation, the positive results of the virtual docking of BZs into the colchicine site of a *T. circumcincta* tubulin model allowed the proposal of such biochemical interaction as partially responsible for the anthelmintic action of BZs. Indeed, although some correlations were observed between experimental activity and docking scores for small groups of compounds of every type I–IV, no true global parallelism could be found between the virtual and experimental results, which ensures that there are other mechanisms of action, yet to be discovered, that would contribute to justifying their effects on eggs and larvae of this important parasite. Finally, it can be added that two compounds with the most relevant results were selected to carry out *in vivo* preclinical efficacy and toxicity assays on gerbils, and that some of the promising results achieved will be published shortly in a specialised parasitological journal.

4. Experimental

4.1. Chemistry

4.1.1. Chemistry general

All commercial chemicals (Aldrich, Alpha, Fischer, SDS) were used as purchased and solvents (Fischer, SDS, Scharlau) purified by the standard procedures prior to use [35]. Reactions were monitored by Thin Layer Chromatography (TLC) (Kieselgel 60 F254 precoated plates, E. Merck, Germany), the spots were detected by exposure to UV light at λ 254 nm, and colourisation with 10% ninhydrin spray, and further heating of the plate. Melting points (Mp) were determined with Mel-Temp apparatus in open capillaries and were uncorrected. Separations by flash column chromatography were performed on Merck 60 silica gel (0.063–0.2 mesh). Infrared spectra were recorded on a FT-IR spectrometer Perkin Elmer System BX, using solid samples in KBr disks. NMR spectra were recorded on a Bruker Avance or Varian Mercury 400 MHz (400 MHz for ^{1}H, 100 MHz for ^{13}C). The spectra were measured in $CDCl_3$, methanol-d_4 or DMSO-d_6, using tetramethylsilane (TMS) as internal standard, chemical shifts (δ) are given in ppm and coupling constants (J) in Hertz (Hz). High resolution mass spectra (HRMS) were obtained by electron spray ionisation-mass spectrometry (ESI-MS) technique (5 kV) on a QSTAR XL mass spectrometer.

4.1.2. Synthesis and characterisation off BZs

4.1.2.1. Procedure for the preparation of the nitrobenzimidazole 3. A mixture of the 4-nitro-1,2-phenylenediamine (153 mg, 1.00 mmol), 4-methoxybenzaldehyde (136 mg, 1.00 mmol) and $Na_2S_2O_5$ (189 mg, 1.00 mmol) in dry DMF (4 mL) was heated to reflux for 16 h. Then, the reaction was cooled to room temperature, and water (20 mL) was added to provide a solid that was filtered off in Büchner. The solid obtained was purified by column chromatography on silica gel with *n*-hexane/ethyl acetate (8:2) as elution system and recrystallised from $CHCl_3$/methanol to obtain 205 mg (75%) of **3,** mp 237–239 °C.

*2-(4-Methoxyphenyl)−5-nitro-1*H*-benzimidazole*, **3**

Its physicochemical properties were identical as those described by Escala [8].

BZs *2-(4-Methoxyphenyl)−1*H*-benzimidazole* **1** and *2-(4-Methoxyphenyl)−5-methyl-1*H*-benzimidazole* **2** were obtained as described [8].

4.1.2.2. Procedure for the reduction of the nitrobenzimidazole 3. A solution of **3** (86 mg, 0.32 mmol) in MeOH (3 mL) in a two-necked round bottom flask was prepared, then Pd-C catalyst (3 mg) was added. Air was removed from the system, and a balloon with H_2 was placed to one of the necks. The mixture was kept at room temperature and under magnetic stirring for 2 h. Then, the Pd-C was removed by filtration through Celite, and the residue washed with MeOH. The solvent was removed in vacuo to give a red-brown solid, that was purified by crystallisation in $CHCl_3$/methanol to provided BZ **4** (69 mg, 90%), mp 196–197 °C.

*5-Amino-2-(4-methoxyphenyl)-1*H*-benzimidazole* **4**

The physicochemical properties were identical as those described by Escala [8].

4.1.2.3. Synthesis of the carbamate 5. A solution of (8 M) NaOH was added to another of BZ **4** (60 mg, 0.25 mmol) in *tert*-butanol (0.31 mL) / water (0.47 mL) (2:3) to reach pH 13. Then, 54.7 mg (0.25 mmol) of di-*tert*-butyl dicarbonate (Boc_2O) in *tert*-butanol (0.16 mL) were added and the mixture kept at room temperature for 90 min. The pH was controlled during the progress of the reaction and maintained at pH 13 by adding the necessary amounts of (8 M) NaOH. When reaction was completed (monitored by TLC), the solution was acidified to pH 5 with a solution of saturated citric acid and the mixture extracted with ethyl acetate. The organic phase was then washed with water, and dried over anhydrous sodium sulfate. Solvent was removed under vacuum, and the crude mixture purified by column chromatography with *n*-hexane/ethyl acetate (1:1) to give BZ **5** 55 mg (65% yield) as a light pink solid, mp: 148–149 °C ($CHCl_3$/methanol).

Tert-*butyl (2-(4-methoxyphenyl)-1*H*-benzimidazol)carbamate* **5**

IR (KBr) ν_{max}: 3420, 2975, 1693 (NH=CO), 1613, 1534, 1476, 1391, 1366, 1250 (C-O), 1158 (C-O), 1026, 835, 754 cm^{-1}. ^1H NMR (400 MHz, $CDCl_3$): δ 7.88 (2H, d, J = 8.4 Hz, H-2´ + 6´), 7.61 (1H, d, J = 1.2 Hz, H-4), 7.37 (1H, d, J = 8.8 Hz, H-7), 7.03 (1H, dd, J_1 = 8.8; J_2 = 1.2 Hz, H-6), 6.72 (2H, d, J = 8.4 Hz, H-3´+ 5´), 3.69 (3H, s, OCH_3), 1.49 (9H, s, $(CH_3)_3$). ^{13}C NMR (100 MHz, $CDCl_3$): δ 160.86 (C-4´), 152.84 (C-2), 152.70 (COOC$(CH_3)_3$), 138.20 (C-7a), 137.60 (C-3a), 133.28 (C-5), 128.19 (C-2' + 6´), 122.30 (C-1´), 115.85 (C-6), 114.18 (C-7 + 3' + 5´), 105.70 (C-4), 80.34 (COOC$(CH_3)_3$), 55.21 (OCH_3), 28.39 ($(CH_3)_3$). HRMS (ESI+) *m/z* calcd. for $C_{19}H_{22}N_3O_3$ $[M + H]^+$, 340.1656, found, 340.1649.

4.1.2.4. Preparation of BZ 6. To a solution of BZ **4** (60 mg, 0.25 mmol) in THF (3.80 mL), Et_3N (0.502 mmol) was added, and then a solution of *p*-toluenesulfonyl chloride (53 mg, 0.28 mmol) in THF (2.00 mL) was added dropwise. The mixture was kept under magnetic stirring for 18 h. at room temperature and under a N_2 atmosphere. Reaction progress was monitored by TLC with *n*-hexane/ethyl acetate (2:8) as eluent. After complexion of the reaction, it was extracted with CH_2Cl_2, washed with water and the crude purified by column chromatography using *n*-hexane/ethyl acetate mixtures of increasing polarity (3:7 to 2: 8). Reaction yield in BZ **6** 55 mg (65%).

N-*(2-(4-Methoxyphenyl)-1*H*-benzimidazol-5-yl)-4-tolylsulfonamide*, **6** A white solid, mp: 196–197 °C ($CHCl_3$/methanol). IR (KBr)

ν_{max} 3342 (NH), 2924, 1611, 1520, 1455, 1430, 1296 (SO_2-N), 1254 (C–O), 1160 (SO_2-N), 1150, 1090, 1027, 966, 935, 811, 663 cm^{-1}. ^1H NMR (400 MHz, CD_3OD): δ 7.90 (2H, d, J = 8.0 Hz, H-2'' + 6´), 7.35 (1H, d, J = 8.8 Hz, H-7), 7.58 (2H, d, J = 8.0 Hz, H-2' + 6´), 7.33 (1H, d, J = 2.4 Hz, H-4), 7.17 (2H, d, J = 8.0 Hz, H-3'' + 5´), 6.95 (2H, d, J = 8.0 Hz, H-3' + 5´), 6.94 (1H, d, J_1 = 8.8; J_2 = 2.4 Hz, H-6), 3.76 (3H, s, OCH_3), 2.25 (3H, s, CH_3). ^{13}C NMR (100 MHz, CD_3OD): δ 161.53 (C-4´), 152.92 (C-2), 143.46 (C-5), 136.80 (C-3a), 136.51 (C-7a), 136.50 (C-4´), 132.48 (C-1´), 129.08 (C-3´´+ 5´), 127.90 (C-2' + 6´), 126.93 (C-2'' + 6´), 121.65 (C-1´), 118.27 (C-6), 114.80 (C-7), 114.06 (C-3' + 5´), 108.50 (C-4), 54.49 (OCH_3), 20.02 (CH_3). HRMS (ESI+) *m/z* calcd. for $C_{21}H_{20}N_3O_3S$ $[M + H]^+$, 394.1220, found, 394.1226.

4.1.2.5. General procedure for BZ 4 acylation. 0.49 mmol of 1,1-carbonildiimidazole (CDI) was added to a solution of 0.41 mmol of the corresponding acid in dry DMF (2 mL), and the mixture was maintained at room temperature for 1 h. Then, 0.37 mmol of BZ **4** was added, and the mixture kept at room temperature with magnetic stirring for 16 h. The progress of the reaction was monitored by TLC, and *n*-hexane/ethyl acetate (1:9) was used as an eluent. After completion of the reaction, the solvent was removed under vacuum on a rotary evaporator, and the solid purified by column chromatography with *n*-hexane/ethyl acetate (2:8) as eluent. Reaction yields ranged within 67–94%.

N-*(2-(4-Methoxyphenyl)-1*H*-benzimidazol-5-yl)-2-(naphthalen-2-yl)-acetamide* **7.** A light brown solid, yield

67%, mp: 237–239 °C (methanol). IR (KBr): ν_{max} 3380, 2970, 1695, 1615, 1535, 1475, 1250, 1025, 830, 754 cm^{-1}. ^1H NMR (400 MHz, C_2D_6SO): δ 10.30 (1H, brs, NH), 10.20 (1H, brs, NH), 8.06 (3H, m, H-1'' + 4'' + 8´), 7.87 (2H, d, J = 8.4 Hz, H-2' + 6´), 7.52 (3H, m, H-5´´+ 6´´+ 7´), 7.51 (1H, m, H-7), 7.40 (1H, m, H-3´), 7.38 (1H, m, H-4), 7.21 (1H, m, H-6), 7.07 (2H, d, J = 8.4 Hz, H-3' + 5´), 3.83 (3H, s, OCH_3), 2.49 (2H, s, CH_2). ^{13}C NMR (100 MHz, C_2D_6SO): δ 168.72 (NHCO), 160.46 (C-4´), 151.21 (C-2), 140.18 (C-5), 134.29 (C-3a + 7a), 133.90 (C-1´), 133.09 (C-8a´), 131.84 (C-4a´), 127.71 (C-4´´+7´), 127.50 (C-3'' + 8´), 127.43 (C-2' + 6´), 126.13 (C-5'' + 6´), 125.59 (C-2´), 122.73 (C-1´), 118.30 (C-6), 114.34 (C-3' + 5´), 110.61 (C-4), 109.14 (C-7), 55.31 (OCH_3), 43.51 (CH_2). HRMS (ESI+) *m/z* calcd. for $C_{26}H_{22}N_3O_2$ $[M + H]^+$, 408.1707, found, 408.1707.

N-*(2-(4-Methoxyphenyl)-1*H*-benzimidazol-5-yl)quinoline-2-carboxamide* **8**

A yellow solid, yield: 94%, mp: 256–257 °C (methanol). ^1H NMR (400 MHz, C_2D_6SO): δ 10.78 (2H, brs), 8.62 (1H, d, J = 8.4 Hz), 8.31 (1H, m), 8.27 (1H, d, J = 8.4 Hz), 8.26 (1H, d, J = 8.4 Hz), 8.25 (2H, d, J = 7.6 Hz), 8.11 (1H, d, J = 8.4 Hz), 7.91 (1H, m), 7.75 (1H, m), 7.65 (1H, m), 7.56 (1H, m), 7.10 (2H, d, J = 7.6 Hz), 3.84 (3H, s). ^{13}C NMR (100 MHz, C_2D_6SO): δ 162.40, 160.55, 151.62, 145.90, 140.80, 138.15, 133.24, 130.54, 130.61, 129.34, 128.87, 128.25, 128.10 (3C), 127.89, 122.69, 118.33 (2C), 116.33, 114.36 (2C), 110.73, 55.32. HRMS (ESI+) *m/z* calcd. for $C_{24}H_{19}N_4O_2$ $[M + H]^+$, 395.1502, found, 395.1498.

Tert-*butyl(1-((2-(4-methoxyphenyl)-1*H*-benzimidazole-5-yl)amino)-1-oxododecan-2-yl)carbamate* **9**

A light brown solid, yield: 69%, mp: 169–170 °C ($CHCl_3$/methanol). ^1H NMR (400 MHz, CD_3OD): δ 7.99 (1H, brs, H-4), 7.93 (2H, d, J = 8.8 Hz, H-2´+6´), 7.45 (1H, d, J = 8.4 Hz, H-7), 7.25 (1H, brd, J = 8.4 Hz, H-6), 6.99 (2H, d, J = 8.8 Hz, H-3´+5´), 4.21 (1H, m, H-2´), 3.81 (3H, s, OCH_3), 1.82 (2H, m, CH_2-3´), 1.76 (2H, m, CH_2-4´), 1.45 (9H, s, $(CH_3)_3$), 1.23 (14H, m, $(CH_2)_7$), 0.84 (3H, t, J = 7.2 Hz, CH_3). ^{13}C NMR (100 MHz, CD_3OD): δ 172.34 (NHCO), 161.47 (C-4´), 156.56 (COOC$(CH_3)_3$), 152.55 (C-2), 137.97 (C-7a), 136.47 (C-3a), 133.43 (C-5), 127.87 (C-2' + 6´), 121.76 (C-1´), 116.06 (C-6), 114.62 (C-7), 114.05 (C-3' + 5´), 105.80 (C-4), 79.22 (COOC$(CH_3)_3$), 55.26 (CH-α), 54.49 (OCH_3), 32.34, 31.63, 29.29, 29.25, 29.20, 28.96, 28.46 ($(CH_3)_3$), 27.38, 25.60, 22.31, 13.06 (CH_3). HRMS (ESI+) *m/z* calcd. for $C_{31}H_{45}N_4O_4$ $[M + H]^+$, 537.3435, found, 537.3423.

4.1.2.6. Obtaining BZ 10 by deprotection of 9. 40 mg (0.074 mmol) of BZ **9** were dissolved in CH_2Cl_2 (3 mL) and kept at 0 °C under stirring. Then, trifluoroacetic acid (0.6 mL) was added, and the reaction is monitored by running TLC [eluent: *n*-hexane / ethyl acetate (1:9)] every 15 min. After the reaction has finished, it was extracted with CH_2Cl_2 and washed with water. The solvent was removed under vacuum on a rotary evaporator, and the crude purified by crystallisation [*n*-hexane / CH_2Cl_2] at 0 °C to provide BZ **10**, 10 mg in 31% yield.

*2-Amino-*N*-(2-(4-methoxyphenyl)-1*H*-benzimidazole-5-yl)dodeca namide, BZ-***10**

A brown solid, mp: 103–105 °C. IR (KBr): ν_{max} 3374 (NH), 3274 (NH), 3450, 2922, 1647 (NHCO), 1614, 1534, 1495, 1454, 1252, 1175, 1035, 830 cm^{-1}. ^1H NMR (400 MHz, $CDCl_3$): δ 8.06 (1H, brs, H-4), 7.89 (2H, d, J = 8.4 Hz, H-2' + 6'), 7.45 (1H, d, J = 8.4 Hz, H-7), 6.97 (1H, d, J = 8.4 Hz, H-6), 6.81 (2H, d, J = 8.4 Hz, H-3'+5'), 3.67 (3H, s, OCH_3), 3.42 (1H, m, H-2'), 1.83 (2H, m, CH_2–3'), 1.47 (2H, m, CH_2–4'), 1.14 (14H, m, $(CH_2)_7$), 0.78 (3H, t, J = 7.2 Hz, CH_3). ^{13}C NMR (100 MHz, $CDCl_3$): δ 173.54 (NHCO), 161.14 (C-4'), 152.10 (C-2), 138.40 (C-7a), 136.40 (C-3a), 133.20 (C-5), 128.03 (C-2' + 6'), 122.30 (C-1'), 119.10 (C-6), 114.38 (C-3' + 5'), 110.20 (C-7), 109.30 (C-4), 55.65 (CH-2'), 55.38 (OCH_3), 34.92, 31.88, 29.56, 29.50 (2C), 29.41, 29.30, 25.98, 22.66, 14.10 (CH_3). HRMS (ESI+) *m/z* calcd. for $C_{26}H_{37}N_4O_2$ $[M + H]^+$ 437.2911, found, 437.2903.

4.1.2.7. General procedure for the preparation of 2-aminobenzimidazole intermediates BZis (1–5). Solutions of the corresponding 1,2-phenylendiamine (0.02 mmol) and cyanogen bromide (0.03 mmol) in aqueous methanol (50% v/v) were prepared separately. Then were mixed in an Erlenmeyer flask and maintained with continuous magnetic stirring at room temperature for 96 h. The reaction was monitored by TLC with ethyl acetate as eluent. After reaction completion, the methanol was removed under vacuum, and the crude purified by column chromatography using ethyl acetate as eluent [28].

*5-Methyl-1*H*-benzimidazol-2-amine,* BZ***i* 1**

A brown solid, yield: 85%, mp: 197–198 °C (methanol). IR (KBr): ν_{max} 3415, 3380, 2920, 1648, 1567, 1487, 1277, 1223, 1106, 890, 868, 807, 798 cm^{-1}. ^1H NMR (CD_3OD): δ 7.04 (1H, d, J = 8.4 Hz, H-7), 6.99 (1H, brs, H-4), 6.80 (1H, dd, J_1 = 8.4; J_2 = 1.6 Hz, H-6), 2.35 (3H, s, CH_3). ^{13}C NMR (100 MHz, CD_3OD): δ 155.09 (C-2), 137.82 (C-3a), 135.46 (C-7a), 129.89 (C-6), 129.47 (C-5), 111.73 (C-4), 110.99 (C-7), 20.18 (CH_3). HRMS (ESI+) *m/z* calcd. for $C_8H_{10}N_3$ $[M + H]^+$, 148.0869, found, 148.0868.

*5-Chloro-1*H*-benzimidazol-2-amine,* BZ***i* 2**

A light brown solid, yield: 85%, mp: 188–189 °C (methanol). ^1H NMR (400 MHz, CD_3OD): δ 7.37 (1H, d, J = 2.0 Hz), 7.31 (1H, d, J = 8.8 Hz), 7.24 (1H, dd, J_1 = 8.8; J_2 = 2.0 Hz). ^{13}C NMR (100 MHz, CD_3OD): δ 153.57, 134.53, 131.73, 127.19, 121.76, 111.86, 111.43. HRMS (ESI+) *m/z* calcd. for $C_7H_7N_3Cl$ $[M + H]^+$, 168.0328, found, 168.0317.

*5-Methoxy-1*H*-benzimidazol-2-amine,* BZ***i* 3**

A black solid, yield: 62%, mp: 184–185 °C (methanol). ^1H NMR (400 MHz, CD_3OD): δ 7.05 (1H, d, J = 8.8 Hz), 6.79 (1H, d, J = 2.4 Hz), 6.61 (1H, dd, J_1 = 8.8; J_2 = 2.4 Hz), 3.77 (3H, s). ^{13}C NMR (100 MHz, CD_3OD): δ 155.21, 155.02, 138.22, 130.76, 111.15, 107.46, 97.19, 54.89. HRMS (ESI+) *m/z* calcd. for $C_8H_{10}N_3O$ $[M + H]^+$, 164.0824, found, 164.0816.

*5,6-Dimethyl-1*H*-benzimidazol-2-amine,* BZ***i* 4**

A dark red solid, yield: 85%, mp: 189–190 °C (methanol). ^1H NMR (400 MHz, CD_3OD): δ 7.04 (2H, s), 2.23 (3H, s), 2.20 (3H, s). ^{13}C NMR (100 MHz, CD_3OD): δ 150.20, 132.32, 132.01, 127.56 (2C), 111.75, 111.46, 18.75 (2C). HRMS (ESI+) *m/z* calcd. for $C_9H_{12}N_3$ $[M + H]^+$, 162.1031, found, 162.1019.

5,6-Dichloro-1H-benzimidazol-2-amine, BZ***i* 5**

A pink solid, yield: 85%, mp: 190–191 °C (methanol). ^1H NMR (400 MHz, C_2D_6SO): δ 8.74 (2H, s), 7.59 (NH_2). ^{13}C NMR (100 MHz, C_2D_6SO): δ 151.98, 130.24 (2C), 125.57 (2C), 113.48, 112.59. HRMS (ESI+) *m/z* calcd. for $C_7H_6N_3Cl_2$ $[M + H]^+$, 201.9939, found, 201.9933.

4.1.2.8. General procedure for the preparation of type II BZs 11 to 30 [29]. To a solution of 0.75 mmol of each BZ*i* and the same proportion of the corresponding aldehyde in 10 mL of absolute EtOH, three drops of glacial acetic acid were added. The mixture was refluxed for 22 h. at 60 °C. Then, $NaBH_4$ (2.62 mmol) was slowly added, and the mixture was heated under reflux for 1 h. Subsequently, of water (7.5 mL) was added, and the $NaBH_4$ excess was neutralised with 2–3% glacial acetic acid. The mixture was cooled to 4 °C for 2 h. in the refrigerator, and then, the solvent was removed in vacuum on a rotary evaporator to provide a precipitate that was purified by column chromatography, eluted with mixtures *n*-hexane/ethyl acetate of increasing the polarity from (1:1) to (1:9). Yields ranged within 17–57%.

N-*Benzyl-5-methyl-1*H*-benzimidazol-2-amine* **11**

A light red solid, yield: 25%, mp: 114–115 °C (methanol). IR (KBr): ν_{max} 3350 (NH), 2918, 1638, 1579, 1490, 1452, 1273, 801, 750, 695 cm^{-1}. ^1H NMR (400 MHz, CD_3OD): δ 7.37 (2H, d, J = 7.2 Hz, H-2' + 6'), 7.30 (2H, t, J = 7.2 Hz, H-3' + 5'), 7.22 (1H, d, J = 7.2 Hz, H-4'), 7.05 (1H, d, J = 7.6 Hz, H-7), 7.04 (1H, d, J = 1.2 Hz, H-4), 6.78 (1H, dd, J_1 = 7.6; J_2 = 1.2 Hz, H-6), 4.54 (2H, s, CH_2), 2.34 (3H, s, CH_3). ^{13}C NMR (100 MHz, CD_3OD): δ 155.37 (C-2), 139.18 (C-5), 137.81 (C-3a), 135.50 (C-7a), 129.50 (C-1'), 128.11 (C-3' + 5'), 126.79 (C-2' + 4' + 6'), 120.92 (C-6), 111.76 (C-4), 111.02 (C-7), 46.05 (CH_2), 20.24 (CH_3). HRMS (ESI+) *m/z* calcd. for $C_{15}H_{16}N_3$ $[M + H]^+$, 238.1266, found, 238.1282.

N-*(4-Methoxybenzyl)-5-methyl-1*H*-benzimidazol-2-amine* **12**

A dark orange solid, yield: 45%, mp: 107–108 °C (methanol). ^1H NMR (400 MHz, CD_3OD): δ 7.30 (2H, d, J = 8.8 Hz, H-2' + 6'), 7.07 (1H, d, J = 7.8 Hz, H-7), 7.04 (1H, d, J = 1.2 Hz, H-4), 6.89 (2H, d, J = 8.8 Hz, H-3' + 5'), 6.77 (1H, dd, J_1 = 7.8; J_2 = 1.2 Hz, H-6), 4.60 (2H, s, CH_2), 3.75 (3H, s, OCH_3), 2.36 (3H, s, CH_3). ^{13}C NMR (100 MHz, CD_3OD): δ 158.73 (C-4'), 155.41 (C-2), 137.92 (C-3a), 137.14 (C-5), 135.40 (C-7a), 131.84 (C-1'), 128.38 (C-2' + 6'), 121.13 (C-6), 114.00 (C-3' + 5'), 111.80 (C-4), 111.10 (C-7), 55.80 (OCH_3), 45.39 (CH_2), 20.36 (CH_3). HRMS (ESI$^+$) *m/z* calcd. for $C_{16}H_{18}N_3O$ $[M + H]^+$, 268.1450, found, 268.1469

*5-Methyl-*N*-(2,3,4-trimethoxybenzyl)-1*H*-benzimidazol-2-amine* **13**

A light yellow oil, yield: 45%. ^1H NMR (400 MHz, CD_3OD): δ 7.10 (1H, d, J = 8.4 Hz), 7.04 (1H, brs), 7.00 (1H, d, J = 8.8 Hz), 6.89 (1H, d, J = 8.4 Hz), 6.65 (1H, d, J = 8.8 Hz), 4.47 (2H, s), 3.85 (3H, s), 3.77 (3H, s), 3.76 (3H, s), 2.34 (3H, s). ^{13}C NMR (100 MHz, CD_3OD): δ 153.64, 153.49, 151.02, 141.83, 131.94, 131.34, 134.24, 123.36, 122.99, 122.49, 111.91, 111.15, 107.50, 61.22, 60.68, 55.84, 41.77, 21.34. HRMS (ESI$^+$) *m/z* calcd. for $C_{18}H_{21}N_3ONa$ $[M + Na]^+$, 350.1475, found, 350.1472.

*5-Methyl-*N*-(naphthalen-2-ylmethyl)-1*H*-benzimidazol-2-amine* **14**

A yellow solid, yield: 17%, mp: 179–180 °C (methanol). ^1H NMR (400 MHz, CD_3OD): δ 7.81 (4H, m), 7.50 (1H, m), 7.41 (2H, m), 7.07 (1H, d, J = 8.0 Hz), 7.01 (1H, d, J = 1.4 Hz), 6.79 (1H, dd, J_1 = 8.0; J_2 = 1.4 Hz), 4.71 (2H, s), 2.34 (3H, s). ^{13}C NMR (100 MHz, CD_3OD): δ 155.38, 137.90, 136.66, 135.42, 133.53, 132.85, 129.63, 127.87, 127.37, 127.25, 125.76, 125.35, 125.28, 125.25, 121.00, 111.77, 111.05, 46.20, 20.22. HRMS (ESI$^+$) *m/z* calcd. for $C_{19}H_{17}N_3Na$ $[M + Na]^+$, 310.1314, found, 310.1304.

N-*(Furan-2-ylmethyl)-5-methyl-1*H*-benzimidazol-2-amine* **15**

A yellow-orange solid, yield: 20%, mp: 136–137 °C (methanol). ^1H NMR (400 MHz, CD_3OD): δ 7.39 (1H, brs), 7.05 (1H, d, J = 8.0 Hz), 7.00 (1H, brs), 6.78 (1H, d, J = 8.0 Hz), 6.30 (1H, brs), 6.27 (1H, brs), 4.49 (2H, s), 2.32 (3H, s). ^{13}C NMR (100 MHz,

CD_3OD): δ 156.10, 153.66, 143.32, 138.65, 136.38, 131.15, 122.46, 113.15, 112.46, 111.32, 107.98, 40.69, 21.59. HRMS (ESI^+) *m/z* calcd. for $C_{13}H_{14}N_3O$ $[M + H]^+$, 228.1131, found, 228.1141.

*5-Methyl-*N*-(thiophen-2-ylmethyl)-1*H*-benzimidazol-2-amine* **16**

An orange oil, yield: 35%. IR (NaCl): ν_{max} 3412, 3375, 2915, 1645, 1567, 1530, 1487, 1223, 1106, 890, 807, 798 cm^{-1}. ^1H NMR (400 MHz, CD_3OD): δ 7.13 (1H, brd, J = 5.2 Hz, H-5′), 7.12 (1H, d, J = 7.2 Hz, H-7), 7.05 (1H, brs, H-4), 6.92 (1H, d, J = 3.2 Hz, H-3′), 6.86 (1H, dd, J_1 = 5.2; J_2 = 3.2 Hz, H-4′), 6.85 (1H, d, J = 7.2 Hz, H-6), 4.70 (2H, s, CH_2), 2.34 (3H, s, CH_3). ^{13}C NMR (100 MHz, CD_3OD): δ 150.12 (C-2), 137.93 (C-2′), 133.79 (C-5), 129.65 (C-3a), 127.32 (C-7a), 127.04 (C-4′), 126.89 (C-3′), 125.77 (C-5′), 124.59 (C-6), 111.98 (C-4), 111.31 (C-7), 42.33 (CH_2), 21.37 (CH_3). HRMS (ESI^+) *m/z* calcd. for $C_{13}H_{14}N_3S$ $[M + H]^+$, 244.0902, found, 244.0897.

N-*Benzyl-5-chloro-1*H*-benzimidazol-2-amine* **17**

A brown-orange solid, yield: 19%, mp: 123–124 °C (methanol). ^1H NMR (400 MHz, CD_3OD): δ 7.37 (2H, m), 7.32 (2H, t, J = 7.2 Hz), 7.24 (1H, m), 7.16 (1H, s), 7.11 (1H, d, J = 7.6 Hz), 6.93 (1H, d, J = 7.6 Hz), 4.56 (2H, s). ^{13}C NMR (100 MHz, CD_3OD): δ 156.24, 138.93, 136.70, 132.10, 128.16 (2C), 126.88 (3C), 125.34, 119.76, 111.67 (2C), 45.93. HRMS (ESI^+) *m/z* calcd. for $C_{14}H_{13}N_3Cl$ $[M + H]^+$, 258.0793, found, 258.0796.

*5-Chloro-*N*-(4-methoxybenzyl)-1*H*-benzimidazol-2-amine* **18**

A yellow solid, yield: 40%, mp: 114–150 °C (methanol). ^1H NMR (400 MHz, CD_3OD): δ 7.32 (2H, d, J = 8.2 Hz), 7.18 (1H, brs), 7.12 (1H, d, J = 7.8 Hz), 6.98 (1H, d, J = 7.8 Hz), 6.88 (2H, d, J = 8.2 Hz), 4.56 (2H, s), 3.77 (3H, s). ^{13}C NMR (100 MHz, CD_3OD): δ 158.10, 156.10, 137.20, 134.00, 131.72, 128.21 (2C), 126.08, 120.11, 113.98 (2C), 111.82, 111.81, 55.69, 45.99. HRMS (ESI^+) *m/z* calcd. for $C_{15}H_{15}ON_3Cl$ $[M + H]^+$, 288.0904, found, 288.0914.

*5-Chloro-*N*-(3,4,5-trimethoxybenzyl)-1*H*-benzimidazol-2-amine* **19**

A light orange solid, yield: 25%, mp: 109–110 °C (methanol). ^1H NMR (400 MHz, $CDCl_3$): δ 7.25 (1H, brs), 7.10 (1H, d, J = 8.0 Hz), 6.99 (1H, d, J = 8.0 Hz), 6.39 (2H, s), 4.41 (2H, s), 3.77 (3H, s), 3.63 (6H, s). ^{13}C NMR (100 MHz, $CDCl_3$): δ 154.73, 152.84 (2C), 137.60, 136.38, 134.20, 133.19, 126.16, 120.80, 111.94 (2C), 103.33 (2C), 60.44, 55.52 (2C), 46.63. HRMS (ESI^+) *m/z* calcd. for $C_{17}H_{19}O_3N_3Cl$ $[M + H]^+$, 328.1110, found, 348.1104.

*5-Chloro-*N*-(furan-2-yl-methyl)-1*H*-benzimidazol-2-amine* **20**

A dark red solid, yield: 21%, mp: 128–129 °C (methanol). IR (KBr): ν_{max} 3411, 2921, 1630, 1603, 1466, 1384, 1266, 1058, 919, 803, 695 cm^{-1}. ^1H NMR (400 MHz, CD_3OD): δ 7.45 (1H, dd, J_1 = 1.2; J_2 = 0.8 Hz, H-5′), 7.20 (1H, d, J = 1.6 Hz, H-4), 7.14 (1H, J = 8.0 Hz, H-7), 6.99 (1H, J_1 = 8.0; J_2 = 1.6 Hz, H-6), 6.34 (1H, dd, J_1 = 3.2; J_2 = 0.8 Hz, H-3′), 6.32 (1H, d, J = 3.2 Hz, H-4′), 4.56 (2H, s, CH_2). ^{13}C NMR (100 MHz, CD_3OD): δ 154.84 (C-2), 151.55 (C-2′), 142.21 (C-5′), 137.46 (C-3a), 134.29 (C-7a), 126.11 (C-5), 121.62 (C-6), 111.65 (C-4), 111.38 (C-7), 109.62 (C-4′), 106.94 (C-3′), 39.21 (CH_2). HRMS (ESI^+) *m/z* calcd. for $C_{12}H_{10}N_3ClO$ $[M + H]^+$, 248.0585, found, 248.0587.

N-*Benzyl-5-methoxy-1*H*-benzimidazol-2-amine* **21**

A dark orange, yield: 45%, mp: 181–182 °C (methanol). ^1H NMR (400 MHz, CD_3OD): δ 7.37 (2H, dd, J_1 = 7.6; J_2 = 1.2 Hz), 7.31 (2H, dd, J_1 = 7.6; J_2 = 7.2 Hz), 7.21 (1H, dd, J_1 = 7.2; J_2 = 1.2 Hz), 7.04 (1H, d, J = 8.4 Hz) 6.80 (1H, d, J = 2.4 Hz), 6.58 (1H, dd, J_1 = 8.4; J_2 = 2.4 Hz), 4.54 (2H, s), 3.76 (3H, s). ^{13}C NMR (100 MHz, CD_3OD): δ 155.65, 155.05, 139.17, 138.92, 131.90, 128.11 (2C), 126.90 (2C), 126.78, 111.15, 107.12, 97.33, 54.89, 46.04. HRMS (ESI^+) *m/z* calcd. for $C_{15}H_{16}N_3O$ $[M + H]^+$, 254.1288, found, 254.1287.

*5-Methoxy-*N*-(4-methoxybenzyl)-1*H*-benzimidazol-2-amine* **22**

A dark yellow solid, yield: 43%, mp: 110–111 °C (methanol). ^1H NMR (400 MHz, CD_3OD): δ 7.30 (2H, d, J = 8.8 Hz), 7.05 (1H, d, J = 8.4 Hz), 6.87 (2H, d, J = 8.8 Hz), 6.80 (1H, d, J = 2.4 Hz), 6.58 (1H, d, J_1 = 8.4; J_2 = 2.4 Hz), 4.56 (2H, s), 3.75 (3H, s), 3.76 (3H, s). ^{13}C NMR (100 MHz, CD_3OD): δ 158.83, 155.81, 155.78, 139.20, 136.00, 130.33, 128.24 (2C), 113.95 (2C), 111.99, 107.77, 97.94, 55.92, 55.13, 46.41. HRMS (ESI^+) *m/z* calcd. for $C_{16}H_{18}N_3O_2$ $[M + H]^+$, 284.1399, found, 284.1339.

*5-Methoxy-*N*-(4-(pyrrolidin-1-yl)benzyl)-1*H*-benzimidazol-2-amine,* **23**

A dark orange solid, yield: 40%, mp: 175–176 °C ($CHCl_3$/methanol). IR (KBr): ν_{max} 3430, 1925, 1620, 1585, 1523, 1487, 1375, 1156, 1110, 802 cm^{-1}. ^1H NMR (400 MHz, CD_3OD+$CDCl_3$): δ 7.25 (2H, d, J = 8.8 Hz, H-2′ + 6′), 7.17 (1H, d, J = 8.4 Hz, H-7), 6.97 (1H, d, J = 2.0 Hz, H-4), 6.73 (1H, dd, J_1 = 8.4; J_2 = 2.0 Hz, H-6), 6.58 (2H, d, J = 8.8 Hz, H-3′ + 5′), 4.54 (2H, s, CH_2), 3.88 (3H, s, OCH_3), 3.32 (4H, m, H-2′′+5′′), 2.10 (4H, m, H-3′′ + 4′′). ^{13}C NMR (100 MHz, CD_3OD+$CDCl_3$): δ 155.06 (C-2), 154.94 (C-5), 147.46 (C-4′), 138.23 (C-3a), 130.71 (C-7a), 128.60 (C-2′ + 6′), 124.46 (C-1′), 111.71 (C-3′ + 5′), 111.39 (C-7), 107.63 (C-6), 97.68 (C-4), 55.89 (OCH_3), 47.62 (C-2′′ + 5′′), 46.52 (CH_2), 25.34 (C-3′′ + 4′′). HRMS (ESI^+) *m/z* calcd. for $C_{19}H_{23}N_4O$ $[M + H]^+$, 323.1866, found, 323.1873.

*5-Methoxy-*N*-((5-methylfuran-2-yl)methyl)-1*H*-benzimidazol-2-amine,* **24**

A dark orange solid, yield: 32%, mp: 141–142 °C ($CHCl_3$/methanol). ^1H NMR (400 MHz, $CDCl_3$): δ 7.09 (1H, d, J = 8.4 Hz), 6.83 (1H, d, J = 2.4 Hz), 6.62 (1H, dd, J_1 = 8.4; J_2 = 2.4 Hz), 6.04 (1H, d, J = 2.8 Hz), 5.81 (1H, d, J = 2.8 Hz), 4.47 (2H, s), 3.74 (3H, s), 2.15 (3H, s). ^{13}C NMR (100 MHz, $CDCl_3$): δ 155.34, 154.45, 152.06, 149.28, 137.61, 129.97, 111.91, 108.31 (2C), 106.23, 97.72, 55.83, 40.25, 13.39. HRMS (ESI^+) *m/z* calcd. for $C_{14}H_{15}N_3O_2Na$ $[M + Na]^+$, 280.1056, found, 280.1046.

*5-Methoxy-*N*-(thiophen-2-yl-methyl)-1*H*-benzimidazol-2-amine,* **25**

A dark brown solid, yield: 32%, mp: 167–168 °C (methanol). ^1H NMR (400 MHz, CD_3OD): δ 7.26 (1H, dd, J_1 = 4.8; J_2 = 0.8 Hz), 7.06 (1H, d, J = 8.4 Hz), 7.05 (1H, dd, J_1 = 3.6; J_2 = 0.8 Hz), 6.93 (1H, dd, J_1 = 4.8; J_2 = 3.6 Hz), 6.81 (1H, d, J = 2.8 Hz), 6.60 (1H, dd, J_1 = 8.4; J_2 = 2.8 Hz), 4.71 (2H, s), 3.77 (3H, s). ^{13}C NMR (100 MHz, CD_3OD): δ 156.53, 156.49, 143.75, 140.50, 133.10, 127.63, 126.39, 125.67, 112.70, 108.63, 98.63, 56.26, 42.55. HRMS (ESI^+) *m/z* calcd. for $C_{13}H_{19}N_3OS$ $[M + H]^+$, 260.0852, found, 280.0855.

N-*(4-Methoxybenzyl)-5,6-dimethyl-1*H*-benzimidazol-2-amine,* **26**

A dark yellow solid, yield: 57%, mp: 157–158 °C (methanol). ^1H NMR (400 MHz, CD_3OD): δ 6.90 (2H, d, J = 8.4 Hz), 6.58 (2H, s), 6.47 (2H, d, J = 8.4 Hz), 4.06 (2H, s), 3.36 (3H, s), 1.87 (6H, s). ^{13}C NMR (100 MHz, CD_3OD): δ 160.45, 156.08, 138.76, 136.76 (2C), 134.60, 132.30, 129.70 (2C), 114.87 (2C), 113.50 (2C), 55.63, 47.02, 20.20 (2C). HRMS (ESI^+) *m/z* calcd. for $C_{17}H_{20}N_3O$ $[M + H]^+$, 282.1606, found, 282.1606.

*5,6-Dimethyl-*N*-(3,4,5-trimethoxybenzyl)-1*H*-benzimidazol-2-amine,* **27**

A dark yellow solid, yield: 40%, mp: 114–115 °C ($CHCl_3$/methanol). IR (KBr): ν_{max} 3250, 3066, 1681, 1648, 1565, 1250, 1220, 1120, 890, 872, 807, 798 cm^{-1}. ^1H NMR (400 MHz, $CDCl_3$): δ 6.99 (2H, s, H-4 + 7), 6.43 (2H, s, H-2′ + 6′), 4.43 (2H, s, CH_2), 3.76 (3H, s, 4′–OCH_3), 3.62 (6H, s, 3′ + 5′–OCH_3), 2.23 (6H, s, CH_3). ^{13}C NMR (100 MHz, $CDCl_3$): δ 154.62 (C-2), 153.27 (C-3′ + 5′), 136.86 (C-4′), 135.12 (C-3a + 7a), 134.27 (C-1′), 129.13 (C-5 + 6), 112.88 (C-4 + 7), 103.87 (C-2′ + 6′), 60.76 (4′–OCH_3), 55.87 (3′ + 5′–OCH_3), 47.18 (CH_2), 20.02 ((CH_3)$_2$). HRMS (ESI^+) *m/z* calcd. for $C_{19}H_{24}N_3O_3$ $[M + H]^+$, 342.1812, found, 342.1807.

N-*Benzyl-5,6-dichloro-1*H*-benzimidazol-2-amine,* **28**

A light brown solid, yield: 17%, mp: 198–199 °C ($CHCl_3$/methanol). ^1H NMR (400 MHz, $CDCl_3$): δ 7.84 (2H, s), 7.39 (2H, m), 7.27 (3H, m), 4.58 (2H, s). ^{13}C NMR (100 MHz, $CDCl_3$): δ 155.73, 142.10 (2C), 137.14 (2C), 128.93 (2C), 127.95, 127.00 (2C), 124.37, 113.31 (2C), 46.96. HRMS (ESI^+) *m/z* calcd. for $C_{14}H_{12}N_3Cl$ $[M + H]^+$, 292.0403, found, 292.0407.

*5,6-Dichloro-*N*-(4-methoxybenzyl)-1*H*-benzimidazol-2-amine,* **29**

A light brown, yield: 18%, mp: 209–210 °C (methanol). IR (KBr): ν_{max} 3339, 2929, 1620, 1597, 1569, 1514, 1455, 1248, 1174, 1030, 824, 865 cm^{-1}. ^1H NMR (400 MHz, CD_3OD): δ 7.28 (2H, s, H-4 + 7), 7.25 (2H, d, J = 8.8 Hz, H-2′ + 6′), 6.88 (2H, d, J = 8.8 Hz, H-3′ + 5′), 4.47 (2H, s, CH_2), 3.76 (3H, s, OCH_3). ^{13}C NMR (100 MHz, CD_3OD): δ 160.49 (C-4′), 158.30 (C-2), 139.08 (C-3a), 134.63 (C-7a), 131.98 (C-5 + 6), 129.64 (C-2′ + 6′), 124.23 (C-1′), 114.91 (C-3′ + 5′), 113.76 (C-4 + 7), 55.63 (OCH_3), 46.80 (CH_2). HRMS (ESI^+) m/z calcd. for $C_{15}H_{14}N_3OCl_2$ [M + H]$^+$, 322.0508, found, 322.0503.

*5,6-Dichloro-*N*-(3,4,5-trimethoxybenzyl)-1H-benzimidazol-2-amine,* **30**

A dark orange solid, yield: 20%, mp: 111–112 °C ($CHCl_3$/methanol). ^1H NMR (400 MHz, $CDCl_3$): δ 7.21 (2H, s), 6.39 (2H, s), 4.37 (2H, s), 3.76 (3H, s), 3.66 (6H, s). ^{13}C NMR (100 MHz, $CDCl_3$): δ 155.13, 153.21 (2C), 139.05 (2C), 137.24, 135.62 (2C), 131.42, 113.22 (2C), 105.19 (2C), 60.76, 56.37 (2C), 47.28. HRMS (ESI^+) m/z calcd. for $C_{17}H_{18}N_3O_3Cl_2$ [M + H]$^+$, 382.0720, found, 382.0717.

4.1.2.9. General procedure for the preparation of amides of types III and IV, BZs 31 to 55. The procedure applied was similar to that indicated in Section 4.1.2.5. To a solution of the corresponding acid (0.31 mmol) in dry DMF (1 mL), 1,1-carbonyldiimidazole (0.31 mmol) was added, and the mixture maintained at room temperature for 1 h. Then, the corresponding 2-aminobenzimidazole intermediate (0.22 mmol) was added and the mixture maintained at room temperature with magnetic stirring for 16 h. The progress of the reaction was monitored by TLC using ethyl acetate as eluent. After the reaction completion, the solvent was removed in vacuum and the crude product chromatographed on silica gel using ethyl acetate as eluent. BZ yields ranged within 20–73%.

N-*(5-Methyl-1H-benzimidazol-2-yl)benzamide* **31**

A light yellow solid, yield: 20%, mp: 244–245 °C ($CHCl_3$/methanol). IR (KBr) ν_{max}: 3345, 2950, 1683, 1645, 1600, 1470, 1190, 887, 780, 745, 683 cm^{-1}. ^1H NMR (400 MHz, CD_3OD): δ 8.07 (2H, dd, J_1 = 8.0; J_2 = 1.6 Hz, H-2′ + 6′), 7.62 (1H, dd, J_1 = 7.8; J_2 = 1.6 Hz, H-4′), 7.54 (2H, dd, J_1 = 8.0; J_2 = 7.8 Hz, H-3' + 5), 7.36 (1H, d, J = 8.4 Hz, H-7), 7.28 (1H, d, J = 1.2 Hz, H-4), 7.03 (1H, dd, J_1 = 8.4; J_2 = 1.2 Hz, H-6), 2.61 (3H, s, CH_3). ^{13}C NMR (100 MHz, $CDCl_3$): δ 169.36 (NHCO), 148.59 (C-2), 134.00 (C-3a), 133.70 (C-5), 132.45 (C-4′), 132.00 (C-7a + 1′), 128.86 (C-3′ + 5′), 128.56 (C-2′ + 6′), 123.54 (C-6), 112.30 (C-4), 112.10 (C-7), 21.47 (CH_3). HRMS (ESI^+) m/z calcd. for $C_{15}H_{14}N_3O$ [M + H]$^+$, 252.1128, found, 252.1128.

*4-Methoxy-*N*-(5-methyl-1H-benzimidazol-2-yl)benzamide* **32**

A white solid, yield: 20%, mp: 234–235 °C (methanol). ^1H NMR (400 MHz, CD_3OD): δ 8.04 (2H, d, J = 8.4 Hz), 7.34 (1H, d, J = 8.0 Hz), 7.29 (1H, d, J = 1.6 Hz), 7.05 (2H, d, J = 8.4 Hz), 7.02 (1H, dd, J_1 = 8.0; J_2 = 1.6 Hz), 3.88 (3H, s), 2.44 (3H, s). ^{13}C NMR (100 MHz, CD_3OD): δ 166.38, 162.21, 148.30, 134.20, 132.00, 130.52 (3C), 130.46, 123.94, 115.22, 114.18 (3C), 55.49, 21.49. HRMS (ESI^+) m/z calcd. for $C_{16}H_{16}N_3O_2$ [M + H]$^+$, 282.1237, found, 282.1234.

*2-Chloro-*N*-(5-methyl-1H-benzimidazol-2-yl)-5-nitrobenzamide* **33**

A yellow solid, yield: 41%, mp: 240–241 °C (methanol). IR (KBr): ν_{max} 3390, 3313, 2924, 1682, 1626, 1558, 1536, 1384, 1270, 1100, 1023, 800 cm^{-1}. ^1H NMR (400 MHz, C_2D_6SO): δ 12.80 (2H, brs, NH+NHCO), 8.58 (1H, d, J = 2.4 Hz, H-6′), 8.25 (1H, dd, J_1 = 8.8; J_2 = 2.4 Hz, H-4′), 7.78 (1H, d, J = 8.8 Hz, H-3′), 7.29 (1H, d, J = 8.4 Hz, H-7), 7.21 (1H, brs, H-4), 6.98 (1H, brd, J = 8.4 Hz, H-6′), 2.35 (3H, s, CH_3). ^{13}C NMR (100 MHz, C_2D_6SO): δ 162.30 (NHCO), 147.50 (C-2), 143.80 (C-5′), 140.22 (C-2′), 136.10 (C-7a), 138.20 (C-3a), 134.39 (C-5), 134.29 (C-1′), 131.43 (C-4′), 130.53 (C-3′), 126.61 (C-6′), 125.42 (C-6), 113.52 (C-4), 113.50 (C-7), 21.62 (CH_3). HRMS (ESI^+) m/z calcd. for $C_{15}H_{12}N_4O_3Cl$ [M + H]$^+$, 331.0592, found, 331.0597.

*3,5-Dimethoxy-*N*-(5-methyl-1H-benzimidazol-2-yl)benzamide* **34**

A light orange, yield: 73%, mp: 155–156 °C (methanol). IR (KBr): ν_{max} 3379, 2920, 1681, 1635, 1568, 1466, 1427, 1351, 1207, 1157, 1063, 832, 803 cm^{-1}. ^1H NMR (400 MHz, C_2D_6SO): δ 8.30 (1H, brs, NH + NHCO), 7.30 (1H, d, J = 7.2 Hz, H-7), 7.29 (2H, t, J = 2.2 Hz, H-2′ + 6′), 7.23 (1H, brs, H-4), 6.69 (1H, t, J = 2.2 Hz, H-4′), 6.94 (1H, brd, J = 7.2 Hz, H-6), 3.80 (3H, s, OCH_3), 3.77 (3H, s, OCH_3), 2.37 (3H, s, CH_3). ^{13}C NMR (100 MHz, C_2D_6SO): δ 166.99 (NHCO), 160.38 (C-3′), 160.30 (C-5′), 149.50 (C-2), 137.80 (C-3a), 137.10 (C-7a), 132.89 (C-5), 130.71 (C-1′), 122.80 (C-6), 113.03 (C-4), 112.99 (C-7), 106.84 (C-4′), 106.02 (C-2′ + 6′), 55.44 ((OCH_3)$_2$), 21.26 (CH_3). HRMS (ESI^+) m/z calcd. for $C_{17}H_{18}N_3O_3$ [M + H]$^+$, 312.1343, found, 312.1338.

*3,4,5-Trimethoxy-*N*-(5-methyl-1H-benzimidazol-2-yl)benzamide* **35**

A light brown solid, yield: 51%, mp: 139–140 °C (methanol). ^1H NMR (400 MHz, C_2D_6SO): δ 12.15 (2H, brs), 7.47 (2H, s), 7.31 (1H, d, J = 8.4 Hz), 7.24 (1H, d, J = 1.6 Hz), 6.93 (1H, dd, J_1 = 8.4; J_2 = 1.6 Hz), 3.85 (6H, s), 3.72 (3H, s), 2.36 (2H, s). ^{13}C NMR (100 MHz, C_2D_6SO): δ 169.36, 153.13 (2C), 149.16, 141.80, 134.30, 132.40, 132.10, 128.81, 123.87, 112.80, 112.10, 105.86 (2C), 60.90, 55.83 (2C), 21.56. HRMS (ESI^+) m/z calcd. for $C_{18}H_{20}N_3O_4$ [M + H]+, 342.1148, found, 342.1445.

N-*(5-Methyl-1H-benzimidazol-2-yl)picolinamide* **36**

A light yellow solid, yield: 31%, mp: 206–207 °C (methanol). IR (KBr): ν_{max} 3235, 2920, 1685, 1621, 1569, 1442, 1410, 1271, 1226, 1170, 1112, 1015, 992, 899, 870, 808, 740, 695 cm^{-1}. ^1H NMR (400 MHz, C_2D_6SO): δ 8.75 (1H, ddd, J_1 = 5.5; J_2 = 1.6; J_3 = 0.9 Hz), 8.21 (1H, ddd, J_1 = 7.8; J_2 = 1.2; J_3 = 0.9 Hz), 8.10 (1H, dt, J_1 = 7.8; J_2 = 1.6 Hz), 7.72 (1H, ddd, J_1 = 7.8; J_2 = 5.5; J_2 = 1.2 Hz), 7.36 (1H, d, J = 8.1 Hz), 7.29 (1H, d, J = 1.6 Hz), 6.94 (1H, d, J_1 = 8.1; J_2 = 1.6 Hz), 2.38 (3H, s). ^{13}C NMR (100 MHz, C_2D_6SO): δ 163.22 (NHCO), 148.93 (C-6), 148.48 (C-2), 145.44 (C-2), 138.28 (C-3a + 4), 137.62 (C-7a), 131.48 (C-5), 127.61 (C-5), 122.69 (C-6 + 3), 115.20 (C-7), 114.13 (C-4), 21.31 (CH_3). HRMS (ESI^+) m/z calcd. for $C_{14}H_{13}N_4O$ [M + H]$^+$, 253.1084, found, 253.1074.

N-*(5-Chloro-1H-benzimidazol-2-yl)benzamide* **37**

A yellow solid, yield: 60%, mp: 244–245 °C (methanol). IR (KBr): ν_{max} 3256, 2917, 1685, 1622, 1563, 1440, 1410, 1271, 1225, 1172, 1113, 1015, 889, 882, 829, 749, 695, 619 cm^{-1}. ^1H NMR (400 MHz, C_2D_6SO): δ 12.29 (2H, brs, NH + NHCO), 8.10 (2H, d, J_1 = 8.0 Hz; J_2 = 1.6 Hz, H-2′ + 6′), 7.63 (1H, dd, J_1 = 7.2; J_2 = 1.6 Hz, H-4′), 7.53 (2H, dd, J = 8.0; J = 7.2 Hz, H-3′ + 5′), 7.49 (1H, d, J = 2.0 Hz, H-4), 7.45 (1H, d, J = 8.0 Hz, H-7), 7.13 (1H, dd, J_1 = 8.0; J_2 = 2.0 Hz, H-6). ^{13}C NMR (100 MHz, C_2D_6SO): δ 167.50 (NHCO), 149.11 (C-2), 137.60 (C-3a), 134.60 (C-7a), 133.63 (C-1′), 132.90 (C-4′), 128.94 (C-3′ + 5′), 128.68 (C-2′ + 6′), 126.01 (C-5), 121.82 (C-6), 115.17 (C-4), 114.10 (C-7). HRMS (ESI^+) m/z calcd. for $C_{14}H_{11}N_3OCl$ [M + H]$^+$, 272.0585, found, 272.0584.

N-*(5-Chloro-1H-benzimidazol-2-yl)-4-methoxybenzamide* **38**

A light pink solid, yield: 55%, mp: 249–250 °C (methanol). ^1H NMR (400 MHz, C_2D_6SO): δ 12.19 (2H, brs), 8.10 (2H, d, J = 8.8 Hz), 7.48 (1H, d, J = 2.0 Hz), 7.44 (1H, d, J = 8.8 Hz), 7.11 (1H, dd, J_1 = 8.8; J_2 = 2.0 Hz), 7.05 (2H, d, J = 8.8 Hz), 3.82 (3H, s). ^{13}C NMR (100 MHz, C_2D_6SO): δ 166.47, 166.13, 149.11, 138.10, 136.30, 130.66 (2C), 125.81, 125.43, 121.62, 114.25 (2C), 108.10, 106.90, 55.95. HRMS (ESI^+) m/z calcd. for $C_{15}H_{13}N_3O_2Cl$ [M + H]$^+$, 302.0691, found, 302.0691.

N-*(5-Chloro-1H-benzimidazol-2-yl)picolinamide* **39**

A white solid, yield: 65%, mp: 223–224 °C (methanol). IR (KBr): ν_{max} 3241, 2915, 1684, 1625, 1560, 1440, 1412, 1273, 1226, 1172, 1110, 1017, 996, 899, 875, 808, 740, 695, 619 cm^{-1}. ^1H NMR (400 MHz, C_2D_6SO): δ 12.00 (2H, brs), 8.65 (1H, brd, J = 4.8 Hz, H-6′), 8.19 (1H, d, J = 7.6 Hz, H-3′), 8.60 (1H, ddd, J_1 = 8.0; J_2 =7.6; J_3 = 1.2 Hz, H-4′), 7.66 (1H, dd, J_1 = 8.0; J_2 = 4.8 Hz, H-5′), 7.50 (1H, d, J = 1.2 Hz, H-4), 7.48 (1H, d, J = 8.4 Hz, H-7), 7.12 (1H, J_1 = 8.4; J_2 = 1.2 Hz, H-6). ^{13}C NMR (100 MHz, C_2D_6SO):

δ 163.75 (NHCO), 149.30 (C-6′), 148.57 (C-2′), 147.19 (C-2), 138.70 (C-3a + 4′), 136.90 (C-7a), 128.16 (C-5′), 126.09 (C-5), 123.24 (C-3′), 121.89 (C-6), 116.10 (C-4), 115.90 (C-7). HRMS (ESI$^+$) *m/z* calcd. for $C_{13}H_{10}N_4OCl$ [M + H]$^+$, 273.0538, found, 273.0544.

N-*(5-Methoxy-1*H*-benzimidazol-2-yl)benzamide* **40**

A white solid, yield: 60%, mp: 195–196 °C ($CHCl_3$/methanol). IR (KBr): ν_{max} 3255, 2915, 1680, 1621, 1565, 1439, 1410, 1270, 1223, 1170, 1112, 1015, 889, 882, 829, 749, 695 cm^{-1}. ^{1}H NMR (400 MHz, $CDCl_3$): δ 11.83 (2H, brs), 8.13 (2H, dd, J_1 = 8.4; J_2 = 1.6 Hz, H-2′ + 6′), 7.52 (1H, m, H-4′), 7.42 (2H, dd, J_1 =8.4; J_2 = 7.2 Hz, H-3′ + 5′), 7.10 (1H, brs, H-4), 6.73 (1H, dd, J_1 = 8.4; J_2 = 2.0 Hz, H-6), 6.70 (1H, d, J = 8.4 Hz, H-7), 3.67 (3H, s, OCH_3). ^{13}C NMR (100 MHz, $CDCl_3$): δ 168.10 (NHCO), 156.40 (C-5), 144.20 (C-2), 136.20 (C-3a), 132.88 (C-4′), 131.88 (C-1′), 130.40 (C-7a), 128.85 (C-3′ + 5′), 128.46 (C-2′ + 6′), 111.73 (C-6), 109.70 (C-7), 108.10 (C-4), 55.75 (OCH_3). HRMS (ESI$^+$) *m/z* calcd. for $C_{15}H_{14}N_3O_2$ [M + H]$^+$, 268.1081, found, 268.1075.

*4-Methoxy-*N*-(5-methoxy-1*H*-benzimidazol-2-yl)benzamide* **41**

A white solid, yield: 57%, mp: 192–193 °C ($CHCl_3$/methanol). ^{1}H NMR (400 MHz, $CDCl_3$): δ 8.18 (2H, d, J = 8.4 Hz), 7.21 (1H, brs), 6.96 (2H, J = 8.4 Hz), 6.81 (1H, dd, J_1 = 9.2; J_2 = 2.4 Hz), 6.76 (1H, brs), 3.86 (3H, s), 3.83 (3H, s). ^{13}C NMR (100 MHz, $CDCl_3$): δ 167.56, 163.29, 156.17, 148.20, 136.40, 130.58 (2C), 130.00, 125.08, 114.07 (2C), 111.34, 107.60, 107.21, 55.64, 55.49. HRMS (ESI$^+$) *m/z* calcd. for $C_{16}H_{16}N_3O_3$ [M + H]$^+$, 298.1186, found, 298.1181.

N-*(5-Methoxy-1*H*-benzimidazol-2-yl)picolinamide* **42**

A light yellow solid, yield: 40%, mp: 175–176 °C ($CHCl_3$/methanol). IR (KBr): ν_{max} 3232, 2915, 1681, 1620, 1567, 1442, 1412, 1270, 1225, 1173, 1112, 1015, 992, 899, 870, 808, 740, 695 cm^{-1}. ^{1}H NMR (400 MHz, $CDCl_3$): δ 8.57 (1H, ddd, J_1 = 5.5; J_2 = 1.9; J_3 = 0.9 Hz, H-6′), 8.26 (1H, ddd, J_1 = 7.6; J_2 = 1.6; J_3 = 0.9 Hz, H-3′), 7.89 (1H, ddd, J_1 = 7.6; J_2 = 7.5; J_3 = 1.9 Hz, H-4′), 7.50 (1H, ddd, J_1 = 7.5; J_2 = 5.5; J_3 = 1.6 Hz, H-5′), 7.40 (1H, d, J = 8.0 Hz, H-7), 7.02 (1H, brs, H-4), 6.86 (1H, d, J = 8.0 Hz, H-6), 3.82 (3H, s, OCH_3). ^{13}C NMR (100 MHz, $CDCl_3$): δ 163.54 (NHCO), 156.15 (C-5), 148.65 (C-6′), 148.17 (C-2′), 147.87 (C-2), 137.02 (C-4′), 136.97 (C-3a), 129.93 (C-7a), 127.32 (C-5′), 122.73 (C-3′), 111.18 (C-6), 100.80 (C-7), 108.50 (C-4), 55.79 (OCH_3). HRMS (ESI$^+$) *m/z* calcd. for $C_{14}H_{13}N_4O_2$ [M + H]$^+$, 269.1033, found, 269.1022.

N-*(5,6-Dimethyl-1*H*-benzimidazol-2-yl)benzamide* **43**

A white solid, yield: 32%, mp: 232–233 °C (methanol). ^{1}H NMR (400 MHz, C_2D_6SO): δ 11.89 (2H, brs), 7.62 (1H, dd, J_1 = 7.8; J_2 = 1.6 Hz), 7.39 (2H, dd, J_1 = 8.0; J_2 = 7.8 Hz), 7.35 (2H, dd, J_1 = 8.0; J_2 = 1.6 Hz), 7.01 (2H, s), 2.31 (6H, s). ^{13}C NMR (100 MHz, C_2D_6SO): δ 168.21, 146.13, 137.22 (2C), 132.80, 132.11, 131,74 (2C), 128.65 (2C), 128.22 (2C), 115.63 (2C), 19.16 (2C). HRMS (ESI$^+$) *m/z* calcd. for $C_{16}H_{16}N_3O$ [M + H]$^+$, 266.1293, found, 266.1299.

N-*(5,6-Dimethyl-1*H*-benzimidazol-2-yl)-4-methoxybenzamide* **44**

A white solid, yield: 28%, mp: 259–260 °C ($CHCl_3$/methanol). ^{1}H NMR (400 MHz, $CDCl_3$): δ 7.99 (2H, d, J = 8.8 Hz), 6.83 (2H, d, J = 8.8 Hz), 6.85 (2H, brs), 3.76 (3H, s), 2.16 (6H, s). ^{13}C NMR (100 MHz, $CDCl_3$): δ 169.06, 162.97, 148.81, 135.80 (2C), 130.61 (2C), 130.52 (2C), 126.43, 115.20 (2C), 114.03 (2C), 55.41, 20.05 (2C). HRMS (ESI$^+$) *m/z* calcd. for $C_{17}H_{18}N_3O_2$ [M + H]$^+$, 296.1394, found, 296.1392.

N-*(5,6-Dichloro-1*H*-benzimidazol-2-yl)benzamide* **45**

A white solid, yield: 26%, mp: 335–336 °C (methanol). ^{1}H NMR (400 MHz, C_2D_6SO): δ 8.09 (2H, dd, J_1 = 7.2; J_2 = 1.6 Hz), 7.69 (2H, s), 7.62 (1H, dd, J_1 = 7.6; J_2 = 1.6 Hz), 7.53 (2H, dd, J_1 = 7.6; J_2 = 7.2 Hz). ^{13}C NMR (100 MHz, C_2D_6SO): δ 166.44, 149.21, 138.10 (2C), 132.69, 128.57 (2C), 128.26 (2C), 125,90 (2C), 123.39, 115.50 (2C). HRMS (ESI$^+$) *m/z* calcd. for $C_{14}H_{10}N_3OCl_2$ [M + H]$^+$, 306.0195, found, 306.0195.

N-*(5,6-Dichloro-1*H*-benzimidazol-2-yl)-4-methoxybenzamide* **46**

A white solid, yield: 30%, mp: 295–296 °C (methanol). ^{1}H NMR (400 MHz, C_2D_6SO): δ 12.45 (1H, brs), 12.01 (1H, brs), 8.10 (2H, d, J = 8.8 Hz), 7.67 (2H, s), 7.07 (2H, d, J = 8.8 Hz), 3.84 (3H, s). ^{13}C NMR (100 MHz, C_2D_6SO): δ 165.78, 162.82, 149.21, 130.50 (2C), 130.37 (2C), 124.55 (2C), 123.26, 116.10 (2C), 113.86 (2C), 55.54. HRMS (ESI$^+$) *m/z* calcd. for $C_{15}H_{12}N_3O_2Cl_2$ [M + H]$^+$, 336.0301, found, 336.0301.

N-*(5-Methyl-1*H*-benzimidazol-2-yl)-2-(3-nitrophenyl)acetamide* **47**

A white solid, yield: 72%, mp: 233–234 °C (methanol). IR (KBr): ν_{max} 3352, 2920, 1690 (NHCO), 1648 (CN), 1605, 1524, 1482, 1350, 1192, 1034, 797, 718 cm^{-1}. ^{1}H NMR (400 MHz, C_2D_6SO): δ 12.03 (2H, brs, NH + NHCO), 8.45 (1H, brs, H-2′), 8.29 (1H, d, J = 7.9 Hz, H-4′), 7.96 (1H, d, J = 7.7 Hz, H-6′), 7.79 (1H, dd, J_1 = 7.9; J_2 =7.7 Hz, H-5′), 7.43 (1H, d, J = 8.0 Hz, H-7), 7.36 (1H, brs, H-4), 7.03 (1H, brd, J = 8.0 Hz, H-6), 4.10 (2H, s, CH_2), 2.49 (3H, s, CH_3). ^{13}C NMR (100 MHz, C_2D_6SO): δ 169.59 (NHCO), 147.69 (C-3′), 146.23 (C-2), 140.50 (C-3a), 138.90 (C-7a), 137.38 (C-1′), 136.38 (C-6′), 130.06 (C-5), 129.84 (C-5′), 124.22 (C-2′), 122.40 (C-6), 121.91 (C-4′), 117.21 (C-4), 111.21 (C-7), 41.47 (CH_2), 21.34 (CH_3). HRMS (ESI$^+$) *m/z* calcd. for $C_{16}H_{15}N_4O_3$ [M + H]$^+$, 311.1139, found, 311.1134.

*2-Hydroxy-*N*-(5-methyl-1*H*-benzimidazol-2-yl)-2-phenylacetamide* **48**

A light yellow solid, yield: 17%, mp: 243–244 °C ($CHCl_3$/methanol). IR (KBr): ν_{max} 3368, 3212, 2922, 1686, 1620, 1575, 1450, 1212, 1067, 810, 694 cm^{-1}. ^{1}H NMR (400 MHz, $CDCl_3$): δ 7.42 (2H, d, J = 6.4 Hz, H-2′ + 6′), 7.21 (3H, m, H-3′ + 4′ + 5′), 7.14 (1H, d, J = 8.0 Hz, H-7), 7.05 (1H, s, H-4), 6.91 (1H, d, J = 8.0 Hz, H-6), 5.29 (1H, s, H-α), 2.31 (3H, s, CH_3). ^{13}C NMR (100 MHz, $CDCl_3$): δ 174.32 (NHCO), 146.88 (C-2), 138.20 (C-3a), 134.50 (C-7a), 132.72 (C-5), 128.87 (C-1′), 128.71 (C-3′ + 5′), 128.65 (C-4′), 126.65 (C-2′ + 6′), 124.15 (C-6), 112.30 (C-4), 110.20 (C-7), 75.12 (CH-α), 21.53 (CH_3). HRMS (ESI$^+$) *m/z* calcd. for $C_{16}H_{16}N_3O_2$ [M + H]$^+$, 282.1237, found, 282.1242.

N-*(5-Methyl-1*H*-benzimidazol-2-yl)-2-(naphthalen-2-yl)acetamide* **49**

A light yellow solid, yield: 32%, mp: 245–246 °C (methanol). IR (KBr): ν_{max} 3359, 2924, 1680 (NHCO), 1645, 1598, 1482, 1433, 1220, 810, 794, 739, 670 cm^{-1}. ^{1}H NMR (400 MHz, C_2D_6SO): δ 11.90 (1H, brs, NH), 11.78 (1H, brs, NHCO), 7.92 (1H, brd, J = 8.8 Hz, H-5′), 7.88 (1H, brd, J = 8.6 Hz, H-8′), 7.81 (1H, d, J = 7.6 Hz, H-4′), 7.69 (1H, d, J = 1.6 Hz, H-1′), 7.46 (1H, m, H-6′), 7.44 (1H, m, H-7′), 7.39 (1H, dd, J_1 = 7.6; J_2 = 1.6 Hz, H-3′), 7.32 (1H, d, J = 8.4 Hz, H-7), 7.25 (1H, d, J = 1.6 Hz, H-4), 6.89 (1H, dd, J_1 = 8.4; J_2 = 1.6 Hz, H-6), 3.92 (2H, s, CH_2), 2.33 (3H, s, CH_3). ^{13}C NMR (100 MHz, C_2D_6SO): δ 171.99 (NHCO), 146.18 (C-2), 141.20 (C-3a), 140.39 (C-3′), 138.60 (C-7a), 134.91 (C-2′), 133.47 (C-8′a), 132.96 (C-5), 132.66 (C-4′a), 128.73 (C-5′), 127.74 (C-8′), 127.62 (C-4′), 126.40 (C-1′), 126.16 (C-7′), 125.03 (C-6′), 117.10 (C-6), 111.30 (C-4), 111.10 (C-7), 42.42 (CH_2), 21.35 (CH_3). HRMS (ESI$^+$) *m/z* calcd. for $C_{20}H_{18}N_3O$ [M + H]$^+$, 316.1444, found, 316.1440.

N-*(5-Methyl-1*H*-benzimidazol-2-yl)thiophene-2-acetamide* **50**

A white solid, yield: 47%, mp: 230–231 °C ($CHCl_3$/methanol). ^{1}H NMR (400 MHz, $CDCl_3$): δ 7.33 (1H, d, J = 4.8 Hz), 7.32 (1H, d, J = 8.0 Hz), 7.24 (1H, d, J = 1.2 Hz), 7.15 (1H, d, J_1 = 6.5; J_2 = 4.8 Hz), 7.06 (1H, d, J = 6.5 Hz), 7.04 (1H, dd, J_1 = 8.0; J_2 = 1.2 Hz), 3.94 (2H, s), 2.44 (3H, s). ^{13}C NMR (100 MHz, $CDCl_3$): δ 171.36, 147.58, 138.10, 133.12, 132.43, 130.10, 128.25, 126.42, 123.45, 110.00, 108.10, 107.10, 38.15, 21.62. HRMS (ESI$^+$) *m/z* calcd. for $C_{14}H_{14}N_3OS$ [M + H]$^+$, 272.0852, found, 272.0860.

*3-Chlorophenyl-*N*-(5,6-dimethyl-1*H*-benzimidazol-2-yl)acetamide* **51**

A light brown solid, yield: 42%, mp: 264–265 °C (methanol). ^{1}H NMR (400 MHz, C_2D_6SO): δ 11.78 (2H, brs), 7.43 (1H, brs), 7.35 (1H, dd, J_1 = 8.0; J_2 = 7.8 Hz), 7.32 (1H, dd, J_1 = 8.0; J_2 = 1.6 Hz), 7.29 (1H, dd, J_1 = 7.8; J_2 = 1.6 Hz), 7.17 (2H, s), 3.75 (2H, s), 2.23 (6H, s). ^{13}C NMR (100 MHz, C_2D_6SO): δ 169.72, 145.77, 138.10 (2C),

137.66, 132.85, 130.17, 129.18, 129.10 (2C), 128.02, 126.75, 111.83 (2C), 41.72, 19.91 (2C). HRMS (ESI$^+$) *m/z* calcd. for $C_{17}H_{17}N_3OCl$ $[M + H]^+$, 314.1055, found, 314.1045.

N-*(5,6-Dichloro-1H-benzimidazol-2-yl)-2-(3-nitrophenyl)acetamide* **52**

A orange solid, yield: 68%, mp: 287–289 °C (methanol). IR (KBr): ν_{max} 3327, 2924, 1690, 1637, 1581, 1526, 1453, 1349, 1297, 1124, 1040, 854, 810, 790, 672, 659 cm^{-1}. ^1H NMR (400 MHz, C_2D_6SO): δ 12.31 (1H, brs, NH), 12.05 (1H, brs, NHCO), 8.13 (1H, dd, $J_1 = 7.6$; $J_2 = 2.0$; $J_3 = 1.8$ Hz, H-4′), 7.79 (1H, dd, $J_1 = 8.0$; $J_2 = 7.6$ Hz, H-5′), 7.65 (1H, ddd, $J_1 = 8.0$; $J_2 = 2.2$; $J_3 = 2.0$ Hz, H-6′), 7.61 (1H, dd, $J_1 = 2.2$; $J_2 = 1.8$ Hz, H-2′), 7.56 (2H, s, 4 + H-7), 3.98 (2H, s, CH_2). ^{13}C NMR (100 MHz, C_2D_6SO): δ 170.30 (NHCO), 148.77 (C-3′), 148.12 (C-2), 140.95 (C-3a + 7a), 136.77 (C-6′), 132.74 (C-1′), 130.21 (C-5′), 124.68 (C-2′), 123.97 (C-6), 123.21 (C-5), 122.34 (C-4′), 118.58 (C-4), 113.12 (C-7), 41.78 (CH_2). HRMS (ESI$^+$) *m/z* calcd. for $C_{15}H_{10}N_4O_3Cl_2$ $[M + H]^+$, 365.0208, found, 365.0015.

Tert-*butyl(1-((5-methoxy-1H-benzimidazol-2-yl)amino)-1-oxododecan-2-yl-carbamate* **54**

A yellow solid, yield: 62%, mp: 113–114 °C ($CHCl_3$/methanol). IR (KBr): ν_{max} 3347, 2919, 2850, 1683, 1642, 1596, 1483, 1462, 1229, 1200, 1029, 857, 787 cm^{-1}. ^1H NMR (400 MHz, $CDCl_3$): δ 7.12 (1H, brs, H-4), 6.86 (1H, brd, $J = 8.0$ Hz, H-6), 6.11 (1H, d, $J = 8.0$ Hz, H-7), 4.68 (1H, m, H-α), 3.82 (3H, s, OCH_3), 1.75 (2H, m), 1.74 (2H, m), 1.45 (9H, s, $(CH_3)_3$), 1.23 (14H, m), 0.84 (3H, t, $J = 6.8$ Hz, CH_3). ^{13}C NMR (100 MHz, $CDCl_3$): δ 174.13 (CONH), 155.68 (5-C), 156.09 (OCOC$(CH_3)_3$), 146.87 (C-2), 133.21 (C-3a), 130.00 (C-7a), 111.40 (C-6), 111.27 (C-7), 95.64 (C-4), 79.64 (OCOC$(CH_3)_3$), 55.65 (OCH_3), 54.99 (CH- α), 31.95, 31.78, 29.61, 29.46, 29.38, 29.33, 29.20, 28.25 (OCOC$(CH_3)_3$), 22.58, 22.40, 14.03 (CH_3). HRMS (ESI$^+$) *m/z* calcd. for $C_{25}H_{41}N_4O_4$ $[M + H]^+$, 461.3122, found, 461.3122.

4.1.2.10. Obtaining BZ 53 by reduction of the nitrobenzimidazole 52. The same protocol than that indicated in 4.1.2.2 was applied. To a solution of BZ **52** (40 mg, 0.109 mmol) in MeOH (3 mL) placed in a two-necked round bottom flask, Pd-C catalyst (3 mg) was added. The air was removed, and a balloon with H_2 was placed to one of the necks. The mixture was kept at room temperature and under magnetic stirring for 2 h. Then, the Pd-C was removed by filtration through Celite, and the residue was washed with MeOH. The solvent was removed in vacuum in a rotary evaporator to provide a solid that was purified by crystallisation in methanol, 14 mg, 39% yield.

*2-(3-Aminophenyl)-*N*-(5,6-dichloro-1H-benzimidazol-2-yl)acetamide* **53**

A light yellow solid, mp: 298–299 °C. IR (KBr): ν_{max} 3420, 3327, 2924, 1695, 1637, 1581, 1526, 1408, 1349, 1297, 1124, 854, 790, 730 cm^{-1}. ^1H NMR (400 MHz, CD $_3$OD): δ 7.59 (2H, s, H-4 + 7), 7.06 (1H, dd, $J_1 = 8.0$; $J_2 = 7.6$ Hz, H-5′), 6.72 (1H, brs, H-2′), 6.69 (1H, d, $J = 7.6$ Hz, H-6′), 6.63 (1H, brd, $J = 8.0$ Hz, H-4′), 3.68 (2H, s, CH_2). ^{13}C NMR (100 MHz, CD $_3$OD): δ 173.06 (NHCO), 150.01 (C-3′), 149.17 (C-2), 141.20 (C-3a + 7a), 136.38 (C-1′), 130.40 (C-5′), 126.80 (C-5 + 6), 119.91 (C-6′), 117.16 (C-2′), 115.45 (C-4′), 113.76 (C-4 + 7), 43.97 (CH_2). HRMS (ESI$^+$) *m/z* calcd. for $C_{15}H_{13}N_4OCl$ $[M + H]^+$, 335.0466, found, 335.0457.

4.1.2.11. Obtaining BZ 55 by deprotection of the Boc group in 54. 100 mg (0.217 mmol) of compound **54** were dissolved in CH_2Cl_2 (3 mL) and kept at 0 °C under stirring. Then, trifluoroacetic acid (1.0 mL) was added. The reaction was monitored every 15 min. by TLC *n*-hexane/ethyl acetate (4:6) using as eluent. After completion of the reaction, it was extracted with CH_2Cl_2, washed with water and the organic layer over anhydrous sodium sulphate. The solvent was removed under vacuo to provide a crude mixture that was purified by column chromatography with *n*-hexane/ethyl acetate (4:6) as eluent to provide BZ **55** 27 mg in 35% yield.

N-*(5-methoxy)-1H-benzimidazol-2-yl)-2-aminododecanamide* **55**

A white solid, yield: 27%, mp: 105–106 °C ($CHCl_3$/methanol). ^1H NMR (400 MHz, $CDCl_3$): δ 7.42 (1H, brs), 7.13 (1H, d, $J = 8.8$ Hz), 6.85 (1H, brd, $J = 8.8$ Hz), 5.92 (1H, d, $J = 9.2$ Hz, NHCO), 4.69 (1H, m, CH- α), 4.62 (2H, brs, NH_2), 3.82 (3H, s), 1.79 (2H, m), 1.65 (2H, m), 1.42 (2H, m), 1.21 (6H, m), 0.84 (3H, t, $J = 6.8$ Hz). ^{13}C NMR (100 MHz, $CDCl_3$): δ 176.54, 157.17, 143.70, 133.07, 129.60, 112.63, 111.99, 96.30, 61.83, 56.19, 35.06, 32.90. 30.72, 30.46, 30.37, 30.35, 30.31, 26.73, 23.68, 15.12. HRMS (ESI$^+$) *m/z* calcd. for $C_{20}H_{33}N_4O_2$ $[M + H]^+$, 361.2598, found, 361.2603.

4.1.3. Molecular docking

T. circumcinta β-tubulin obtained by homology modelling used as a target for docking studies was the same as has been described in a previous work.[8] Docking calculations were performed using GLIDE integrated into the Schrödinger Molecular Modelling Suite (Schrödinger, Inc., USA, 2016.4) according the methodology reported in the work; with the only difference of allowing the free rotation of the hydroxyl and sulfanyl groups of the colchicine site during the grid generation.

4.2. Biological assays

More than fifty BZs derivatives were screened *in vitro* to prove their effects on eggs and third-stage larvae (L3) of *T. circumcincta* by means of the Egg Hatch Assay (EHA) and the Larval Migration Inhibition Assay (LMIA), respectively. Cytotoxicity assays were also performed on Caco-2 and HepG2 cells in order to calculate the selectivity index (SI) of each compound.

4.2.1. Animals

Two animals were used to obtain the necessary material to carry out the *in vitro* experiments. Two months-old Merino lambs were infected with 20,000 L3 of *T. circumcincta.* All protocols carried out were performed according to current national and European regulations of animal wellbeing (R.D 53/2013 and EU Directive 2010/63/EU) at the facilities of the Instituto de Ganadería de Montaña (IGM, CSIC, León, Spain).

4.2.2. Egg hatch assay (EHA)

The eggs were extracted from fresh faecal material of infected animals by sieving, centrifugation and flotation in a solution of saturated sodium-chloride. Each compound was first tested in a susceptible strain of the GIN at concentration of 50 µM in order to select those with activities higher than 97%. Then, their half maximal effective concentration (EC_{50}) was calculated using eight serial dilutions (1:2) ranging from 50 to 0.39 µM. Thiabendazole at 0.49 µM (equivalent to 0.1 µg/mL; the known cut-off value used to classify field susceptible and resistant strains according to Coles et al. [36] was used as positive control and DMSO at 0.5% as negative. The EHA was performed using a similar protocol described by Coles et al. [36] Briefly, each compound was incubated with fresh eggs in 24-well culture plates for 48 h at 23 °C. The concentration of eggs per well was 150 in a final volume of 2 mL. All compounds were tested in duplicate during three different days to ensure the accuracy of results. After 48 h of incubation, all eggs and larvae present in each well were counted and the ovicidal activity was estimated by following the formulas:

% Egg hatching per well

$$= (\text{number of L1/number of L1 larvae and eggs}) \times 100.$$

% Ovicidal activity

$$= [100 - (\%\ \text{Egg hatching per well}/\%\ \text{Egg hatching in control well})] \times 100.$$

Dose-response curves were fitted by nonlinear regression using the computer program Sigma Plot V 10.0 (Systat Software, Inc., San José, California; USA). The EC_{50} values and R^2 values were calculated. The results were expressed as the mean of the EC_{50} and the standard error of the mean (SEM).

4.2.3. Larval migration inhibition assay

Infective L3 obtained from coprocultures were used to carry out the LMIA. For this, fresh faeces from infected lambs were cultured in small closed boxes aerated and humidified twice a week and placed in a climatic chamber at 25 °C for ten days to allow the hatching of eggs and the development of the larvae to the infective stage. Then, the larvae were stored in ventilated cell culture flasks at 6–10 °C in a fridge for a maximum period of three months.

The assay was performed similarly to the method described previously by Demeler et al.[37] and the procedure followed was the same as for the EHA. Firstly, an initial screening of all compounds at 50 µM was performed. Briefly, L3 were incubated with the different compounds for 24 hours in the dark at 28 °C in 48-well culture plates. Then, the content of the wells was transferred to a 96-wells MultiScreen-Mesh Filter Plate (Sigma-Aldrich) and left for a further 24 h period to allow the motile L3 to pass through the sieves for counting. 0.5% DMSO was used as negative control in each assay.

The efficacy of the compound was expressed as the larval migration inhibition following the formula:

% Larval migration inhibition = [(number of larvae migrating through sieves in negative controls wells – number of larvae migrating through sieves in treatment wells) / number of larvae migrating through sieves in negative controls wells.] x 100.

4.3. Cytotoxicity assay

Those compounds with activities higher than 95% at a 50 µM concentration in the initial screening were selected to carry out cytotoxicity assays on two human cell lines: the human colorectal adenocarcinoma Caco-2 (ATCC® HTB-37™) and the human hepatocarcinoma HepG2 (ATCC® HB-8065™), to assess the toxicity on a cell line of intestinal origin and to assess the systemic toxicity of the compounds, respectively.

Briefly, 10,000 cells were seeded on 96 well-plates containing RPMI 1640 Medium supplemented with 2.0 g/L sodium bicarbonate (Fisher Scientific®), 1% (w/v) L-glutamine (Sigma-Aldrich®) and 25 mM HEPES buffer, pH 7.6, 10% (v/v) inactivated foetal bovine serum and antibiotic cocktail containing 100 U/mL penicillin, and 100 mg/mL streptomycin. Cultures were incubated at 37 °C in a humidified atmosphere containing 5% CO_2. After 24 h, different concentrations of testing compounds (ranging 1 to 100 µM) were added for a period of 72 h. After this time, the viability of the cells was assessed using the Alamar Blue (Thermo Fisher) staining method according to manufacturer's recommendations.

Cell viability expressed as the fluorescence emitted by resorufin at 590 nm was plotted against the corresponding concentration added to cell culture and fitted using the software package for scientific data analysis SigmaPlot 10.0 with the aim to estimate the half cytotoxic concentration (CC_{50}) of each compound. As an estimation of the safety of each compound, selectivity index (SI) with respect to HepG2 cells was calculated by dividing CC_{50} by EC_{50}.

Supporting information

^1H, ^{13}C NMR and HRMS spectra of relevant compounds. Additional results of docking studies. Physicochemical Drug-Likeness and Toxicity risks for selected BZs.

Declaration of Competing Interest

The authors declare that they have no known competing financial interests or personal relationships that could have appeared to influence the work reported in this paper.

Data availability

Data will be made available on request.

Acknowledgements

Financial support came from MINECO: RETOS (AGL2016-79813-C2-1R/2R) and Junta de Castilla y León co-financed by FEDER, UE [LE020P17]. EVG was funded by FPU17/00627; VCGA and MAB are recipients of Junta de Castilla y Leon (JCyL) (LE082-18, LE051-18, respectively) and MMV by the Spanish "Ramon y Cajal" Programme (Ministerio de Economía y competitividad; MMV, RYC-2015-18368).

Supplementary materials

Supplementary material associated with this article can be found, in the online version, at doi:10.1016/j.molstruc.2022.133735.

References

[1] R.L. Pullan, J.L. Smith, R. Jasrasaria, S.J. Brooker, Global numbers of infection and disease burden of soil transmitted helminth infections in 2010, Parasites Vectors 7 (2014) 1–19, doi:10.1186/1756-3305-7-37.
[2] T.M. Craig, Gastrointestinal nematodes, diagnosis and control, Vet. Clin. North Am. Food Anim. Pract. 34 (2018) 185–199, doi:10.1016/j.cvfa.2017.10.008.
[3] F. Jackson, R.L. Coop, The development of anthelmintic resistance in sheep nematodes, Parasitology (2000) 120, doi:10.1017/s0031182099005740.
[4] E. Papadopoulos, E. Gallidis, S. Ptochos, Anthelmintic resistance in sheep in Europe: a selected review, Vet. Parasitol. 189 (2012) 85–88, doi:10.1016/j.vetpar.2012.03.036.
[5] M. Martínez-Valladares, T. Geurden, D.J. Bartram, J.M. Martínez-Pérez, D. Robles-Pérez, A. Bohórquez, E. Florez, A. Meana, F.A. Rojo-Vázquez, Resistance of gastrointestinal nematodes to the most commonly used anthelmintics in sheep, cattle and horses in Spain, Vet. Parasitol. 211 (3–4) (2015) 228–233.
[6] M. Zajíčková, L.T. Nguyen, L. Skálová, L. Raisová Stuchlíková, P. Matoušková, Anthelmintics in the future: current trends in the discovery and development of new drugs against gastrointestinal nematodes, Drug Discov. Today (2020), doi:10.1016/j.drudis.2019.12.007.
[7] E.L. Gutiérrez, M.S. Souza, L.F. Diniz, J. Ellena, Synthesis, characterization and solubility of a new anthelmintic salt: mebendazole nitrate, J. Mol. Struct. 1161 (2018) 113–121, doi:10.1016/j.molstruc.2018.02.060.
[8] N. Escala, E. Valderas-García, M.Á. Bardón, V.C. Gómez de Agüero, R. Escarcena, J.L. López-Pérez, F.A. Rojo-Vázquez, A. San Feliciano, R. Balaña-Fouce, M. Martínez-Valladares, E. Olmo, Synthesis, bioevaluation and docking studies of some 2-phenyl-1*H*-benzimidazole derivatives as anthelminthic agents against the nematode *Teladorsagia circumcincta*, Eur. J. Med. Chem. 208 (2020) 112554, doi:10.1016/j.ejmech.2020.112554.
[9] M. Abongwa, R.J. Martin, A.P. Robertson, A brief review on the mode of action of antinematodal drugs, Acta Vet 67 (2017) 137e152, doi:10.1515/acve-2017-0013.
[10] Spartan20. Wavefunction, Inc. 18401 Von Karman Ave., Suite 435. Irvine, CA 92612. https://www.wavefun.com/.
[11] U.S. Sørensen, D. Strøbæk, P. Christophersen, C. Hougaard, M.L. Jensen, E.Ø. Nielsen, D. Peters, L. Teuber, Synthesis and structure−activity relationship studies of 2-(*N*-Substituted)-aminobenzimidazoles as potent negative gating modulators of small conductance Ca^{2+}-activated K^+ channels, J. Med. Chem. 51 (23) (2008) 7625–7634, doi:10.1021/jm800809f12.
[12] J. Ha Lee, M. Hyun An, E. Hyun Choi, H.Y. Park Choo, G. Han, a facile synthesis of 2-acyl and 2-alkylaminobenzimidazoles for 5-lipoxygenase Inhibitors, Heterocycles 70 (1) (2006) 571, doi:10.3987/com-06-s(w)25.
[13] T.C. Kühler, M. Swanson, B. Christenson, A.C. Klintenberg, B. Lamm, J. Fägerhag, R. Gatti, M. Ölwegard-Halvarsson, V. Shcherbuchin, T. Elebring, J.E. Sjöström, Novel structures derived from 2-[[(2-Pyridyl)methyl]thio]-1*H*-benzimidazole as anti-*Helicobacter pylori* agents, Part 1, J. Med. Chem. 45 (19) (2002) 4282–4299, doi:10.1021/jm0208673.
[14] NF. Abdel-Ghaffar, Synthesis, reactions, structure-activity relationship of 2-benzimidazole analogs as anticancer agents and study their molecular docking, Pharm. Chem. 5 (5) (2013) 243–257.
[15] W. Nawrocka, B. Sztuba, M.W. Kowalska, H. Liszkiewicz, J. Wietrzyk, A. Nasulewicz, M. Pelczyńska, A. Opolski, Synthesis and antiproliferative activity *in vitro* of 2-aminobenzimidazole derivatives, Farm. Sci. 59 (2) (2004) 83–91, doi:10.1016/j.farmac.2003.12.001.

[16] V.S. Pilyugin, Y.E. Sapozhnikov, N.A. Sapozhnikova, Acyl derivatives of 2-aminobenzimidazole and their fungicide activity, Russ. J. Gen. Chem. 74 (5) (2004) 738–743, doi:10.1023/b:rugc.0000039088.870.
[17] V.S. Pilyugin, Y.E. Sapozhnikov, A.M. Davydov, G.E. Chikisheva, T.P. Vorob'eva, E.V. Klimakova, G.V. Kiseleva, S.L. Kuznetsova, R.D. Davletov, N.A. Sapozhnikova, R.K. Yumadilov, 13C NMR spectra and biological activity of *N*-(1*H*-benzimidazol-2-yl)benzamides, Russ. J. Gen. Chem. 76 (10) (2006) 1653–1659, doi:10.1134/s1070363206100264.
[18] R.D. Davletov, G.E. Chikisheva, R.N. Galiakhmetov, Search for environmentally less harmful fungicides in a series of benzimidazole derivatives, Bašk. Him. Ž. 17 (2) (2010) 28–32.
[19] G.E. Chikisheva, Y.E. Sapozhnikov, R.K. Mudarisova, L.I. Buslaeva, Z.B. Galieva, R.D. Davletov, Synthesis and fungicidal activity of 2-benzoylaminobenzimidazole complex compounds with copper, Russ. J. Appl. Chem. 86 (2) (2013) 285–288, doi:10.1134/s10704272130226220.
[20] K.L. Obydennov, T.A. Kalinina, N.A. Galieva, T.V. Beryozkina, Y. Zhang, Z. Fan, T.V. Glukhareva, V.A. Bakulev, Synthesis, fungicidal activity and molecular docking of 2-acylamino and 2-thioacylamino derivatives of 1*H*-benzo[*d*]imidazoles as anti-tubulin agents, J. Agric. Food Chem. 69 (40) (2021) 12048–12062, doi:10.1021/acs.jafc.1c03325.
[21] F. Odame, R. Betz, E.C. Hosten, J. Krause, M. Isaacs, H.C. Hoppe, S.D. Khanye, Y. Sayed, C. Frost, K.A. Lobb, Z.R. Tshentú, A new synthetic method for tetraaza-tricyclic derivatives and evaluation of their biological properties, ChemistrySelect 3 (48) (2018) 13613–13618, doi:10.1002/slct.20180293022.
[22] K. Garg, Y. Bansal, G. Bansal, R.K. Goel, Design, synthesis, and PASS-assisted evaluation of novel 2-substituted benzimidazole derivatives as potent anthelmintics, Med. Chem. Res. 23 (2014) 2690–2697, doi:10.1007/s00044-013-0856-1.
[23] K. Ding, A. Wang, M.A. Boerneke, S.M. Dibrov, T. Hermann, Aryl-substituted aminobenzimidazoles targeting the hepatitis C virus internal ribosome entry site, Bioorg. Med. Chem. Lett. 24 (14) (2014) 3113–3117, doi:10.1016/j.bmcl.2014.05.009.
[24] X. He, S.K. Lakkaraju, M. Hanscom, Z. Zhao, J. Wu, B. Stoica, A.D. MacKerell, A.I. Faden, F. Xue, Acyl-2-aminobenzimidazoles: a novel class of neuroprotective agents targeting mGluR5, Bioorg. Med. Chem. 23 (9) (2015) 2211–2220, doi:10.1016/j.bmc.2015.02.05425.
[25] J.P. Powers, S. Li, J.C. Jaen, J. Liu, N.P.C. Walker, Z. Wang, H. Wesche, Discovery and initial SAR of inhibitors of interleukin-1 receptor-associated kinase-4, Bioorg. Med. Chem. Lett. 16 (11) (2006) 2842–2845, doi:10.1016/j.bmcl.2006.03.020.
[26] K. Starcevic, I. Caleta, D. Cincic, B. Kaitner, M. Kralj, K. Ester, G. Karminski-Zamola, Synthesis, crystal structure determination, and antiproliferative evaluation of novel benzazolyl benzamides, Heterocycles 68 (11) (2006) 2285–2299, doi:10.3987/COM-06-10844.
[27] E. Valderas-García, J. de la Vega, M.Á. Bardón, V.C.G. de Agüero, R. Escarcena, J.L. López-Pérez, F.A. Rojo-Vázquez, A. San Feliciano, E. del Olmo, R. Balaña-Fouce, M. Martínez-Valladares, Anthelmintic activity of aminoalcohol and diamine derivatives against the gastrointestinal nematode *Teladorsagia circumcincta*, Vet. Parasitol. 296 (2021) 109496, doi:10.1016/j.vetpar.2021.109496.
[28] Y. Bansal, M. Kaur, O. Silakari, Benzimidazole–ibuprofen/mesalamine conjugates: potential candidates for multifactorial diseases, Eur. J. Med. Chem. 89 (2015) 671–682, doi:10.1016/j.ejmech.2014.10.081.
[29] K.S. Tikhomirova, I.E. Tolpygin, A.B. Starikov, M.A. Kaz'mina, New fluorogenic chemosensors derived from benzimidazole, Chem. Heterocycl. Compd. 53 (2017) 179–185, doi:10.1007/s10593-017-2037-5.
[30] E.R. Morgan, J. van Dijk, Climate and the epidemiology of gastrointestinal nematode infections of sheep in Europe, Vet. Parasitol. 189 (2012) 8–14, doi:10.1016/J.VETPAR.2012.03.028.
[31] P.J. Dawson, W.E. Gutteridge, K. Keith Gull, A comparison of the interaction of anthelmintic benzimidazoles with tubulin isolated from mammalian tissue and the parasitic nematode *Ascaridia galli*, Biochem. Pharmacol. 33 (7) (1984) 1069–1074.
[32] M.M. Barrowman, S.E. Marriner, J.A. Bogan, The binding and subsequent inhibition of tubulin polymerization in *Ascaris suum (in vitro)* by benzimidazole anthelmintics, Biochem. Pharmacol. 33 (19) (1984) 3037–3040.
[33] Y. Zhou, J. Xu, Y. Zhu, Y. Duan, M. Zhou, Mechanism of action of the benzimidazole fungicide on *Fusarium graminearum*: interfering with polymerization of monomeric tubulin but not polymerized Microtubule, Phytopathology 106 (8) (2016) 807–813 2016 Aug, doi:10.1094/PHYTO-08-15-0186-R.
[34] J.W. Tracy, L.T. Webster, Drugs used in the chemotherapy of helminthiasis, in: J.G. Hardman, L.E. Limbind, A.G. Gilman (Eds.), Goodman and Gilman's the Pharmacological Basis of Therapeutics, l0th ed, E-McGraw-Hill, 2001, pp. 1134–1136.
[35] W.L.F. Armarego, D.D. Perrin, Purification of Laboratory Chemicals, 4th ed, Butterworth-Heinemann, 1997.
[36] G.C. Coles, F. Jackson, W.E. Pomroy, R.K. Prichard, G. Von Samson-Himmelstjerna, A. Silvestre, M.A. Taylor, J. Vercruysse, The detection of anthelmintic resistance in nematodes of veterinary importance, Vet. Parasitol. 136 (2006) 167–185, doi:10.1016/j.vetpar.2005.11.019.
[37] J. Demeler, U. Küttler, G. von Samson-Himmelstjerna, Adaptation and evaluation of three different *in vitro* tests for the detection of resistance to anthelmintics in gastrointestinal nematodes of cattle, Vet. Parasitol. 170 (2010) 61–70, doi:10.1016/J.VETPAR.2010.01.032.

III.4. ARTÍCULO 4

Este artículo está relacionado con el objetivo 5 del Trabajo de Tesis. Esta publicación no computa dentro de los 3 artículos requeridos para la defensa de tesis en modalidad de artículos.

A partir de los resultados in vitro frente a *Teladorsagia circumcincta* de los Bzs de tipo I, II y III, se seleccionó el compuesto Bz.xxxx para su ensayo in vivo en corderos. Para ello hubo que sintetizar 25 gramos de compuesto, lo que fue necesario hacer en el escalado del proceso de síntesis.

Novel compound shows in vivo anthelmintic activity in gerbils and sheep infected by *Haemonchus contortus*

Elora Valderas-García, Nerea Escala, María Álvarez-Bardón, Verónica Castilla-Gómez de Agüero, Maria Cambra-Pellejà, Laura González del Palacio, Raquel Vallejo García, Jennifer de la Vega, Arturo San Feliciano, Esther del Olmo, María Martínez-Valladares, Rafael Balaña-Fouce

En: *Scientific Reports* 2022, 12, 13004; doi: 10.1038/s41598-022-17112-3

Factor de Impacto: 4,997
Quartil: Q1

scientific reports

Check for updates

OPEN

Novel compound shows in vivo anthelmintic activity in gerbils and sheep infected by *Haemonchus contortus*

Elora Valderas-García[1,2,5], Nerea Escala[3,5], María Álvarez-Bardón[2], Verónica Castilla-Gómez de Agüero[1,4], Maria Cambra-Pellejà[1,4], Laura González del Palacio[1,4], Raquel Vallejo García[4], Jennifer de la Vega[3], Arturo San Feliciano[3], Esther del Olmo[3], María Martínez-Valladares[1,4]✉ & Rafael Balaña-Fouce[2]✉

The control of gastrointestinal nematodes in livestock is becoming increasingly difficult due to the limited number of available drugs and the rapid development of anthelmintic resistance. Therefore, it is imperative to develop new anthelmintics that are effective against nematodes. Under this context, we tested the potential toxicity of three compounds in mice and their potential anthelmintic efficacy in Mongolian gerbils infected with *Haemonchus contortus*. The compounds were selected from previous in vitro experiments: two diamine (AAD-1 and AAD-2) and one benzimidazole (2aBZ) derivatives. 2aBZ was also selected to test its efficacy in sheep. In Mongolian gerbils, the benzimidazole reduced the percentage of pre-adults present in the stomach of gerbils by 95% at a dose of 200 mg/kg. In sheep, there was a 99% reduction in the number of eggs shed in faeces after 7 days at a dose of 120 mg/kg and a 95% reduction in the number of worm adults present in the abomasum. In conclusion, 2aBZ could be considered a promising candidate for the treatment of helminth infections in small ruminants.

Gastrointestinal parasitism, especially caused by helminth species, is a major constraint in livestock production systems. These infections impair animal health seriously causing reductions in weight, meat and milk production and fertility[1]. One of the most important species, not only because of its global distribution but also because of its pathogenic potential, is *Haemonchus contortus*[2]. This abomasum parasite has a blood-feeding behavior that causes anemia and can lead to death in heavily infected animals[1,3]. In Europe, annual economic losses produced by helminth infections can reach 357 million euros in sheep and 1.8 billion euros in livestock in general[4]. Globally, these losses have been estimated at approximately 10 billion euros per year[5]. Currently, anthelmintics applied in the veterinary field basically include benzimidazoles, imidazothiazoles and macrocyclic lactones[6]. Their good therapeutic profiles including broad-spectrum of action, good tolerability and low costs are in part responsible for their excessive use for a long time. This has led to the development of varying degrees of drug resistance among nematodes for all groups of anthelmintics compromising their efficacy and control[7–11]. Therefore, the introduction of new drugs is urgently required to overcome the resistance to the current marketed drugs. However, despite this urgent need for innovation, their development is very slow since only three new compounds have been approved as anthelmintics in the last 20 years: emodepside[12], monepantel[13] and derquantel[14]. One of the main reasons is that drug discovery requires large sources of investment and funding[15].

The objective of the current experiment was to assess the tolerance and the in vivo anthelmintic potential of three novel synthetic compounds identified in a previous phenotypic platform against the gastrointestinal nematode infecting sheep *Teladorsagia circumcincta*. One benzimidazole and two diamine derivatives were selected from a total of 220 compounds based on their in vitro ovicide and larvicide activity but also their high selective

[1]Instituto de Ganadería de Montaña, CSIC-Universidad de León, 24346 Grulleros, León, Spain. [2]Departamento de Ciencias Biomédicas, Facultad de Veterinaria, Universidad de León, 24071 León, Spain. [3]Departamento de Ciencias Farmacéuticas: Química Farmacéutica, Facultad de Farmacia, Universidad de Salamanca, CIETUS, IBSAL, 37007 Salamanca, Spain. [4]Departamento de Sanidad Animal, Facultad de Veterinaria, Universidad de León, 24071 León, Spain. [5]These authors contributed equally: Elora Valderas-García and Nerea Escala. ✉email: mmarva@unileon.es; rbalf@unileon.es

III.5. ARTÍCULO 5

Este artículo está relacionado con el objetivo 6 del Trabajo de Tesis. Esta publicación no computa dentro de los 3 artículos requeridos para la defensa de tesis en modalidad de artículos.

Algunos de los Bzs de tipo I obtenidos fueron ensayados en otras especies de nematodos gastrointestinales, concretamente en *Trichuris muris y Heligmosomoides polygyrus.*

Benzimidazole and aminoalcohol derivatives show in vitro anthelmintic activity against *Trichuris muris* and *Heligmosomoides polygyrus*

Elora Valderas-García, Cécile Häberli, María Álvarez-Bardón, Nerea Escala, Verónica Castilla-Gómez de Agüero, Jennifer de la Vega, Esther Del Olmo, Rafael Balaña-Fouce, Jennifer Keiser, María Martínez-Valladares

En: *Parasites & Vectors* 2022, 15, 1; doi: 10.21203/rs.3.rs-1250014/v2

Factor de Impacto: 4,052
Quartil: Q1

Valderas-García *et al. Parasites & Vectors* (2022) 15:243
https://doi.org/10.1186/s13071-022-05347-y

Parasites & Vectors

SHORT REPORT

Open Access

Benzimidazole and aminoalcohol derivatives show in vitro anthelmintic activity against *Trichuris muris* and *Heligmosomoides polygyrus*

Elora Valderas-García[1,2], Cécile Häberli[3,4], María Álvarez-Bardón[2], Nerea Escala[5], Verónica Castilla-Gómez de Agüero[1,6], Jennifer de la Vega[5], Esther del Olmo[5], Rafael Balaña-Fouce[2], Jennifer Keiser[3,4] and María Martínez-Valladares[1,6*]

Abstract

Background: Infections by gastrointestinal nematodes cause significant economic losses and disease in both humans and animals worldwide. The discovery of novel anthelmintic drugs is crucial for maintaining control of these parasitic infections.

Methods: For this purpose, the aim of the present study was to evaluate the potential anthelmintic activity of three series of compounds against the gastrointestinal nematodes *Trichuris muris* and *Heligmosomoides polygyrus* in vitro. The compounds tested were derivatives of benzimidazole, lipidic aminoalcohols and diamines. A primary screening was performed to select those compounds with an ability to inhibit *T. muris* L_1 motility by > 90% at a single concentration of 100 µM; then, their respective IC_{50} values were calculated. Those compounds with IC_{50} < 10 µM were also tested against the adult stage of *T. muris* and *H. polygyrus* at a single concentration of 10 µM.

Results: Of the 41 initial compounds screened, only compounds AO14, BZ6 and BZ12 had IC_{50} values < 10 µM on *T. muris* L_1 assay, showing IC_{50} values of 3.30, 8.89 and 4.17 µM, respectively. However, only two of them displayed activity against the adult stage of the parasites: BZ12 killed 81% of adults of *T. muris* (IC_{50} of 8.1 µM) and 53% of *H. polygyrus* while BZ6 killed 100% of *H. polygyrus* adults (IC_{50} of 5.3 µM) but only 17% of *T. muris*.

Conclusions: BZ6 and BZ12 could be considered as a starting point for the synthesis of further structurally related compounds.

Keywords: *Trichuris muris*, *Heligmosomoides polygyrus*, Anthelmintic, Benzimidazole, Diamine, Aminoalcohol

Background

Soil transmitted helminths (STHs) are a group of human parasitic nematodes that affect around 1.5 billion of the world's population causing substantial disease and disability [1]. These infections are more common in people living in low- and middle-income countries, in areas with poor access to adequate drinking water, sanitation and hygiene [2]. Of particular importance are infections caused by roundworms (*Ascaris lumbricoides*), whipworms (*Trichuris trichiura*) and hookworms (*Necator americanus* or *Ancylostoma duodenale*) [3]. According to the latest studies, the global incidence of *T. trichiura*

*Correspondence: mmarva@unileon.es

[1] Instituto de Ganadería de Montaña, CSIC-Universidad de León, 24346 Grulleros, León, Spain
Full list of author information is available at the end of the article

III.6. ARTÍCULO 6

Este artículo está relacionado con los objetivos 7 y 8 del Trabajo de Tesis.

Algunos compuestos con estructura de Bz presentan actividad antiprotozoaria. Inicialmente, los derivados de tipo I, II y III fueron ensayados in vitro frente *Plasmodium falciparum*, *Leishmania donovani* y *Trypanosoma cruzi,* encontrándose diferentes perfiles de actividad. En este trabajo se indica la actividad anti-*Plasmodium* de algunos Bz.

Entre las enfermedades transmitidas por vectores, la malaria es la que más muertes causa a nivel global. El arsenal terapéutico en el caso de malaria es amplio y variado, sin embargo, se han encontrado resistencias a casi todos los fármacos disponibles, por lo que es necesario encontrar nuevas alternativas terapéuticas.

En un primer cribado con compuestos representativos de las familias I, II y III, se encontraron buenos indicios de actividad para los derivados de la familia III. Así, en este trabajo se explora la actividad in vitro de los derivados 2-picolinamido-Bz en una cepa sensible a cloroquina, seleccionando los más activos para su ensayo frente a una cepa resistente. Además, se estudió el efecto de algunos compuestos a nivel celular, evaluando la integridad de la membrana, la producción intracelular de especies reactivas de hidrógeno (ROS), cambios en el potencial de membrana mitocondrial y la biocristalización de la hemozoína.

Antiplasmodial activity, structure-activity relationship and studies on the action of novel benzimidazole derivatives

Nerea Escala, Laura M. Pineda, Michelle G. Ng, Lorena M. Coronado, Carmenza Spadafora, Esther del Olmo

En: *Scientific Reports* 2022, 13, 285; doi: 10.1038/s41598-022-27351-z

Factor de Impacto: 4,997
Quartil: Q1

scientific reports

Check for updates

OPEN

Antiplasmodial activity, structure–activity relationship and studies on the action of novel benzimidazole derivatives

Nerea Escala[1], Laura M. Pineda[2], Michelle G. Ng[2], Lorena M. Coronado[2], Carmenza Spadafora[2]✉ & Esther del Olmo[1]✉

Malaria cases and deaths keep being excessively high every year. Some inroads gained in the last two decades have been eroded especially due to the surge of resistance to most antimalarials. The search for new molecules that can replace the ones currently in use cannot stop. In this report, the synthesis of benzimidazole derivatives guided by structure–activity parameters is presented. Thirty-six molecules obtained are analyzed according to their activity against *P. falciparum* HB3 strain based on the type of substituent on rings A and B, their electron donor/withdrawing, as well as their dimension/spatial properties. There is a preference for electron donating groups on ring A, such as Me in position 5, or better, 5, 6-diMe. Ring B must be of the pyridine type such as picolinamide, other modifications are generally not favorable. Two molecules, 1 and 33 displayed antiplasmodial activity in the high nanomolar range against the chloroquine sensitive strain, with selectivity indexes above 10. Activity results of 1, 12 and 16 on a chloroquine resistance strain indicated an activity close to chloroquine for compound 1. Analysis of some of their effect on the parasites seem to suggest that 1 and 33 affect only the parasite and use a route other than interference with hemozoin biocrystallization, the route used by chloroquine and most antimalarials.

Malaria is a potentially mortal febrile disease that is caused by protozoa of the genus *Plasmodium*. The parasite is transmitted by the bite of an infected female *Anopheles* mosquito[1]. Malaria is a preventable and treatable disease; however, it continues to be a global health problem, and according to the World Health Organization (WHO) 2021 report[2], 241 million cases were reported in 2020, being the African continent the region with the highest global malaria burden[2]. Since 2021, the WHO recommends the use of the RTS,S/AS01 vaccine (Mosquirix™) among children living in regions with moderate to high *Plasmodium falciparum* (*Pf*) transmission[3], although the efficacy of this vaccine is of only 28.3% in approximately 4 years[4]. The best existing treatment is the artemisinin-based combination therapy (ACT), artemether–lumefantrine, artesunate–amodiaquine, artesunate–mefloquine, artesunate–sulfadoxine–pyrimethamine, and dihydroartemisinin–piperaquine. A sixth ACT (artesunate–pyronaridine) has recently been included[5]. However, in the last year's antimalarial drug resistances to ACT have appeared, with a mutation in the Kelch13 gene strongly related to artemisinin resistances, and the Greater Mekong subregion is the most affected, presenting a new threat for the management of malaria[6]. Recently, the same resistance has also been identified in Rwanda, which to date had not been reported in the African continent[7]. The need for new antimalarials is a pressing task.

The benzimidazole skeleton (BZ) plays an important role in the medicinal chemistry field. Substitutions in different positions of the molecule provide compounds with a wide variety of applications such as antihypertensive[8], antidiabetic[9], antitumoral[10], antimicrobial[11] or anti-inflammatory[12], among others.

In the last 5 years several research groups have worked on the synthesis of BZ derivatives with potential antimalarial activity. On the one hand, 2-phenyl-1*H*-benzimidazole derivatives exhibited a good activity in vitro against *P. falciparum* with IC_{50} values of the most potent compounds ranging from 18 nM to 1.30 μM[13–16]. The inclusion of a spacer between the BZ nucleus and the aromatic fragment in C-2 give the molecules the possibility to adopt different conformations. In this way, Attram et al. included an amino group in C-2, obtaining

[1]Departamento de Ciencias Farmacéuticas: Química Farmacéutica, Facultad de Farmacia, Universidad de Salamanca, CIETUS, IBSAL, 37007 Salamanca, Spain. [2]Center of Cellular and Molecular Biology of Diseases, Instituto de Investigaciones Científicas y Servicios de Alta Tecnología, City of Knowledge, Clayton, Apartado 0816-02852, Panama City, Panama. ✉email: cspadafora@indicasat.org.pa; olmo@usal.es

in vitro fast-acting anti-*Plasmodium* compounds with a hit compound which showed an IC_{50} of 79 nM against the chloroquine-sensitive strain NF54 and 335 nM against the multi-resistant strain K1[17]. The introduction of an acrylonitrile group as a linker also showed good *Pf* inhibitory activity of BZ derivatives, with an IC_{50} value for the best compound of 0.69 and 3.41 μM in 3D7 and RKL9 strains, respectively[18].

Substitutions in the *N*-1 position of BZ provides good antiplasmodial derivatives. Thus, some research groups have synthetized *N*-1 aryl, hetaryl or alkyl derivatives obtaining interesting results, with activities ranging from 6.4 nM to 1.5 μM for most active compounds[19–23].

Tricyclic derivatives such as pyrido[1,2-*a*]benzimidazole seem to be a good alternative for malaria treatment, providing compounds with submicromolar IC_{50} values, and reductions of parasitemia above 95%[24–28]. The bioactivity of Schiff bases attached to BZ nucleus is described in previous literature; based on it, the antimalarial activity of some novel derivatives has been evaluated recently, exhibiting favorable results in vitro[29] and with some derivatives displaying IC_{50} values ranging from 26.9 to 28.3 μg/mL. More recently, Aragon et al.[30] described the antiplasmodial activity of some metal-based Schiff bases-BZ with EC_{50} values ranging from 12.8 to 18.3 μg/mL.

Furthermore, the obtaining of derivatives related to the antiallergic drug astemizole[31–33] or lerisetron[34], showed congeners with good IC_{50} values, from 47 nM to 1.7 μM against NF54 and K1 strains; moreover, derivatives related to some natural products, as carvacrol, showed activity values of 0.48 – 1.76 μg/mL[35]. Ferroquine, a ferrocenyl-chloroquine in phase 2b studies, led to Baartzes et al. to the obtaining and evaluation of ferrocenyl and neutral and cationic iridium (III) and rhodium (III) aminoquinoline-benzimidazole hybrids[36,37] and 2(2-pyridyl) benzimidazole[38]. In the same sense, iridium(III), rhodium(III) and ruthenium (II) BZ-complexes were also tested against *Pf*[39]. Organometallic-BZ complexes exhibited IC_{50} values in the low submicromolar range (0.12–5.17 μM).

Bearing these facts in mind, in the present study we explore the in vitro activity of some BZ derivatives against *Pf*. These compounds bear an amide spacer between the BZ nucleus and the heterocyclic fragment (ring B). The amide fragment allows the molecules the possibility of adopting an exocyclic tautomerization, which could contribute to establish an additional interaction with its target and perhaps increase the activity of the compounds. The introduction of electron donor or acceptor groups on ring A would allow, on the one hand, to enhance (or not) the formation of the exocyclic tautomer and, on the other hand, to increase the BZ size to fit better with the target, or establish an additional bond as could happen with the methoxy group (an additional hydrogen bond could be established) thus increasing the activity. Regarding ring B, the convenience of medium-sized (pyridine) or larger (quinoline, isoquinoline) heterocycles has been explored. Even the presence of certain substituents (type and position) on the pyridine ring. Additionally, the cytotoxicity against the Vero cell line for most active compounds is described, and the corresponding selectivity index (SI) calculated. A set of mechanistic studies were included for some compounds with good activities but inadequate selectivity and they were compared in head-to-head experiments with the lead compounds BZ **1** and **33** to obtain clues on the possible differentiation between them in terms of their action on the parasites.

Results and discussion

Chemical synthesis. To obtain the 2-arylcarbamidoBZ derivatives, the corresponding 2-amino-1*H*-benzimidazole intermediate (**AI**) should be previously synthesized. The procedure to obtain **AI 1–5** is indicated in a Escala et al. previous work[40]. Here we indicate as an example compound **AI-6** obtaining, solutions of the 4-nitro-1,2-phenylendiamine and cyanogen bromide in aqueous methanol (50% v/v) were prepared separately. Then, the solutions were mixed and maintained with continuous magnetic stirring at room temperature for 48 h[41], to provide **AI-6** in 95% yield. The coupling of intermediates **AI-1**/**AI-6** with different acids in the presence of 1,1′-carbonyldiimidazole (DCI) as catalyst at room temperature for 16 h, allowed us to obtain BZ **1** to **29** and BZ **33** to **36** with yields ranging from 27 to 69%, (Fig. 1).

BZ **30** was obtained by the reduction of **29** under H_2 atmosphere with a yield of 85%. BZ **31** was synthetized by coupling **30** with 2-(Boc-amino)decanoic acid and DCI in 32% yield. The procedure for obtaining 2-(Boc-amino)decanoic acid is indicated in Valderas et al[42]. Boc deprotection of **31** with trifluoroacetic acid provided the corresponding free amino derivative **32** in 76%.

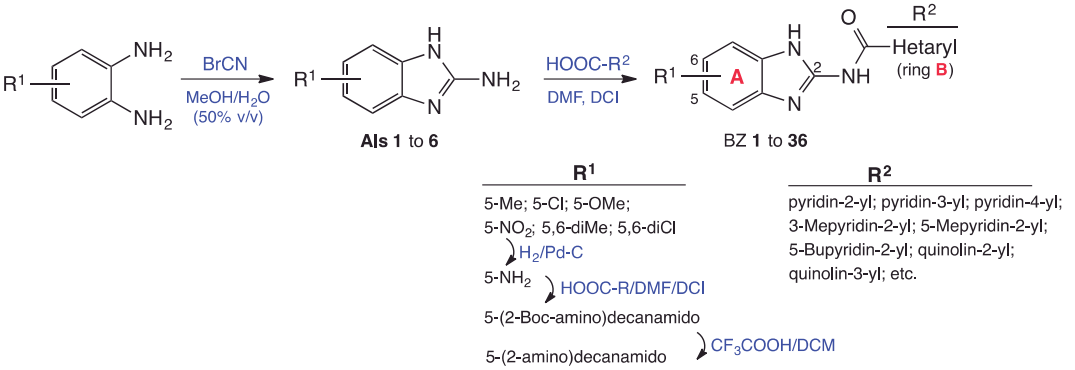

Figure 1. Procedure for the synthesis of 2-amidobenzimidazole derivatives.

All the compounds obtained (intermediate and final) were properly characterized according to their physicochemical properties. For experimental details, description of synthesized intermediates and characterization of the most active final compounds see the Experimental: Chemistry section; for the rest of the compounds see Supplementary Information.

Antiplasmodial activity. In vitro *activity of BZ.* All BZ derivatives were tested at 10 μM against the HB3 strain of *Pf*, and for those compounds with a percentage of growth inhibition (% GI) higher than 50%, the IC_{50} values were determined. In addition, their cytotoxicity on epithelial Vero cell cultures was evaluated to calculate their selectivity indexes (SI), Table 1. An index of 10 or above is expected for a lead compound.

In Table 1 compounds are organized first according to the substituent on ring A, and then by ring B complexity (general structure: Fig. 2). Ring A displays electron donating groups, EDG, (5-CH_3, 5-OCH_3, 5-NH_2, 5-NHCOR, or 5,6-diCH_3) or electron withdrawing, EWG, (5-Cl, 5-NO_2 or 5,6-diCl) in the BZ system, while ring B heterocycle can be a pyridine with the nitrogen in *ortho*, *meta* or *para* position, a quinoline or an isoquinoline. In addition, the presence of certain substituents (methyl, butyl, chloro, cyano, phenyl) on the pyridine ring has been explored, as well as its position.

Eleven derivatives (BZ **1** to **11**) displaying a methyl group on C-5 BZ were obtained. Compounds **1**, **2**, **3** showed in ring B a pyridine fragment with the nitrogen in 2′ (*ortho*), 3′(*meta*) or 4′(*para*) position. As observed

N°	R^1	R^2	GI[a] (%)	IC_{50} (μM)	Cytotoxicity[b] CC_{50} (μM)	SI
1	5-CH_3	pyridin-2-yl	**93.5**	**0.98**	**14.8**	**14.5**
2	5-CH_3	pyridin-3-yl	0.0	nc	nc	nc
3	5-CH_3	pyridin-4-yl	0.0	nc	nc	nc
4	5-CH_3	3-methylpyridin-2-yl	92.4	2.5	6.8	2.8
5	5-CH_3	5-methylpyridin-2-yl	100.0	1.5	4.5	1.6
6	5-CH_3	5-butylpyridin-2-yl	90.9	2.4	6.6	2.7
7	5-CH_3	5-phenylpyridin-2-yl	57.5	7.8	19.5	2.5
8	5-CH_3	5-cyanopyridin-2-yl	37.4	nc	nc	nc
9	5-CH_3	quinolin-2-yl	73.1	14.1	63.0	4.5
10	5-CH_3	quinolin-4-yl	60.5	nc	nc	nc
11	5-CH_3	isoquinolin-1-yl	0.0	nc	nc	nc
12	5-Cl	pyridin-2-yl	91.4	1.8	15.4	8.7
13	5-Cl	3-methylpyridin-2-yl	87.3	2.8	8.6	3.0
14	5-Cl	3-chloropyridin-2-yl	11.9	nc	nc	nc
15	5-Cl	4-methoxypyridin-2-yl	89.8	1.5	2.0	1.4
16	5-Cl	5-methylpyridin-2-yl	85.6	2.4	7.2	3.0
17	5-Cl	5-butylpyridin-2-yl	89.7	3.5	3.4	1.0
18	5-Cl	5-phenylpyridin-2-yl	99.2	2.3	0.6	0.3
19	5-Cl	6-methylpyridin-2-yl	28.0	nc	nc	nc
20	5-Cl	quinoline-2-yl	25.9	nc	nc	nc
21	5-Cl	quinolin -3-yl	0.0	nc	nc	nc
22	5-Cl	quinolin -4-yl	88.9	2.3	16.1	6.9
23	5-Cl	isoquinolin-1-yl	53.7	nc	nc	nc
24	5-Cl	6-methoxy-quinolin-2-yl	22.3	nc	nc	nc
25	5-OCH_3	pyridin-2-yl	50.9	nc	nc	nc
26	5-OCH_3	5-methylpyridin-2-yl	93.5	3.3	11.1	3.4
27	5-OCH_3	5-butylpyridin-2-yl	100.0	1.2	8.5	7.4
28	5-OCH_3	5-phenylpyridin-2-yl	72.7	4.4	14.6	3.3
29	5-NO_2	pyridin-2-yl	96.0	5.1	13.9	2.7
30	5-NH_2	pyridin-2-yl	0.0	nc	nc	nc
31	5-$NHCOC_9H_{18}(NHBoc)$[c]	pyridin-2-yl	71.8	8.5	26.8	3.16
32	5-$NHCOC_9H_{18}(NH_2)$[d]	pyridin-2-yl	72.3	6.8	16.41	2.43
33	5,6-diCH_3	pyridin-2-yl	**100.0**	**0.85**	**13.2**	**15.4**
34	5,6-diCH_3	5-butylpyridin-2-yl	74.2	3.4	3.2	1.0
35	5,6-diCH_3	5-phenylpyridin-2-yl	64.7	7.3	9.7	1.3
36	5,6-diCl	pyridin-2-yl	81.9	2.4	11.8	5.0
Chloroquine			100.0	**0.028**	nc	nc

Table 1. Growth inhibition, IC_{50} cytotoxicity and selectivity index of 2-amidobenzimidazole derivatives in HB3 *P. falciparum* parasites. *nc* not calculated. [a]Growth inhibition percentage (%) at 10 μM, [b]cytotoxicity tested in Vero cells, [c]2-(Boc-amino)decanamido, [d]2-amino-decanamido. Significant values are in bold.

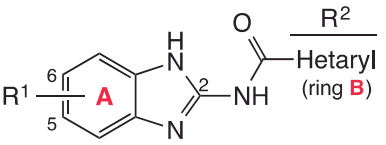

Figure 2. General structure of 2-amidobenzimidazole derivatives.

in the results for antiplasmodial activity (Table 1) there is a clear preference for the *ortho* position since the picolinamide **1** reduced by 93.5% the growth of *Pf*, while the nicotinamide **2**, or the isonicotinamide **3** were inactive. BZ **1** showed an IC_{50} equal to 0.98 μM and an SI of 14.5. Then, the presence of certain substituents on the picolinamide fragment, their position (C-3′ or 5′) and electronical character (EWD, EDG) were explored, as well as the convenience of bulky fragments (quinoline, isoquinoline). EDG as methyl in C-3′ (IC_{50} = 2.5 μM for **4**) and specially in C-5′ (IC_{50} = 1.5 μM for **5**) are favorable, therefore new fragments in position C-5′ (Bu, Phe, CN) were introduced. The butyl derivative **6** with IC_{50} equal to 2.4 μM was slightly less potent than **5**, and the EWG 5-cyano **8** was inactive, electron rich fragments as the phenyl **7** were less potent than **5** (IC_{50} = 7.8 μμM). Of the bulkier groups (**9**, **10** and **11**) only the quinolin-2-yl **9** showed IC_{50} = 14.1 μM. These modifications, along with new others were introduced in combination with 5-Cl in ring A (BZ **12** to **24**). The effect of a methyl group in C-3′ (compound **13**) was similar to that of BZ **4** with IC_{50} = 2.8 μM and SI = 3.0, and an EWG as chloro (**14**) in that position was not suitable for the activity with only 11.9% GI of *Pf*. The combination 5-Cl/5′-Me (BZ **16**) was less efficient than the 5-Me/5′-Me (**5**), and the 5-Cl/6′-Me (**19**) was inactive. A methoxy group in position 4′ (BZ **15**) was introduced as EDG, which turned out to be the most potent compound of this group with IC_{50} = 1.5 μM, however, the picolinamide **12**, with a slightly lower activity, showed a higher SI of 8.7. In this case, of the bulkier fragments **20** to **24**, the quinolin-4-yl **22** showed good growth inhibitory effect with IC_{50} = 2.3 μM and SI = 6.9. Four derivatives with 5-OMe were synthesized (**25** to **28**); here the 5′-butylpyridin-2-yl **27** was the most potent with IC_{50} = 1.2 μM and SI = 7.4.

The 5-NO_2/pyridin-2-yl **29** displayed moderate *Pf* inhibitory effect with IC_{50} = 5.1 μM. The activity was lost by reduction of the nitro group to an amino (BZ **30**), and recovered by modification to a long chain amide derivative, compounds **31** and **32**.

Disubstitution on ring A (5,6-diMe or (5,6-diCl) combined with pyridin-2-yl, 5-butylpyridin-2-yl, or 5-phenylpyridin-2-yl (BZ **33** to **36**) indicated that EDG associated with pyridin-2-yl (**33**) was an excellent combination, with IC_{50} = 0.85 μM and SI = 15.4, which is thirty times less active than the reference compound, chloroquine.

In general, and after the results showed in Table 1 we can state that the best association are EDG´s (one or two) in ring A combined with pyridine-2-yl in ring B.

Cellular effect studies. The integrity of the plasma membrane under the action of certain antiplasmodial compounds was assessed through the use of two methodologies. First, the absorption of propidium iodide, to which intact membranes are impermeable, was measured. Second, the presence of heme in the culture media, which indicates a leakage of the contents of the erythrocyte or its complete lysis (hemolysis), was analyzed. None of them showed any significant hemolysis action, however, some permeation in the membrane, although not significant, is caused by BZ **5**, **16** and **26**, while BZ **1** and **33** are the best in keeping the membrane well preserved (Fig. 3). This result is in agreement with the lower toxicity exhibited by the two latter with respect to the other three compounds.

Also, the intracellular production of oxygen reactive species (ROS) was monitored for the same antiplasmodial compounds. The level of ROS production was compared between the samples and that of the untreated parasites. Three compounds, BZ **5, 16** and **26,** showed no significant difference at any point. However, samples BZ **1** and **33** caused an early significant decrease in the natural level of ROS produced by *Pf* infection, which tapers off by t = 9 h (Fig. 4). This could explain why the latter, again, are the ones that are more effective in generating harm with the least toxicity given that they cause a transient shortage of oxidative reactions, which seem to last only enough to affect the parasite but not the epithelial Vero cells tested for cytotoxicity. This would point to the conformation of such molecules targeting a specific molecule or process of the parasite.

Changes in mitochondrial membrane potential, another common hallmark of programed cell death, were analyzed in the samples that had promising activities toward *P. falciparum* cultures. The results of adding 1 μM of each compound can be seen in Fig. 5. While four of the compounds tested do not show a significant departure from what happens to the mitochondrial membrane in the untreated controls, BZ **26** shows an effect from t = 6 h onward (Fig. 5), shifting toward the damaging effect of the positive control, which could perhaps be due to an additional interaction between the oxygen of the methoxy group attached to ring A with its specific target. Noteworthy, the two best antiplasmodial compounds, BZ **1** and BZ **33** do not show a difference with the untreated control up to t = 6 h, but there is a changing tendency at t = 9 h, that could suggest that only at that time those two compounds could start reaching the mitochondria. This could probably be explained by the presence of the unsubstituted picolinamide fragment, therefore more polar and less soluble in the membrane, making it harder or slower to permeate into the erythrocyte and then into the parasite, with respect to the other three.

Finally, the interference of the BZ derivatives with hemozoin biocrystallization was measured in the two most promising samples (BZ **1** and **33**) together with one sample that was not selective towards *Pf* (BZ **16**) Fig. 6. The mechanism used by *Pf* to prevent intoxication with free heme once hemoglobin is degraded is to form hemozoin

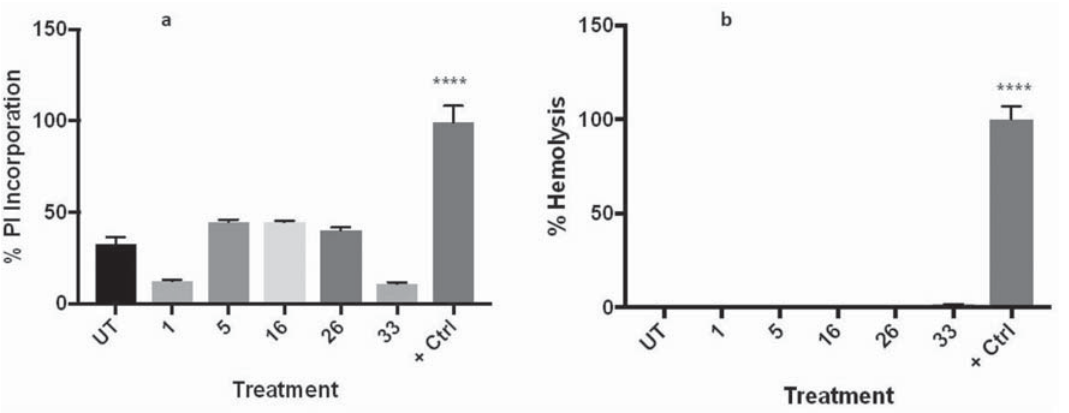

Figure 3. Membrane integrity tests. BZ **1**, **5**, **16**, **26** and **33** were tested in triplicates in two independent experiments. (**a**) Incorporation of propidium iodide (PI) was analyzed through fluorometry after 3 h incubation with the compounds. (**b**) Hemolysis was measured by light absorbance 24 h after exposure to the compounds. One-way ANOVA with Turkey´s comparison was used for analysis of significance. ****$p < 0.001$.

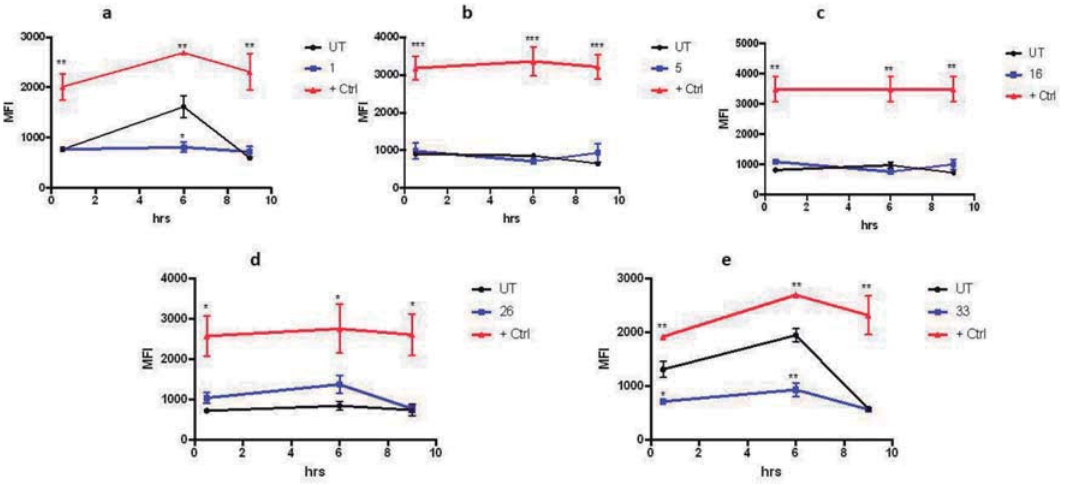

Figure 4. Effect of selected benzimidazole derivatives on ROS production. Five potent compounds were incubated with *P. falciparum*-infected cultures and the production of reactive oxygen species was measured through fluorometry at 0.5, 6 and 9 h after their addition at 1 μM. As positive control, a sample containing hydrogen peroxide at 200 μM was added. Samples were measured in triplicates. One-way ANOVA with Turkey´s comparison was used to measure significance with respect to the untreated control at each different time point. n = 2. (**a**) BZ **1**, (**b**) BZ **5**, (**c**) BZ **16**, (**d**) BZ **26** and (**e**) BZ **33.** *$p < 0.05$, **$p < 0.01$, ***$p < 0.005$.

crystals that capture heme. Mefloquine and other common antimalarials interfere with this pathway, resulting in the death of the parasite. All the compounds tested here seem to interfere, but at a low level, with this process, but it clearly is not the main target of BZ **1** and BZ **33** against the parasite, given that a non-selective compound as BZ **16** gives the same, small level of disruption of the process as the other two. To explore a possible mechanism of action, three derivatives with different level of activities against *Pf* HB33 (BZ **1**, **12** and **16**) were also tested against *Pf* HB7G8, a strain that has developed chloroquine resistance (Table 2).

Table 2 shows that two of the compounds tested (**1** and **16**), unlike CQ, did not show an increase in their IC_{50} when confronted with a strain that has developed ways to detoxify from CQ, suggesting that some derivatives, as these two, might be targeting another pathway than CQ. On the other hand, the concentration of BZ **12** has to be doubled, with respect to *Pf* HB3, to achieve 50% killing in *Pf* 7G8, aligning with the notion that other BZ

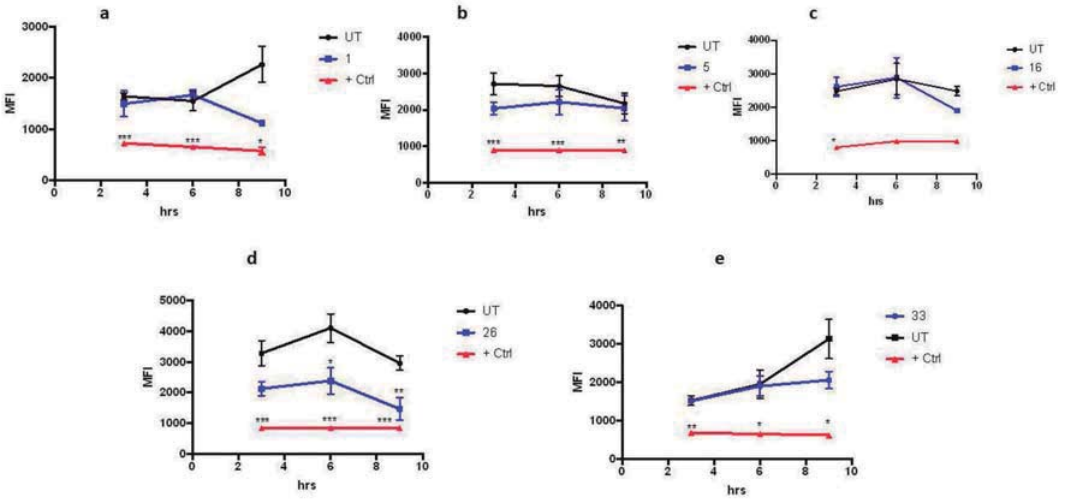

Figure 5. Changes to mitochondrial membrane potential caused by antiplasmodial compounds. Fluorometry was used to measure the effects on the mitochondria of *P. falciparum* parasites caused by treatment with compounds that show activity against their growth in culture. A membrane disruptor (CCCP) was added as a positive control and untreated cultures were used as the negative one. All compounds were tested at 1 µM in triplicates, n = 3. (**a**) BZ **1**, (**b**) BZ **5**, (**c**) BZ **16**, (**d**) BZ **26** and (**e**) BZ **33**. *p < 0.05, **p < 0.01, ***p < 0.005.

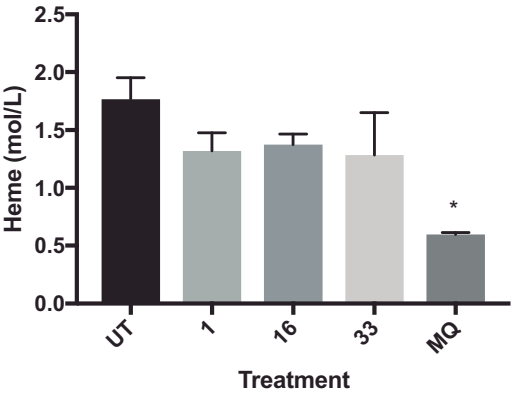

Figure 6. Influence in the biocrystallization of hemozoin in *P. falciparum*. Compounds **1, 16** and **33** were added to *Pf* cultures and the amount of hemozoin produced was analyzed after 36 h. Mefloquine (MQ) was used as a positive control. The experiment was performed in triplicates and analyzed with one-way ANOVA. *p < 0.05.

Nº	R^1	R^2	7G8 *Pf* IC_{50} (µM)	Cytotoxicity[a] CC_{50} (µM)	SI
1	5-CH_3	pyridin-2-yl	0.95	14.8	15.6
12	5-Cl	pyridin-2-yl	3.60	15.4	4.2
16	5-Cl	5-methylpyridin-2-yl	2.60	7.2	2.7
CQ*			**0.23**	nc	nc

Table 2. Growth inhibition, $IC_{50,}$ cytotoxicity and selectivity index of 2-amidobenzimidazole derivatives in 7G8 *P. falciparum* parasites. [a]cytotoxicity tested in Vero cells.

derivatives share a mechanism of action that participates at some point in the one used by chloroquine, possibly related with disturbing the ability of the parasite to synthetize hemozoin.

Significant values are in bold.

ADME-toxicity profiles and physicochemical properties. In silico studies were performed through SwissADME (http://www.swissadme.ch/) and admetSAR (http://lmmd.ecust.edu.cn/admetsar2) online free servers to analyze the druggability and toxicity risks of most active compounds (Table 3). The most active BZs fulfill Lipinski's Rule of Five and the Rule of Three of lead-likeness with MW values in the range of 252.27 and 286.72 g/mol, clogP values between 2.52 and 3.17, three H-bond acceptors for BZ **1**, **5**, **16** and **33** and four for BZ **26**, and H-donors in all of them equal to 2.

Other properties as solubility, with values from − 4.81 to − 4.00 and topological polar surface area with 70.67 values for **1**, **5**, **16** and **33** and 79.90 for BZ **26** are favorable. Very good intestinal absorption, and blood brain barrier penetration with potential access to the central nervous system are shown in compounds **1**, **5**, **16** and **33.** This trait is especially necessary in their potential use to treat cerebral malaria, and is not predicted for BZ **26**, suggesting that the latter compound would work better in other manifestations of the infection. Plasma protein binding levels from 73.3 to 100% were predicted, which ensures a good distribution of the drug. None of the compounds showed mutagenic values except **1,** oddly enough given that compound **5**, which is structurally very similar, is not mutagenic. None of the compounds seem to be tumorigenic.

Conclusions

A series of benzimidazole derivatives were synthetized and a structure–activity analysis performed, with the aim of improving their antiplasmodial activity. Some of the derivatives displayed IC_{50s} in the mid nanomolar range but were highly toxic. A number of mechanistic studies were conducted with a number of derivatives that had shown activity against the parasites, to try to understand the different response of the two best compound, BZ **1** and **33**, which showed high nanomolar activity with a good SI against *P. falciparum* parasites. Thus, for comparison reasons, these two lead compounds with nanomolar activity and selectivity index > 10 were analyzed together with other few molecules that were very active but, at the same time, toxic. None of the molecules showed a potent hemolytic activity; however, some of them caused harm to the membrane, which is an undesirable effect, that was diminished for BZ **1** and BZ **33**. In the production of reactive oxygen species and their effects on the potential of the mitochondrial membrane, BZ **1** and BZ **33** seem to differ from the other compounds tested, although in the interference with hemozoin crystallization they do not. These results, together, hint at a mechanism of action used by BZ **1** and BZ **33** that differ from the other compounds tested. This seems to be confirmed for **1,** when it made no difference to its IC_{50} to have it tested against a CQ-resistant strain. Compounds **1** and **33** displayed a methyl as electron donor group in ring A (one for **1** and two for **33**) and a non-substituted picolinamide fragment in ring B. These are characteristics that should be considered when trying to optimize their activity, which can be considered very good, given that the chloroquine activity differs from **1** and **33** only by some tenths of nano molarity and they seem to act through a different route than the signature antimalarial.

	BZ				
Properties	**1**	**5**	**16**	**26**	**33**
MW	252.27	266.30	286.72	282.30	266.30
H-A[a]	3	3	3	4	3
H-D[a]	2	2	2	2	2
Log P	2.52	2.83	3.17	2.53	2.83
Rotatable bonds	2	2	2	3	2
TPSA	70.67	70.67	70.67	79.90	70.67
Drug-likeness	Yes	Yes	Yes	Yes	Yes
Lead-likeness	Yes	Yes	Yes	Yes	Yes
Log S	− 4.23	− 4.24	− 4.81	− 4.00	− 4.13
HIA	High	High	High	High	High
BBB	Yes	Yes	Yes	No	Yes
PPB	76.4	100.0	100	100	73.3
P-g substrate	Yes	No	No	Yes	Yes
Mutagenic	Yes	No	No	No	No
Tumorigenic	No	No	No	No	No

Table 3. ADMET properties of most active compounds against *Pf. MW* molecular weight, *Log P* lipophilicity, *PSA* topological polar surface area Å^2, *Log S* aqueous solubility, *HIA* human intestinal absorption %, *BBB* blood–brain barrier, *PPB* plasma protein binding %. [a]H-A Acceptor, H–D Donor.

Experimental

Chemistry. *General experimental procedures.* All commercial chemicals (Aldrich, Alpha, Fischer, SDS) were used as purchased and solvents (Fischer, SDS, Scharlau) purified by the standard procedures prior to use[43]. Reactions were monitored by Thin Layer Chromatography (TLC) (Kieselgel 60 F254 precoated plates, E. Merck, Germany), the spots were detected by exposure to UV light at λ 254 nm, and colorization with 10% ninhydrin spray, and further heating of the plate. Melting points (mp) were determined with Mel-Temp apparatus in open capillaries and were uncorrected. Separations by flash column chromatography were performed on Merck 60 silica gel (0.063–0.2 mesh). NMR spectra were recorded on a Bruker Avance 400 MHz, Varian Mercury 400 MHz (400 MHz for ^{1}H, 100 MHz for ^{13}C) or Varian Mercury 200 MHz (200 MHz for ^{1}H, 500 MHz for ^{13}C). The spectra were measured either in $CDCl_3$, methanol-d_6 or DMSO-d_6, using tetramethylsilane (TMS) as internal standard, chemical shifts (δ) are given in ppm and coupling constants (*J*) in Hertz. High resolution mass spectra (HRMS) were obtained by electron spray ionization-mass spectrometry (ESI–MS) technique (5 kV) on a QSTAR XL mass spectrometer.

General procedures for the preparation of active compounds. *Procedure for obtaining intermediate amino compounds, AIs 1–6.* The obtaining process was the same as that described in Escala[40]; solutions of 1.00 g (6.53 mmol) 4-nitro-1,2-phenylendiamine and cyanogen bromide 1.04 g (9.80 mmol) in aqueous methanol (50% v/v) were prepared separately. The solutions were then mixed in an Erlenmeyer flask and maintained with continuous magnetic stirring at room temperature for 48 h, obtaining 1.10 g (6.20 mmol) 95%[41].

*5-Nitro-1*H*-benzimidazol-2-amine* **AI 6**, orange solid; mp: 231 °C; ^{1}H NMR (400 MHz, CD_3OD): δ 8.10 (d, *J* = 1.6 Hz, 1H), 8.07 (dd, *J* = 8.4 and 1.6 Hz, 1H), 7.43 (d, *J* = 8.4 Hz, 1H); ^{13}C NMR (100 MHz, CD_3OD): δ 153.90, 143.45, 136.39, 131.10, 118.91, 111.06, 106.89; HRMS (m/z): $[M]^+$ calcd. for $C_7H_7N_4O_2$ $[MS+H]^+$, 179.0491; found, 179.0410.

AIs 1–**5** were described in Escala[40].

Coupling of intermediate amines with the corresponding acids. BZ 4, 5, 6, 13, 15, 16, 18, 22, 26, 27, 33 and 36. The protocol described in Escala et al.[40] was applied. To a solution of the corresponding acid (1.3 mmol) in dry DMF (1 mL), DCI (1.3 mmol) was added, and the mixture maintained at room temperature for 1 h. Then, the corresponding 2-aminobenzimidazole intermediate (1.0 mmol) was added and the mixture maintained at room temperature with magnetic stirring for 16 h. The progress of the reaction was monitored by TLC using ethyl acetate as eluent. After completion of the reaction, the solvent was removed in vacuo in a rotary evaporator and the obtained solid was purified by silica gel chromatography using ethyl acetate as eluent. Reaction yields ranged between 30–69%.

3-Methyl-N-*(5-methyl-1*H*-benzimidazol-2-yl)picolinamide* **4**, a dark pink solid; mp: 173 °C; yield: 63%; ^{1}H NMR (400 MHz, $CDCl_3$): δ 11.00 (brs, 2H), 8.40 (d, *J* = 4.8 Hz, 1H), 7.61 (d, *J* = 7.6 Hz, 1H), 7.36 (dd, *J* = 7.6 and 4.8 Hz, 1H), 7.35 (d, *J* = 8.0 Hz, 1H), 7.25 (brs, 1H), 7.02 (dd, *J* = 8.0 and 1.2 Hz, 1H), 2.77 (s, 3H), 2.45 (s, 3H); ^{13}C NMR (100 MHz, $CDCl_3$): δ 165.0, 146.3, 146.0, 144.8, 141.2, 137.8, 136.7, 132.7, 131.8, 126.9, 123.4, 117.1, 110.8, 21.6, 20.5; HRMS (m/z): $[M]^+$ calcd. for $C_{15}H_{15}N_4O$ $[MS+H]^+$, 267.1240; found, 267.1236.

5-Methyl-N-*(5-methyl-1*H*-benzimidazol-2-yl)picolinamide* **5**, a white solid; mp: 256 °C; yield: 55%; ^{1}H NMR (400 MHz, DMSO): δ 8.60 (d, *J* = 1.2 Hz, 1H), 8.11 (d, *J* = 7.6 Hz, 1H), 7.91 (dd, *J* = 7.6 and 1.2 Hz, 1H), 7.35 (d, *J* = 8.4 Hz, 1H), 7.28 (d, *J* = 1.2 Hz, 1H), 6.93 (dd, *J* = 8.4 and 1.2 Hz, 1H), 2.43 (s, 3H), 2.37 (s, 3H); ^{13}C NMR (100 MHz, DMSO): δ 163.6, 149.6, 146.3, 145.9, 138.8, 138.3, 137.3, 132.9, 130.8, 123.1, 122.7, 114.3, 114.1, 21.7, 18.5; HRMS (m/z): $[M]^+$ calcd. for $C_{15}H_{15}N_4O$ $[MS+H]^+$, 267.1240; found, 267.1236.

5-Butyl-N-*(5-methyl-1*H*-benzimidazol-2-yl)picolinamide* **6**, a dark yellow solid, mp: 245 °C; yield: 52%; ^{1}H NMR (400 MHz, $CDCl_3$): δ 8.43 (d, *J* = 1.6 Hz, 1H), 8.18 (d, *J* = 8.0 Hz, 1H), 7.69 (dd, *J* = 8.0 and 1.6 Hz, 1H), 7.40 (d, *J* = 8.0 Hz, 1H), 7.30 (brs, 1H), 7.04 (brd, *J* = 8.0 Hz, 1H), 2.69 (t, *J* = 7.6 Hz, 2H), 2.46 (s, 3H), 1.63 (m, 2H), 1.37 (m, 2H), 0.94 (t, *J* = 7.2 Hz, 3H); ^{13}C NMR (100 MHz, $CDCl_3$): δ 163.9, 148.9, 146.1, 145.7, 142.7, 137.1 (2C), 132.8, 131.9, 123.6, 122.5, 117.2, 116.8, 32.9, 32.7, 22.2, 21.6, 13.8; HRMS (m/z): $[M]^+$ calcd. for $C_{18}H_{21}N_4O$ $[MS+H]^+$, 309.1710; found, 309.1700.

N-*(5-Chloro-1*H*-benzimidazol-2-yl)-3-methylpicolinamide* **13**, an orange solid; mp: 180 °C; yield: 47%; ^{1}H NMR (400 MHz, DMSO): δ 11.52 (brs, 2H), 8.38 (d, *J* = 4.0 Hz, 1H), 7.70 (d, *J* = 7.2 Hz, 1H), 7.41 (dd, *J* = 7.2 and 4.0 Hz, 1H), 7.34 (d, *J* = 2.0 Hz, 1H, 1H), 7.33 (d, *J* = 8.4 Hz, 1H), 6.98 (dd, *J* = 8.4 and 1.2 Hz, 1H), 2.49 (s, 3H); ^{13}C NMR (100 MHz, DMSO): δ 165.0, 146.9, 146.9, 146.2, 140.7, 138.5, 134.6, 133.8, 126.7, 125.5, 121.3, 115.4, 114.2, 19.2; HRMS (m/z): $[M]^+$ calcd. for $C_{14}H_{12}N_4OCl$ $[MS+H]^+$, 287.0694; found, 287.0688.

N-*(5-Chloro-1*H*-benzimidazol-2-yl)-4-methoxypicolinamide* **15**, a light pink; mp: 245 °C; yield: 53%; ^{1}H NMR (400 MHz, DMSO): δ 8.54 (d, *J* = 5.6 Hz, 1H), 7.67 (d, *J* = 2.4 Hz, 1H), 7.52 (d, *J* = 2.0 Hz, 1H), 7.49 (d, *J* = 8.4 Hz, 1H), 7.26 (dd, *J* = 5.6 and 2.4 Hz, 1H), 7.14 (dd, *J* = 8.4 and 2.0 Hz, 1H), 3.92 (s, 3H); ^{13}C NMR (100 MHz, DMSO): δ 166.9, 163.1, 150.6, 150.0, 146.7, 139.5, 135.5, 125.8, 121.7, 114.0 (2C), 113.5, 109.0, 56.0; HRMS (m/z): $[M]^+$ calcd. for $C_{14}H_{12}N_4O_2Cl$ $[MS+H]^+$, 303.0643; found, 303.0638.

N-*(5-Chloro-1*H*-benzimidazol-2-yl)-5-methylpicolinamide* **16**, an orange solid; mp: 201 °C; yield: 69%; ^{1}H NMR (400 MHz, $CDCl_3$): δ 8.46 (d, *J* = 1.2 Hz, 1H), 8.16 (d, *J* = 8.0 Hz, 1H), 7.73 (dd, *J* = 8.0 and 1.2 Hz, 1H), 7.51 (d, *J* = 1.6 Hz, 1H), 7.42 (d, *J* = 8.4 Hz, 1H), 7.20 (dd, *J* = 8.4 and 1.6 Hz, 1H), 2.46 (s, 3H); ^{13}C NMR (100 MHz, $CDCl_3$): δ 164.0, 149.3, 147.0, 145.0, 138.4, 138.0, 137.2, 134.8, 125.8, 122.8, 122.5, 114.8 (2C), 18.7; HRMS (m/z): $[M]^+$ calcd. for $C_{14}H_{12}N_4OCl$ $[MS+H]^+$, 287.0694; found, 287.0688.

N-*(5-Chloro-1*H*-benzimidazol-2-yl)-5-phenylpicolinamide* **18**, a white solid; mp: 214 °C; yield: 39%; ^{1}H NMR (400 MHz, DMSO): δ 9.05 (d, *J* = 2.0 Hz, 1H), 8.37 (dd, *J* = 8.0 and 2.0 Hz, 1H), 8.27 (d, *J* = 8.0 Hz, 1H), 7.83 (dd, *J* = 8.6 and 1.6 Hz, 2H), 7.55 (m, 3H), 7.50 (d, *J* = 2.0 Hz, 1H), 7.48 (d, *J* = 8.4 Hz, 1H), 7.15 (dd, *J* = 8.4 and 2.0 Hz, 1H); ^{13}C NMR (100 MHz, DMSO): δ 163.2, 148.6, 147.0, 146.8, 140.1, 139.9, 139.1, 135.9, 135.9, 129.3

(2C), 129.1, 127.3 (2C), 125.6, 123.0, 121.5, 116.2, 114.8; HRMS (m/z): $[M]^+$ calcd. for $C_{19}H_{14}N_4OCl$ $[MS+H]^+$, 349.0851; found, 349.0845.

N-*(5-Chloro-1*H*-benzimidazol-2-yl)quinoline-4-carboxamide* **22**, a yellow solid; mp: 262 °C; yield: 50%; ^{1}H NMR (400 MHz, DMSO): δ 9.04 (d, *J* = 4.4 Hz, 1H), 8.32 (dd, *J* = 8.8 and 1.2 Hz, 1H), 8.13 (dd, *J* = 8.8 and 1.6 Hz, 1H), 7.85 (ddd, *J* = 8.8; 8.4 and 1.2 Hz, 1H), 7.83 (d, *J* = 4.4 Hz, 1H), 7.70 (ddd, *J* = 8.8; 8.4 and 1.6 Hz, 1H), 7.53 (d, *J* = 2.0 Hz, 1H), 7.50 (d, *J* = 8.4 Hz, 1H), 7.18 (dd, *J* = 8.4 and 2.0 Hz, 1H); ^{13}C NMR (100 MHz, DMSO): δ 168.1, 150.6, 148.6, 148.3, 141.0, 137.3, 134.3, 130.5, 129.9, 128.2, 125.8 (2C), 124.4, 122.2, 120.5, 115.5, 114.2; HRMS (m/z): $[M]^+$ calcd. for $C_{17}H_{12}N_4OCl$ $[MS+H]^+$, 323.0694; found, 323.0888.

N-*(5-Methoxy-1*H*-benzimidazol-2-yl)-5-methylpicolinamide* **26**, a light yellow solid; mp: 213 °C; yield: 30%; ^{1}H NMR (400 MHz, $CDCl_3$): δ 8.47 (s, 1H), 8.14 (d, *J* = 8.0 Hz, 1H), 7.42 (d, *J* = 8.0 Hz, 1H), 7.25 (d, *J* = 8.4 Hz, 1H), 7.05 (brs, 1H), 6.89 (d, *J* = 8.0 Hz, 1H), 3.84 (s, 3H), 2.44 (3H, s); ^{13}C NMR (100 MHz, $CDCl_3$): δ 164.0, 155.7, 149.5, 145.7, 145.1, 138.3, 137.9, 136.5, 128.3, 122.5, 112.5, 111.9, 98.0, 55.9, 18.7; HRMS (m/z): $[M]^+$ calcd. for $C_{15}H_{15}N_4O_2$ $[MS+H]^+$, 283.1190; found, 283.1141.

*5-Butyl-N-(5-methoxy-1*H*-benzimidazol-2-yl)picolinamide* **27**, a dark yellow solid; mp: 129 °C; yield: 49%; ^{1}H NMR (400 MHz, $CDCl_3$): δ 10.84 (brs, 2H), 8.33 (d, *J* = 2.4 Hz, 1H), 8.16 (dd, *J* = 8.0 and 2.4 Hz, 1H), 7.65 (d, *J* = 8.0 Hz, 1H), 7.37 (d, *J* = 8.8 Hz, 1H), 7.00 (brs, 1H), 6.83 (dd, *J* = 8.8 and 1.2 Hz, 1H), 3.78 (s, 3H), 2.64 (t, *J* = 8.0 Hz, 2H), 1.59 (m, 2H), 1.31 (m, 2H), 0.90 (t, *J* = 7.2 Hz, 3H); ^{13}C NMR (100 MHz, $CDCl_3$): δ 163.8, 156.2, 148.7, 146.1, 145.6, 142.7, 137.2 (2C), 129.5, 122.6, 116.5, 111.2, 99.2, 55.8, 32.9, 32.8, 22.2, 13.8; HRMS (m/z): $[M]^+$ calcd. for $C_{18}H_{21}N_4O_2$ $[MS+H]^+$, 325.1659; found, 325.1652.

N-*(5,6-Dimethyl-1*H*-benzimidazol-2-yl)picolinamide* **33**, a yellow solid; mp: 221 °C; yield: 49%; ^{1}H NMR (400 MHz, $CDCl_3$): δ 11.0 (brs, 2H, D_2O), 8.59 (dd, *J* = 4.8 and 1.2 Hz, 1H), 8.28 (d, *J* = 8.0 Hz, 1H), 7.90 (ddd, *J* = 8.0; 7.2 and 1.2 Hz, 1H), 7.50 (dd, *J* = 7.2 and 4.8 Hz, 1H), 7.28 (brs, 2H), 2.35 (s, 6H); ^{13}C NMR (100 MHz, $CDCl_3$): δ 163.5, 148.7, 148.0, 145.5, 137.7, 137.1 (2C), 131.0 (2C), 127.3, 122.7, 115.2 (2C), 20.3 (2C); HRMS (m/z): $[M]^+$ calcd. for $C_{15}H_{15}N_4O$ $[MS+H]^+$, 267.1240; found, 267.1235.

N-*(5,6-Dichloro-1*H*-benzimidazol-2-yl)picolinamide* **36**, a yellow solid; mp: 281 °C; yield: 46%; ^{1}H NMR (400 MHz, DMSO): δ 12.60 (brs, 1H), 11.52 (brs, 1H), 8.77 (dd, *J* = 4.8 and 1.2 Hz, 1H), 8.21 (dd, *J* = 8.0 and 1.6 Hz, 1H), 8.11 (ddd, *J* = 8.0; 7.2 and 1.2 Hz, 1H), 7.74 (ddd, *J* = 7.2; 4.8 and 1.6 Hz, 1H), 7.72 (s, 2H); ^{13}C NMR (100 MHz, DMSO): δ 163.5, 149.1, 148.1, 147.8, 138.5, 132.4 (2C), 128.0, 123.9 (2C), 123.0, 118.4 (2C); HRMS (m/z): $[M]^+$ calcd. for $C_{13}H_9N_4OCl_2$ $[MS+H]^+$, 307.0148; found, 307.0145.

BZs N-*(5-methyl-1*H*-benzimidazol-2-yl)picolinamide* **1**, N-*(5-chloro-1*H*-benzimidazol-2-yl)picolinamide* **12** were described in Escala[40].

Biology. *Parasites and cultures.* The chloroquine-sensitive strain HB3 and chloroquine-resistance 7G8 strain HB3 of *P. falciparum* were used throughout. Infected erythrocytes were kept in culture using the protocol established by Haynes et al.[44], basically utilizing human O^+ erythrocytes kept in an RPMI medium supplemented with glutamine and 10% human serum incubated in an atmosphere of 90% N_2, 5% O_2 and 5% CO_2.

Hemolysis assay. Tests were performed in 96-well plates as described previously by Costa-Lotufo et al. The negative control contained only red blood cells in RPMI medium. All compounds were tested at 10 µM. A positive control, 20 µL of 0.1% Triton X-100 added to culture media, inducing 100% hemolysis, was used. Samples and controls were incubated at 37 °C. After 24 h, they were centrifuged collecting the supernatant which was read at 415 nm in a spectrophotometer.

Propidium iodide (PI) incorporation assay. Manufacturer's instructions (BD PharmingenTM) were followed. Briefly, 200 µL of parasite culture at 2% parasitemia or uninfected erythrocytes, at 2% hematocrit, were incubated with each compound for 3 h at 37 °C. Untreated samples were cultured in the same plate. After incubation, 2 µL of Propidium Iodide was added and incubated for 15 min at RT while protected from light. Fluorescence was read in a fluorometer at excitation and emission wavelengths of 485/20 and 645/40 nm, respectively.

Mitochondrial membrane potential (Dy) measurements. The membrane potential was measured in a flow cytometer after staining *P. falciparum* cultures with the DiOC6(3) dye at 10 nM (Thermo Fisher, Waltham, MA, USA). Samples were incubated for 45 min at 37 °C in the dark. Following incubation, cells were washed and resuspended using 200 µL of phosphate-buffered saline (PBS) and analyzed immediately after. The mitochondrial membrane disrupter, CCCP (50 µM), incubated for 1 h, was used as a positive control. The fluorescence intensity of stained cells was calculated using FCS Express 4 (De Novo Software, Glendale, CA, USA). As negative control, uninfected red blood cells were used and their signal was subtracted from that of the infected red blood cells.

Intracellular reactive oxygen species (ROS) production in P. falciparum. Intracellular ROS formation was measured in a fluorimeter using the CM-H_2DCFDA reactive dye from Molecular Probes® (Eugene OR, USA). Hydrogen peroxide was used as a positive control at a final concentration of 200 µM. The level of ROS present was inferred through the amount of oxidized DCF[45].

In vitro β-hemozoin formation. The hemozoin polymerization assay was developed on the basis of the differential solubility of hemozoin and heme and was first used by Pandey et al. to quantify the amount of production of hemozoin by *Pf* parasites[46]. Using the methodology described by Tripathi et al.[47], schizonts and late trophozoites at a parasitemia of 2–4% were used to obtain a parasite lysate. After overnight incubation with the samples, the

absorbance of the final hemozoin pellet dissolved in NaOH was measured at 405 nm. Supernatants of soluble heme and hemozoin pellets were taken from washing steps and precipitated with concentrated (6 M) HCl. Pellets obtained were measured in a Fourier transformed infrared spectrometer (FT-IR) (Bruker, Germany) in attenuated total reflection (ATR) mode, at RT. The Beer-Lambert equation was used to calculate the final amount of hemozoin.

Ethics statement. Human blood used in this study was collected from a pool of volunteers who signed informed consents. This protocol was approved by the bioethical committee of The Gorgas Memorial Institute of Health Sciences in Panama for this study through note 221/CBI/ICGES/21. All methods were performed in accordance with relevant guidelines and regulations.

Data availability

All the information required to reproduce the experiments (chemistry, activity assays and cellular activities) is included in the manuscript, and the rest in the Supplementary Material.

Received: 24 August 2022; Accepted: 30 December 2022
Published online: 06 January 2023

References

1. Ashley, E. A., Pyae Phyo, A. & Woodrow, C. J. Malaria. *Lancet* **391**(10130), 1608–1621. https://doi.org/10.1016/s0140-6736(18)30324-6 (2018).
2. World Malaria Report. World Health Organization. https://www.who.int/teams/global-malaria-programme/reports/world-malaria-report-2021 (2021). Accessed 10 December 2022.
3. WHO recommends groundbreaking malaria vaccine for children at risk. https://www.who.int/news/item/06-10-2021-who-recommends-groundbreaking-malaria-vaccine-for-children-at-risk (2021). Accessed 10 December 2022.
4. Olotu, A. *et al.* Seven-year efficacy of RTS, S/AS01 malaria vaccine among young African children. *N. Engl. J. Med.* **374**, 2519–2529. https://doi.org/10.1056/NEJMoa1515257 (2016).
5. Guideline for Malaria. World Health Organization. https://www.who.int/publications/i/item/guidelines-for-malaria (2021). Accessed 10 December 2022.
6. Menard, D. & Dondorp, A. Antimalarial drug resistance: A threat to malaria elimination. *Cold Spring Harb. Perspect. Med.* https://doi.org/10.1101/cshperspect.a025619 (2017).
7. Uwimana, A. *et al.* Expanding home-based management of malaria to all age groups in Rwanda: Analysis of acceptability and facility-level time-series data. *Trans. R. Soc. Trop. Med. Hyg.* **112**(11), 513–521. https://doi.org/10.1093/trstmh/try093 (2018).
8. Vyas, V. K. & Ghate, M. Substituted benzimidazole derivatives as angiotensin II -AT1 receptor antagonist: A review. *Mini Rev. Med. Chem.* **10**(14), 1366–1384. https://doi.org/10.2174/138955710793564151 (2010).
9. Gaba, M., Singh, S. & Mohan, C. Benzimidazole: An emerging scaffold for analgesic and anti-inflammatory agents. *Eur. J. Med. Chem.* **76**, 494–505. https://doi.org/10.1016/j.ejmech.2014.01.030 (2014).
10. Shrivastava, N. *et al.* Benzimidazole scaffold as anticancer agent: Synthetic approaches and structure-activity relationship. *Arch. Pharm.* https://doi.org/10.1002/ardp.201700040 (2017).
11. Bansal, Y., Kaur, M. & Bansal, G. Antimicrobial potential of benzimidazole derived molecules. *Mini Rev. Med. Chem.* **19**(8), 624–646. https://doi.org/10.2174/1389557517666171101104024 (2019).
12. Veerasamy, R., Roy, A., Karanakaran, R. & Rajak, H. Structure-activity relationship analysis of benzimidazoles as emerging anti-inflammatory agents: An overview. *Pharmaceuticals* **14**(7), 633. https://doi.org/10.3390/ph14070663 (2021).
13. L'abbate, F. P. *et al.* Hemozoin inhibiting 2-phenylbenzimidazoles active against malaria parasites. *Eur. J. Med. Chem.* **159**, 243–254. https://doi.org/10.1016/j.ejmech.2018.09.060 (2018).
14. Doganc, F. *et al.* Synthesis, in vitro antiprotozoal activity, molecular docking and molecular dynamics studies of some new monocationic guanidinobenzimidazoles. *Eur. J. Med. Chem.* **221**, 113545. https://doi.org/10.1016/j.ejmech.2021.113545 (2021).
15. Openshaw, R. *et al.* A diverse range of hemozoin inhibiting scaffolds act on *Plasmodium falciparum* as heme complexes. *ACS Infect. Dis.* **7**(2), 362–376. https://doi.org/10.1021/acsinfecdis.0c00680 (2021).
16. Purwono, B., Nurohmah, B. A., Fathurrohman, P. Z. & Syahri, J. Some 2-arylbenzimidazole derivatives as an antimalarial agent: Synthesis, activity assay, molecular docking and pharmacological evaluation. *Rasayan J. Chem.* **14**(1), 94–100. https://doi.org/10.31788/RJC.2021.1416088 (2021).
17. Attram, H. D., Wittlin, S. & Chibale, K. Incorporation of an intramolecular hydrogen bonding motif in the side chain of antimalarial benzimidazoles. *Med. Chem. Comm.* https://doi.org/10.1039/c8md00608c (2019).
18. Sharma, K. *et al.* Synthesis of novel benzimidazole acrylonitriles for inhibition of *Plasmodium falciparum* growth by dual target inhibition. *Arch. Pharm.* https://doi.org/10.1002/ardp.201700251 (2017).
19. Raphemot, R. *et al. Plasmodium* PK9 inhibitors promote growth of liver-stage parasites. *Cell Chem. Biol.* **26**(3), 411–419. https://doi.org/10.1016/j.chembiol.2018.11.003 (2018).
20. Jacobs, L., de Kock, C., Taylor, D., Pelly, S. C. & Blackie, M. A. L. Synthesis of five libraries of 6,5-fused heterocycles to establish the importance of the heterocyclic core for antiplasmodial activity. *Bioorg. Med. Chem.* **26**(21), 5730–5741. https://doi.org/10.1016/j.bmc.2018.10.029 (2018).
21. Oduselu, G. O., Ajani, O. O., Ajamma, Y. U., Brors, B. & Adebiyi, E. Homology modelling and molecular docking studies of selected substituted benzo[*d*]imidazol-1-yl)methyl)benzimidamide scaffolds on *Plasmodium falciparum* adenylosuccinate lyase receptor. *Bioinform. Biol. Insights* **13**, 1–10. https://doi.org/10.1177/1177932219865533 (2019).
22. Devine, S. M. *et al.* Discovery and development of 2-aminobenzimidazoles as potent antimalarials. *Eur. J. Med. Chem.* **221**, 113518. https://doi.org/10.1016/j.ejmech.2021.113518 (2021).
23. Dziwornu, G. A. *et al.* Antimalarial benzimidazole derivatives incorporating phenolic Mannich base side chains inhibit microtubule and hemozoin Formation: Structure–activity relationship and in vivo oral efficacy studies. *J. Med. Chem.* **64**(8), 5198–5215. https://doi.org/10.1021/acs.jmedchem.1c00354 (2021).
24. Ndakala, A. J. *et al.* Antimalarial pyrido[1,2-*a*]benzimidazoles. *J. Med. Chem.* **54**(13), 4581–4589. https://doi.org/10.1021/jm200227r (2011).
25. Singh, K. *et al.* Antimalarial pyrido[1,2-*a*]benzimidazoles: Lead optimization, parasite life cycle stage profile, mechanistic evaluation, killing kinetics, and in vivo oral efficacy in a mouse model. *J. Med. Chem.* **60**(4), 1432–1448. https://doi.org/10.1021/acs.jmedchem.6b01641 (2017).
26. Mayoka, G. *et al.* Structure-activity relationship studies and Plasmodium life cycle profiling identifies pan-active *N*-aryl-3-trifluoromethyl pyrido[1,2-*a*]benzimidazoles which are efficacious in an in vivo mouse model of malaria. *J. Med. Chem.* **62**(2), 1022–1035. https://doi.org/10.1021/acs.jmedchem.8b01769 (2018).

27. Okombo, J. *et al.* Antimalarial pyrido[1,2-*a*]benzimidazole derivatives with Mannich base side chains: Synthesis, pharmacological evaluation and reactive metabolite trapping studies. *ACS Infect. Dis.* **5**(3), 372–384. https://doi.org/10.1021/acsinfecdis.8b00279 (2019).
28. Leshabane, M. *et al.* Benzimidazole derivatives are potent against multiple life cycle stages of *Plasmodium falciparum* malaria parasites. *ACS Infect. Dis.* **7**(7), 1945–1955. https://doi.org/10.1021/acsinfecdis.0c00910 (2021).
29. Fonkui, T. Y., Ikhile, M. I., Njobeh, P. B. & Ndinteh, D. T. Benzimidazole Schiff base derivatives: Synthesis, characterization and antimicrobial activity. *BMC Chem. Biol.* **13**(1), 127. https://doi.org/10.1186/s13065-019-0642-3 (2019).
30. Aragón-Muriel, A. *et al.* In vitro evaluation of the potential pharmacological activity and molecular targets of new benzimidazole-based Schiff base metal complexes. *Antibiotics* **10**(6), 728. https://doi.org/10.3390/antibiotics10060728 (2021).
31. Tian, J. *et al.* Astemizole analogues with reduced hERG inhibition as potent antimalarial compounds. *Bioorg. Med. Chem.* **25**(24), 6332–6344. https://doi.org/10.1016/j.bmc.2017.10.004 (2017).
32. Kumar, M. *et al.* Multistage antiplasmodium activity of astemizole analogues and inhibition of hemozoin formation as a contributor to their mode of action. *ACS Infect. Dis.* **5**(2), 303–315. https://doi.org/10.1021/acsinfecdis.8b00272 (2018).
33. Mambwe, D. *et al.* Structure–activity relationship studies reveal new astemizole analogues active against *Plasmodium falciparum in vitro*. *ACS Med. Chem. Lett.* **12**(8), 1333–1341. https://doi.org/10.1021/acsmedchemlett.1c00328 (2021).
34. Mueller, R. *et al.* Lerisetron analogues with antimalarial properties: Synthesis, structure-activity relationship studies, and biological assessment. *ACS Omega* **5**(12), 6967–6982. https://doi.org/10.1021/acsomega.0c00327 (2020).
35. Bhoi, R. T., Rajput, J. D. & Bendre, R. S. An efficient synthesis of rearranged new biologically active benzimidazoles derived from 2-formyl carvacrol. *Res. Chem. Intermed.* **48**, 401–422. https://doi.org/10.1007/s11164-021-04601-9 (2022).
36. Baartzes, N. *et al.* Bioisosteric ferrocenyl aminoquinoline-benzimidazole hybrids: Antimicrobial evaluation and mechanistic insights. *Eur. J. Med. Chem.* **15**(180), 121–133. https://doi.org/10.1016/j.ejmech.2019.06.069 (2019).
37. Baartzes, N. *et al.* Antimicrobial evaluation of neutral and cationic iridium(III) and rhodium(III) aminoquinoline-benzimidazole hybrid complexes. *Eur. J. Med. Chem.* **206**, 112694. https://doi.org/10.1016/j.ejmech.2020.112694 (2020).
38. Jordaan, L. *et al.* Investigating the antiplasmodial activity of substitutedcyclopentadienyl rhodium and iridium complexes of 2-(2-pyridyl)benzimidazole. *J. Organomet. Chem.* **962**, 122273. https://doi.org/10.1016/j.jorganchem.2022.122273 (2022).
39. Rylands, L. *et al.* Structure-activity relationship studies of antiplasmodial cyclometallated ruthenium(II), rhodium(III) and iridium(III) complexes of 2-phenylbenzimidazoles. *Eur. J. Med. Chem.* **161**, 11–21. https://doi.org/10.1016/j.ejmech.2018.10.019 (2018).
40. Escala, N. *et al.* Further and new target-based benzimidazole anthelmintics active against *Teladorsagia circumcincta*. *J. Mol. Struct.* **1269**, 133735. https://doi.org/10.1016/j.molstruc.2022.133735 (2022).
41. Bansal, Y., Kaur, M. & Silakari, O. Benzimidazole–ibuprofen/mesalamine conjugates: Potential candidates for multifactorial diseases. *Eur. J. Med. Chem.* **89**, 671–682. https://doi.org/10.1016/j.ejmech.2014.10.081 (2015).
42. Valderas-García, E. *et al.* Anthelmintic activity of aminoalcohol and diamine derivatives against the gastrointestinal nematode *Teladorsagia circumcincta*. *Vet. Parasitol.* **296**, 109496. https://doi.org/10.1016/j.vetpar.2021.109496 (2021).
43. Armarego, W. L. F. *Purification of Laboratory Chemicals* 8th edn. (Butterworth-Heinemann, 2017).
44. Haynes, J. D., Diggs, C. L., Hines, F. A. & Desjardins, R. E. Culture of human malaria parasites *Plasmodium falciparum*. *Nature* **263**(5580), 767–769. https://doi.org/10.1038/263767a0 (1976).
45. Jakubowski, W. & Bartosz, G. 2,7-dichlorofluorescin oxidation and reactive oxygen species: What does it measure?. *Cell Biol. Int.* **24**(10), 757–760. https://doi.org/10.1006/cbir.2000.0556 (2000).
46. Pandey, A., Singh, N., Tekwani, B., Puri, S. & Chauhan, V. Assay of β-hematin formation by malaria parasite. *J. Pharm. Biomed. Anal.* **20**(1–2), 203–207. https://doi.org/10.1016/s0731-7085(99)00021-7 (1999).
47. Tripathi, A. K., Khan, S. I., Walker, L. A. & Tekwani, B. L. Spectrophotometric determination of de novo hemozoin/β-hematin formation in an in vitro assay. *Anal. Biochem.* **325**, 85–91. https://doi.org/10.1016/S0731-7085(99)00021-7 (2004).

Acknowledgements

EO thanks to the Spanish Ministry of Science and Innovation for the Financial support (grant MINECO: RETOS, AGL2016-79813- C2-2R), and the Ministery of Environment: Endowment for Water, Protected Areas and Wildlife, Panama, (012-37). CS acknowledges partial funding for this work by the Endowment for Water, Protected Areas and Wildlife from the Ministry of Environment of Panama (Desarrollo de un Banco de Microorganismos (BIOBANCO) Panamá). CS and LMC were partially funded by the National System of Investigation of Panama (SNI023-2022) and (SNI60-2022), respectively.

Author contributions

E.O. initiated the project and designed the compounds. N.E. did synthesis, purification and characterization of the compounds obtained, under the supervision of E.O. C.S. designed the biological protocols. L.M.P. and M.G.N. performed bioscreens, antiplasmodial and cytotoxic bioassays. L.M.C. performed mechanistic studies. N.E., E.O. and C.S. wrote the manuscript. C.S. conceptualized and supervised the biological studies. All authors read and approved the final manuscript.

Competing interests

The authors declare no competing interests.

Additional information

Supplementary Information The online version contains supplementary material available at https://doi.org/10.1038/s41598-022-27351-z.

Correspondence and requests for materials should be addressed to C.S. or E.O.

IV. DISCUSIÓN DE RESULTADOS

IV.1. BENZALFTALIDAS Y FTALAZINONAS. Actividad frente a *T. circumcincta*

Las infecciones por helmintos afectan tanto a humanos como a animales. En el caso de los animales, reviste especial atención las infecciones por nematodos gastrointestinales en el ganado rumiante en pastoreo, y sobre todo en el ovino, ya que genera pérdidas económicas elevadas en las explotaciones ganaderas. La administración masiva e incontrolada de fármacos ha generado resistencias a los medicamentos convencionales a nivel mundial, lo que limita el número de fármacos disponibles, existiendo una necesidad urgente de encontrar nuevas alternativas terapéuticas.

Teniendo en cuenta los resultados de actividad de benzalftalidas y ftalazinonas obtenidos previamente por el grupo de investigación, se sintetizaron varios compuestos con estructuras de benzalftalida (Bf **13**-**24**) y ftalazinona (Ft **25**, **31**-**36**). Los derivados de Bf se obtuvieron por dos procedimientos diferentes. El procedimiento ***A***, se basa en reaccionar en un aparato Dean-Stark anhídridos ftálicos con el ácido fenilacético correspondientes en presencia de acetato potásico a 220 ºC. Mientras que en el procedimiento ***B***, se mezclan los reactivos homogéneamente y se irradian en un microondas a 230 ºC durante 20 minutos. Por la vía ***B*** se obtuvieron unos rendimientos ligeramente más altos (46-65%) que con la ***A*** (51-80%). Haciendo reaccionar las Bf-**7** y **19** con las correspondientes hidrazinas y trietilamina a 80 ºC se sintetizaron las Pt **16**, **25**, **30**, **32** y **37**, con rendimientos entre 23 y 77%. El resto de las Pt se obtuvieron por la reacción de **25** con el haluro correspondiente en condiciones básicas.

Seis compuestos (**1**, **7**, **13**, **19**, **26** y **37**) mostraron inhibición de la eclosión de huevos en cepa sensible de *T. circumcincta* superior al 96% a una concentración de 50 μg/mL. Entre ellos, destacan la Bf **19** (R_1 = 5(6)-CH_3; R_2 = 4´-Cl) y la Ft **26** (R_1 = H; R_2 = CH_3) con un valor de inhibición del 100% y unos índices de selectividad (IS) por encima de 10. El compuesto **26** mostró una actividad del 99% en la prueba de mortalidad de larvas en la cepa sensible y, además, mostró una inhibición de la eclosión de huevos mayor en la cepa resistente de *T. circumcincta* a 10 μg/mL (99,4%) que en la cepa sensible (76,1%).

IV.2. BENZIMIDAZOLES TIPO I. Actividad frente a *T. circumcincta*

Los compuestos con núcleo de benzimidazol (Bz) (albendazol, fenbendazol, mebendazol, entre otros) son los más frecuentemente utilizados para el tratamiento de las infecciones por nematodos gastrointestinales. Se sabe que actúan sobre el sitio de colchicina de la β-tubulina inhibiendo la formación de los microtúbulos, lo que conduce a la destrucción de la estructura celular y por tanto a la muerte del parásito. Además, se conocen las principales mutaciones asociadas al desarrollo de resistencias, que afectan a tres aminoácidos fundamentalmente (F167Y, E198A y F200Y) y producen una disminución en la afinidad por la β-tubulina, y por tanto la reducción en la eficacia del fármaco. Estos fármacos presentan un fragmento de carbamato en la posición C-2 del Bz, por lo que se decidió sustituir dicho fragmento por otro rico en electrones de tipo fenilo con diferentes sustituciones.

Se puso a punto el proceso de obtención de los Bzs, que se abordó por dos vías diferentes. La ruta ***A***, implica dos pasos de reacción, en el primero se obtienen las sales de sodio de los 1-hidroxifenilmetanosulfonatos a partir de los correspondientes aldehídos, que se consigue con un rendimiento del 100%, éstas se han reaccionar con las *orto*-fenilendiaminas sustituidas en presencia de DMF y a 110-120 ºC, generando los Bzs con rendimiento del 43 a 87%. La ruta ***B*** es directa, haciendo reaccionar las *orto*-fenilendiaminas con los aldehídos en presencia de metabisulfito sódico en las mismas condiciones anteriores, generando los Bzs con rendimientos del 40 al 73%. En general la vía ***A*** produce unos rendimientos ligeramente superiores a la ***B***.

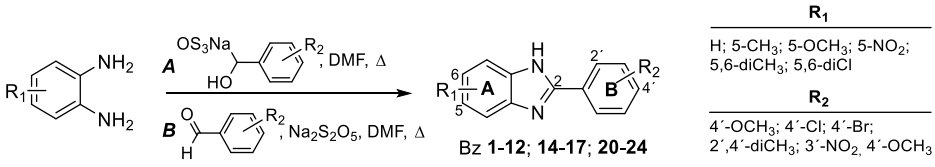

Esquema IV.2.1. Procesos de síntesis para la obtención de derivados de 2-fenilbenzimidazol.

Los Bzs **13**, **18** y **19** se obtuvieron por reducción con H_2/Pd-C a partir de sus respectivos nitro-derivados.

Todos los compuestos obtenidos fueron caracterizados convenientemente según sus propiedades fisicoquímicas. Así, los puntos de fusión van de 112 a 307 ºC; en los espectros

de IR se observan bandas intensas correspondiente al fragmento de Bz a 3315 (N-H), 1613 y 1535 (Ar C-C), 1460 y 1384 (C=N) cm^{-1}, además de las correspondientes a las distintas sustituciones como son, C-Cl a 676 cm^{-1}, C-NO_2 a 1511 y 1349 cm^{-1}, C-NH_2 a 3306 y 1340 cm^{-1}. Las moléculas son bastante polares por lo que hubo que hacer los espectros de RMN ^1H y ^{13}C en metanol-d_4 o DMSO-d_6, a modo de ejemplo se indican los desplazamientos del compuesto **2** (R_1 = H, R_2 = *p*-Cl), uno de los compuestos más potentes ensayados, ^1H RMN (400 MHz, CD_3OD): δ 7,27 (2H, m), 7,57 (2H, d, *J* = 8.0 Hz), 7,61 (2H, m), 8,06 (2H, d, *J* = 8,0 Hz). ^{13}C NMR (100 MHz, CD_3OD): δ 124,2 (2C), 129,3 (4C), 129,6, 130,4 (2C), 137,4 (3C), 152,2. HRMS (ESI^+) calcd. para $C_{13}H_{10}ClN_2$ $[M+H]^+$: 229,0533, encontrada: 229,0536.

Todos los compuestos sintetizados fueron ensayados frente a una cepa sensible de *T. circumcincta*, determinando el efecto ovicida (inhibición de la eclosión de los huevos), Tabla IV.2.1. Aquellos compuestos que mostraron una actividad ovicida >98% se probaron también frente a una cepa resistente. Adicionalmente, se evaluó la citotoxicidad en células Caco-2 y HepG2 humanas.

Se obtuvieron tres Bz sin sustitución en anillo A (compuesto **1**, **2** y **3**), 19 monosustituidos (de **4** a **22**) y 2 disustituidos (**23** y **24**). Sobre el anillo B presentan mono- o di-sustituciones con átomos dadores (CH_3, OCH_3, NH_2) y atractores de electrones (Cl, Br, NO_2).

Todos los compuestos fueron ensayados a una concentración de 50 µM. Atendiendo a la relación entre la estructura y la actividad de los Bzs, los compuestos **1** (R_2 = 4´-OCH_3), **2** (R_2 = 4´-Cl) y **3** (R_2 = 4´-Br); **4** (R_1 = 5-CH_3, R_2 = 4´-OCH_3) y **5** (R_1 = 5-CH_3, R_2 = 4´-Cl); **8** (R_1 = 5-Cl, R_2 = 4´-OCH_3) y **9** (R_1 = 5-Cl, R_2 = 4´-Cl); y **21** (R_1 = 5-OCH_3, R_2 = 4´-Cl) y **22** (R_1 = 5-OCH_3, R_2 = 4´-Br) fueron capaces de detener la eclosión de huevos de *T. circumcincta* de cepa sensible en más del 98%. Se observa una clara preferencia por determinados sustituyentes en C-4´ del fenilo (anillo B) en relación la potencia antihelmíntica. Así, la presencia de agrupaciones 4´-OCH_3, 4´-Br o 4´-Cl aumentaron el efecto en mayor medida. Compuestos que análogamente en R_1 mostraban CH_3, Cl, OCH_3 (o no sustitución).

Tabla IV.2.1. Efecto inhibitorio de los Bz sobre la eclosión de huevos en cepas sensible y resistentes de *T. circumcincta*. Índices de citotoxicidad y selectividad.

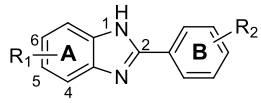

Compuesto			*T. circumcincta* cepa sensible		*T. circumcincta* cepa resistente		Citotoxicidad [a]		Índices de selectividad [b]			
Bz	**R_1**	**R_2**	**Inhib. eclosión** % a 50 µM	**Ovicida** CE_{50}, µM	**Inhib. eclosión** % a 50 µM	**Ovicida** CE_{50}, µM	**Caco-2**	**HepG2**	**IS*s*** Caco-2	**IS*r*** Caco-2	**IS*s*** HepG2	**IS*r*** HepG2
1	H	4-OCH_3	**100**	**15,78 ± 0,12**	18,2	>50	56,80 ± 8,12	43,08 ± 3,42	3,60	<1	2,73	<1
2	H	4-Cl	**99,5**	**9,04 ± 0,23**	**86,4**	**14,47 ± 1,05**	42,63 ± 6,50	51,46 ± 6,27	**4,72**	2,94	**5,69**	3,56
3	H	4-Br	**99,8**	**6,30 ± 0,23**	65,8	<50	39,17 ± 2,46	38,36 ± 2,36	**6,22**	*nc*	**6,09**	*nc*
4	5-CH_3	4-OCH_3	**100**	**12,21 ± 0,29**	**81,1**	**24,80 ± 0,99**	11,60 ± 3,42	18,75 ± 1,92	0,95	0,47	1,53	0,76
5	5-CH_3	4-Cl	**99,5**	**15,23 ± 0,78**	71,8	<50	28,06 ± 1,35	27,11 ± 1,69	1,84	<1	1,78	<1
6	5-CH_3	2,5-diCH_3	0,80	>50	na	nc	9,14 ± 232	>25	nc	nc	nc	nc
7	5-CH_3	3-NO_2, 4-OCH_3	1,11	>50	na	nc	9,07 ± 2,35	>25	nc	nc	nc	nc
8	5-Cl	4-OCH_3	**100**	**13,74 ± 0,46**	**89,6**	**25,76 ± 3,48**	37,38 ± 3,38	36,03 ± 3,02	2,72	1,45	2,62	1,39
9	5-Cl	4-Cl	**99,6**	**6,54 ± 0,40**	**94,0**	**20,90 ± 0,50**	22,58 ± 1,69	17,54 ± 0,91	3,45	1,08	2,68	0,84
10	5-Cl	4- NO_2	1,25	>50	na	nc	19,14 ± 2,05	21,73 ± 1,65	nc	nc	nc	nc
11	5-Cl	2,5-diCH_3	4,00	>50	na	nc	23,28 ± 2,47	30,22 ± 3,35	nc	nc	nc	nc
12	5-Cl	3-NO_2, 4-OCH_3	0,97	>50	na	nc	67,31 ± 15,31	53,43±16,61	nc	nc	nc	nc
13	5-Cl	3-NH_2, 4-OCH_3	1,00	>50	na	nc	34,70 ± 4,32	44,91 ± 5,94	nc	nc	nc	nc
14	5-NO_2	4-OCH_3	3,16	>50	na	nc	14,37 ± 3,69	22,98±19,57	nc	nc	nc	nc
15	5-NO_2	4-Cl	1,61	>50	na	nc	12,29 ± 1,09	14,64 ± 0,83	nc	nc	nc	nc
16	5-NO_2	2,5-diCH_3	4,02	>50	na	nc	16,78 ± 9,16	>12,5	nc	nc	nc	nc
17	5-NO_2	3-NO_2, 4-OCH_3	0,88	>50	na	nc	13,38 ± 3,02	13,64 ± 4,85	nc	nc	nc	nc
18	5-NH_2	4-OCH_3	0,50	>50	na	nc	>25	>50	nc	nc	nc	nc
19	5-NHpic [c]	4-OCH_3	17,1	>50	na	nc	83,17 ± 45,84	22,76 ± 2,08	nc	nc	nc	nc
20	5-OCH_3	4-OCH_3	44,1	>50	na	nc	21,80 ± 1,47	19,11 ± 3,68	nc	nc	nc	nc
21	5-OCH_3	4-Cl	**98,2**	25,60 ± 1,25	70,6	<50	28,94 ± 1,47	21,33 ± 1,20	1,13	nc	0,83	nc
22	5-OCH_3	4-Br	**99,9**	**15,34 ± 0,55**	**98,9**	**15,99 ± 0,42**	21,69 ±1,61	13,48 ± 0,64	1,41	1,36	0,87	0,84
23	5,6-diCH_3	4-OCH_3	17,4	>50	na	nc	13,01 ± 1,23	31,66 ± 4,09	nc	nc	nc	nc
24	5,6-diCl	4-OCH_3	0,44	>50	na	nc	16,68 ± 1,46	26,37 ± 2,29	nc	nc	nc	nc
	Tiabendazol (TBZ)		100	0,43 ± 0,02	100	1,53 ± 0,06	>300	>300	*>697*	*>196*	*>697*	*>196*

[a] Determinado por el método Alamar Blue. [b] Índice de selectividad: IS = CC_{50}(Caco-2 o HepG2) / CE_{50}(*T.c.*), relativo a cepas susceptibles (ISs) y resistentes (ISr). [c] picolinamida; na: no apreciable; nc: no calculado. Los valores de inhibición de eclosión **>80%** y **>90%**, los valores de CE_{50} **<10** y **<20 µM** y los valores IS **> 4** se han resaltado en negrita para facilitar las comparaciones. En **azul** compuestos con actividad menor a 26 µM en cepa resistente.

Además, **2**, **4**, **8**, **9** y **22** produjeron una inhibición significativa de la eclosión de los huevos, entre un 81,1 y un 98,9%, en la cepa resistente de *T. circumcincta* utilizada en el estudio. Sorprendentemente, a pesar de la similitud estructural de Bz **1** con las sustancias más potentes de la serie, este compuesto pierde gran parte de su capacidad inhibitoria frente a la cepa resistente, Tabla IV.2.1.

Adicionalmente, se ensayó la actividad larvicida de **4**, **9** y **22** en ambas cepas de *T. circumcincta,* Tabla IV.2.2. Se observa que Bz **9** y **22** ensayados a dosis 50 µM mataron

prácticamente todas las larvas L1 tanto en la cepa sensible como en la resistente. Posteriormente, se calculó el valor de CE_{50} en ambas cepas, siendo de 5,01 y 28,06 μM en la cepa sensible y 11,66 y 28,99 μM en la resistente para los derivados **9** y **22**, respectivamente. Estos valores son dos órdenes más bajos del encontrado para el compuesto de referencia levamisol (LEV) con CE_{50} = 1782 y 2410 en cepa sensible y resistente, respectivamente. Además, el compuesto más potente, Bz **9**, mostró un valor SI y SIr mejor que LEV.

Tabla IV.2.2. Efectos larvicidas de los Bz activos sobre larvas sensible y resistentes de *T. circumcincta.*

	***T. circumcincta* L1** cepa sensible		***T. circumcincta* L1** cepa resistente		**Citotoxicidad** [a]	**Índice Selectividad**[b]	
Bz	**Mortalidad** % a 50 μM	**Larvicida** CE_{50} μM	**Mortalidad** % a 50 μM	**Larvicida** CE_{50} μM	**Caco-2** CC_{50} μM	**SI*s*** Caco-2	**SI*r*** Caco-2
4	40,9	>50	*nt*	*nd*	11,60 ± 3,42	0,95	0,47
9	100	**5,01 ± 0,04**	100	**11,66 ± 0,21**	22,58 ± 1,69	**4,51**	1,94
22	100	**28,06 ± 2,95**	99,3	**28,99 ± 3,32**	21,69 ± 1,61	0,77	0,75
LEV	0	1782 ± 26	0	2410 ± 23	2912 ± 970	1,63	1,20

[a,b] reproducido de la Tabla 1 para comparación con el compuesto de referencia levamisol (LEV). IS = CC_{50}(Caco-2) / CE_{50}(L1). *s*,*r*: relacionado con L1 y cepas sensibles y resistentes, respectivamente. *nd:* no determinado**.** *nt*: no testado. EC_{50} valores **< 10** y **< 30** μM y SI valores **>4** puestos en negrita para facilitar la comparación.

Con el fin de justificar la diferente actividad encontrada para algunos Bzs frente a cepas sensibles y resistentes de *T. circumcincta*, y para comprender mejor la base molecular de sus propiedades inhibidoras, se realizaron estudios de docking y modelado molecular de todos los compuestos descritos en este estudio. Así, se buscó la secuencia de β–tubulina de *T. circumcincta* y se obtuvo la estructura 3D por homología molecular con la herramienta SWISS-MODEL Workspace, que posteriormente fue validada con el servidor Rampage (http://mordred.bioc.cam.ac.uk/~rapper/rampage.php), observándose un 92,7% de homología en la región requerida.

El sistema de Bz en los compuestos con $R_1 \neq H$ puede dar lugar a mezclas tautoméricas. Por lo que se hicieron cálculos computacionales al nivel DFT, MN15/6-31+G(d,p) para ambos tautómeros con los Bz más potentes, observándose que el tautómero con el sustituyente en C-6 (B) es unas 0,5-1 kcal/mol más estable que el sustituido en C-5 (A) (Esquema IV.2.2), y ha de ser la forma predominante a nivel del receptor.

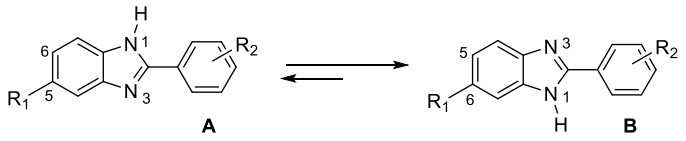

Esquema IV.2.2. Cambio de equilibrio tautomérico y numeración sistemática para los Bzs mono-sustituidos no simétricos.

La predicción del ranking de actividad de los Bzs por el sistema de acoplamiento en el modelo de homología de tubulina de *T. circumcincta* está de acuerdo con los resultados de actividad ovicida (CE_{50}) obtenidos experimentalmente. De hecho, los Bzs más potentes (ver Tabla IV.2.1) aparecen posicionados en los primeros lugares del ranking energético según la función GlideScore implementada en GLIDE. Curiosamente, la conformación activa de los compuestos más activos corresponde a la del tautómero de menor energía. En la Fig. IV.2.1 se muestran las poses de acoplamiento de los ligandos más significativos y en la Fig. IV.2.2 los mapas 2D.

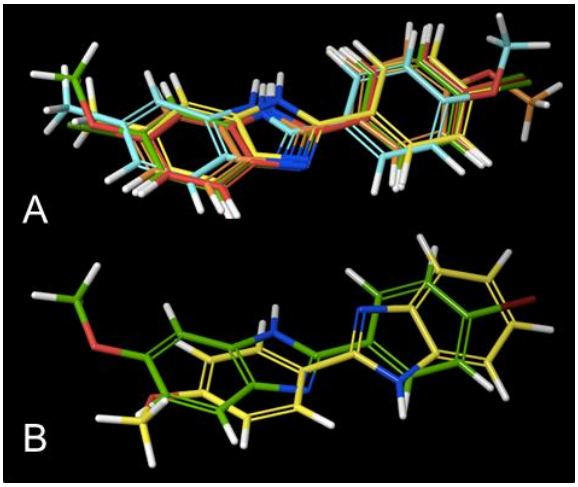

Figura IV.2.1. A: Superposición de los BZs más potentes (4: azul, 5: amarillo, 8: marrón, 9: rojo, y 22: verde) en el sitio de colchicina de la tubulina de *T. circumcincta*. B: Superposición de los Bzs 1 (amarillo) y 22 (verde).

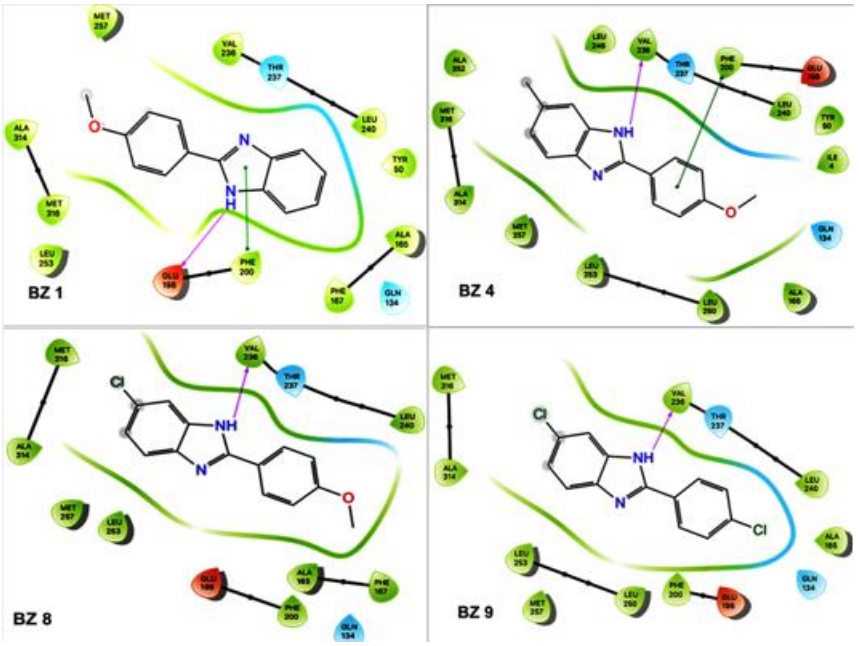

Figura IV.2.2. Mapas de interacción 2D de algunos Bzs, obtenidos de los estudios docking sobre el sitio de colchicina de la tubulina de *T. circumcincta.*

Se observó que, en el sitio de unión de la colchicina, los compuestos más activos establecen, normalmente, un enlace por puente de hidrógeno con carbonilo del péptido Val236 a través de su BzN-H que actúa como donante. Además, algunos de los Bzs más potentes presentan interacciones de apilamiento π entre el Bz y la tubulina Phe200 (Fig. IV.2.3).

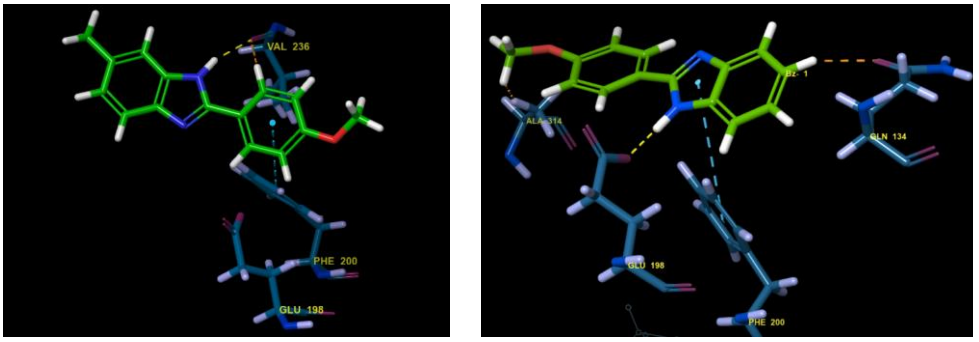

Figura IV.2.3. Bz 4 establece un puente de hidrogeno (líneas discontinuas de color amarillo) entre su 1-BzN-H y el carbonilo de la amida Val236 *(izquierda*), mientras que Bz 1 establece enlaces por puente de hidrogeno con el Glu198 (*derecha*).

Curiosamente, como se muestra en las Fig. IV.2.2 y IV.2.3, el Bz **1** sin sustituyente en el anillo A, interactúa con la tubulina de manera inversa a la mayoría de los compuestos de la serie (también se observa en el Bz **8**). Es decir, establece el enlace del BzN-H con el grupo γ-carboxilo de Glu198 en lugar del carbonilo de la amida en Val236, que es el aceptor de enlace H común para la mayoría de los Bz, y que adicionalmente muestran interacciones de apilamiento π con el grupo fenilo de Phe200 a través de su núcleo de imidazol (Fig. IV.3 *izda*). Este modelo diferente de interacción podría explicar la pérdida de actividad de Bz **1** frente a las cepas resistentes. De hecho, como se describe en la bibliografía[163] las mutaciones asociadas con cepas resistentes a Bz para *T. circumcincta* y *Haemonchus contortus* son en realidad Phe167Tyr, Glu198Ala y Phe200Tyr, y como se muestra gráficamente Glu198 y Phe200 están directamente involucradas en interacciones tubulina-Bzs, que deberían resultar perturbadas en cierta medida por tales mutaciones.

De este trabajo se concluye que algunos 2-fenilbenzimidazoles mostraron actividad ovicida remarcable frente a *T. circumcincta* en cepa sensible (>98%) y resistente (>80%) a 50 μM. Siendo **3** el Bz más potente en la cepa sensible (CE_{50} de 6,30 μM y IS de 6,22) y **2** (CE_{50} de 14,47 μM y IS de 2,94) en la resistente. Los Bz **9** y **22** produjeron la inhibición de la motilidad y la muerte en L1 de *T. circumcincta*, aunque ninguno de ellos mostró una inhibición significativa de la motilidad en la etapa L3. Esto representa el punto de partida de investigaciones más profundas y completas para obtener mejores candidatos con efectos sobre las larvas L3, una mayor potencia nematicida y una mayor selectividad.

[163] Beech, R.N.; Skuce, P.; Bartley, D.J.; Martin, R.J.; Prichard, R.K.; Gilleard, S. Anthelmintic resistance: markers for resistance or susceptibility? *Parasitology* **2010**, 138(2), 160e174. doi: 10.1017/S0031182010001198

IV.3. BENZIMIDAZOLES TIPO II-IV. Actividad frente a *T. circumcincta*

En este trabajo, se buscó progresar en la búsqueda de nuevas moléculas con esqueleto base de benzimidazol (Bz) que fueran más potentes y selectivas que las obtenidas con anterioridad, y que pudieran utilizarse como tratamiento alternativo para las infecciones por helmintos gastrointestinales en el ganado ovino en pastoreo. Para ello, se diseñó un cribado computacional por docking con más de cien estructuras nuevas y diversos grupos funcionales (atractores, dadores de electrones), considerando además los diferentes tautómeros y especies protonadas.

Los valores de XP obtenidos del docking GLIDE para estas estructuras eran inferiores a -10 kcal/mol, mejorando los valores previos de los 2-fenilbenzimidazoles (-9 kcal/mol) del Artículo 2, y que podría deberse a una mayor interacción entre las nuevas moléculas y la diana. Así, se observaron nuevas interacciones Bz-β-tubulina, como por ejemplo el enlace por puente de hidrógeno (enlace H) entre el fragmento de imidazol y el residuo Glu198 de la β-tubulina, junto a las ya conocidas en los 2-fenilBz: enlace H con la Val236 y de apilamiento π con el aminoácido Phe200 de la β-tubulina de *Teladorsagia circumcincta*.

Estos estudios condujeron a la selección de tres grupos estructurales de Bz, compuestos que mostraban un espaciador entre el anillo de Bz y el aromático/hetearomático (**B**) con función de amina (tipo II), amida (tipo III) y acetamida (tipo IIIa, en el artículo tipo IV), es decir, son Bz que muestran un grupo amino en C-2 y por tanto contienen un fragmento de guanidina, Fig. IV.3.1, lo que posibilita la existencia de diferentes formas tautoméricas a nivel del receptor. Se puso a punto el método de obtención de las diferentes familias, se purificaron e identificaron adecuadamente los compuestos obtenidos y se prepararon las muestras para ensayo in vitro frente a huevos y larvas de *T. circumcincta*. Todos los compuestos fueron ensayados a una concentración fija de 50 μM; para aquellos Bz que mostraron una inhibición superior al 90% se calculó la CE_{50} y se determinó su toxicidad en células Caco-2 y HepG2 con el fin de calcular el índice de selectividad.

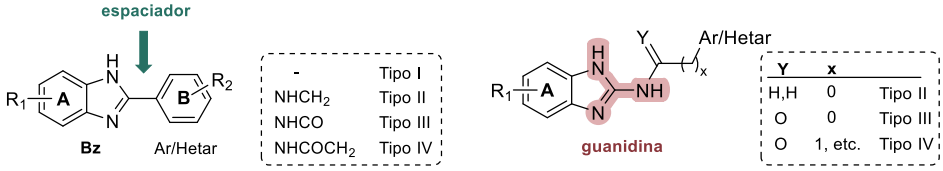

Figura IV.3.1. Estructura general de los nuevos benzimidazoles.

Los nuevos compuestos tipo I fueron obtenidos siguiendo el método ***B*** descrito en el Artículo 2, en el cual se hacen reaccionar la *o*-fenilendiamina correspondiente con un arilaldehído en presencia de metabisulfito sódico ($Na_2S_2O_5$) y DMF como disolvente, manteniendo la mezcla durante 16 horas a reflujo. Bz **4** se obtuvo por reducción del nitro derivado de **3** con H_2/Pd-C con un rendimiento del 90%. Los compuestos **5** a **10** fueron sintetizados a partir del Bz **4** con unos rendimientos entre 65 y 94%. Así, tratando la amina **4** con dicarbonato de di-*terc*-butilo (Boc_2O) se obtiene el carbamato **5**, mientras que el tratamiento con cloruro de tosilo en presencia de trietilamina conduce a la sulfamida **6**. Las amidas **7**, **8** y **9** se obtuvieron por acoplamiento de la amina **4** con el ácido correspondiente utilizando de 1,1´-carbonildiimidazol (CDI) como agente acoplante . Por último, la desprotección del grupo *terc*-butoxicarbonilo (Boc) en el compuesto **9** con ácido trifluoroacético dio lugar a la aminoamida **10**, Esquema IV.3.1.

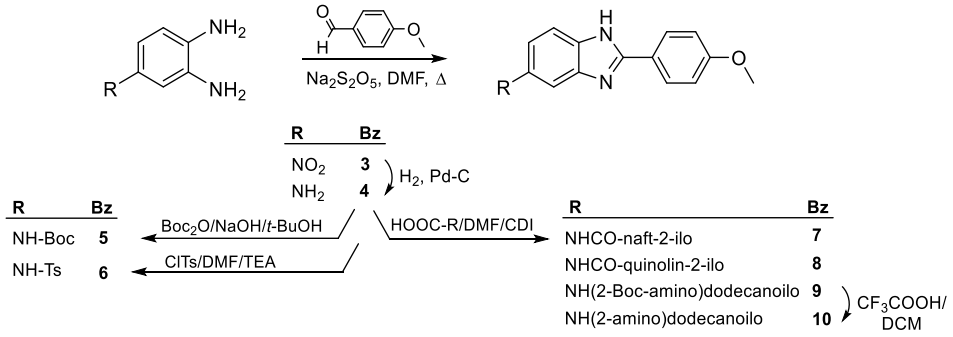

Esquema IV.3.1. Esquema de obtención de los benzimidazoles **4** a **10**.

La obtención de los derivados de tipo II, III y IV, se realiza en un proceso de dos pasos. En primer lugar, ha de obtenerse la correspondiente amina intermedia (Bz*i*) por tratamiento de la *o*-fenilendiamina con bromuro de cianógeno en metanol/agua v/v al 50%, a temperatura ambiente durante 72 horas generando los Bz*i* con rendimiento entre 62 y 85%. La síntesis de los derivados tipo II se realiza por condensación de la correspondiente Bz*i* con un aldehído, en etanol absoluto y presencia de ácido acético glacial a 60 °C durante 22 horas, seguido de reducción de la imina con borohidruro de sodio ($NaBH_4$) con rendimientos entre 17 y 57%. La obtención de los compuestos tipo III y IV se realiza por tratamiento de la Bz*i* con un ácido y CDI como agente acoplante, a temperatura ambiente durante 16 horas, con rendimientos del 17 al 73%, Esquema IV.3.2.

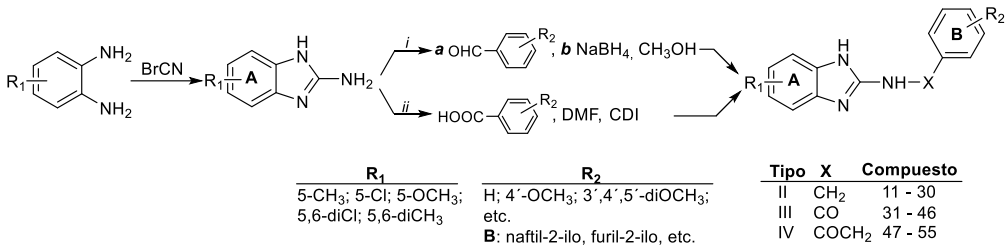

Esquema IV.3.2. Esquema de obtención de los benzimidazoles **tipo II**, **III** y **IV**.

Se estableció de manera inequívoca la estructura de todos los compuestos obtenidos mediante técnicas espectroscópicas de IR, HRMS, RMN ^{1}H, RMN ^{13}C, y 2D-RMN en algunos casos. Así, los puntos de fusión de los derivados de tipo I van de 103 a 257 °C, los del tipo II de 107 a 210 °C y los del tipo III y IV de 105 a 336 °C. En los espectros de IR se observan bandas de absorción a 3315 (N-H), 1613 y 1535 (Ar C-C), 1460 y 1384 (C=N) cm^{-1} del fragmento de 2-aminoBz, además de las correspondientes a las distintas sustituciones como, C-Cl a 650 cm^{-1}, C-NO_2 a 1550 y 1350 cm^{-1}, C-NH_2 a 3350 y 1300 cm^{-1}. Los espectros de RMN ^{1}H y ^{13}C se hicieron en cloroformo-d, metanol-d_4 o DMSO-d_6, a modo de ejemplo se indican los desplazamientos del Bz **42** (tipo III, R_1 = OCH_3, R^2 = NHCO-piridin-2-ilo), uno de los compuestos obtenidos más potentes. ^{1}H RMN (400 MHz, $CDCl_3$): δ 8,57 (1H, ddd, J_1 = 5,5; J_2 = 1,9; J_3 = 0,9 Hz, H-6'), 8,26 (1H, ddd, J_1 = 7,6; J_2 = 1,6; J_3 = 0,9 Hz, H-3'), 7,89 (1H, ddd, J_1 = 7,6; J_2 = 7,5; J_3 = 1,9 Hz, H-4'), 7,50 (1H, ddd, J_1 = 7,5; J_2 = 5,5; J_3 = 1,6 Hz, H-5'), 7,40 (1H, d, J = 8,0 Hz, H-7), 7,02 (1H, sa, H-4), 6,86 (1H, d, J = 8,0 Hz, H-6), 3,82 (3H, s, OCH_3). ^{13}C RMN (100 MHz, $CDCl_3$): δ 163,5 (NHCO), 156,2 (C-5), 148,7 (C-6'), 148,2 (C-2'), 147,9 (C-2), 137,0 (C-4'), 137,0 (C-3a), 129,9 (C-7a), 127,3 (C-5'), 122,7 (C-3'), 111,2 (C-6), 100,8 (C-7), 108,5 (C-4), 55,8 (OCH_3).

Se realizaron ensayos in vitro de los 55 Bz obtenidos frente a la cepa sensible de *T. circumcincta*, en los que se evaluó la actividad ovicida (mediante el ensayo de inhibición de eclosión de huevos) y larvicida (ensayo de inhibición de migración de larvas), utilizando como fármacos de referencia tiabendazol y levamisol, para el primer y segundo ensayo, respectivamente, Tablas IV.3.1 a IV.3.3.

Se obtuvieron diez derivados de tipo I, todos ellos con una agrupación 4´-metoxifenilo en C-2. En relación con las sustituciones sobre el anillo A, uno de los compuestos no muestra sustitución, Bz **1**, los compuestos **2** y **4** presentan grupos dadores de electrones (CH_3, NH_2),

el **3** un atractor de electrones (NO_2), y los derivados **5** a **10** grupos voluminosos sobre una agrupación tipo amida, Fig. IV.3.2.

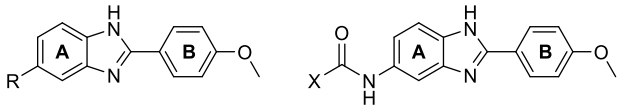

Figura IV.3.2. Estructura general de los benzimidazoles tipo I.

Solo los compuestos **1** (R_1 = H) y **2** (R_1 = CH_3) fueron capaces de inhibir la eclosión de huevos en un 100%, y el **2** además inhibió la migración de larvas en un 40,9%. Los derivados amídicos **6** (X = tosilo), **7** (X = 2-naftilmetilo), **8** (X = quinolin-2-ilo) y **9** (X = 2-Boc-aminododecanoilo) mostraron buena inhibición de migración larvaria con valores entre 39,1 y 48,9%, semejante a la encontrada para el compuesto **2,** Tabla IV.3.1.

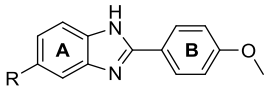

Tabla IV.3.1. Inhibición de eclosión de huevos y migración de larvas de *T. circumcincta* por derivados tipo I.

		Inhibición % (a 50 μM)	
Bz (I)	**R**	**Eclosión de huevos (EH)**	**Migración de larvas (LM)**
1	H	**100** [a]	nc
2	CH_3	**100** [a]	**40,9** [a]
3	NO_2	3,2 [a]	nc
4	NH_2	<1 [a]	nc
5	BocNH	<1	8,7
6	tosiloNH	<1	**48,9**
7	2-naftiloCH_2CONH	<1	**43,8**
8	2-quinoliniloCONH	<1	**38,7**
9	2-Boc-aminododecanoilo-NH	<1	**39,1**
10	2-aminododecanoilo-NH	1,4	13,2
Tiabendazol		**100**	nc
Levamisol		nc	**100**

Boc = *terc*-butoxicarbonilo; nc: no calculado; [a] Resultados del Artículo 2. Valores de EHI >90% y valores LMI >25% se indican en negrita.

Se obtuvieron 20 derivados del tipo II, sobre el anillo A muestran sustituciones con átomos dadores (CH_3, OCH_3) y atractores de electrones (Cl). De ellos, 15 presentan mono-sustitución (de **11** a **25**) y 5 disustitución (de **26** a **30**). Sobre el anillo B presentan fragmentos aromáticos (fenilo, naftilo) y heteroaromáticos (furilo, tienilo).

Desafortunadamente, ningún Bz de tipo II mostró inhibición de la eclosión de huevos, (valores <1%). Sin embargo, 7 inhibieron la migración de larvas, **11** (R = CH_3, **B** = fenilo), **12**

(R = CH_3, **B** = 4´-metoxifenilo), **13** (R = CH_3, **B** = 2´,3´,4´-trimetoxifenilo), **14** (R = CH_3, **B** = naft-2-ilo), **26** (R = diCH_3, **B** = 4´-metoxifenilo), **28** (R = diCl, **B** = fenilo) y el **29** (R = diCl, **B** = 4´-metoxifenilo) con unos valores entre 26,5 y 54,9%. Se observa con relación al anillo A una preferencia por átomos dadores de electrones [mono-metilo (**11**, **12**, **13**, **14**) o di-metilo (**26**)]. En relación con el anillo B, ninguno de los compuestos de tipo heterocíclico (furilo, 5-metilfur-2-ilo, tienilo) mostró algún tipo de actividad, existiendo una clara preferencia por un fragmento de fenilo sin sustituir, o con sustituciones (4´-metoxifenilo, 2´,3´,4´-trimetoxifenilo, 3´,4´,5´-trimetoxifenilo), incluso de tamaño mayor como el naft-2-ilo.

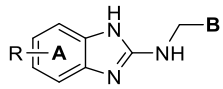

Tabla IV.3.2. Inhibición de eclosión de huevos y migración de larvas de *T. circumcincta* por derivados tipo II.

			Inhibición % (a 50 µM)	
Bz (II)	**R**	**B**	**Eclosión de huevos (EH)**	**Migración de larvas (EH)**
11	5-CH_3	fenilo	1,1	**36,3**
12	5-CH_3	4´-OCH_3fenilo	1,1	**40,3**
13	5-CH_3	2´,3´,4´-triOCH_3fenilo	<1	**54,9**
14	5-CH_3	naft-2-ilo	<1	**41,5**
15	5-CH_3	furan-2-ilo	<1	22,5
16	5-CH_3	tiofen-2-ilo	<1	<1
17	5-Cl	fenilo	<1	4,6
18	5-Cl	4´-OCH_3fenilo	<1	12,1
19	5-Cl	3´,4´,5´-triOCH_3fenilo	<1	1,4
20	5-Cl	furan-2-ilo	1,7	9,2
21	5-OCH_3	fenilo	<1	10,7
22	5-OCH_3	4´-OCH_3fenilo	1,1	14,6
23	5-OCH_3	4´-(1-pirrolidinil)fenilo	1,0	16,4
24	5-OCH_3	5´-CH_3fur-2-ilo	<1	15,8
25	5-OCH_3	tiofen-2-ilo	<1	20,0
26	5,6-diCH_3	4´-OCH_3fenilo	<1	**49,8**
27	5,6-diCH_3	3´,4´,5´-triOCH_3fenilo	<1	<1
28	5,6-diCl	fenilo	2,1	**31,9**
29	5,6-diCl	4´-OCH_3fenilo	1,3	**26,5**
30	5,6-diCl	3´,4´,5´-triOCH_3fenilo	<1	<1
Tiabendazol			**100,0**	nc
Levamisol			nc	**100,0**

nc: no calculado. Valores de LMI >25% se indican en negrita.

Se obtuvieron 16 BZ de tipo III (**31**-**46**) y 9 de tipo IV (**47**-**55**), con sustituciones análogas al tipo II, sobre el anillo A átomos dadores y atractores de electrones, mono- y di-sustituciones y sobre anillo B grupos aromáticos o heteroaromáticos.

Los compuestos **31** (R = CH_3, **B** = fenilo), y **43** (R = diCH_3, **B** = fenilo), mostraron muy buena inhibición de la eclosión de huevos, 95,5 y 91,2, respectivamente. Además, los Bz **36** (R = CH_3, **B** = piridin-2-ilo), **37** (R = Cl, **B** = fenilo), **39** (R = Cl, **B** = piridin-2-ilo), **40** (R = OCH_3, **B**

= fenilo) y **42** (R = OCH_3, **B** = piridin-2-ilo), produjeron una inhibición de 100%. El compuesto **39**, inhibió también la migración de larvas en un 51,2%. Entre los compuestos del tipo IV, los Bz **48** (R = CH_3, **B** = α-hidroxibencilo), **50** (R = CH_3; **B** = 2-tiofenilmetil) y **53** (R = 5,6-diCl, **B** = 3-aminobencilo) produjeron la inhibición de migración de larvas entre 25,5 y 41,2%. Se observa que un fenilo o un piridin-2-ilo en B confiere actividad ovicida al Bz. Sin embargo, no se ve una clara preferencia por los sustituyentes del anillo A, aunque sí parece haber una preferencia por sistemas monosustituídos.

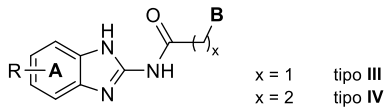

Tabla IV.3.3. Inhibición de eclosión de huevos y migración de larvas de *T. c.* en derivados tipo III y IV.

			Inhibición % (a 50 μM)	
Bz (III)	**R_1**	**R_2**	**Eclosión de huevos (EH)**	**Migración de larvas (LM)**
31	5-CH_3	fenilo	**95,5**	<1
32	5-CH_3	4′-OCH_3fenilo	<1	8,8
33	5-CH_3	2′-Cl,5′-NO_2fenilo	<1	22,5
34	5-CH_3	3′,5′-diOCH_3fenilo	<1	<1
35	5-CH_3	3′,4′,5′-triOCH_3fenilo	<1	6,9
36	5-CH_3	piridin-2-ilo	**100,0**	<1
37	5-Cl	fenilo	**100,0**	<1
38	5-Cl	4′-OCH_3fenilo	39,9	<1
39	5-Cl	piridin-2-ilo	**100,0**	**51,2**
40	5-OCH_3	fenilo	**100,0**	15,1
41	5-OCH_3	4′-OCH_3fenilo	<1	<1
42	5-OCH_3	piridin-2-ilo	**100,0**	<1
43	5,6-diCH_3	fenilo	**91,2**	7,2
44	5,6-diCH_3	4′-OCH_3fenilo	<1	<1
45	5,6-diCl	fenilo	<1	3,6
46	5,6-diCl	4′-OCH_3fenilo	<1	3,3
Bz (IV)				
47	5-CH_3	3′-NO_2bencilo	<1	21,9
48	5-CH_3	α-OHbencilo	<1	**34,2**
49	5-CH_3	2′-naftilmetilo	<1	2,3
50	5-CH_3	2′-tienilmetilo	1,0	**25,5**
51	5,6-diCH_3	3′-Clbencilo	<1	2,5
52	5,6-diCl	3′-NO_2bencilo	<1	15,1
53	5,6-diCl	3′-NH_2bencilo	<1	**41,2**
54	5-OCH_3	1-Boc-aminododecanoilo	<1	20,4
55	5-OCH_3	1-aminododecanoilo	<1	<1
Tiabendazol			**100,0**	nc
Levamisol			nc	**100,0**

nc: no calculado. Los valores de EHI >90% y los valores LMI >25% se indican en negrita.

En la siguiente etapa se seleccionaron los compuestos que presentaron una actividad EH >90% y se determinó la CE_{50}, también, se evaluaron los valores CC_{50} de citotoxicidad en Caco-2 y HepG2 para calcular los índices de selectividad (IS), Tabla IV.3.4.

Tabla IV.3.4. Valores de CE_{50} de los compuestos más potentes frente a la eclosión de huevos de *T. circumcincta*, citotoxicidad en células HepG2 e índices de selectividad (IS).

Bz	***T. circumcincta* EHI,** CE_{50} (μM)	**Citotoxicidad** [a] (CC_{50}, μM)	**IS** [b]
31	1,51±0,03	**27,59 ± 10,40**	18,3
36	1,52±0,03	**36,91 ± 8,08**	**24,3**
37	1,58±0,03	**>50** [c]	**>31**
39	1,47±0,15	**>25** [c]	>17
40	1,35±0,12	**>50** [c]	**>37**
42	**0,92±0,06**	**101,80 ± 37,52**	**111**
Tiabendazol[d]	0,34±0,02	786,99 ± 275,51	2315

[a] Determinado por el método Alamar Blue. [b] IS = CC_{50} (HepG2) / CE_{50} (*T.c.*). [c] Compuestos con problemas de solubilidad. [d] Resultados de tiabendazol recogidos del Artículo 2. Los valores de CE_{50} <1 μM, CC_{50} >25 μM and IS >20 se indican en negrita.

Según se observa en la Tabla IV.3.4, la CE_{50} de los seis compuestos (**31**, **36**, **37**, **39**, **40** y **42**), está entre 0,92 y 1,58 μM. **42** fue el compuesto más potente, con un tercio del valor del compuesto de referencia (tiabendazol), y un IS de 111. La dificultad para disolver los compuestos **37**, **39** y **40** no permitió calcular sus valores CC_{50}, estando por encima de 50, 25 y 50 μM, respectivamente.

Como se ha indicado anteriormente, se estudió la interacción teórica entre los derivados de Bz activos y la β-tubulina de *T. circumcincta* para encontrar la correlación entre los resultados de actividad ovicida y larvicida, y la inhibición de la enzima. Al igual que en el Artículo 2, se estudiaron los equilibrios tautoméricos observando que los Bz de tipo I se comportaban de manera similar al estudio previo. El fragmento de guanidina, en el caso de los compuestos de tipo II tiende a la protonación a pH = 7 ± 2, por lo que fue el aplicado en el estudio. Los derivados de tipo III y IV, sin embargo, mostraron un comportamiento diferente que probablemente se debe a la estabilización por conjugación del carbonilo, Esquema IV.3.3.

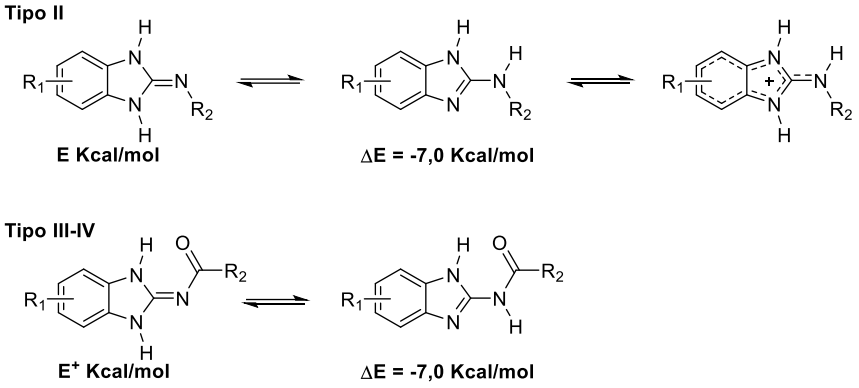

Esquema IV.3.3. Equilibrios tautoméricos y químicos para derivados de Bz tipo **II** - **IV**. Energías genéricas calculadas (DFT RWB97X-D/6-31+G*) para BZ aminas (E) y amidas (E') y diferencias (Δ) entre sus respectivos tautómeros.

La presencia del fragmento de guanidina en los nuevos Bz proporciona mayor presencia de átomos dadores de enlaces de hidrógeno, lo que contribuye a aumentar la interacción con la tubulina y por tanto la afinidad formando complejos más estables. En la Fig. IV.3.3 se puede observar que, además de las interacciones que se establecen en los 2-fenilBz de tipo I (enlace BzN-H al residuo Val236 e interacciones de apilamiento π), los compuestos tipo II-IV muestran interacciones diferentes, como el enlace BzN-H al residuo Cys239 del Bz **6**, el BzN-H al residuo Glu198 de la amina protonada Bz**14** y los tautomeros exocíclicos de los 2-amidoBz **42** y **53**.

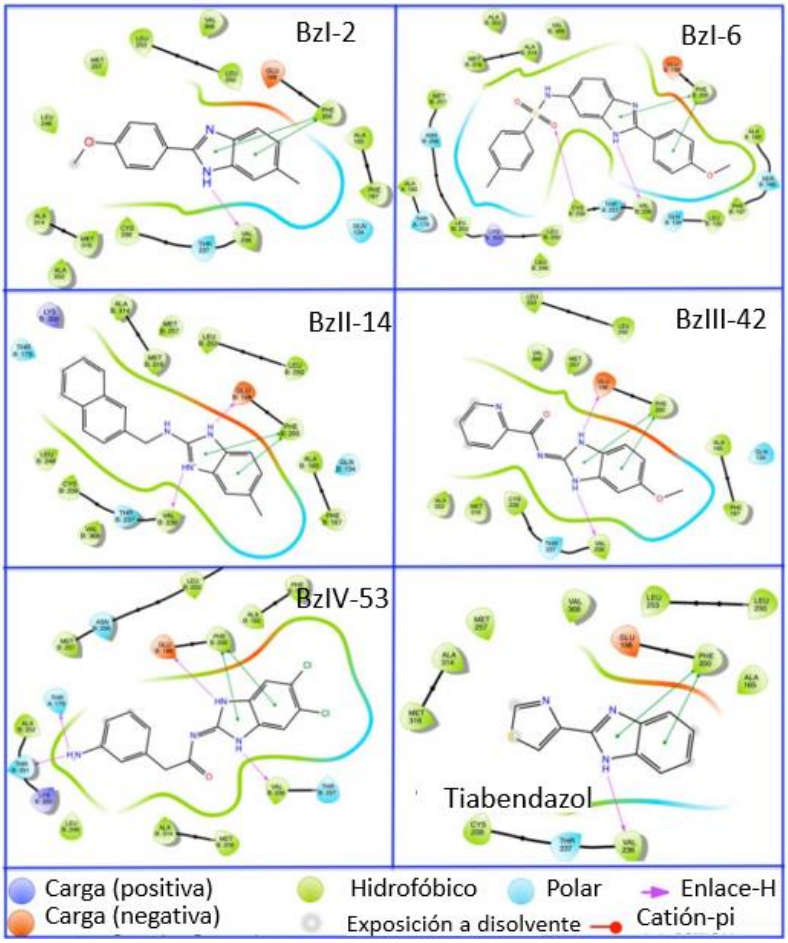

Figura IV.3.3. Mapas de interacción 2D de tubulina modelada de *T. circumcincta* con ejemplos de los cuatro tipos de Bz, el derivado BZ **2** y el fármaco de referencia tiabendazol.

Además, como se observa en el derivado **53** (R_1 = 5,6-diCl, R_2 = 3-NH_2bencilcarbonilo, Bz tipo IV) los grupos funcionales presentes en el fragmento B pueden mejorar la interacción con la diana. Concretamente para este caso, se puede observar el enlace de hidrógeno con el grupo amino y las Thr179 y 351 (Fig. IV.3.4, A1 y A2). Análogamente, la presencia de otros sustituyentes podría causar un impedimento estérico reduciendo la estabilidad entre el compuesto y la diana como en el caso de los compuestos **44** (R_1 = 5,6-diCH_3, R_2 = 4´-metoxifenilo, Bz tipo III) y **46** (R_1 = 5,6-diCl, R_2 = 4´-metoxifenilo, Bz tipo III) (Fig. IV.3.4, B1 y B2).

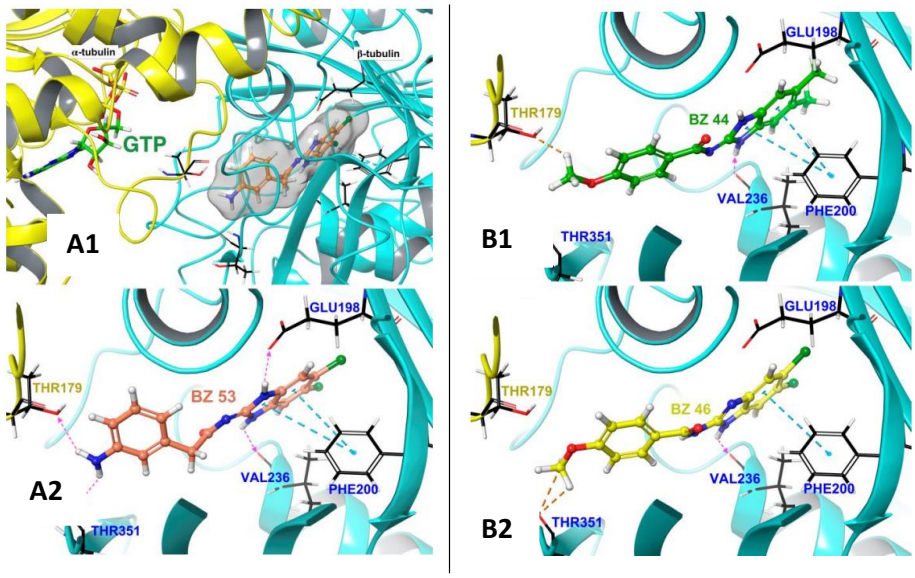

Figura IV.3.4. A1 y A2: Docking de la amida **53** en el sitio de colchicina de la tubulina modelada de *T. circumcincta*. A2: Detalles de las interacciones de apilamiento Phe200 - BZ π (en forma de T) y los enlaces H del N-H en las posiciones 1 y 3 con Val236 y Glu198 residuos de β-tubulina, así como entre los 3 -aminofenilo y el residuo de α-tubulina (amarillo) Thr179, o el de β-tubulina (azul) Thr351.
B1: Complejo de acoplamiento de la benzamida **44**, que muestra su mala interacción (línea discontinua dorada) con el residuo Thr179 de la α-tubulina, y sin el enlace H habitual para los compuestos de tipo III entre BZN-H y Glu198. B2: Complejo similar del análogo de dicloro **46** que muestra las malas interacciones con el residuo Thr351 de β-tubulina.

Los resultados experimentales de LMI encontrados para los compuestos **53** (41,2%), **46** (3,3%) y **44** (<1%) están de acuerdo con lo acabado de indicar, y van en paralelo con los valores de energía de acoplamiento obtenidos (G-score) de -10,79, -10,42 y -9,98 kcal/mol, respectivamente.

Por otro lado, se observa que algunos Bz de los diferentes tipos se acoplan con orientaciones similares al sitio de la colchicina, mientras que otros del mismo tipo lo hacen en orientaciones opuestas, Fig. IV.3.5. A. Esto se ve reflejado en los resultados de LMI donde los compuestos **14** y **20**, ambos de tipo II, inhiben la migración larvaria en un 41,5 y 9,2%, respectivamente, el valor de energía de acoplamiento refleja esta diferencia, mientras que en el compuesto **14** muestra un valor de -10,47 kcal/mol, en **20** es de -9,20 kcal/mol, Fig. IV.3.4. B.

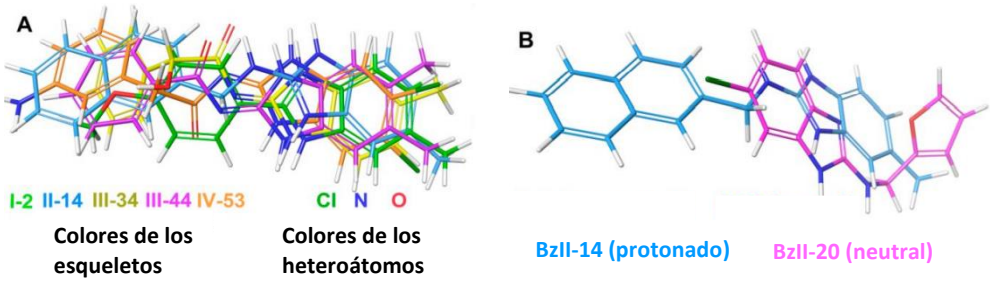

Figura IV.3.5. (A) Superposición de BZ seleccionadas de tipos I–IV acopladas en el modelo de tubulina de *T. circumcincta.* (B) Diferente disposición de los sistemas BZ (A) y naftilo/furano (B) en las aminas acopladas II-**14** y II-**20**, respectivamente.

De acuerdo con lo expuesto, entre los más de 50 derivados de Bz obtenidos con estructuras de diferentes familias (**I**-**IV**), cinco BZ de tipo III mostraron un 100% de actividad ovicida frente a una cepa sensible a tiabendazol de *T. circumcincta*, y otros dos, >90% a 50 μM. Diez de los derivados presentaron actividad larvicida mayor a 40%. El compuesto **13** (tipo II) fue el compuesto larvicida más activo, inhibiendo en un 54,9% la migración de larvas; el compuesto **39** (tipo III) mostró actividad ovicida (CE_{50} 1,47 μM, IS >17) y larvicida, y el **42** (tipo **III**), fue el compuesto más potente y ovicida específico mostrando valores de CE_{50} de 0,92 μM y el IS más elevado, 110. Dos Bz fueron seleccionados para realizar ensayos in vivo con el fin de determinar su toxicidad en ratón, su eficacia preclínica en jerbos y posteriormente en corderos.

IV.4. ENSAYOS IN VIVO. Actividad frente a *Haemonchus contortus*

Como ya se ha indicado, las infecciones por nematodos gastrointestinales que afectan al ganado rumiante y más específicamente a ovino, suponen un problema muy importante de salud animal a nivel mundial, porque a pesar de la variedad de fármacos existentes en el arsenal terapéutico se han encontrado resistencias en la mayoría de ellos.

El grupo de investigación ha sintetizado más de 220 compuestos con esqueleto base de benzalftalida y ftalazinona (Artículo 1), benzimidazol (Artículos 2 y 3), aminoalcohol y diaminas lipídicas,[11] que fueron ensayados frente a huevos y larvas en una cepa sensible de *T. circumcincta*, incluso algunos en un aislado resistente por el grupo colaborador de la Universidad de León. Estos estudios permitieron seleccionar dos diaminas, **AAD-1** y **AAD-2** y, un benzimidazol, **2aBZ**, para ensayos in vivo.

Las cantidades necesarias para el tratamiento de corderos infectados, con un peso entre 10 y 13 Kg, son muy elevadas, por lo que se aplicó un paso intermedio utilizando jerbos (de 50 a 150 g de peso), con el fin de seleccionar el o los compuestos más potentes y seguros. Para la infección se utilizó *Haemonchus contortus*, nematodo que produce una infección muy semejante a *Teladorsagia* y que se considera un buen modelo de tricostrongílido animal.

Se sintetizaron las cantidades de compuesto necesarias para estudios de toxicidad en ratón y de infección en jerbos.

En primer lugar, no se observaron signos de toxicidad en ratones a dosis de 250 mg/Kg. Después, se trataron jerbos infectados a dosis única de 200 y 10 mg/Kg, observándose que el benzimidazol **2aBZ** era el más potente produciendo una reducción del 95,63% en vermes pre-adultos a la dosis superior, la disminución de la dosis en un 20% bajo la eficacia a la tercera parte (30,64%). Le sigue en eficacia la diamina **AAD-2** (44,99% de reducción a 200 mg/Kg) y después **AAD-1** (20,54% de reducción), Tabla IV.4.1.

Tabla IV.4.1. Actividad antihelmíntica de los compuestos **2aBz**, **AAD-1** y **AAD-2** vía oral a dosis única en jerbos infectados con *H. contortus*.

Compuesto	Dosis (mg /kg)	% Reducción[a]	
		L4 (%)	Pre-adultos (%)
2aBz	200	0,00	95,63
2aBz	10	0,00	30,64
AAD-1	200	3,73	20,54
AAD-1	10	1,25	0,00
AAD-2	200	16,50	44,99

[a] Valor medio de n = 6

Además, se observó que los animales tratados conseguían el peso normal a lo largo del experimento, comparado con el grupo control, y que después del sacrifico no mostraban lesiones en órganos vitales, ni macroscópicas, ni microscópicas. Estos resultados permitieron seleccionar el compuesto **2aBz** para ensayos in vivo en corderos, por lo que hubo que sintetizar 25 gramos de compuesto. Para el experimento se utilizaron 4 corderos infectados, a los que se administró una dosis única de 120 mg/Kg de **2aBz** vía oral el día 7 post-infección consiguiéndose una reducción del 99,13% del número de huevos de heces y del 95,45% del número de vermes en el abomaso en comparación con el grupo control. Adicionalmente, no se observaron muertes, ni signos de toxicidad relacionados con el tratamiento, Fig. IV.4.1.

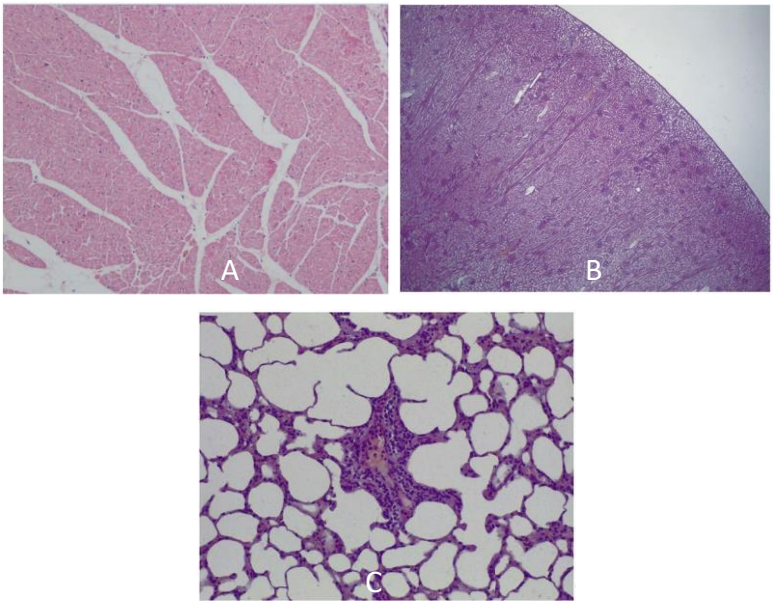

Figura IV.4.1. Cortes histológicos de algunos órganos vitales de corderos tratados con **2aBZ**. *A*) Corazón (cardiomiocitos y epicardio normales, 100x). *B*) Riñón (estructuras renales normales, glomérulo, túbulo proximal y túbulo distal, 40x). *C*) Del grupo control, pulmón (alveolos normales con bajo número de células mononucleares perivasculares, también presente en corderos tratados, 200x).

De todo ello se puede concluir, que el compuesto **2aBZ** podría constituir un candidato para el tratamiento de las infecciones por *H. contortus* y otros nematodos gastrointestinales en rumiantes y, además, servir de base estructural para la obtención de compuestos más eficaces, aunque **2aBZ** muestra una actividad significativa y buena tolerancia a dosis de 120 mg/Kg en corderos.

IV.5. BENZIMIDAZOLES: Actividad frente a otros nematodos

Las geohelmintiasis afectan a nivel mundial a unos de 1.500 millones de personas que viven, fundamentalmente, en zonas ingresos medios y bajos, con un acceso deficiente al agua potable y a los sistemas de salud. Entre ellas se encuentran las infecciones producidas por gusanos redondos como *Ascaris lumbricoides*, gusanos látigo como *Trichuris trichiura*, o lombrices como *Necator americanus* o *Ancylostoma duodenale*, siendo las producidas por *T. trichura* las que afectan a un mayor número de personas (800 millones en el mundo).[164] También, en los animales las infecciones por helmintos constituyen un importante problema de salud, ya que tienen un impacto crucial sobre el bienestar animal en el ganado rumiante.

Los fármacos disponibles para el tratamiento de la infección por *T. trichiura* son Bzs, ivermectina, levamisol y pamoato de pirantel.[165] Desafortunadamente, se han descrito resistencias frente a todos ellos debido a su uso masivo e incorrecto, por lo que es necesario encontrar nuevas alternativas terapéuticas.[166]

T. muris es un nematodo de ratones, muy semejante al parásito humano *T. trichiura*, debido a su reactividad cuando se cruza, por lo que se usa a menudo en estudios relacionados. Por otro lado, *Heligmosomoides polygyrus* es una lombriz intestinal natural de los roedores, que ocasiona infecciones crónicas alterando la respuesta inmunitaria del huésped, por lo que se usa ampliamente como modelo parasitario gastrointestinal en estudios inmunológicos, farmacológicos y toxicológicos. Así, se ensayaron in vitro algunos de los Bz indicados en los artículos 2 y 3 (15 compuestos), junto con varios aminoalcoholes (15) y diaminas (11) alifáticas frente a larvas L1 y formas adultas de *T. muris y H. polygyrus*.[167]

Cinco de los Bz evaluados presentaron un porcentaje de inhibición de la motilidad >90% a 100 μM. Entre ellos, los derivados **6** (R_1 = 5-Cl, R_2 = 4´-Cl) y **12** (R_1 = 5-NO_2, R_2 = 4´-Cl) mostraron valores de CI_{50} <10 μM frente a L1 de *T. muris*. Teniendo en cuenta estos resultados, se evaluó su actividad frente a larvas adultas de *T. muris* y *H. polygyrus* a una

[164] CDC, Trichuriasis. Disponible en: https://www.cdc.gov/dpdx/trichuriasis/index.html. Acesso 21 febrero 2023
[165] WHO, Model List of Essential Medicines. Disponible en: https://www.who.int/groups/expert-committee-on-selection-and-use-of-essential-medicines/essential-medicines-lists. Acceso 21 febrero 2023
[166] Moser, W.; Schindler, C.; Keiser, J. Efficacy of recommended drugs against soil transmitted helminths: systematic review and network meta-analysis. *BFJ***, 2017**, 358, j4307. doi: 10.1136/bmj.j4307
[167] Bancroft, A.J.; Grencis, R.K. Immunoregulatory molecules secreted by *Trichuris muris*. *Parasitology*, **2021**, 148, 1757-1763. doi: 10.1017/ S0031182021000846

concentración de 10 μM. Además, el compuesto Bz **12** mató el 81,7% de los gusanos adultos de *T. muris*, y el **6** el 100% de los adultos de *H. polygyrus* (Tabla IV.5.1).

Tabla IV.5.1. Actividad antihelmíntica de los compuestos **6** y **12**.

Bz	***T. muris***		***H. polygyrus***	
	L1 CI_{50} (μM)	**Adultos (%) a 10 μM**	**Adultos (%) a 10 μM**	**CI_{50} (μM)**
6	4,17	17,2	**100**	5,3
12	8,89	**81,7**	53,3	nc

nc: no calculado.

A pesar de que los resultados no muestren valores muy relevantes, estas estructuras de Bz podrían considerarse como un punto de partida para la obtención de nuevos compuestos antihelmínticos.

IV.6. BENZIMIDAZOLES TIPO III. Actividad frente a *Plasmodium falciparum*

La malaria o paludismo continúa siendo en el siglo XXI un reto importante para los sistemas de salud a nivel global. Se trata de una enfermedad protozoaria transmitida, generalmente, por mosquitos hembra del género *Anopheles*. Se conocen cinco especies de *Plasmodium* causantes de la enfermedad, *P. falciparum*, *P. vivax*, *P. ovale*, *P. malariae* y *P. knowlesi*, siendo las dos primeras las más peligrosas.

El arsenal terapéutico disponible para el tratamiento de la malaria es bastante amplio, sin embargo, la aparición de resistencias a muchos de los fármacos antimaláricos pone de manifiesto la necesidad de desarrollar nuevas moléculas.

Se puede encontrar en la bibliografía información sobre la actividad anti-*Plasmodium* de algunas familias de Bz, así, en este trabajo se han obtenido 36 derivados de 2-amidobenzimidazoles (tipo III), que han sido ensayados frente a la cepa HB3 de *P. falciparum*. En un primer cribado se evaluó la capacidad inhibitoria de los compuestos a 10 μM, y se calculó la CI_{50} de aquellos que producían una inhibición mayor al 50%, determinándose adicionalmente la citotoxicidad en células Vero con el fin de establecer sus índices de selectividad. Además, se evaluaron los compuestos más potentes frente a la cepa *Pf*7G8 resistente a cloroquina.

Como se ha indicado en el Artículo 3, la síntesis de los 2-amidoBz se lleva a cabo en un proceso de dos pasos. Primero, se obtienen los 2-aminoBz intermedios (Bz*i* **1** a **6**, AIs **1** a **6** en este artículo) con rendimientos del 62 al 85%. El Bz*i* **6** se obtuvo con un rendimiento del 95% y su punto de fusión era de 231 ºC. Después, el ácido carboxílico correspondiente se activa por tratamiento con CDI en DMF durante 1 hora a temperatura ambiente, y se añade el Bz*i* manteniéndolo la mezcla de reacción en las mismas condiciones durante 16 horas. Así, se obtuvieron los compuestos **1**-**29**, **33**-**36** en un rendimiento de 27 a 69%. La amina **30** se obtienen por tratamiento de **29** disuelto en metanol con H_2/Pd-C con un rendimiento de 85%. El compuesto **31** se sintetizó por acoplamiento del ácido 2-(Boc-amino)decanoico con **30** (obtenido convenientemente según el protocolo indicado en del Olmo, 2006[168]), catalizado con CDI. La retirada del grupo Boc en Bz **31** con ácido trifluoroacético llevó a la amina **32** con un rendimiento de 76%, Esquema IV.6.1.

[168] del Olmo, E.; Plaza, A.; Muro, A.; Martínez-Fernández, A.R.; Nogal-Ruiz, J.J.; López-Pérez, J.L.; San Feliciano, A. Synthesis and evaluation of some lipidic aminoalcohols and diamines as immunomodulators. *Bioorg. Med. Chem. Lett.* **2006**, 16(23), 6091-6095. doi: 10.1016/j.bmcl.2006.08.113

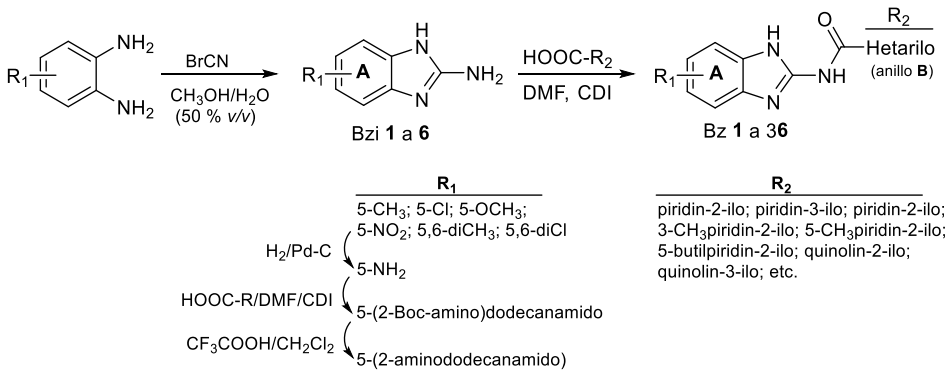

Esquema IV.6.1. Proceso de síntesis de los derivados 2-amidobenzimidazol.

Todos los compuestos obtenidos han sido purificados por cromatografía en columna y cristalización en algún caso, y su estructura determinada de manera inequívoca mediante técnicas espectroscópicas, IR, RMN ^{1}H, RMN ^{13}C y HRMS. Los puntos de fusión de los derivados oscilan entre 129 y 335 ºC.

Los espectros de RMN ^{1}H y ^{13}C se hicieron en cloroformo-d, metanol-d_4 o DMSO-d_6, como ejemplo se indican los desplazamientos del Bz **1** (R_1 = CH_3, R_2 = NHCO-piridin-2-ilo), uno de los compuestos con mayor actividad anti-*Plasmodium*. ^{1}H RMN (400 MHz, C_2D_6SO): δ 12,00 (2H, sa), 8,65 (1H, da, *J* = 4,8 Hz, H-6'), 8,19 (1H, d, *J* = 7,6 Hz, H-3'), 8,60 (1H, ddd, J_1 = 8,0; J_2 =7,6; J_3 = 1,2 Hz, H-4'), 7,66 (1H, dd, J_1 = 8,0; J_2 = 4,8 Hz, H-5'), 7,50 (1H, d, *J* = 1,2 Hz, H-4), 7,48 (1H, d, *J* = 8,4 Hz, H-7), 7,12 (1H, J_1 = 8,4; J_2 = 1,2 Hz, H-6). ^{13}C NMR (100 MHz, C_2D_6SO): δ 163,8 (NHCO), 149,3 (C-6'), 148,6 (C-2'), 147,2 (C-2), 138,7 (C-3a + 4'), 136,9 (C-7a), 128,2 (C-5'), 126,1 (C-5), 123,2 (C-3'), 121,9 (C-6), 116,1 (C-4), 115,9 (C-7).

Los derivados obtenidos mostraban sobre el anillo A mono- o di-sustituciones con átomos dadores (CH_3, OCH_3 y NH_2), o atractores de electrones (Cl, NO_2) o grupos de tamaño voluminoso (**31** y **32**). El anillo B presentan derivados de piridina o quinolina.

Tabla IV.6.1. Porcentajes de inhibición de crecimiento. CI_{50}, citotoxicidad e índices de selectividad.

Bz	R_1	R_2	PIC [a] (%)	CI_{50} (μM)	Citotoxicidad CC_{50} (μM)	IS
1	5-CH_3	piridin-2-ilo	**93,5**	**0,98**	14,8	**14,5**
2	5-CH_3	piridin-3-ilo	0,0	nc	nc	nc
3	5-CH_3	piridin-4-ilo	0,0	nc	nc	nc
4	5-CH_3	3´-CH_3piridin-2-ilo	**92,4**	2,5	6,8	2,8
5	5-CH_3	5´-CH_3piridin-2-ilo	**100**	1,5	4,5	1,6

6	5-CH_3	5´-butilpiridin-2-ilo	**90,9**	2,4	6,6	2,7
7	5-CH_3	5´-fenilpiridin-2-ilo	57,5	7,8	19,5	2,5
8	5-CH_3	5´-CNpiridin-2-ilo	37,4	nc	nc	nc
9	5-CH_3	quinolin-2-ilo	73,1	14,1	63,0	4,5
10	5-CH_3	quinolin-4-ilo	60,5	nc	nc	nc
11	5-CH_3	isoquinolin-1-ilo	0,0	nc	nc	nc
12	5-Cl	piridin-2-ilo	**91,4**	1,8	15,4	8,7
13	5-Cl	3´-CH_3piridin-2-ilo	87,3	2,8	8,6	3,0
14	5-Cl	3´-Clpiridin-2-ilo	11,9	nc	nc	nc
15	5-Cl	4´-OCH_3piridin-2-ilo	89,8	1,5	2,0	1,4
16	5-Cl	5´-CH_3piridin-2-ilo	85,6	2,4	7,2	3,0
17	5-Cl	5´-butilpiridin-2-ilo	89,7	3,5	3,4	1,0
18	5-Cl	5´-fenilpiridin-2-ilo	**99,2**	2,3	0,6	0,3
19	5-Cl	6´-CH_3piridin-2-ilo	28,0	nc	nc	nc
20	5-Cl	quinolin-2-ilo	25,9	nc	nc	nc
21	5-Cl	quinolin-3-ilo	0,0	nc	nc	nc
22	5-Cl	quinolin-4-ilo	88,9	2,3	16,1	6,9
23	5-Cl	isoquinolin-1-ilo	53,7	nc	nc	nc
24	5-Cl	6´-OCH_3quinolin-2-ilo	22,3	nc	nc	nc
25	5-OCH_3	piridin-2-ilo	50,9	nc	nc	nc
26	5-OCH_3	5´-CH_3piridin-2-ilo	**93,5**	3,3	11,1	3,4
27	5-OCH_3	5´-butilpiridin-2-ilo	**100**	1,2	8,5	7,4
28	5-OCH_3	5´-fenilpiridin-2-ilo	72,7	4,4	14,6	3,3
29	5-NO_2	piridin-2-ilo	**96,0**	5,1	13.9	2,7
30	5-NH_2	piridin-2-ilo	0,0	nc	nc	nc
31	5-NHCO-C_9H_{18}(NHBoc)	piridin-2-ilo	71,8	8,5	26,8	3,2
32	5-NHCO-C_9H_{18}(NH_2)	piridin-2-ilo	72,3	6,8	16,4	2,4
33	5,6-diCH_3	piridin-2-ilo	**100**	**0,85**	13,2	**15,4**
34	5,6-diCH_3	5´-butilpiridin-2-ilo	74,2	3,4	3,2	1,0
35	5,6-diCH_3	5´-fenilpiridin-2-ilo	64,7	7,3	9,7	1,3
36	5,6-diCl	piridin-2-ilo	81,9	2,4	11,8	5,0
Cloroquina			100	0,028		

[a] PIC: porcentaje de inhibición de crecimiento. Boc: *terc*-butoxicarbonilo. nc: no calculado.

Los compuestos **1** (R_1 = 5-CH_3, R_2 = piridin-2-ilo), **4** (R_1 = 5-CH_3, R_2 = 3´-metilpiridin-2-ilo), **6** (R_1 = 5-CH_3, R_2 = 5´-butilpiridin-2-ilo), **12** (R_1 = 5-Cl, R_2 = piridin-2-ilo), **18** (R_1 = 5-Cl, R_2 = 5´-fenilpiridin-2-ilo), **26** (R_1 = 5-OCH_3, R_2 = 5´-metilpiridin-2-ilo) y **29** (R_1 = 5-NO_2, R_2 = piridin-2-ilo) inhibieron el crecimiento de la cepa sensible de *P. falciparum* en más del 90% a una concentración de 10 μM y mostraron valores de CI_{50} entre 0,98 y 5,1 μM. El derivado **15** (R_1 = 5-Cl, R_2 = 4´-metoxipiridin-2-ilo) presentó un valor de 1,5 μM (inhibición de crecimiento 89,8%). Por otro lado, los derivados **5** (R_1 = 5-CH_3, R_2 = 5´-metilpiridin-2-ilo), **27** (R_1 = 5-OCH_3, R_2 = 5´-butilpiridin-2-ilo) y **33** (R_1 = 5,6-diCH_3, R_2 = piridin-2-ilo) fueron capaces de inhibir el crecimiento en un 100% a la misma concentración.

Cabe resaltar la actividad de los Bz **1** y **33**, con CI_{50} de 0,98 y 0,85 μM, respectivamente, es decir, unas 30 veces menos potentes que el fármaco control, cloroquina. Se observa una clara relación entre la posición del nitrógeno en la piridina y la actividad anti-*Plasmodium,* así, el compuesto **1** (*orto*) es muy activo, mientras que **2** (*meta*) y **3** (*para*) son inactivos. De manera general los derivados de piridin-2-ilo con cualquiera de las combinaciones en el anillo A: metilo (**1**), cloro (**12**), nitro (**29**), dimetilo (**33**) o dicloro (**36**) muestran una excelente potencia de inhibición, que varía entre 100 y el 81,9%, bajando al 51% en el derivado metoxilado **25** y perdiéndose totalmente en la amina **30**. Se estudió la influencia en la actividad anti-*Plamodium* con relación a la presencia de determinados sustituyente sobre el anillo de piridin-2-ilo, Fig. IV.6.1. En general, la presencia de átomos dadores de electrones (CH_3, OCH_3, Bu) en posiciones 3, 4 o 5 son buenas para la actividad, y desfavorable en 6; tampoco conviene la presencia de átomos atractores de electrones en 3 (Bz **14**) o 5 (Bz **8**). La presencia de un fragmento rico en electrones como un fenilo en posición 5 (Bz **18**) es favorable para la actividad anti-*Plasmodium*.

Se investigó la conveniencia de fragmentos heterocíclicos de mayor tamaño, tipo quinolina o isoquinolina, Fig. IV.6.2. No se aprecia una clara preferencia en los quinolin derivados, así, en R_1 = CH_3 es más conveniente una sustitución en C-2 del fragmento quinolinico (Bz **9**), mientras que en R_1 = Cl es mejor la sustitución en 4 (Bz **22,** CI_{50} de 2,3 μM). Un fragmento de isoquinolina, amido en C-1 a la agrupación Bz-NHCO- no es favorable para la actividad (Bz **11** y **23**).

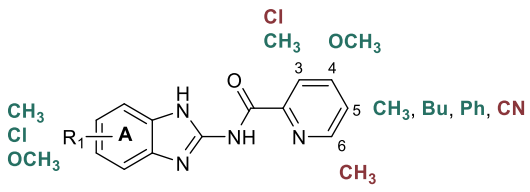

Figura IV.6.1. Derivados de 2-picolinamidoBz, en **rojo** posición o grupos desfavorables.

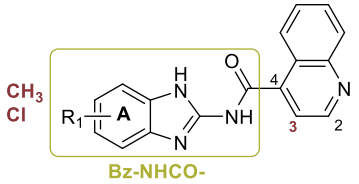

Figura IV.6.2. Derivados de 2-quinolincarboxamida, en **rojo** posición o grupos desfavorables.

Se seleccionaron tres compuestos, **1** (CI_{50} 0,98 μM), **12** (CI_{50} 1,8 μM) y **16** (CI_{50} 2,4 μM) con rangos de actividad diferentes para su evaluación frente a la cepa resistente 7G8 de *P. falciparum*.

Tabla IV.6.2. Porcentajes de inhibición de crecimiento en cepa *Pf*7G8. CI_{50}, citotoxicidad e índices de selectividad de algunos 2-amidobenzimidazoles.

Bz	R_1	R_2	*Pf*7G8 CI_{50} (µM)	Citotoxicidad CC_{50} (µM)	IS
1	5-CH_3	piridin-2-ilo	0,95	14,8	15,6
12	5-Cl	piridin-2-ilo	3,60	15,4	4,2
16	5-Cl	3´-CH_3piridin-2-ilo	2,60	7,2	2,7
Cloroquina			0,23	nc	nc

Como se observa en la Tabla IV.6.2 los compuestos **1** y **16**, mantuvieron la potencia anti-*Plasmodium* en la cepa resistente *Pf*7G8, **12** redujo la potencia la mitad y cloroquina perdió un orden de actividad. En esta cepa Bz **1** es 4 veces menos potente que cloroquina.

Con el fin de estudiar los efectos de algunos Bzs a nivel celular, se evaluó el comportamiento de los compuestos **1**, **5**, **16**, **26** y **33**. Por un lado, se estudió la integridad de la membrana plasmática midiendo la absorción de yoduro de propidio y la presencia del grupo hemo en el medio de cultivo, Fig. IV.6.3, pudiendo observar que los Bz **5**, **16** y **26** producían permeabilidad en la membrana, siendo los compuestos **1** y **33** los que mejor la conservaron y, que podría estar relacionado con la menor toxicidad encontrada para ellos. Ninguno de los compuestos mostró capacidad hemolítica.

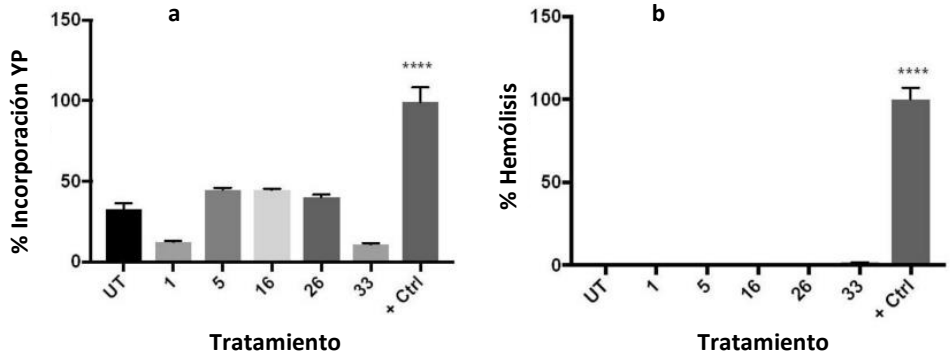

Figura IV.6.3. Evaluación de la integridad de la membrana. a) Incorporación de yoduro de propidio. b) Hemólisis.

Además, la menor toxicidad de los compuestos **1** y **33** podría estar relacionada con la disminución de la producción intracelular de especies reactivas de oxígeno (ROS) durante un rango específico de tiempo, Fig. IV.6.4.

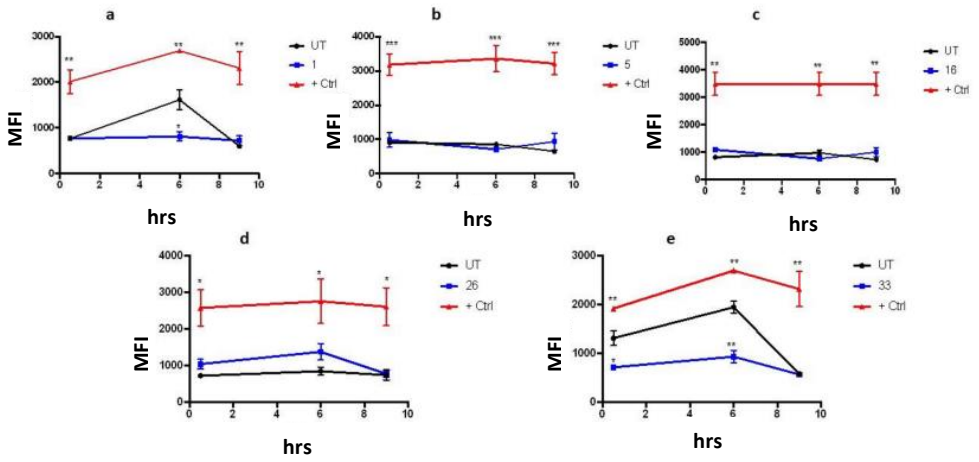

Figura IV.6.4. Efecto de los Bz seleccionados sobre la producción de ROS.

Estos mismos compuestos, no produjeron cambios en el potencial de membrana mitocondrial frente al control a las 6 horas, sin embargo, a las 9 horas cambia la tendencia, lo que indica que los compuestos tardan más en llegar a la mitocondria, probablemente por la presencia del grupo piridin-2-ilo sin sustituir, que al ser más polar es menos soluble en la membrana que los otros derivados, Fig. IV.6.5.

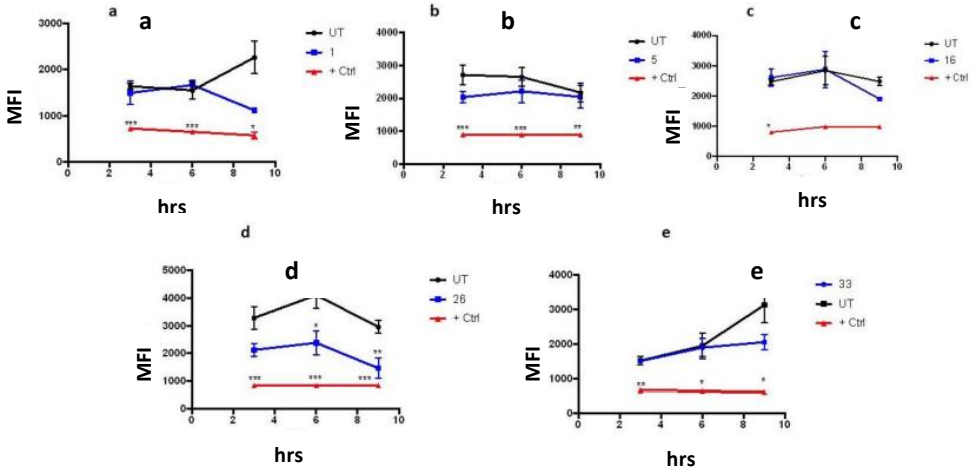

Figura IV.6.5. Cambio del potencial de membrana mitocondrial causado por los Bz seleccionados.

Finalmente, se estudió la interferencia de **1**, **16** y **33** con la biocristalización de la hemozoína, el principal mecanismo de acción de fármacos como cloroquina, mefloquina y

otros antimaláricos, Fig. IV.6.6, observando que éste no es el principal mecanismo de acción de estos Bzs frente a *P. falciparum*.

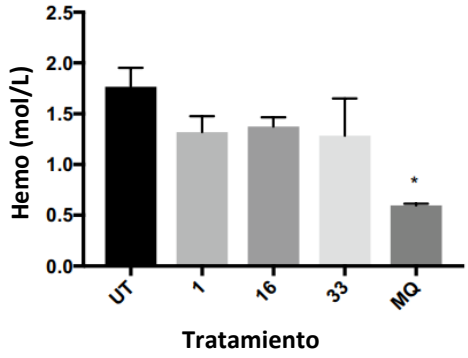

Figura IV.6.6. Biocristalización de la hemozoína en los Bzs **1**, **16** y **33**.

En resumen, en este trabajo se sintetizaron, purificaron, caracterizaron y evaluaron treinta y seis derivados de 2-amidobenzimidazol frente a una cepa sensible a cloroquina de *P. falciparum*, seis de ellos (**1**, **5**, **15**, **27** y **33**) mostraron una CI_{50} igual o inferior a 1,5 μM, presentando desafortunadamente alta toxicidad. Los compuestos **1**, **12** y **16** se ensayaron en la cepa *Pf*7G8 manteniendo su valor de CI_{50}, menos Bz **12** que bajo a la mitad. En los estudios de mecanismo de acción realizados sobre los Bz **1**, **5**, **16**, **26** y **33** se observa que, **5**, **16** y **26** modificaron la permeabilidad de la membrana; **1**, **16** y **26** disminuyeron el potencial de membrana a partir de las 9 horas; no se observa una variación en la producción de especies reactivas de oxígeno en ninguno de los cinco Bzs y, que ninguno de los tres Bzs (**1**, **16** y **33**) ensayados en la interferencia en la producción cristales de hemozoína producían su inhibición.

Con todo ello se puede decir, que el esqueleto de benzimidazol-2-ilo-picolinamida constituye un excelente cabeza de serie para la obtención de derivados prometedores para el tratamiento de la malaria.

VI. CONCLUSIONES

Del estudio realizado en este trabajo se deducen las siguientes conclusiones:

De los trabajos de síntesis química

1. Se han obtenido 35 derivados de benzalftalida (Bf), de ellos 32 son mezclas de regioisómeros en posiciones 5 ó 6 que no se han llegado a separar. La síntesis se realiza por el método *a*) usando un Dean-Stark, en presencia de tolueno y a temperaturas superiores a 210 ºC, o por el método *b*) por irradiación en microondas. Los rendimientos de reacción son superiores por el método *b*).
2. Se han obtenido 22 ftalazinonas (Ft), de ellas 16 son mezclas de regioisomeros en posiciones 6 ó 7. Las ftalazinonas se obtienen por tratamiento directo de las Bf con hidrazinas, y adicionalmente, haciendo reaccionar Fts con hidrógeno en sobre el nitrógeno amídico con derivados halogenados en medio básico.
3. Se han obtenido 186 derivados de benzimidazol (Bz), que se han clasificado en 3 familias en función al tipo de unión entre el anillo de benzimidazol y el fragmento en C-2. Directamente unidos (familia I); con un espaciador de tipo metilamino (familia II); o carbonilamino/acetilamino/acrilamido (familia III).
    3.1. De los 85 compuestos de la familia I, 22 presentaban un heterociclo en el anillo B y 9 un fragmento alifático. Estos compuestos se obtienen bien por la vía *a)* en un proceso de dos pasos, donde primero se forman las sales de metansulfonato a partir del aldehído correspondiente, que se hacen reaccionar con las fenilendiaminas adecuadas; o por la vía *b)* en un proceso directo, haciendo reaccionar las fenilendiaminas con aldehídos en presencia de metabisulfito sódico; los rendimientos de reacción son ligeramente superiores por la vía *a*.
    3.2. Se han introducido diferentes modificaciones sobre el benceno del benzimidazol (anillo A) y el fragmento aromático/heteroaromático en C-2 (anillo B), con fin de establecer relaciones entre la estructura y la actividad. Incluso se han obtenido compuestos tricíclicos de tipo benzimidazol-1,3-diazina-2,6-diona.
    3.3. La obtención de las familias II y III implica la formación de los 2-aminobenzimidazoles correspondientes, que por un lado se hacen reaccionar

con aldehídos, seguido de reducción con borohidruro sódico para dar lugar a compuestos de la familia II; y por otro se tratan con diferentes ácidos (previamente activados con CDI) para obtener compuestos de la familia III.

3.4. Se han obtenido 23 benzimidazoles de la familia II, de los cuales 8 contenían un heterociclo en B.

3.5. Entre los 78 compuestos obtenidos de la familia III, 53 eran derivados de formamida, 7 de acetamida y 9 de acrilamida, 38 contenían un fragmento heterocíclico en B y 4 eran de tipo alifático.

4. Con el fin de ampliar la variación estructural de los compuestos a ensayar, se han obtenido 8 derivados de 2-benzimidazolona (Bzo).

De los resultados de actividad frente a Teladorsagia circumcincta

1. Se ensayaron las benzalftalidas y ftalazinonas in vitro frente a huevos (ensayo de inhibición de eclosión de huevos "EHI") y larvas (ensayo de inhibición de motilidad de larvas "LMI") de una cepa sensible de *T. circumcincta*. Solo 4 Bzs mostraron valores de EHI superiores el 97%, destacando Bf-8 con CE_{50} de 30,6 e IS 10,2. De las ftalazinonas solo dos resultaron activas, mostrando Pt-130 una CE_{50} 26,7 e IS 13,6. Se determinó la EHI de Bf-8 y Pt-130 en una cepa resistente de *T. circumcincta* a 10 µg/mL mostrando Pt-130 un 99.4% de inhibición.

2. De los 30 benzimidazoles de la familia I ensayados, 9 mostraron actividad ovicida entre 6,30 y 25,60 µM frente a una cepa sensible de *T. circumcincta*, la actividad disminuyó en una cepa resistente de *T. circumcincta,* siendo BzI.0040 el más activo con CE_{50} de 14,47 e IS de 5,69 frente a la cepa HepG2.

   Se ensayaron 8 Bzs-familia I frente a larvas L1 de *T. circumcincta*, siendo BzI.2040 el más potente, tanto en una cepa sensible como en otra resistente con valores de CE_{50} entre 5,01 y 11,66 µM, respectivamente, mostrando además un IS 4,51 frente a células Caco-2.

a. De los 20 benzimidazoles de la familia II ensayados ninguno mostró actividad ovicida y 7 mostraron actividad larvicida entre 26,5 y 54,9% a 50 µM en una cepa sensible de *T. circumcincta*.

b. Se ensayaron 25 benzimidazoles de la familia III en una cepa sensible de *T.c.* Cinco mostraron EHI del 100% a 50 μM y cuatro LMI entre 25,5 y 51,2% a 50 μM. El ovicida más potente BzIII.3330 mostró CE_{50} 0,92 μM, que es un tercio menor que el fármaco control tiabendazol (CE_{50} 0,34 μM), e IS de 101,8 frente a células HepG2. El larvicida más potente BzIII.2330 mostró 51,2% de inhibición a 50 μM.

c. Los estudios de docking y modelado molecular de los Bzs-familia I frente a la β-tubulina de *T. circumcincta*, indicaban una preferencia por el tautómero con los sustituyentes en C-6 frente a C-5 en su unión a la enzima. Se observa, además, para los compuestos más potentes uniones por puentes de hidrógeno entre la Val236 y el BzN-H, así como interacciones de apilamiento π en el anillo de benzimidazol y la Phe200 en la tubulina. También, se aprecia una diferente orientación a nivel de la β-tubulina para aquellos compuestos que perdían actividad frente a la cepa de *T. circumcincta* resistente.

   Estudios de docking y modelado molecular para Bzs-familia III, la más activa, indican una unión adicional a nivel de la diana para algunos de los compuestos, entre el BzN-H y la Cys239 y/o el Glu198, lo que explicaría su mayor potencia.

d. Se seleccionó el 2aBz de la familia III para ensayos in vivo. Se hizo el escalado del proceso de síntesis para obtener las cantidades necesarias (25 g) para tratar a los corderos infectados.

   Los estudios de toxicidad en ratón indicaron que el compuesto no producía lesiones en órganos vitales. Experimentos con jerbos infectados con *Haemonchus contortus* y tratados con 2aBz a dosis de 200 mg/Kg producían una reducción de formas pre-adultas del 95,6%, y en corderos infectados con *H. contortus* y tratados a dosis de 120 mg/Kg se producía una reducción en el número de huevos del 99,1% y del 95,5% en el número de vermes adultos en el abomaso.

Frente a Trichuris muris y Heligmosomoides polygyrus

7. Se evaluaron 15 Bzs de la familia III frente a larvas L1 y adultos de *T. muris* y *H. polygyrus*. BzI.2040 fue el más activo frente a ambas especies, con CI_{50} de 4,17 μM frente a L1 de *T.m*. y de 5,3 μM frente a formas adultas de *H.p*.

Frente a protozoos

Plasmodium falciparum, Leishmania donovani, Trypanosoma cruzi

8. Ninguna de las benzalftalidas, ni de las ftalazinonas mostraron valores de inhibición del crecimiento significativos frente a los tres parásitos, y los de las benzimidazolonas fueron muy bajos.

9. De los 183 benzimidazoles ensayados, los de la familia III fueron los más activos frente a *Plasmodium falciparum*, siendo BzIII.6330 el más potente con CI_{50} de 0,85 μM, es decir, 30 veces menor que el fármaco control cloroquina. El mecanismo de acción de BzIII.6330 no está relacionado con la interferencia de la biocristalización de hemozoína.

   Tres Bzs de la familia III mostraron valores de CI_{50} entre 0,35 y 0,16 μM frente a *L. donovani.*

   Cuatro Bzs de diferentes familias mostraron valores de CI_{50} entre 0,81 y 0,69 μM frente a *T.cruzi.*

Actividad antitumoral

10. Se ensayaron 77 Bzs frente a las líneas tumorales HeLa, MDA-MB-231 y MCF-7, mostrando valores de actividad muy bajos.

Actividad antiviral

Dengue, Zika, Chikungunya

11. La actividad de los 90 benzimidazoles ensayados en dengue y zika no fue significativa, mientras que en ensayos frente a CHIKV, 9 compuestos mostraron valores significativos, destacando la actividad de BzIb.1071.100 con valor de Rf $10^{2,0}$ a 2,5 μM.

VII. CÓDIGOS Y ESTRUCTURAS

VII.1. CÓDIGOS

Benzalftalidas

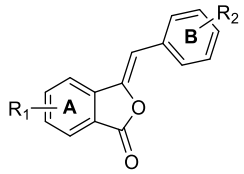

Compuesto					
Nº	**R_1**	**R_2**	**Código tesis**	**Art. 1**	**Cap. 5[a]**
1	H	3´-NO_2	Bf-1		x
2	H	4´-CH_3	Bf-2		x
3	H	4´-isopropilo	Bf-3		x
4a	5-CH_3	H	Bf-4a	**13a**	
4b	6-CH_3	H	Bf-4b	**13b**	
5a	5-CH_3	3´-NO_2	Bf-5a		x
5b	6-CH_3	3´-NO_2	Bf-5b		x
6a	5-CH_3	2´-Cl	Bf-6a	**18a**	
6b	6-CH_3	2´-Cl	Bf-6b	**18b**	
7a	5-CH_3	4´-OCH_3	Bf-7a	**14a**	
7b	6-CH_3	4´-OCH_3	Bf-7b	**14b**	
8a	5-CH_3	4´-Cl	Bf-8a	**19a**	
8b	6-CH_3	4´-Cl	Bf-8b	**19b**	
9a	5-CH_3	4´-SCH_3	Bf-9a	**22a**	
9b	6-CH_3	4´-SCH_3	Bf-9b	**22b**	
10a	5-CH_3	4´-fenilo	Bf-10a		x
10b	5-CH_3	4´-fenilo	Bf-10b		x
11a	5-CH_3	2´,4´-diCl	Bf-11a	**20a**	
11b	6-CH_3	2´,4´-diCl	Bf-11b	**20b**	
12a	5-CH_3	3´,4´-diOCH_3	Bf-12a	**15a**	
12b	6-CH_3	3´,4´-diOCH_3	Bf-12b	**15b**	
13a	5-CH_3	3´,4´-OCH_2O	Bf-13a	**16a**	
13b	6-CH_3	3´,4´-OCH_2O	Bf-13b	**16b**	
14a	5-CH_3	3´,4´-diCl	Bf-14a	**21a**	
14b	6-CH_3	3´,4´-diCl	Bf-14b	**21b**	
15a	5-CH_3	3´,4´,5´-triOCH_3	Bf-15a	**17a**	
15b	6-CH_3	3´,4´,5´-triOCH_3	Bf-15b	**17b**	
16a	5-CH_3	naft-1-ilo	Bf-16a	**23a**	
16b	6-CH_3	naft-1-ilo	Bf-16b	**23b**	
17a	5-CH_3	naft-2-ilo	Bf-17a	**24a**	
17b	6-CH_3	naft-2-ilo	Bf-17b	**24b**	
18a	5-NO_2	3´-OCH_3	Bf-18a		x
18b	6-NO_2	3´-OCH_3	Bf-18b		x
19a	5-COOH	4´-OCH_3	Bf-19a		x
19b	6-COOH	4´-OCH_3	Bf-19b		x

[a] Proceso de síntesis y descripción de propiedades fisicoquímicas en capítulo V.

Ftalazinonas

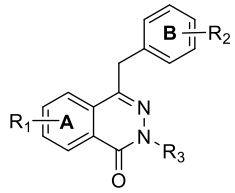

Compuesto						
Nº	**R_1**	**R_2**	**R_3**	**Código tesis**	**Art. 1**	**Cap. 5[a]**
20	H	4´-Cl	H	Ft-1	**25**	
21	H	4´-Cl	CH_2CH_2OH	Ft-2	**31**	
22	H	4´-Cl	3´-NO_2-fenilo	Ft-3	**33**	
23	H	4´-Cl	imidazolidin-2-ilo	Ft-4	**34**	
24	H	4´-Cl	3´-OHbencilo	Ft-5	**35**	
25	H	4´-Cl	3´-(4´-OCH_3-fenil)propilo	Ft-6	**36**	
26a	6-COOH	4-OCH_3	H	Ft-7a		x
26b	7-COOH	4-OCH_3	H	Ft-7b		x
27a	6-COOH	4-OCH_3	CH_3	Ft-8a		x
27b	7-COOH	4-OCH_3	CH_3	Ft-8b		x
28a	6-COOH	4-OCH_3	*terc*-butilo	Ft-9a		x
28b	7-COOH	4-OCH_3	*terc*-butilo	Ft-9b		x
29a	6-COOH	4-OCH_3	fenilo	Ft-10a		x
29b	7-COOH	4-OCH_3	fenilo	Ft-10b		x
30a	6-CONH-ciclohexilo	4-OCH_3	H	Ft-11a		x
30b	7-CONH-ciclohexilo	4-OCH_3	H	Ft-11b		x
31a	6-CONH-1-feniletilo	4-OCH_3	CH_3	Ft-12a		x
31b	7-CONH-1-feniletilo	4-OCH_3	CH_3	Ft-12b		x
32a	6-CONH-1-OHpropilo	4-OCH_3	*terc*-butilo	Ft-13a		x
32b	6-CONH-1-OHpropilo	4-OCH_3	*terc*-butilo	Ft-13b		x
33a	6-CONH-tiazol-2-ilo	4-OCH_3	fenilo	Ft-14a		x
33b	7-CONH-tiazol-2-ilo	4-OCH_3	fenilo	Ft-14b		x

[a] Proceso de síntesis y descripción de propiedades fisicoquímicas en capítulo V.

Benzimidazoles

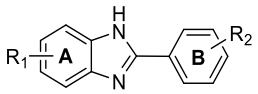

Tipo I

Compuesto						
Nº	**R_1**	**R_2**	**Código tesis**	**Art. 2**	**Art. 3**	**Cap. 5[a]**
34	H	4′-CH_3	BzI.0020			x
35	H	4′-OCH_3	BzI.0030	**1**	**1**	
36	H	4′-Cl	BzI.0040	**2**		
37	H	3′-Cl	BzI.0041			x
38	H	4′-Br	BzI.0050	**3**		
39	H	4′-NO_2	BzI.0060			x
40	H	4′-pirrolidin-1-ilo	BzI.0090			x
41	5-CH_3	4′-OCH_3	BzI.1030	**4**	**2**	
42	5-CH_3	4′-Cl	BzI.1040	**5**		
43	5-CH_3	3′-Cl	BzI.1041			x
44	5-CH_3	4′-NO_2	BzI.1060			x
45	5-CH_3	3′-NO_2	BzI.1061			x
46	5-CH_3	2′-NO_2	BzI.1062			x
47	5-CH_3	4′-NH_2	BzI.1070			x
48	5-CH_3	3′-NH_2	BzI.1071			x
49	5-CH_3	3′-OH	BzI.1081			x
50	5-CH_3	2′-OH	BzI.1082			x
51	5-CH_3	4′-pirrolidin-1-ilo	BzI.1090			x
52	5-CH_3	3′-(4′′-COOHfenilo)	BzI.1110			x
53	5-CH_3	4′-toliloxi	BzI.1120			x
54	5-CH_3	2′,5′-diCH_3	BzI.1140	**6**		
55	5-CH_3	3′-OH, 4′-OCH_3	BzI.1160			x
56	5-CH_3	3′-NO_2, 4′-OCH_3	BzI.1190	**7**		
57	5-CH_3	3′-NH_2, 4′-OCH_3	BzI.1200			x
58	5-CH_3	indol-5-ilo	BzI.1241			x
59	5-CH_3	3′,4′,5′-OCH_3	BzI.1252			x
60	5-CH_3	furan-2-ilo	BzI.1300			x
61	5-CH_3	5′-CH_3furan-2-ilo	BzI.1301			x
62	5-CH_3	5′-NO_2furan-2-ilo	BzI.1302			x
63	5-CH_3	benzofuran-2-ilo	BzI.1303			x
64	5-CH_3	5′-Brbenzofuran-2-ilo	BzI.1304			x
65	5-CH_3	tiofen-2-ilo	BzI.1310			x
66	5-CH_3	3′-CH_3tiazol-2-ilo	BzI.1311			x
67	5-CH_3	5′-(4′-CH_3piperazin-1-il)tiazol-2-ilo	BzI.1312			x
68	5-CH_3	4′-CH_3imidazo-5-ilo	BzI.1320			x
69	5-CH_3	piridin-2-ilo	BzI.1330			x
70	5-CH_3	quinolin-2-ilo	BzI.1360			x
71	5-CH_3	8′-OHquinolin-2-ilo	BzI.1362			x
72	5-CH_3	quinolin-4-ilo	BzI.1380			x

Compuesto						
Nº	**R_1**	**R_2**	**Código tesis**	**Art. 2**	**Art. 3**	**Cap. 5[a]**
73	5-Cl	4´-OCH_3	BzI.2030	**8**		
74	5-Cl	4´-Cl	BzI.2040	**9**		
75	5-Cl	4´-NO_2	BzI.2060	**10**		
76	5-Cl	4´-pirrolidin-1-ilo	BzI.2090			x
77	5-Cl	2´,5´-diCH_3	BzI.2140	**16**		
78	5-Cl	3´-NO_2, 4´-OCH_3	BzI.2190	**12**		
79	5-Cl	3´-NH_2, 4´-OCH_3	BzI.2200	**13**		
80	5-OCH_3	4´-OCH_3	BzI.3030	**20**		
81	5-OCH_3	4´-Cl	BzI.3040	**21**		
82	5-OCH_3	4´-Br	BzI.3050	**22**		
83	5-NO_2	4´-OCH_3	BzI.4030	**14**	**3**	
84	5-NO_2	4´-Cl	BzI.4040	**15**		
85	5-NO_2	4´-pirrolidin-1-ilo	BzI.4090			x
86	5-NO_2	2´,5´-diCH_3	BzI.4140	**16**		
87	5-NO_2	3´-NO_2, 4´-OCH_3	BzI.4190	**17**		
88	5-NO_2	benzofuran-2-ilo	BzI.4303			x
89	5-NH_2	H	BzI.5010			x
90	5-NH_2	4´-OCH_3	BzI.5030	**18**	**4**	
91	5-NH_2	2´,5´-diCH_3	BzI.5140			x
92	5-NH_2	benzofuran-2-ilo	BzI.5303			x
93	5,6-diCH_3	4´-OCH_3	BzI.6030	**23**		
94	5,6-diCl	4´-OCH_3	BzI.7030	**24**		
95	5,6-benceno	4´-Cl	BzI.8040			x

[a] Proceso de síntesis y descripción de propiedades fisicoquímicas en capítulo V.

[a] Proceso de síntesis y descripción de propiedades fisicoquímicas en capítulo V.

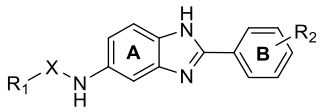

Tipo I.a

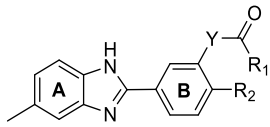

Tipo I.b

	Compuesto							
Nº	**X**	**Y**	**R_1**	**R_2**	**Código tesis**	**Art. 2**	**Art. 3**	**Cap. 5[a]**
Tipo I.a								
96	SO_2	-	tosilo	4´-OCH_3	BzIa.5030.020		6	
97	CO	-	2´,4´-diF-Ph	4´-OCH_3	BzIa.5030.130			**x**
98	CO	-	naft-2-ilo	4´-OCH_3	BzIa.5030.220		7	
99	CO	-	piridin-2-ilo	4´-OCH_3	BzIa.5030.330	19		
100	CO	-	quinolin-2-ilo	4´-OCH_3	BzIa.5030.360		8	
101	CO	-	2-Bocaminodecanoilo	4´-OCH_3	BzIa.5030.00δ			x
102	CO	-	2-aminodecanoilo	4´-OCH_3	BzIa.5030.00γ			x
103	CO	-	2-Boc-aminododecanoilo	4´-OCH_3	BzIa.5030.00α		9	
104	CO	-	2-aminododecanoilo	4´-OCH_3	BzIa.5030.00β		10	
105	CO	-	*terc*-butiloxicarbonilo	4´-OCH_3	BzIa.5030.00ε		5	
106	CO	-	glutarilo	4´-OCH_3	BzIa.5030.00τ			x
107	CO	-	3´,4´,5´-triOCH_3Ph	2´,5´-diCH_3	BzIa.5140.252			x
108	CO	-	2-Bocaminododecanoilo	2´,5´-diCH_3	BzIa.5140.00α			x
109	CO	-	2-aminododecanoilo	2´,5´-diCH_3	BzIa.5140.00β			x
				B				
110	CO	-	piridin-2-ilo	Benzofuran	BzIa.5303.330			x
111	CO	-	2-Boc-aminodecanoilo	Benzofuran	BzIa.5303.00δ			x
112	CO	-	2-aminodecanoilo	Benzofuran	BzIa.5303.00γ			x
Tipo I.b								
113	CO	NH	CH_2-Ph-Ph	-	BzIb.1071.100			x
114	CO	NH	piridin-2-ilo	-	BzIb.1071.330			x
115	CO	NH	isoquinolin-1-ilo	-	BzIb.1071.390			x
116	CO	O	CH_2-Ph-Ph	-	BzIb.1081.100			x
117	CO	O	CH_2-Ph-Ph	4´-OCH_3	BzIb.1160.100			x

[a] Proceso de síntesis y descripción de propiedades fisicoquímicas en capítulo V. Boc: *terc*-butiloxicarbonilo.

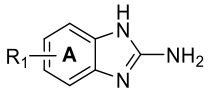

2-Aminobenzimidazoles intermedios (Bz*i*)

Compuesto					
Nº	**R_1**	**R_2**	**Código tesis**	**Art. 3**	**Art. 4**
118	5-CH_3	2-NH_2	Bz*i*-1	Bz*i*-1	
119	5-Cl	2-NH_2	Bz*i*-2	Bz*i*-2	
120	5-OCH_3	2-NH_2	Bz*i*-3	Bz*i*-3	
121	5-NO_2	2-NH_2	Bz*i*-4		AI-6
122	5,6-diCH_3	2-NH_2	Bz*i*-5	Bz*i*-4	
123	5,6-diCl	2-NH_2	Bz*i*-6	Bz*i*-5	

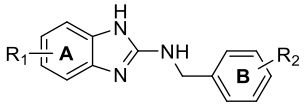

Tipo II

Compuesto					
Nº	**R_1**	**R_2**	**Código tesis**	**Art. 3**	**Cap. 5[a]**
124	5-CH_3	H	BzII.1010	11	
125	5-CH_3	4′-CH_3	BzII.1020		x
126	5-CH_3	4′-OCH_3	BzII.1030	12	
127	5-CH_3	naft-2-ilo	BzII.1220	14	
128	5-CH_3	2′,3′,4′-triOCH_3	BzII.1250	13	
129	5-CH_3	furan-2-ilo	BzII.1300	15	
130	5-CH_3	tiofen-2-ilo	BzII.1310	16	
131	5-Cl	H	BzII.2010	17	
132	5-Cl	4′-OCH_3	BzII.2030	18	
133	5-Cl	3′,4′,5′-OCH_3	BzII.2252	19	
134	5-Cl	furan-2-ilo	BzII.2300	20	
135	5-OCH_3	H	BzII.3010	21	
136	5-OCH_3	4′-OCH_3	BzII.3030	22	
137	5-OCH_3	4′-pirrolidin-1-ilo	BzII.3090	23	
138	5-OCH_3	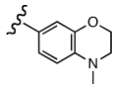	BzII.3231		x
139	5-OCH_3	5′-CH_3-furan-2-ilo	BzII.3301	24	
140	5-OCH_3	tiofen-2-ilo	BzII.3310	25	
141	5-OCH_3	*N*-CH_3indol-3-ilo	BzII.3321		x
142	5,6-diCH_3	4′-OCH_3	BzII.6030	26	
143	5,6-diCH_3	3′,4′,5′-OCH_3	BzII.6252	27	
144	5,6-diCl	H	BzII.7010	28	
145	5,6-diCl	4′-OCH_3	BzII.7030	29	
146	5,6-diCl	3′,4′,5′-OCH_3	BzII.7252	30	

[a] Proceso de síntesis y descripción de propiedades fisicoquímicas en capítulo V.

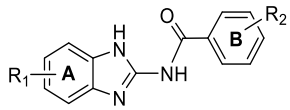

Tipo III

	Compuesto					
Nº	**R_1**	**R_2**	**Código tesis**	**Art. 3**	**Art. 4**	**Cap. 5[a]**
147	5-CH_3	H	BzIII.1010	31		
148	5-CH_3	4´-OCH_3	BzIII.1030	32		
149	5-CH_3	2´-Cl, 5´-NO_2	BzIII.1150	33		
150	5-CH_3	3´,5´-diOCH_3	BzIII.1210	34		
151	5-CH_3	6-NH_2naft-2-ilo	BzIII.1230			x
152	5-CH_3	benzotriazol-5-ilo	BzIII.1240			x
153	5-CH_3	3´,4´,5´-triOCH_3	BzIII.1252	35		
154	5-CH_3	α-OHbencilo	BzIII.1260	48		
155	5-CH_3	piridin-2-ilo	BzIII.1330	36	1	
156	5-CH_3	3´-CH_3piridin-2-ilo	BzIII.1331		4	
157	5-CH_3	5´-CH_3piridin-2-ilo	BzIII.1334		5	
158	5-CH_3	5´-butilpiridin-2-ilo	BzIII.1335		6	
159	5-CH_3	5´-CNpiridin-2-ilo	BzIII.1336		8	
160	5-CH_3	5´-fenilpiridin-2-ilo	BzIII.1337		7	
161	5-CH_3	piridin-3-ilo	BzIII.1340		2	
162	5-CH_3	piridin-4-ilo	BzIII.1350		3	
163	5-CH_3	quinolin-2-ilo	BzIII.1360		9	
164	5-CH_3	quinolin-4-ilo	BzIII.1380		10	
165	5-CH_3	isoquinolin-1-ilo	BzIII.1390		11	
166	5-CH_3	2-aminodecanoilo	BzIII.1000b			x
167	5-CH_3	glutarilo	BzIII.1000t			x
168	5-CH_3	glutarilo cerrado	BzIII.1000c			x
169	5-CH_3	glutarilo cerrado N-butilo	BzIII.1000bc			x
170	5-Cl	H	BzIII.2010	37		
171	5-Cl	4´-OCH_3	BzIII.2030	38		
172	5-Cl	ibuprofenilo	BzIII.2270			x
173	5-Cl	piridin-2-ilo	BzIII.2330	39	12	
174	5-Cl	3´-CH_3piridin-2-ilo	BzIII.2331		13	
175	5-Cl	3´-Clpiridin-2-ilo	BzIII.2332		14	
176	5-Cl	4´-OCH_3piridin-2-ilo	BzIII.2333		15	
177	5-Cl	5´-CH_3piridin-2-ilo	BzIII.2334		16	
178	5-Cl	5´-butilpiridin-2-ilo	BzIII.2335		17	
179	5-Cl	5´-fenilpiridin-2-ilo	BzIII.2337		18	
180	5-Cl	6´-CH_3piridin-2-ilo	BzIII.2338		19	
181	5-Cl	quinolin-2-ilo	BzIII.2360		20	
182	5-Cl	6´-OCH_3quinolin-2-ilo	BzIII.2361		24	
183	5-Cl	quinolin-3-ilo	BzIII.2370		21	
184	5-Cl	quinolin-4-ilo	BzIII.2380		22	
185	5-Cl	isoquinolin-1-ilo	BzIII.2390		23	
186	5-OCH_3	H	BzIII.3010	40		
187	5-OCH_3	4´-OCH_3	BzIII.3030	41		
188	5-OCH_3	piridin-2-ilo	BzIII.3330	42	25	

Compuesto						
Nº	**R_1**	**R_2**	**Código tesis**	**Art. 3**	**Art. 4**	**Cap. 5[α]**
189	5-OCH_3	5´-CH_3piridin-2-ilo	BzIII.3334		**26**	
190	5-OCH_3	5´-butilpiridin-2-ilo	BzIII.3335		**27**	
191	5-OCH_3	5´-fenilpiridin-2-ilo	BzIII.3337		**28**	
192	5-OCH_3	2-Boc-aminododecanoilo	BzIII.3000a	**54**		
193	5-OCH_3	2-aminododecanoilo	BzIII.3000b	**55**		
194	5-OCH_3	glutarilo	BzIII.3000t			x
195	5-NO_2	piridin-2-ilo	BzIII.4330		**29**	
196	5-NH_2	piridin-2-ilo	BzIII.5330		**30**	
197	5-NHCO-2-Bocaminodecanoilo	piridin-2-ilo	BzIII.5330.00δ		**31**	
198	5-NHCO-2-aminodecanoilo	piridin-2-ilo	BzIII.5330.00γ		**32**	
200	5,6-diCH_3	H	BzIII.6010	**43**		
201	5,6-diCH_3	4´-OCH_3	BzIII.6030	**44**		
202	5,6-diCH_3	piridin-2-ilo	BzIII.6330		**33**	
203	5,6-diCH_3	5´-butilpiridin-2-ilo	BzIII.6335		**34**	
204	5,6-diCH_3	5´-fenilpiridin-2-ilo	BzIII.6337		**35**	
205	5,6-diCl	H	BzIII.7010	**45**		
206	5,6-diCl	4´-OCH_3	BzIII.7030	**46**		
207	5,6-diCl	piridin-2-ilo	BzIII.7330		**36**	
208	5,6-diCl	2-Boc-aminododecanoilo	BzIII.7000a			x

[α] Proceso de síntesis y descripción de propiedades fisicoquímicas en capítulo V. Boc: *terc*-butiloxicarbonilo.

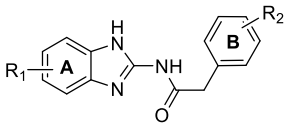

Tipo III.a

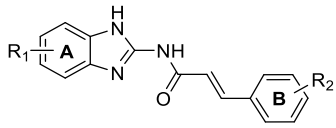

Tipo III.b

Nº	Compuesto R_1	R_2	Código tesis	Art. 3	Cap. 5[a]
	Tipo III.a				
209	5-CH_3	3´-NO_2	BzIIIa.1061	47	
210	5-CH_3	3´,4´-OCH_2O	BzIIIa.1180		x
211	5-CH_3	naftil-2-ilo	BzIIIa.1220	49	
212	5-CH_3	tiofen-2-ilo	BzIIIa.1310	50	
213	5,6-diCH_3	3´-Cl	BzIIIa.6041	51	
214	5,6-diCl	3´-NO_2	BzIIIa.7061	52	
215	5,6-diCl	3´-NH_2	BzIIIa.7071	53	
	Tipo III.b				
216	5-CH_3	H	BzIIIb.1010		x
217	5-CH_3	4-OCH_3	BzIIIb.1030		x
218	5-CH_3	3´-NO_2	BzIIIb.1061		x
219	5-CH_3	3´,4´-OCH_2O	BzIIIb.1180		x
220	5-CH_3	3´,4´-diOCH_3, 4´-OH	BzIIIb.1251		x
221	5-CH_3	3´,4´,5´-OCH_3	BzIIIb.1252		x
222	5-Cl	3´,4´-OCH_3	BzIIIb.2170		x
222	5-Cl	3´,4´,5´-OCH_3	BzIIIb.2252		x
223	5-OCH_3	3´,4´,5´-triOCH_3	BzIIIb.3252		x

[a] Proceso de síntesis y descripción de propiedades fisicoquímicas en capítulo V.

Benzimidazolonas

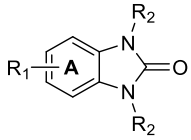

Nº	Compuesto R_1	R_2	R_3	Código tesis	Cap. 5[a]
224	5(6)-CH_3	-	-	Bzo-1	x
225	5(6)-NO_2	-	-	Bzo-2	x
226	5(6)-NO_2	etilo	etilo	Bzo-3	x
227	5(6)-NH_2	etilo	etilo	Bzo-4	x
228	5(6)-NHCO-piridin-2-ilo	etilo	etilo	Bzo-5	x
229	5(6)-NHCO-5´-butilpiridin-2-ilo	etilo	etilo	Bzo-6	x
230	5(6)-NHCOBocaminodecanoilo	etilo	etilo	Bzo-7	x
231	5(6)-NHCOaminodecanoilo	etilo	etilo	Bzo-8	x

[a] Proceso de síntesis y descripción de propiedades fisicoquímicas en capítulo V. Boc: *terc*-butiloxicarbonilo.

VII.2. ESTRUCTURAS

Benzalftalidas

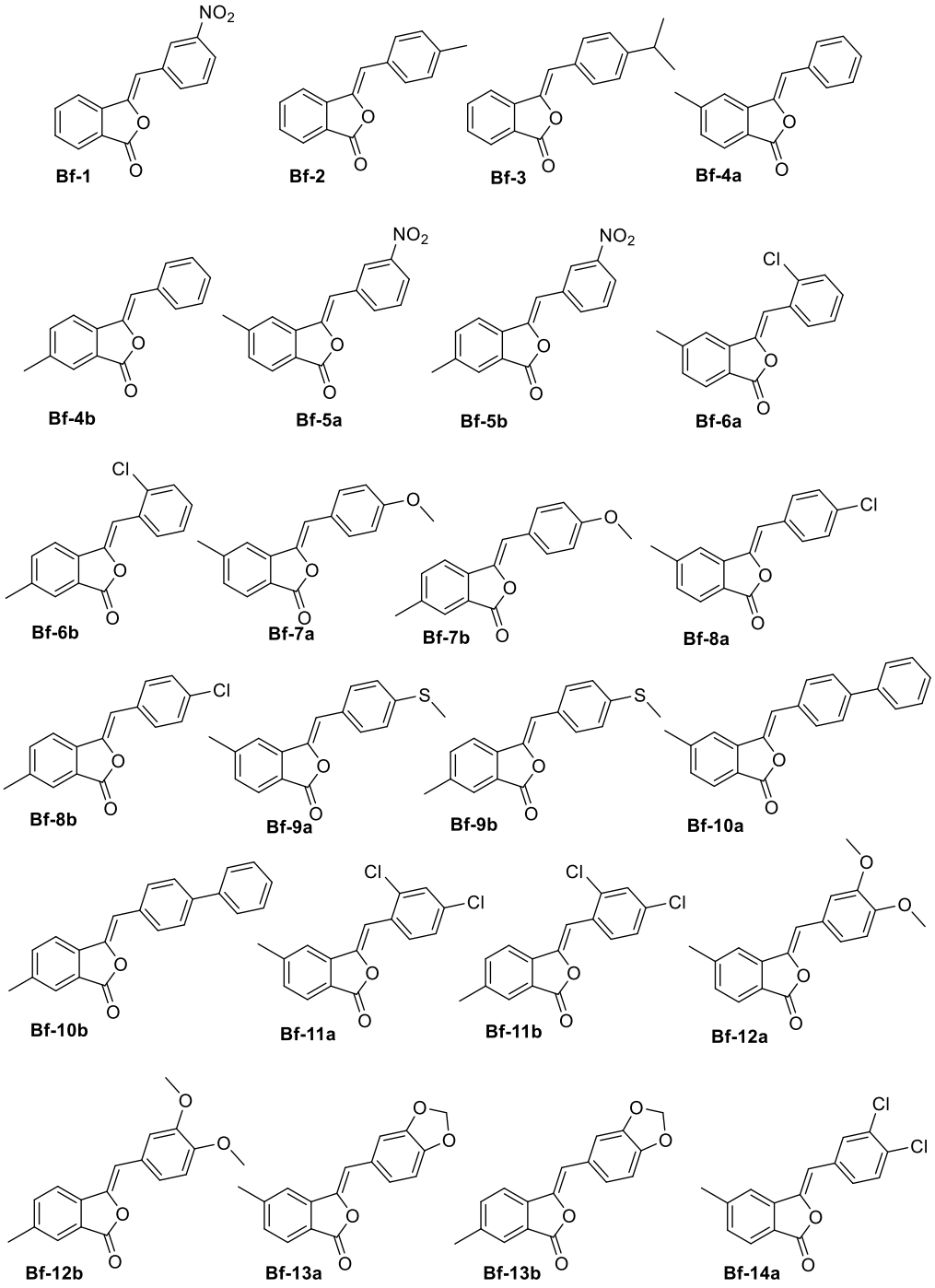

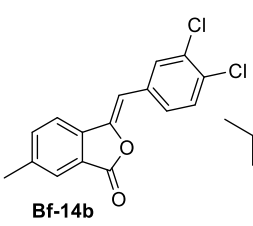

Bf-14b

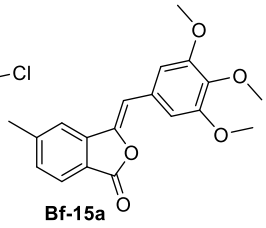

Bf-15a

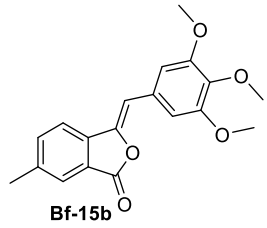

Bf-15b

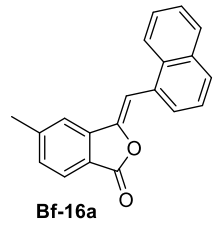

Bf-16a

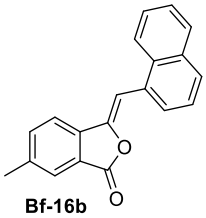

Bf-16b

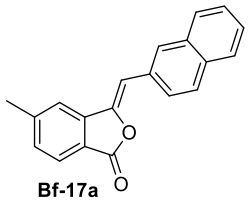

Bf-17a

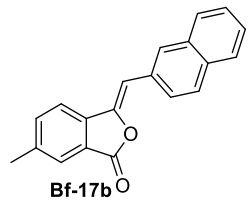

Bf-17b

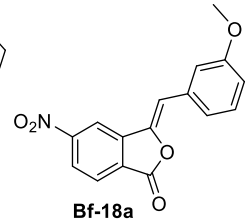

Bf-18a

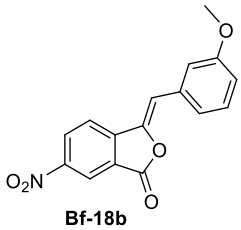

Bf-18b

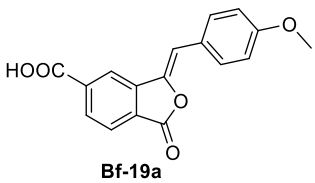

Bf-19a

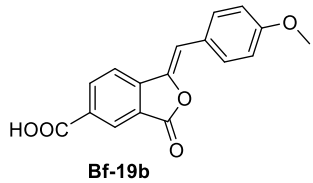

Bf-19b

Ftalazinonas

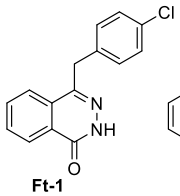

Ft-1

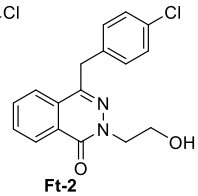

Ft-2

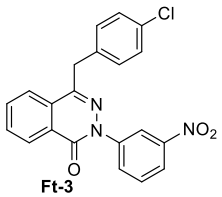

Ft-3

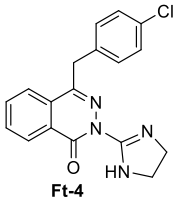

Ft-4

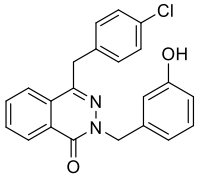

Ft-5

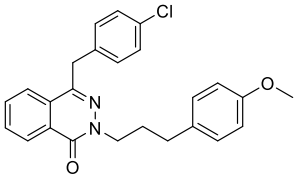

Ft-6

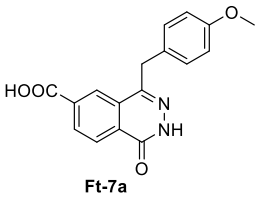

Ft-7a

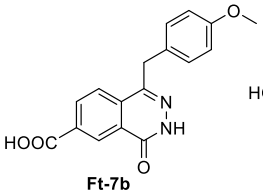

Ft-7b

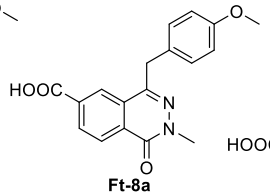

Ft-8a

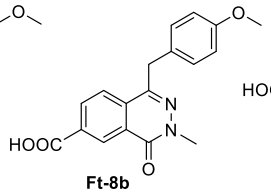

Ft-8b

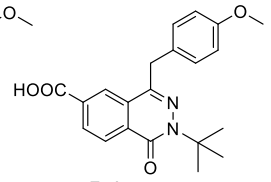

Ft-9a

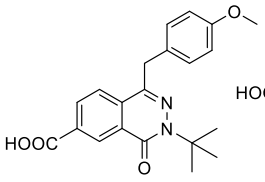

Ft-9b

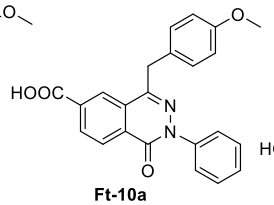

Ft-10a

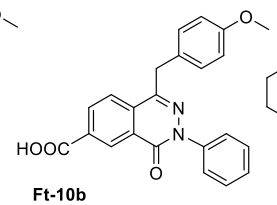

Ft-10b

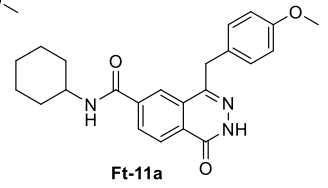

Ft-11a

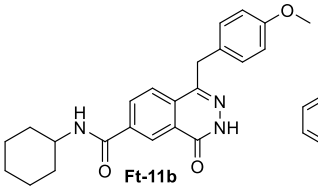

Ft-11b

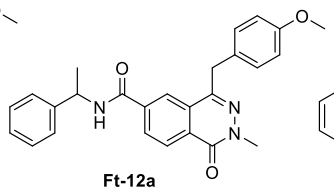

Ft-12a

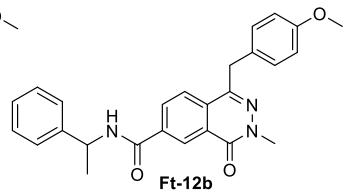

Ft-12b

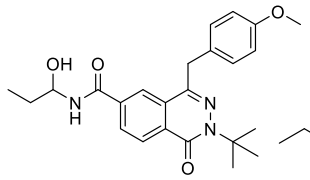

Ft-13a

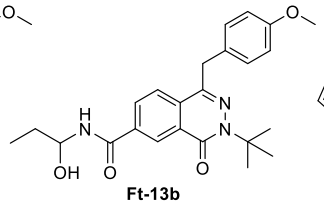

Ft-13b

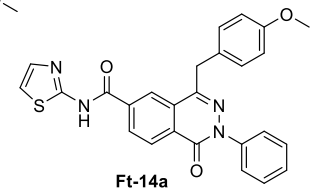

Ft-14a

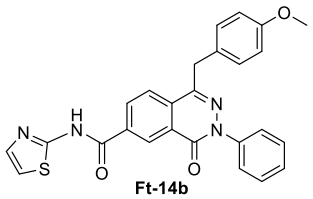

Ft-14b

Benzimidazoles

Familia I

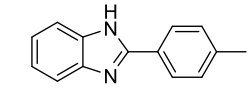

Bzl.0020

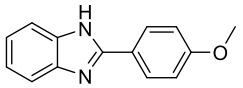

Bzl.0030

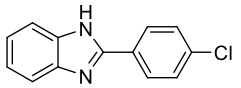

Bzl.0040

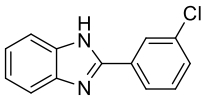

Bzl.0041

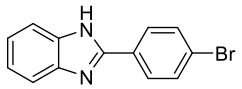

Bzl.0050

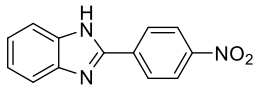

Bzl.0060

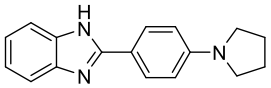

Bzl.0090

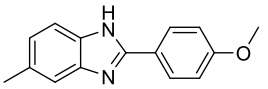

Bzl.1030

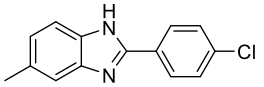

Bzl.1040

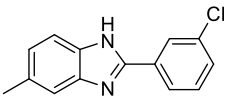

Bzl.1041

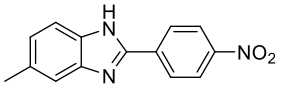

Bzl.1060

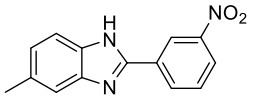

Bzl.1061

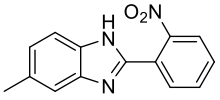

Bzl.1062

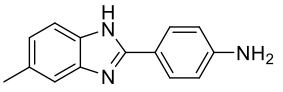

Bzl.1070

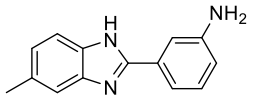

Bzl.1071

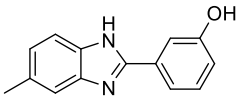

Bzl.1081

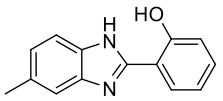

Bzl.1082

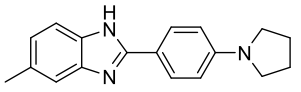

Bzl.1090

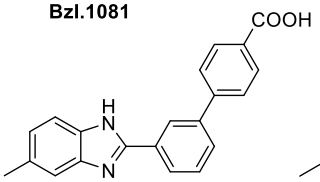

Bzl.1110

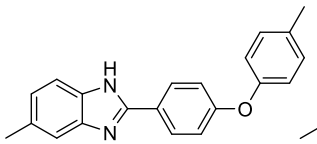

Bzl.1120

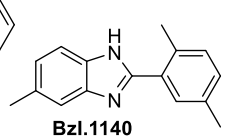

Bzl.1140

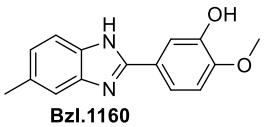

Bzl.1160

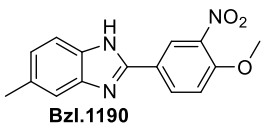

Bzl.1190

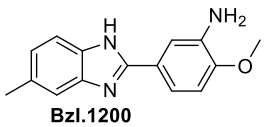

Bzl.1200

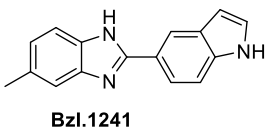

Bzl.1241

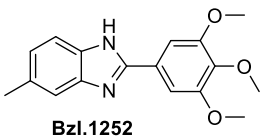

Bzl.1252

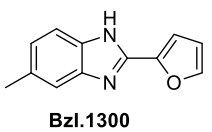

Bzl.1300

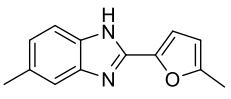

Bzl.1301

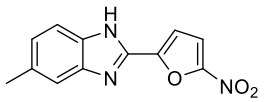

Bzl.1302

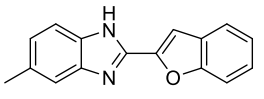

Bzl.1303

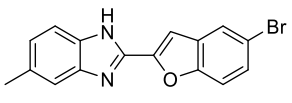

Bzl.1304

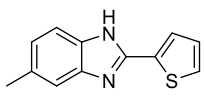

Bzl.1310

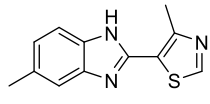

Bzl.1311

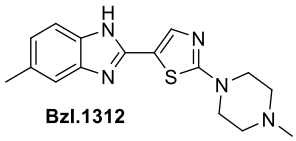

Bzl.1312

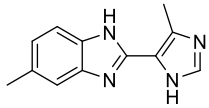

Bzl.1320

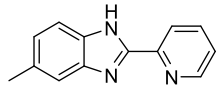

Bzl.1330

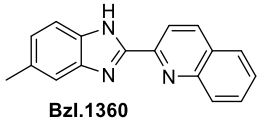

Bzl.1360

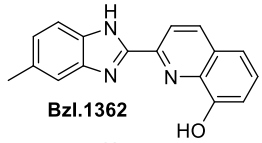

Bzl.1362

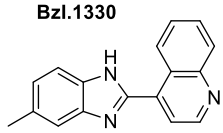

Bzl.1380

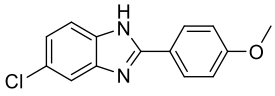

Bzl.2030

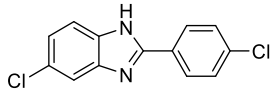

Bzl.2040

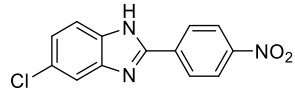

Bzl.2060

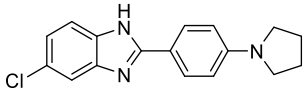

Bzl.2090

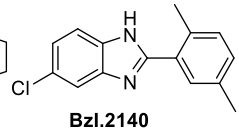

Bzl.2140

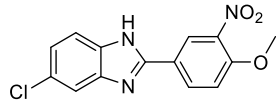

Bzl.2190

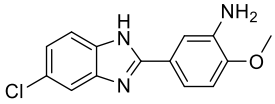

Bzl.2200

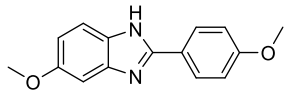

Bzl.3030

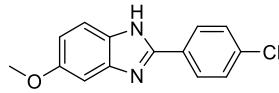

Bzl.3040

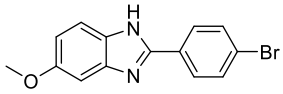

Bzl.3050

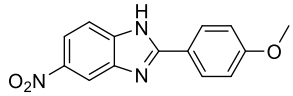

Bzl.4030

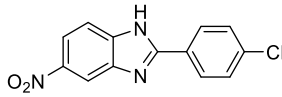

Bzl.4040

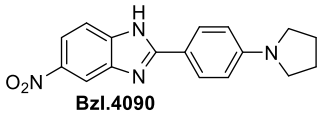

Bzl.4090

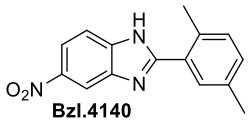

Bzl.4140

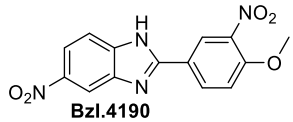

Bzl.4190

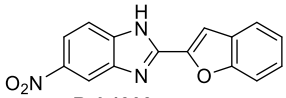

Bzl.4303

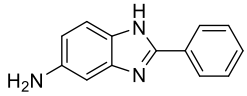

Bzl.5010

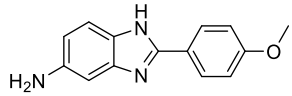

Bzl.5030

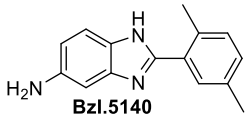

Bzl.5140

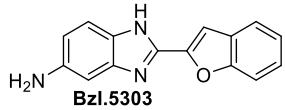

Bzl.5303

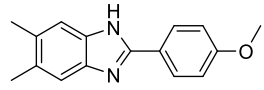

Bzl.6030

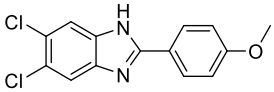

Bzl.7030

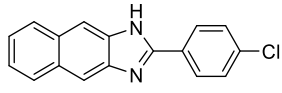

Bzl.8040

Subfamilia Ia

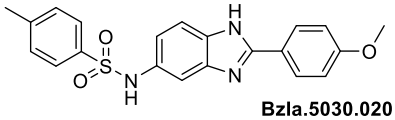

Bzla.5030.020

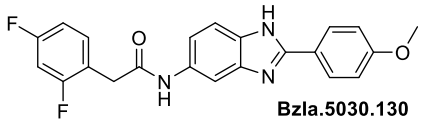

Bzla.5030.130

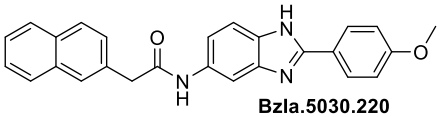

Bzla.5030.220

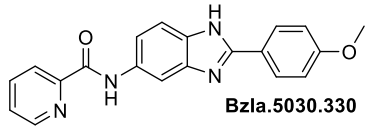

Bzla.5030.330

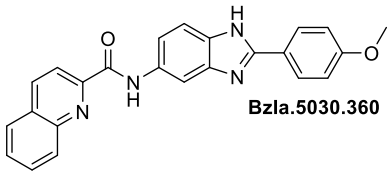

Bzla.5030.360

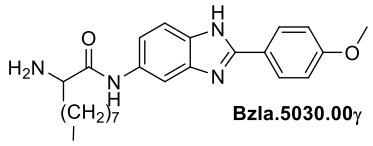

Bzla.5030.00γ

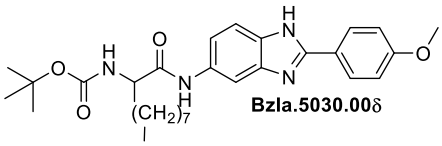

Bzla.5030.00δ

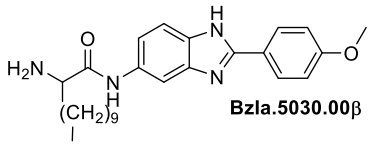

Bzla.5030.00β

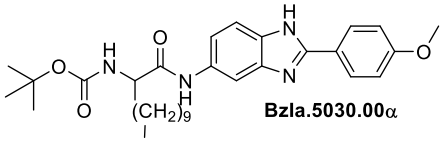

Bzla.5030.00α

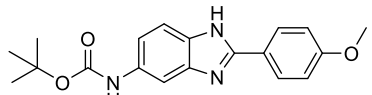

Bzla.5030.00ε

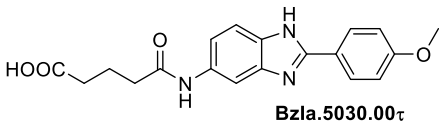

Bzla.5030.00τ

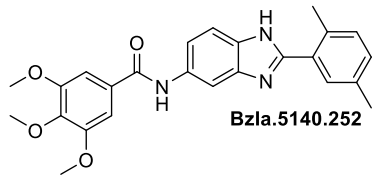

Bzla.5140.252

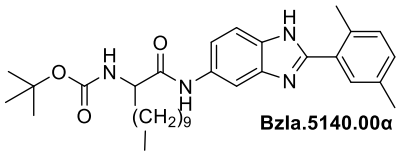

Bzla.5140.00α

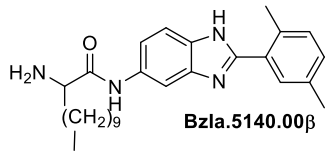

Bzla.5140.00β

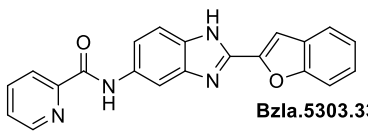

Bzla.5303.330

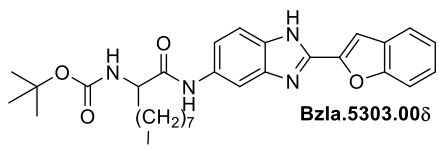

Bzla.5303.00δ

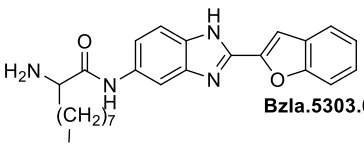

Bzla.5303.00γ

Subfamilia Ib

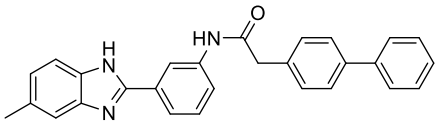

Bzlb.1071.100

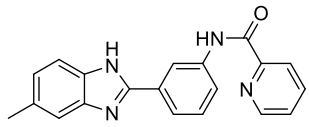

Bzlb.1071.330

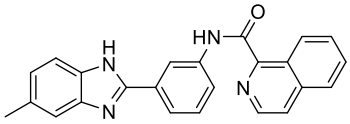

Bzlb.1071.390

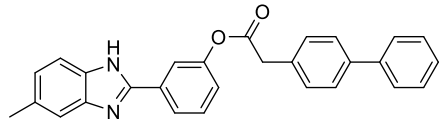

Bzlb.1081.100

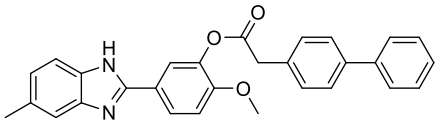

Bzlb.1160.100

2-Aminobenzimidazoles intermedios

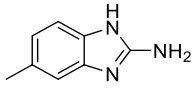

Bz*i*-1

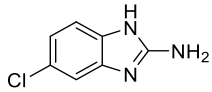

Bz*i*-2

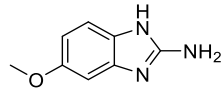

Bz*i*-3

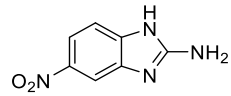

Bz*i*-4

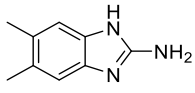

Bz*i*-5

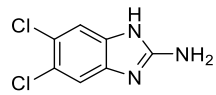

Bz*i*-6

Familia II

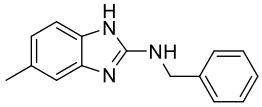
BzII.1010

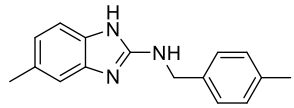
BzII.1020

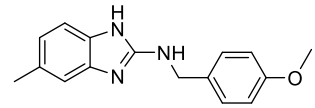
BzII.1030

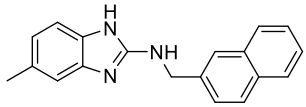
BzII.1220

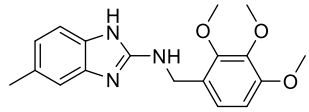
BzII.1250

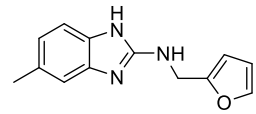
BzII.1300

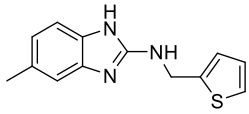
BzII.1310

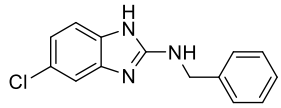
BzII.2010

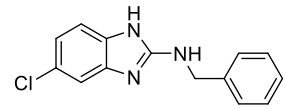
BzII.2030

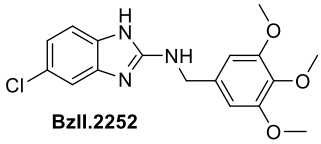
BzII.2252

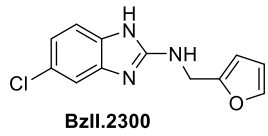
BzII.2300

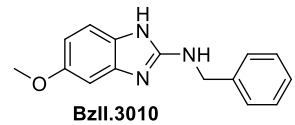
BzII.3010

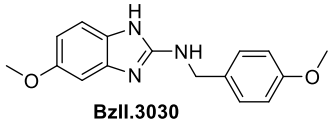
BzII.3030

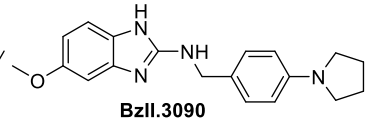
BzII.3090

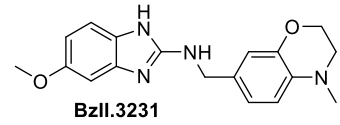
BzII.3231

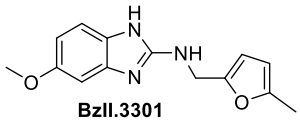
BzII.3301

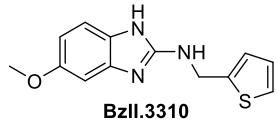
BzII.3310

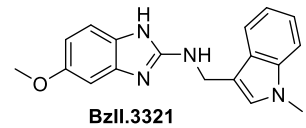
BzII.3321

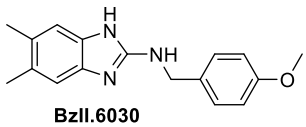
BzII.6030

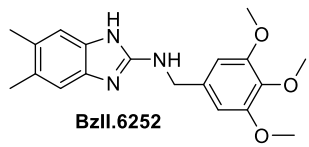
BzII.6252

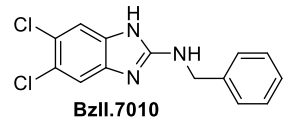
BzII.7010

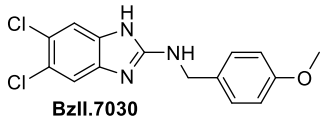
BzII.7030

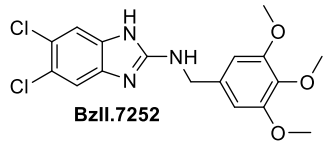
BzII.7252

Familia III

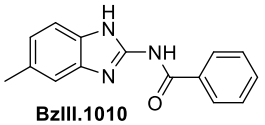
BzIII.1010

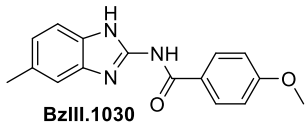
BzIII.1030

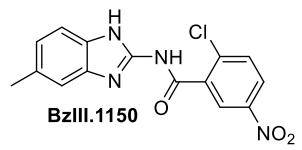
BzIII.1150

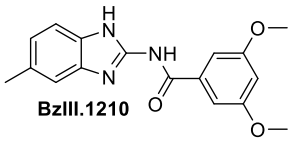
BzIII.1210

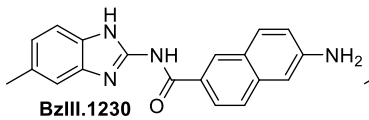
BzIII.1230

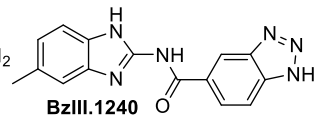
BzIII.1240

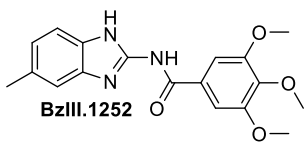
BzIII.1252

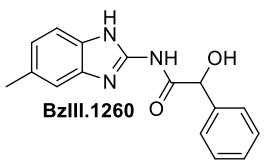
BzIII.1260

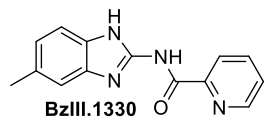
BzIII.1330

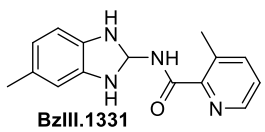
BzIII.1331

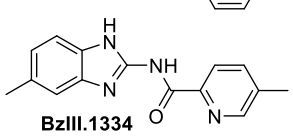
BzIII.1334

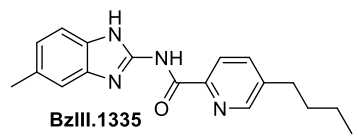
BzIII.1335

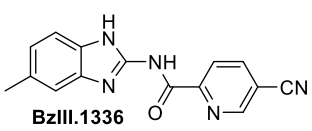
BzIII.1336

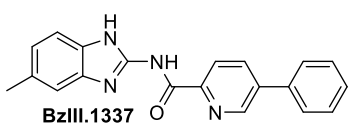
BzIII.1337

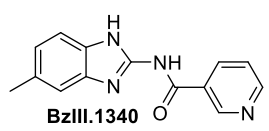
BzIII.1340

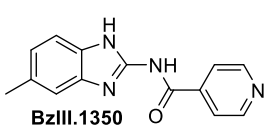
BzIII.1350

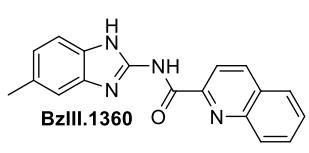
BzIII.1360

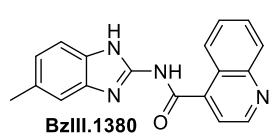
BzIII.1380

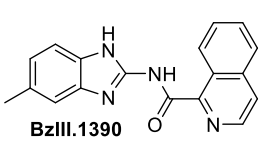
BzIII.1390

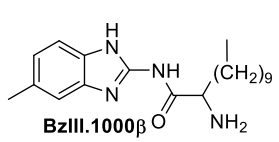
BzIII.1000β

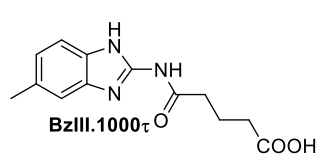
BzIII.1000τ

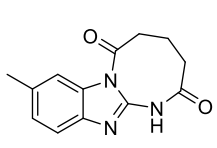
BzIII.1000c

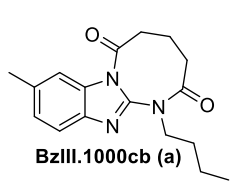
BzIII.1000cb (a)

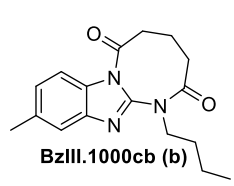
BzIII.1000cb (b)

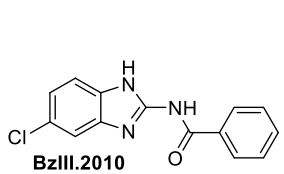
BzIII.2010

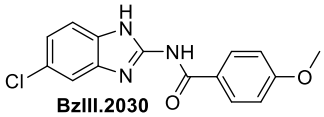
BzIII.2030

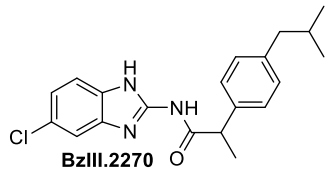
BzIII.2270

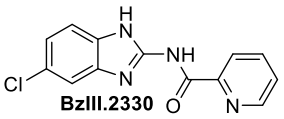
BzIII.2330

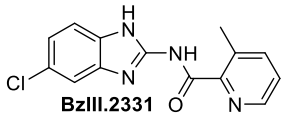
BzIII.2331

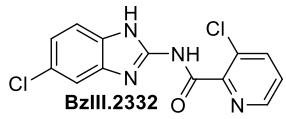
BzIII.2332

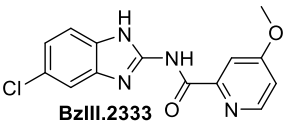
BzIII.2333

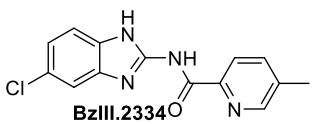
BzIII.2334

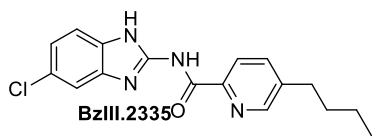
BzIII.2335

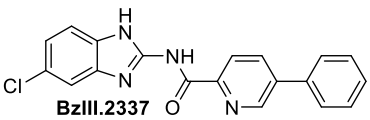
BzIII.2337

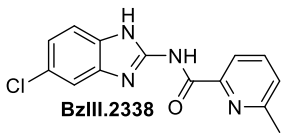
BzIII.2338

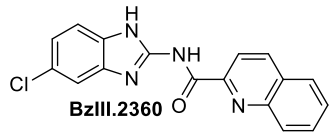
BzIII.2360

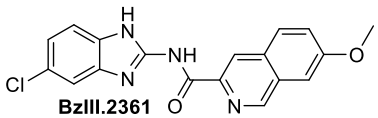
BzIII.2361

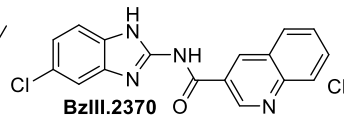
BzIII.2370


BzIII.2380

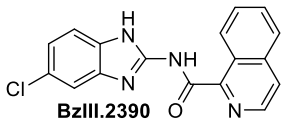
BzIII.2390

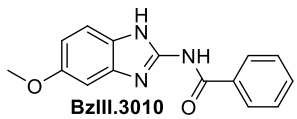
BzIII.3010

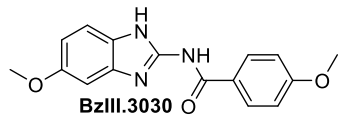
BzIII.3030

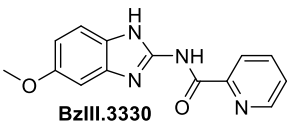
BzIII.3330

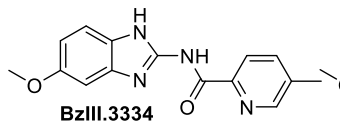
BzIII.3334

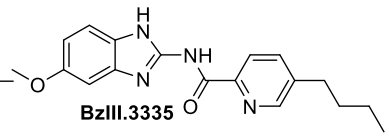
BzIII.3335

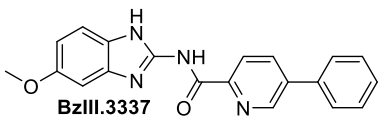
BzIII.3337

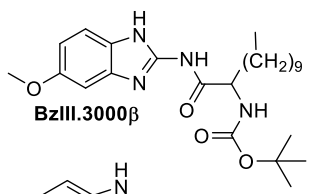
BzIII.3000β

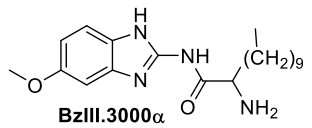
BzIII.3000α

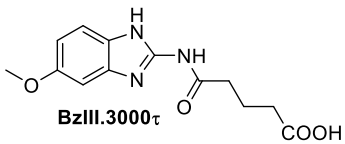
BzIII.3000τ

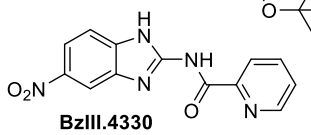
BzIII.4330

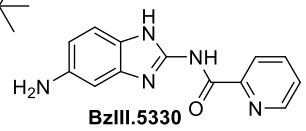
BzIII.5330

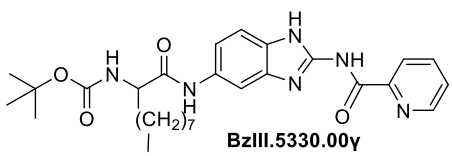
BzIII.5330.00γ

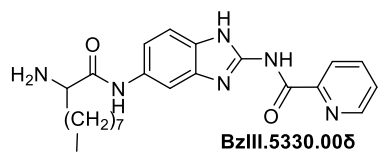
BzIII.5330.00δ

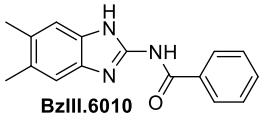
BzIII.6010

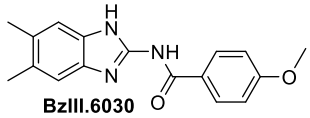
BzIII.6030

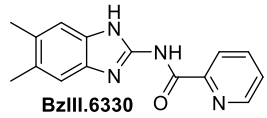
BzIII.6330

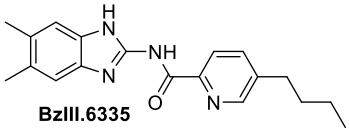
BzIII.6335

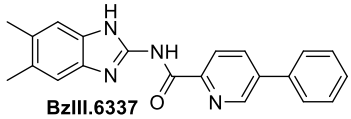
BzIII.6337

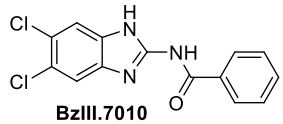
BzIII.7010

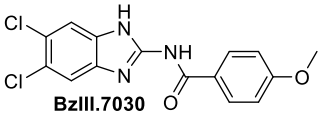
BzIII.7030

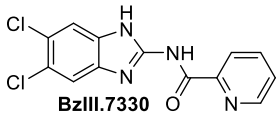
BzIII.7330

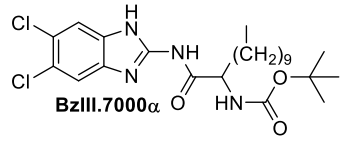
BzIII.7000α

Subfamilia IIIa

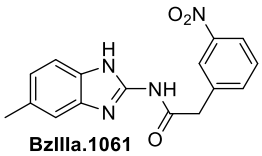
BzIIIa.1061

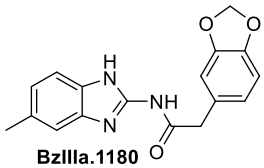
BzIIIa.1180

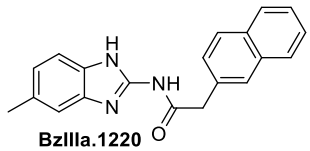
BzIIIa.1220

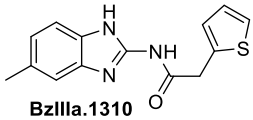
BzIIIa.1310

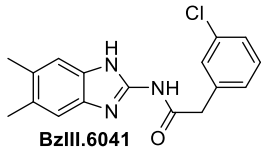
BzIII.6041

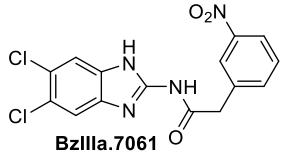
BzIIIa.7061

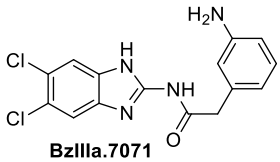
BzIIIa.7071

Subfamilia IIIb

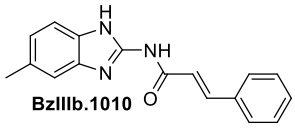
BzIIIb.1010

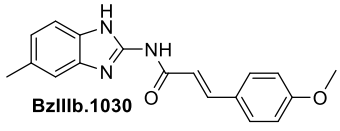
BzIIIb.1030

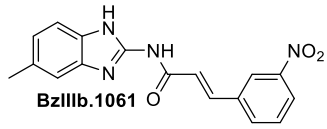
BzIIIb.1061

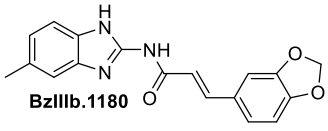
BzIIIb.1180

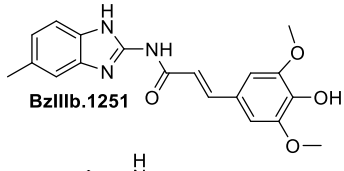
BzIIIb.1251

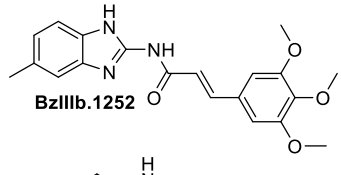
BzIIIb.1252

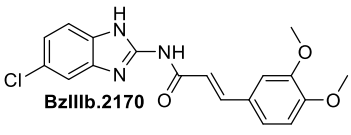
BzIIIb.2170

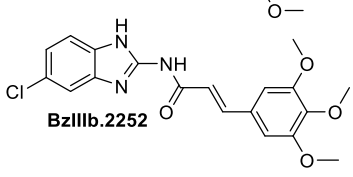
BzIIIb.2252

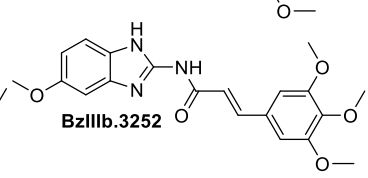
BzIIIb.3252

Benzimidazolonas

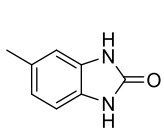
Bzo-1

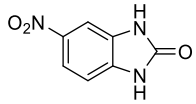
Bzo-2

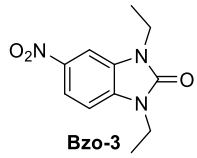
Bzo-3

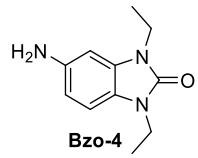
Bzo-4

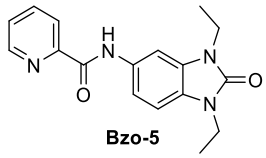
Bzo-5

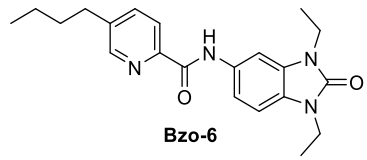
Bzo-6

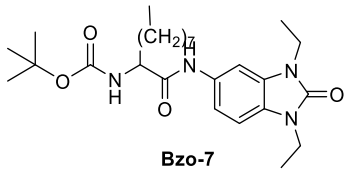
Bzo-7

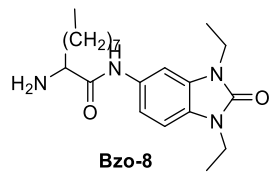
Bzo-8

VIII. ANEXOS

ANEXO 1

La caracterización fisicoquímica de todos los compuestos obtenidos en este Trabajo de Tesis Doctoral está disponible en forma de tablas en el CD adjunto.

ANEXO 2

Los espectros de RMN de ^{1}H, ^{13}C y HR-MS de todos los compuestos obtenidos en este Trabajo de Tesis Doctoral están disponibles en el CD adjunto.